

Airey, Gordon Dan (1997) Rheological characteristics of polymer modified and aged bitumens. PhD thesis, University of Nottingham.

**Access from the University of Nottingham repository:**

<http://eprints.nottingham.ac.uk/13431/1/362996.pdf>

**Copyright and reuse:**

The Nottingham ePrints service makes this work by researchers of the University of Nottingham available open access under the following conditions.

- Copyright and all moral rights to the version of the paper presented here belong to the individual author(s) and/or other copyright owners.
- To the extent reasonable and practicable the material made available in Nottingham ePrints has been checked for eligibility before being made available.
- Copies of full items can be used for personal research or study, educational, or not-for-profit purposes without prior permission or charge provided that the authors, title and full bibliographic details are credited, a hyperlink and/or URL is given for the original metadata page and the content is not changed in any way.
- Quotations or similar reproductions must be sufficiently acknowledged.

Please see our full end user licence at:

[http://eprints.nottingham.ac.uk/end\\_user\\_agreement.pdf](http://eprints.nottingham.ac.uk/end_user_agreement.pdf)

**A note on versions:**

The version presented here may differ from the published version or from the version of record. If you wish to cite this item you are advised to consult the publisher's version. Please see the repository url above for details on accessing the published version and note that access may require a subscription.

For more information, please contact [eprints@nottingham.ac.uk](mailto:eprints@nottingham.ac.uk)

**UNIVERSITY OF NOTTINGHAM**  
**DEPARTMENT OF CIVIL ENGINEERING**



**Rheological Characteristics  
of Polymer Modified and  
Aged Bitumens**

by

**Gordon Dan Airey**

Thesis submitted to the University of Nottingham  
for the degree of Doctor of Philosophy

October 1997

**To Julie**

# Abstract

The demands on asphalt pavements, as a result of the growth in traffic volumes, traffic loads and tyre contact pressures, has resulted in an increased interest in the use of modified bitumens, particularly over the last ten years. Of the various types of modified and specialised binders that are available worldwide, polymer modified bitumens (PMB's) have tended to be the most popular. Polymer modification significantly alters the rheological characteristics of the binder, thereby requiring the use of fundamental rheological testing methods rather than empirical methods, to provide an indication of the performance of the binder and subsequently the asphalt mixture.

This thesis is concerned with the use of a Dynamic Shear Rheometer (DSR) to quantify the fundamental rheological characteristics of various unaged and aged PMB's. The parallel plate testing methodology used with the Bohlin Model DSR50 Dynamic Shear Rheometer requires accurate temperature control by means of a circulating fluid bath, a combination of different plate diameters and sample geometries, and the use of small strains in order to measure the linear viscoelastic rheological characteristics of a bitumen specimen.

Conventional and dynamic shear rheometry testing of various penetration grade bitumens, semi-crystalline ethylene vinyl acetate (EVA) PMB's and thermoplastic rubber styrene butadiene styrene (SBS) PMB's have indicated that the rheological characteristics differ considerably between the unmodified and polymer modified bitumens as well as between the plastomeric EVA and elastomeric SBS PMB's. The DSR dynamic rheological parameters of complex modulus and phase angle indicate that the modification mechanism of EVA PMB's consists of the crystallisation of rigid three dimensional networks within the bitumen. These rigid crystalline structures increase the stiffness and elastic component of the viscoelastic balance of the PMB up to the temperature associated with the melting of the copolymer. The modification mechanism of SBS PMB's consists of the establishment of a highly elastic network within the



bitumen that increases the elasticity and stiffness, particularly at high temperatures. The higher melting temperature of the SBS copolymer allows the rheological character of the SBS PMB to extend to temperatures greater than those found for EVA PMB's.

DSR measurements of the rheological changes associated with laboratory ageing of EVA PMB's indicate that the ageing mechanism is linked to a chemical change of the copolymer due to fusion of the crystallites. This chemical change leads to a degradation of the polymer and, therefore, a transition of the rheological behaviour towards that of an unmodified bitumen.

The rheological changes associated with the ageing of SBS PMB's is linked to a breakdown of the molecular structure of the SBS copolymer to form a lower molecular weight polymer substructure. This results in an increased viscous behaviour after ageing compared to the increased elastic behaviour found for unmodified bitumens.

# Acknowledgements

I would like to thank all those who have provided the assistance, advice, encouragement and funding without which this research would not have been possible.

I wish, particularly, to thank the following persons and organisations:

- Professor S.F. Brown, my supervisor, for his guidance and advice throughout the research period notwithstanding his own heavy workload.
- The European Commission who have provided the financial support for the Brite Euram research project entitled "Quality Analysis of Polymer Modified Bitumen Products by Microscopy Image Analysis with Fluorescent Light" which included part of the research work undertaken in this thesis.
- The partners involved in the Brite Euram project at the Danish Road Institute, Dansk Vejteknologi Ramboll, Jean Lefebvre, Ooms Avenhorn b.v., G.M. Idorn Ramboll and the French Building Research Institute (CSTB), particularly B. Brule, M. Maze, S. Gazeau, R. van Rooijen, J. Sundahl and V. Wegan.
- Ooms Avenhorn b.v. and Jean Lefebvre for the supply of the materials tested in this thesis and Ooms Avenhorn b.v. and Dansk Vejteknologi for the rolling thin film oven (RTFO) and pressure ageing vessel (PAV) ageing of the bitumen.
- My colleagues in the Pavement and Geotechnics Research Group at the University of Nottingham, especially Andy Collop, Barry Brodrick, Shane Malkin, Ehsan Sharegh, Paul Sanders, Hamdi Ibrahim, Nick Thom, Gerry Barnes and Gary Hayes.

# **Declaration**

The work described in this thesis was conducted at the University of Nottingham, Department of Civil Engineering between July 1994 and September 1997. I declare that the work is my own and has not been submitted for a degree of another university.

# Table of Contents

	<b>Page</b>
<b>Abstract</b> .....	i
<b>Acknowledgements</b> .....	iii
<b>Declaration</b> .....	iv
<b>Table of Contents</b> .....	v
<b>List of Figures</b> .....	x
<b>List of Tables</b> .....	xvi
<b>1 Introduction</b> .....	<b>1</b>
1.1 Background .....	1
1.2 Mechanical Properties of Bituminous Mixtures .....	2
1.3 Modification of Bitumen .....	5
1.4 Bituminous Binder Standardisation and Specifications .....	7
1.5 Objectives of Research .....	10
1.6 Scope of Research .....	13
<b>2 Literature Review</b> .....	<b>14</b>
2.1 Introduction .....	14
2.2 Bitumen Constitution (Chemical Composition) .....	15
2.2.1 Elemental Composition of Bitumen .....	15
2.2.2 Molecular Structure .....	16
2.2.3 Fractional Composition of Bitumen .....	17
2.2.4 Functionality and Polarity .....	26
2.2.5 Thermochemical Behaviour of Bitumen .....	28

	<b>page</b>
2.3	Bitumen Structure . . . . . 30
2.3.1	Colloidal Model . . . . . 30
2.3.2	SHRP Microstructural Model . . . . . 31
2.4	Bitumen Rheology . . . . . 32
2.4.1	Definition of Rheology . . . . . 32
2.4.2	Conventional Physical Property Tests . . . . . 33
2.4.3	Viscoelastic Behaviour of Bitumen . . . . . 37
2.4.4	Dynamic Mechanical Analysis . . . . . 47
2.4.5	Time-Temperature Superposition Principle . . . . . 57
2.4.6	Rheological Data Representation . . . . . 66
2.4.7	Rheological Models . . . . . 67
2.4.8	SHRP Binder Specification . . . . . 69
2.5	Bitumen Ageing . . . . . 70
2.6	Bitumen Modification . . . . . 75
2.6.1	Reclaimed Rubber Products . . . . . 76
2.6.2	Fillers . . . . . 77
2.6.3	Fibres . . . . . 77
2.6.4	Catalysts (Organo-Manganese Compounds) . . . . . 77
2.6.5	Extenders (Sulphur Addition) . . . . . 78
2.6.6	Polymer Modified Bitumens . . . . . 78
2.6.7	Fluorescent Microscopy . . . . . 82
2.7	Summary . . . . . 84
<b>3</b>	<b>Bitumen Rheology Testing Procedure . . . . . 87</b>
3.1	Introduction . . . . . 87
3.2	Dynamic Shear Rheometry . . . . . 89
3.3	Factors Affecting DSR Rheological Testing . . . . . 91
3.3.1	Temperature . . . . . 91

	page
3.3.2 Strain Amplitude, Stress Level and Frequency of Oscillation .....	93
3.3.3 Sample Preparation and Geometry .....	94
3.4 Repeatability of DSR Rheological Testing .....	102
3.5 Discussion .....	110
3.6 Conclusions .....	111

<b>4 The Rheological Characteristics of Polymer Modified Bitumens .....</b>	<b>113</b>
4.1 Introduction .....	113
4.2 Experimental Design .....	114
4.2.1 Materials .....	114
4.2.2 Testing Programme .....	116
4.3 Chemical Analysis of Polymer Modified Bitumens .....	118
4.3.1 Differential Scanning Calorimetry of EVA PMB's .....	118
4.3.2 High Performance Gel Permeation Chromatography of SBS PMB's .....	121
4.4 Conventional Physical Property Tests .....	121
4.4.1 Penetration and Softening Point .....	121
4.4.2 DSC Enthalpy Correlation .....	125
4.4.3 Temperature Susceptibility .....	126
4.5 Viscosity Testing .....	127
4.5.1 High Temperature Viscosity Analysis .....	127
4.5.2 Bitumen Test Data Chart .....	129
4.5.3 Zero Shear Viscosity Analysis .....	133
4.6 Dynamic Mechanical Analysis .....	140
4.6.1 Van der Poel's Nomograph .....	140
4.6.2 Complex Modulus Isochronal Plots .....	143

	<b>page</b>
4.6.3	Phase Angle Isochronal Plots . . . . . 147
4.6.4	Complex Modulus Master Curves . . . . . 150
4.6.5	Phase Angle Master Curves . . . . . 153
4.6.6	Black Diagrams . . . . . 159
4.6.7	Cole-Cole Diagrams . . . . . 163
4.7	Discussion . . . . . 163
4.8	Conclusions . . . . . 170

**5 Rheological Characteristics of Aged Unmodified and Polymer Modified Bitumens . . . . . 171**

5.1	Introduction . . . . . 171
5.2	Experimental Design . . . . . 172
5.2.1	Materials . . . . . 172
5.2.2	Testing Programme . . . . . 173
5.3	Penetration Grade Bitumen . . . . . 175
5.3.1	Chemical Characterisation of the Effect of Ageing . . . . . 175
5.3.2	Conventional Empirical Tests . . . . . 179
5.3.3	Dynamic Mechanical Analysis . . . . . 180
5.3.4	Discussion . . . . . 184
5.4	Semi-crystalline Polymer Modified Bitumen . . . . . 186
5.4.1	Differential Scanning Calorimetry Analysis of the Effect of Ageing . . . . . 186
5.4.2	Conventional Tests . . . . . 188
5.4.3	Dynamic Mechanical Analysis . . . . . 189
5.4.4	Discussion . . . . . 204
5.5	Elastomeric Polymer Modified Bitumen . . . . . 206
5.5.1	Chemical Characterisation of the Effect of Ageing . . . . . 206
5.5.2	Conventional Tests . . . . . 209

	<b>page</b>
5.5.3 Dynamic Mechanical Analysis .....	209
5.5.4 Discussion .....	221
5.6 Conclusions .....	222
<b>6 Discussion, Conclusions and Recommendations for Future Research .....</b>	<b>224</b>
6.1 Discussion .....	224
6.2 Conclusions .....	231
6.3 Recommendations for Future Research .....	236
<b>References .....</b>	<b>240</b>
<b>Appendix A - DSR Testing Protocol</b>	
<b>Appendix B - DSR Data for Unaged Bitumens and PMB's</b>	
<b>Appendix C - DSR Data for RTFOT and PAV Aged Bitumens and PMB's</b>	
<b>Appendix D - DSR Data for Unaged, RTFOT and PAV Aged Sealoflex PMB</b>	



# List of Figures

	<b>Page</b>
Figure 2.1: Types of molecules found in bitumen .....	17
Figure 2.2: Non-linear behaviour of bitumen .....	36
Figure 2.3: Viscoelastic response to an applied load .....	37
Figure 2.4: Viscoelastic response of bitumen under creep loading .....	38
Figure 2.5: Linear viscoelastic response of bitumen .....	39
Figure 2.6: Nomograph for determining the stiffness modulus of bitumens ....	46
Figure 2.7: Dynamic oscillatory stress-strain functions .....	50
Figure 2.8: Dynamic test outputs from dynamic mechanical analysis (DMA) ..	50
Figure 2.9: Relationship between complex modulus, storage modulus, loss modulus and phase angle .....	52
Figure 2.10: Dynamic Shear Rheometer testing geometry .....	56
Figure 2.11: Time-temperature superposition principle .....	58
Figure 2.12: Time-temperature superposition in the construction of a master curve .....	62
Figure 2.13: Typical complex modulus master curve for bitumen .....	62
Figure 2.14: Changes in fractional chemical composition as a function of ageing .....	72
Figure 2.15: EVA copolymer structure .....	79
Figure 2.16: SBS copolymer structure .....	81
Figure 3.1: Principles of operation of torsional-type Dynamic Shear Rheometers .....	89
Figure 3.2: Definitions of stiffness moduli from dynamic shear rheometry tests .....	90
Figure 3.3: Viscoelastic behaviour of bitumen .....	90
Figure 3.4: Testing arrangement in Dynamic Shear Rheometer .....	92

Figure 3.5:	Strain sweeps used to determine linear region . . . . .	94
Figure 3.6:	Isothermal plot of complex modulus for Middle East 80/100 pen . .	98
Figure 3.7:	Isothermal plot of phase angle for Middle East 80/100 pen . . . . .	98
Figure 3.8:	Isochronal plot at 0.02 Hz for Middle East 80/100 pen . . . . .	100
Figure 3.9:	Isochronal plot at 10 Hz for Middle East 80/100 pen . . . . .	100
Figure 3.10:	Black diagram for Middle East 80/100 pen . . . . .	101
Figure 3.11:	Complex modulus versus $\log(1 + \tan\delta)$ for Middle East 80/100 pen . . . . .	101
Figure 3.12:	Isochronal plot at 10 Hz for 7% EVA - Russian 80 pen . . . . .	103
Figure 3.13:	Black diagram for 7% EVA - Russian 80 pen . . . . .	103
Figure 3.14:	Isochronal plot at 10 Hz for 7% SBS - Russian 80 pen . . . . .	104
Figure 3.15:	Black diagram for 7% SBS - Russian 80 pen . . . . .	104
Figure 3.16:	Isothermal plot of complex modulus for repeatability study . . . . .	106
Figure 3.17:	Isothermal plot of phase angle for repeatability study . . . . .	106
Figure 3.18:	Histogram of repeatability study for complex modulus . . . . .	108
Figure 3.19:	Histogram of repeatability study for phase angle . . . . .	108
Figure 4.1:	DSC plot for Venezuelan - EVA PMB's . . . . .	120
Figure 4.2:	HP-GPC plot for Venezuelan - SBS PMB's . . . . .	120
Figure 4.3:	Modification indices for Penetrations of PMB's . . . . .	123
Figure 4.4:	Modification indices for Softening Points of PMB's . . . . .	123
Figure 4.5:	Relationship between Softening Point modification indices and DSC enthalpy . . . . .	125
Figure 4.6:	High temperature viscosity for Russian PMB's . . . . .	128
Figure 4.7:	Zero shear viscosity - SHRP method for Middle East 80/100 pen .	130
Figure 4.8:	Zero shear viscosity - Puzinauskas method for Middle East 80/100 pen . . . . .	130
Figure 4.9:	Zero shear viscosity - SHRP method for 7% EVA - Russian 80 pen . . . . .	132

	<b>page</b>
Figure 4.10: Zero shear viscosity - SHRP method for 7% SBS - Russian 80 pen .....	132
Figure 4.11: BTDC for Russian - EVA PMB .....	134
Figure 4.12: BTDC for Russian - SBS PMB .....	134
Figure 4.13: Viscosity-temperature plot for Middle East - EVA PMB's .....	135
Figure 4.14: Viscosity-temperature plot for Russian PMB's .....	135
Figure 4.15: Viscosity-temperature plot for Venezuelan PMB's .....	136
Figure 4.16: Modification indices for viscosity for Middle East PMB's .....	138
Figure 4.17: Modification indices for viscosity for Russian PMB's .....	138
Figure 4.18: Modification indices for viscosity for Venezuelan PMB's .....	139
Figure 4.19: G* versus van der Poel's stiffness for Middle East - EVA PMB's ..	141
Figure 4.20: G* versus van der Poel's stiffness for Russian - EVA PMB's .....	142
Figure 4.21: Complex modulus isochronal plot at 0.02 Hz for Russian PMB's ..	144
Figure 4.22: Complex modulus isochronal plot at 1 Hz for Russian PMB's .....	144
Figure 4.23: Modification indices for complex modulus at 0.02 Hz for Russian PMB's .....	146
Figure 4.24: Modification indices for complex modulus at 1 Hz for Russian PMB's .....	146
Figure 4.25: Complex modulus at 0.1 Hz for EVA copolymer and Russian 80 pen .....	147
Figure 4.26: Phase angle isochronal plot at 0.02 Hz for Russian PMB's .....	148
Figure 4.27: Phase angle isochronal plot at 1 Hz for Russian PMB's .....	148
Figure 4.28: Phase angles at 0.1 Hz for EVA copolymer and Russian 80 pen ..	149
Figure 4.29: Complex modulus master curve for Middle East - EVA PMB's ...	151
Figure 4.30: Complex modulus master curve for Russian - EVA PMB's .....	151
Figure 4.31: Complex modulus master curve for Venezuelan - EVA PMB's ...	152
Figure 4.32: Complex modulus master curve for 7% EVA - Russian PMB .....	152
Figure 4.33: Complex modulus master curve for Russian - SBS PMB's .....	154
Figure 4.34: Complex modulus master curve for Venezuelan - SBS PMB's .....	154

	<b>page</b>
Figure 4.35: Complex modulus master curve for 7% SBS - Russian PMB . . . . .	155
Figure 4.36: Phase angle master curve for Middle East - EVA PMB's . . . . .	155
Figure 4.37: Phase angle master curve for Russian - EVA PMB's . . . . .	156
Figure 4.38: Phase angle master curve for Venezuelan - EVA PMB's . . . . .	156
Figure 4.39: Phase angle master curve for Russian - SBS PMB's . . . . .	158
Figure 4.40: Phase angle master curve for Venezuelan - SBS PMB's . . . . .	158
Figure 4.41: Black diagram for Middle East - EVA PMB's . . . . .	160
Figure 4.42: Black diagram for Russian - EVA PMB's . . . . .	160
Figure 4.43: Black diagram for Venezuelan - EVA PMB's . . . . .	161
Figure 4.44: Black diagram for Russian - SBS PMB's . . . . .	161
Figure 4.45: Black diagram for Venezuelan - SBS PMB's . . . . .	162
Figure 4.46: Cole-Cole diagram for Middle East - EVA PMB's . . . . .	162
Figure 4.47: Cole-Cole diagram for Russian - EVA PMB's . . . . .	164
Figure 4.48: Cole-Cole diagram for Venezuelan - EVA PMB's . . . . .	164
Figure 4.49: Cole-Cole diagram for Russian - SBS PMB's . . . . .	165
Figure 4.50: Cole-Cole diagram for Venezuelan - SBS PMB's . . . . .	165
Figure 4.51: Deformation versus number of loading cycles for rheological analysis and fundamental testing . . . . .	169
Figure 5.1: HP-GPC molecular size parameters . . . . .	175
Figure 5.2: Complex modulus master curve for Russian 80 pen bitumen . . . . .	181
Figure 5.3: Phase angle master curve for Russian 80 pen bitumen . . . . .	181
Figure 5.4: Isochronal plot at 0.02 Hz for Venezuelan 70/100 pen bitumen . . .	183
Figure 5.5: Isochronal plot at 1 Hz for Venezuelan 70/100 pen bitumen . . . . .	183
Figure 5.6: Black diagram for Venezuelan 70/100 pen bitumen . . . . .	185
Figure 5.7: Cole-Cole diagram for Russian 80 pen bitumen . . . . .	185
Figure 5.8: DSC plots for 5% EVA with 95% Venezuelan 70/100 pen bitumen . . . . .	186
Figure 5.9: Complex modulus master curve for 7% EVA - Russian 80 pen . . .	191
Figure 5.10: Phase angle master curve for 7% EVA - Russian 80 pen . . . . .	191

Figure 5.11:	Isochronal plot at 0.02 Hz for 7% EVA - Russian 80 pen . . . . .	192
Figure 5.12:	Isochronal plot at 1 Hz for 7% EVA - Russian 80 pen . . . . .	194
Figure 5.13:	Black diagram for 7% EVA - Russian 80 pen . . . . .	194
Figure 5.14:	Complex modulus master curve for 7% EVA - Venezuelan 70/100 pen . . . . .	197
Figure 5.15:	Phase angle master curve for 7% EVA - Venezuelan 70/100 pen . .	197
Figure 5.16:	Isochronal plot at 0.02 Hz for 7% EVA - Venezuelan 70/100 pen .	199
Figure 5.17:	Isochronal plot at 1 Hz for 7% EVA - Venezuelan 70/100 pen . . .	199
Figure 5.18:	Black diagram for 7% EVA - Venezuelan 70/100 pen . . . . .	200
Figure 5.19:	Complex modulus master curve for 7% EVA - Middle East 80/100 pen . . . . .	201
Figure 5.20:	Phase angle master curve for 7% EVA - Middle East 80/100 pen .	201
Figure 5.21:	Isochronal plot at 0.02 Hz for 7% EVA - Middle East 80/100 pen . . . . .	203
Figure 5.22:	Isochronal plot at 1 Hz for 7% EVA - Middle East 80/100 pen . . .	203
Figure 5.23:	Black diagram for 7% EVA - Middle East 80/100 pen . . . . .	204
Figure 5.24:	FTIR analysis of aged SBS PMB's . . . . .	207
Figure 5.25:	HP-GPC plots for 7% SBS with 93% Venezuelan 70/100 pen bitumen . . . . .	208
Figure 5.26:	Complex modulus master curve for 7% SBS - Russian 80 pen . . . .	212
Figure 5.27:	Phase angle master curve for 7% SBS - Russian 80 pen . . . . .	212
Figure 5.28:	Cole-Cole diagram for 7% SBS - Russian 80 pen . . . . .	214
Figure 5.29:	Isochronal plot at 0.02 Hz for 7% SBS - Russian 80 pen . . . . .	214
Figure 5.30:	Isochronal plot at 1 Hz for 7% SBS - Russian 80 pen . . . . .	216
Figure 5.31:	Black diagram for 7% SBS - Russian 80 pen . . . . .	216
Figure 5.32:	Complex modulus master curve for 7% SBS - Venezuelan 70/100 pen . . . . .	218
Figure 5.33:	Phase angle master curve for 7% SBS - Venezuelan 70/100 pen . .	218
Figure 5.34:	Isochronal plot at 0.02 Hz for 7% SBS - Venezuelan 70/100 pen . .	220

	<b>page</b>
Figure 5.35: Isochronal plot at 1 Hz for 7% SBS - Venezuelan 70/100 pen . . . .	220
Figure 5.36: Black diagram for 7% SBS - Venezuelan 70/100 pen . . . . .	221
Figure 6.1: Complex modulus master curve for Sealoflex . . . . .	228
Figure 6.2: Isochronal plot at 1 Hz for Sealoflex . . . . .	228
Figure 6.3: Isochronal plot at 0.02 Hz for unaged, RTFOT and PAV aged Sealoflex . . . . .	229
Figure 6.4: Isochronal plot at 1 Hz for unaged, RTFOT and PAV aged Sealoflex . . . . .	230
Figure 6.5: Black diagram for unaged, RTFOT and PAV aged Sealoflex . . . . .	230

# List of Tables

	<b>Page</b>
Table 2.1: Penetration and viscosity graded bitumens . . . . .	33
Table 3.1: Suggested disk diameters for DSR rheology testing . . . . .	95
Table 3.2: SHRP suggested disk diameters for DSR rheology testing . . . . .	95
Table 3.3: DSR test conditions for sample geometry . . . . .	97
Table 3.4: SHRP fatigue parameter, $G^* \sin \delta$ for the 25 mm and 8 mm configurations . . . . .	97
Table 3.5: Percentage variation of complex modulus with regard to DSR measuring equipment and transducers . . . . .	105
Table 3.6: Percentage variation of phase angle with regard to DSR measuring equipment and transducers . . . . .	107
Table 3.7: Percentage variation of complex modulus for Bohlin DSR50 . . . . .	109
Table 3.8: Percentage variation of phase angle for Bohlin DSR50 . . . . .	109
Table 4.1: SARA analysis of base bitumens . . . . .	114
Table 4.2: Empirical test data for base bitumens . . . . .	115
Table 4.3: Variations in DSC parameters due to modification of EVA PMB's . . . . .	119
Table 4.4: Penetration and Softening Point for PMB's . . . . .	122
Table 4.5: Temperature susceptibility of PMB's as measured by PI . . . . .	126
Table 4.6: Zero shear viscosities, $\eta_0$ , for Middle East 80/100 pen bitumen . . . . .	129
Table 4.7: Superpave upper temperature PG grading . . . . .	169
Table 5.1: Changes in chemical composition due to ageing . . . . .	176
Table 5.2: Increase in oxidative products during ageing . . . . .	177
Table 5.3: Changes in HP-GPC molecular size parameters due to ageing . . . . .	178
Table 5.4: Changes in conventional test data due to ageing . . . . .	179
Table 5.5: Changes in complex modulus and phase angle due to ageing . . . . .	182
Table 5.6: Variations in DSC parameters due to ageing for EVA PMB's . . . . .	187

		page
Table 5.7:	Changes in conventional test data due to ageing for EVA PMB's ..	188
Table 5.8:	Complex modulus ageing indices for EVA PMB's .....	190
Table 5.9:	Phase angles for unaged, RTFOT and PAV aged Russian - EVA PMB's .....	193
Table 5.10:	Phase angles for unaged, RTFOT and PAV aged Venezuelan - EVA PMB's .....	198
Table 5.11:	Phase angles for unaged, RTFOT and PAV aged Middle East - EVA PMB's .....	202
Table 5.12:	Increase in oxidative products during ageing for SBS PMB's .....	206
Table 5.13:	Changes in conventional test data due to ageing for SBS PMB's ..	209
Table 5.14:	Complex modulus ageing indices for SBS PMB's .....	210
Table 5.15:	Phase angles for unaged, RTFOT and PAV aged Russian - SBS PMB's .....	213
Table 5.16:	Phase angles for unaged, RTFOT and PAV aged Venezuelan - SBS PMB's .....	219



# 1 Introduction

## 1.1 Background

The term “bitumen” originated in Sanskrit, where the words “jatu” meaning pitch and “jatu-krit” meaning pitch creating, referred to the pitch produced by some resinous trees. The Latin equivalent is claimed to be originally “gwitu-men” or “pixtu-men”, which was subsequently shortened to “bitumen” when passing via French to English [1].

The origins of bitumen as an engineering material date from 3800 to 3000 B.C. when surface seepages of “natural” bitumen were used as mortar for masonry and water proofing in the Euphrates and Indus Valleys [2]. In the middle of 19th century attempts were made to utilise rock asphalt from European deposits for road surfacing and from this there was a slow development of the use of natural products for this purpose, followed by the advent of coal tar and later of bitumen manufactured from crude oil.

Although “natural” bitumens, such as Trinidad Lake Asphalt, are still used, most present day applications make use of bitumen manufactured from crude oil. The manufacturing of bitumen from crude oil involves the processes of distillation, blowing and blending. The crude oil, which is a complex mixture of hydrocarbons of different molecular weight, is refined by fractional distillation to separate gas, gasoline, kerosine, gas oil and long residue (heaviest fraction consisting of a complex mixture of high molecular weight hydrocarbons). The long residue is then further distilled under vacuum at 350°C to 400°C to produce short residue, which is the feedstock used in the manufacturing of different grades of bitumen. The physical properties of the short residue may be further modified by processes such as air ratification (blowing) or blending of different short residues.

The four principal crude oil producing areas in the world are the U.S.A., the Middle East, the Caribbean countries and Russia. Crude oils differ in both their physical and chemical properties. Physically, they range from viscous black liquids to free-flowing straw

coloured liquids. Chemically, they may be predominantly paraffinic, naphthenic or aromatic, with combinations of the first two being common [1]. Heavy crudes contain a much smaller proportion of volatile matter than lighter crudes and contain more of the heteroatoms nitrogen, sulphur, oxygen and metals. Heavy crudes also tend to be more naphthenic and aromatic compared to the lighter crudes which tend to be more paraffinic [3]. This makes them difficult to process and the bitumens obtained from these crudes may need to be produced by solvent precipitation processes rather than normal distillation processes.

Although bitumen can be used for a wide variety of applications, the principal use is for road building and, to a lesser extent, airfield pavements which, together, account for approximately 85% of the worldwide consumption of bitumen [4]. In 1994, over fifty million tonnes of bitumen was used for road building with most of the roads being in the United States and Europe. The use of bitumen in combination with mineral aggregate to form an asphalt mixture results in a road construction material that not only has good qualities as a surfacing layer but, when correctly designed, provides the structural component layer of flexible pavement construction. In 1993, 31 million tonnes of bituminous material and approximately 2 million tonnes of bitumen were used in road construction and maintenance in the United Kingdom compared to the total road paving demand of ready-mixed concrete of approximately 6 million tonnes [5]. Based on these statistics it can be concluded that bitumen is not only an important engineering material but also a vital component in pavement engineering.

## **1.2 Mechanical Properties of Bituminous Mixtures**

The analytical approach to the design of pavements requires the consideration of two material property aspects. Firstly, the load-deformation or stress-strain characteristics which are used in the analysis procedure to calculate the stresses and strains in the pavement structure and generally consist of the elastic stiffness and Poisson's ratio of the materials. And, secondly, the performance characteristics of the materials which determine the likely mode of failure. The two primary structural distress modes for

pavement layers are (1) fatigue cracking of the bound layers, such as the asphalt layers and (2) excessive permanent deformation (rutting) of both the bound and unbound material layers.

The mechanical properties of bituminous mixtures are strongly dependent upon the properties of the binder and the volumetric proportions of the three mixture components of aggregate, bitumen and air voids. Bitumens are thermoplastic materials that behave like glass at low temperatures, in that they are very elastic and brittle, and like a fluid at very high temperatures, in that they possess the ability to flow when subjected to shear loading. At moderate temperatures they behave in a viscoelastic manner, possessing both elastic and viscous properties, the relative proportion depending on many factors but dominated by temperature and rate of loading. It is this fundamental rheological property of bitumens that makes them versatile binders for paving mixtures and, therefore, widely used as such in virtually all of the habitable climates found on earth.

The basic parameters used for the characterisation of the volumetric composition of an asphalt mixture are the binder content and air void content. For asphalt mixture design purposes, the analysis of the volumetric proportions serves as a first screening of the mix formulation. However, for a complete evaluation of the performance of the asphalt mixture, the following mechanical properties of elastic stiffness, resistance to fatigue and thermal cracking, and resistance to permanent deformation are of paramount importance. In addition, the asphalt mixture must be durable, being able to exist for a long period of time without significant deterioration of the above mechanical properties.

The elastic stiffness of a bituminous mixture indicates its ability to spread loads and protect the underlying layers by distributing the wheel loads and influencing the traffic induced stresses and strains throughout the pavement. The rate of loading, corresponding to vehicle speeds, and temperature affect the elastic stiffness of the asphalt material. The stress-strain characteristic of an asphalt mixture is essentially elastic for short loading times, but long loading times and high temperatures lead to a viscous response, characterised by low stiffness and permanent deformation problems.

Fatigue resistance of an asphalt mixture is the ability of the mixture to withstand repeated bending without fracture. Fatigue is one of the common forms of distress in asphalt pavements and manifests itself in the form of cracking under repeated traffic loading. Fatigue failure of asphalt pavements is defined as the number of loading cycles a pavement can withstand before fracture (cracking) occurs, with the criteria for fatigue cracking generally being accepted as the maximum tensile strain on the underside of the bituminous layer [6]. Although tensile strain is the parameter that controls the initiation of fatigue cracks, their subsequent propagation is controlled by tensile stress at the crack tip [7].

Permanent deformation of asphalt pavements is a phenomenon caused by the repeated passage of heavily loaded vehicles under conditions of high road temperatures. The permanent deformation develops primarily through shear displacement [8,9], though there may be a degree of densification under traffic, particularly in pavements which are not adequately compacted during construction.

Rutting has always been one of the primary problems that engineers have associated with asphalt pavements but, in recent years, rutting, caused by increased axle loads and traffic densities, has become the major reason why asphalt pavements lose their smoothness and serviceability, leading to premature replacement. To combat the rutting problem, highway engineers have tried using leaner, stiffer mixtures but this has generally resulted in more failures from fatigue cracking.

Low temperature thermal cracking is attributed to tensile stresses induced in the asphalt pavement as the temperature drops to an extremely low temperature [10]. These tensile stresses develop as a result of the tendency of the pavement to contract at extremely low temperatures. The friction between the pavement and the base layer resists this contraction and if the tensile stress induced in the pavement equals the strength of the asphalt mixture, at that temperature, micro-cracking will develop at the edge and surface of the pavement. Under repeated temperature cycles, the transverse crack will penetrate the full depth of the asphalt pavement. Several factors influence thermal cracking, such

as material, environment and pavement structural geometry. However, the single most important factor that affects the degree of thermal cracking in an asphalt mixture is the temperature-stiffness relationship of the bitumen.

Although durability is not a mechanical property, an asphalt mixture will not retain its mechanical properties in the long term unless the mixture is durable. The durability of bituminous mixtures is defined as their resistance to damage caused by environmental factors. There are many factors that affect durability, such as the chemical composition of the bitumen, the type and grading of the aggregate, the interaction between the bitumen and the aggregate, bitumen content, mixture permeability, construction practice and climate. However, the two primary factors that affect durability are, firstly, the embrittlement of the bitumen due to age hardening and, secondly, water damage of the asphalt mixture [11].

### **1.3 Modification of Bitumen**

The consensus from the Eurasphalt & Eurobitume Congress held in Strasbourg, France in May 1996 is that conventional binders cannot totally fulfill the greater demands presently being placed upon asphalt pavements [12]. Asphalt mixture performance with conventional bitumen binders seems to be hitting a performance ceiling which can only be overcome by using modified binders and, therefore, although bitumen modifiers have been used for 50 years, it is not surprising that the range and use of modified binders is increasing to meet these higher demands [13]. This increase over the last ten years can be attributed, in part, to the increased demands on asphalt pavements as a result of the significant increase in traffic volumes, traffic loads and tyre pressures leading to premature rutting of the pavement.

Bitumen modifiers are more commonly used in Europe than in the United States. Polymers have been used to modify bitumen for 20 to 30 years in Europe, particularly in France, Germany, Sweden and Italy, but only for approximately 15 years in the United States. In Europe in 1993 an average of 4% of the bitumen used in asphalt pavements was

modified, ranging from 8% in France to 0.5% in Portugal. The possible reason for the greater use of modified binders in Europe is that contracts that require contractor guarantees for hot mix asphalt (HMA) performance for several years have a greater chance of prompting the use of bitumen modifiers to obtain performance and reduce life cycle costs. Contracts requiring low initial costs as the governing factor will usually discourage modifiers with their higher initial costs, unless they are specified.

The financial benefits of bitumen modification can, therefore, only be appreciated once whole life costing of the road construction is undertaken. Heavily trafficked roads, such as motorways, or roads with difficult access for maintenance, will generally benefit from bitumen modification and the enhanced asphalt mixture performance. In these cases, the combination of higher initial costs and lower maintenance costs tends to provide a more cost effective solution than the low initial costs and increased maintenance requirements of an unmodified asphalt mixture.

A major market requirement is that premium bitumens, such as modified bitumens, must maintain all the existing benefits of asphalt pavements as well as giving additional benefits. A better performance in one particular property at the expense of other important properties or at the expense of Health and Safety Executive (HSE) considerations is, therefore, not desirable.

During the last decade a lot of research work has been carried out on polymer modified bitumens (PMB's) and asphalt mixtures (PMA's). The potential value of PMB's is that polymers can significantly improve the performance of asphalt mixtures and substantially increase the service life of highway surfaces. Specifically, the addition of polymers significantly improves various bitumen properties, such as elasticity, cohesion, stiffness and adhesive, resulting in a substantial improvement in the performance and quality of asphalt pavements with the asphalt mixture being more stable at warmer temperatures and more flexible at colder temperatures. In addition to rutting resistance, a premium polymer can provide a degree of flexibility or elasticity to an asphalt mixture, thereby improving the fatigue and thermal cracking characteristics of the mixture.

The benefits of polymer modification have been reported in many papers. However, modification of bitumen with polymers requires a sound understanding of the interrelationship of the bitumen and the polymer. Inappropriate bitumen/polymer blends may not result in improved performance of the asphalt mixture. In addition, the use of polymers may result in stiffer and harsher asphalt mixtures which are going to be more difficult to handle during manufacturing, transporting, placement and compaction.

Polymer modification is not the only way to improve binder performance. Extra-hard bitumens are widely used with high stiffness and therefore an advantage in load distribution in the pavement structure. Multi-grade binders are another emerging binder type where the good low temperature properties of a softer bitumen and the deformation resistance of a harder bitumen are combined.

## **1.4 Bituminous Binder Standardisation and Specifications**

Historically, empirical binder properties have been used to provide an indication of the performance of asphalt mixtures. For example, Softening Point has been used to predict the permanent deformation resistance of the pavement at high service temperatures and Fraass breaking point has been used as a performance indicator of low temperature brittle fracture of the pavement.

With the advent of higher axle loads and increasing traffic volumes, there has been an increase in the use of PMB's and other specialised binders. Such modification may significantly alter the rheological properties of the binder, which are not necessarily characterised by conventional, empirical binder properties. This has led to an increasing interest in the use of fundamental rheological parameters to specify bituminous binders. In the USA, the Strategic Highway Research Programme (SHRP) has developed specifications which classify the grade of bitumen on the basis of its performance in a number of rheological tests [14].

In the UK, new specifications for modified binders in both hot rolled asphalt (HRA)

wearing course and surface dressing also require rheological measurements and it is proposed that rheological data will be required for all road applications. The specification (Highways Agency Clause 943) is still in draft but some contracts already request rheological information for both applications. The draft specifications, once finalised, will eventually be adopted in the Specifications for Highways Works where the data required will consist of measurements of the shear stiffness of the binder as a function of frequency and temperature [15].

### **European Committee for Standardisation (CEN) Approach**

The standardisation and characterisation of bituminous binders are prepared by the Technical Committee (TC) for bituminous binders dealing with oil products (TC 19). This TC is divided into five groups, each corresponding to a Working Group (WG) for pure bitumen, cut-back and fluxed bitumen, emulsions, modified bitumen and industrial grade bitumen.

The primary goal of CEN is to harmonize existing standards in Europe in order to eliminate trade barriers. Therefore, the CEN working group, WG1, which deals with paving grade bitumen, has proposed a European specification based on traditional and commonly used methods. The intention of this specification is to control the equality of bituminous binders by well known traditional methods

The CEN specification for paving grade bitumen is focused on a Ring and Ball Softening Point related to the highest summer temperature. Considering this temperature and the traffic load, the required grade can be chosen. However, the grades do not take into account any variation in temperature. The other mandatory tests include the Penetration test and resistance to hardening using the Rolling Thin Film Oven Test (RTFOT) or the Rotating Flask Test. Optional tests do, to a limited extent, allow the variation of temperature to be included, with the Fraass breaking point indicating the cold temperature behaviour of the bitumen. However, several of these optional tests have been criticized for poor reliability, such as the Fraass and wax content tests. [16].



With regard to polymer modified bitumens (PMB's), the CEN specification draft [17] covers ready-to-use PMB's for hot plant mixtures and surface treatments. Except for classical methods, the only generally known national standard test for PMB's was the elastic recovery test. However, the first European workshop on the rheology of bituminous binders in Brussels in April 1995, indicated that classical, empirical test methods are unsuitable for PMB's and that PMB standardisation should be rheologically based. Unfortunately, such methods have not yet been implemented on a routine basis and consequently, at present, a performance related specification for PMB's based on fundamental properties is not possible.

### **Strategic Highway Research Program (SHRP) Approach**

As compared to the CEN specification, SHRP follows a completely different approach leading to a Performance Graded (PG) binder classification as part of the Superpave system [14]. The Superpave system is the culmination of five years and \$50 million of research effort in bitumen and asphalt materials. The binder specification section of the Superpave system incorporates a number of new and adopted test procedures to measure the physical properties over the complete range of the binder service life. The condition of the bitumen is simulated at various stages of its service life with the test temperatures being related to those in the field and the binder being thermally treated before testing to simulate the ageing caused by mixing, paving and service life. The test procedures evaluate the ability of the binder to do its part in preventing the three critical distresses of asphalt pavements: rutting, fatigue cracking and low temperature cracking.

The rutting and fatigue performance of the binder are determined by measuring the shear stiffness and viscoelastic balance of the bitumen using a Dynamic Shear Rheometer (DSR). The thermal cracking resistance of the binder is determined by measuring the bending stiffness of the bitumen in the Bending Beam Rheometer (BBR).

At present there is no equivalent to the DSR in the CEN specifications. Although, the Penetration and Softening Point can be considered as empirical viscosity or stiffness values, they are only suitable for paving grade bitumen and not for PMB's. The BBR can

be considered as a functional equivalent to the Fraass test. Both tests are executed at low temperatures and intended to prevent thermal cracking, although the Fraass is a breaking test whereas the BBR is a bending test. The BBR and the additional low temperature SHRP Direct Tension Test (DTT), which is a breaking test, can be considered as future replacements for Fraass in future CEN standards.

Although the SHRP specification has the advantage of incorporating the fundamental properties of the material, the method still lacks practical experience on a broad basis and the applicability of the rutting, fatigue and thermal cracking parameters to special materials, such as PMB's.

## **1.5 Objectives of Research**

Greater use is being made of modified bituminous binders to improve the performance of flexible pavements and, therefore, there is an universal need to have laboratory tests for both binders and mixtures that reliably predict field performance. Although PMB's have been used to enhance the performance of asphalt mixtures for 30 years, it is only recently that there have been the means of performing fundamental rheological characterisation of PMB's in order to provide a better understanding of their behaviour.

The DSR is one such means that can be used to determine the rheological characteristics of bitumens over a wide range of temperature and loading rate conditions. However, the use of the DSR is still in its infancy when compared with well established measurements such as Penetration, Softening Point and viscosity. These conventional tests recognise the importance of closely controlled conditions and appropriate calibration to obtain reproducible and comprehensive results, particularly for specification purposes. In contrast, the rheological properties obtained with the DSR, still require considerable research effort to overcome the uncertainties, contradictions and blind alleys associated with fundamental rheological testing. The first European workshop on the rheology of bituminous binders and the Eurasphalt and Eurobitume Congress have shown that there is continued development of analytical techniques and rheological testing methods which

will provide a means of obtaining a better understanding of the contribution of modifiers and special binders to the field of asphalt technology.

The SHRP proposals represented an undoubted advance in putting forward a global framework for assessing the properties of bituminous binders related to the in-service performance of bituminous mixtures. With Superpave, bitumen is now an engineered product and no longer simply a by-product of the refining operation. Research over the past few years, however, has shown the need not only to assess the value of these proposals but also to explore other concepts and approaches before finalising specifications.

With regard to precision, a statistical evaluation of the DSR test, undertaken by Anderson [18] and using various plate diameters and test temperatures, has concluded that measurements of  $G^*$  are still more variable than desired while phase angle measurements are very repeatable. The fundamental rheological binder equipment is also significantly more expensive than the traditional equipment used prior to Superpave.

The research in this thesis is concerned with three areas:

- The laboratory techniques associated with the testing geometry and procedure used with dynamic shear rheological testing of bitumens and PMB's,
- The applicability of conventional empirically based tests and fundamental dynamic shear tests at describing the rheological characteristics of bitumens and PMB's, and
- Explanation of the ageing mechanisms associated with the changes in the rheological characteristics of aged bitumens and PMB's.

Although the Dynamic Mechanical Analysis (DMA) [19,20] procedure is now well known with various pieces of standard DSR equipment and testing methods, there is still limited guidance of how to evaluate and quantify the rheological data with regard to the screening of possibly unrealistic or misleading results. Research into the practical

limitations associated with DSR testing, with different testing configurations, testing parameters and materials, should help to lessen the uncertainties associated with this relatively new piece of rheological testing equipment.

Although, DMA has been widely used to test the rheological characteristics of paving grade bitumens, Philipps [21] has found that for unmodified bitumens, conventional tests plus van der Poel's empirically based bitumen stiffness model [22] can provide the same type of rheological information as the Superpave tests. The main advantage of DMA would, therefore, seem to be in the evaluation of PMB's where Penetration, Softening Point and van der Poel's model are not applicable.

The CEN specifications for paving grade bitumens are, at present, still empirically based with the first stage PMB specification only applicable as a quick characterisation for product control of the binder. A second step is, therefore, urgently needed and should be based on fundamental rheological properties as proposed by SHRP. However, the fact that at present empirical tests, such as Penetration and Softening Point, will still be used for PMB's, necessitates a critical evaluation of the suitability and limitations of the different testing methods, empirical and fundamental, at accurately describing the rheological characteristics of various types of PMB's at different levels of modification.

The last area of the thesis is concerned with the ageing of PMB's and the potential to evaluate this ageing by means of DMA. Although the rheological and chemical changes associated with the ageing of unmodified paving grade bitumens (oxidation of the bitumen components leading to the hardening of the bitumen) are well known and understood, these changes are not fully understood for PMB's. An understanding of the ageing mechanisms of PMB's would reduce the risk and uncertainty associated with their use.

## 1.6 Scope of Research

The scope of the thesis consists of a literature review followed by three chapters, each focusing on one of the three objectives of the thesis, and finally a chapter presenting the final discussions, conclusions and recommendations for future research work.

The literature review summarises the principal findings with regard to the chemical constitution, physical structure, physical properties and rheological characteristics of bitumen. The literature review also presents information on bitumen ageing and briefly describes various forms of bitumen modification, most specifically polymer modification. The three main chapters of the thesis address the topics of practicality of conducting DSR testing, rheological characteristics of polymer modified bitumens as measured by conventional and fundamental test methods and rheological changes associated with the ageing of unmodified and polymer modified bitumens. The research in this thesis emphasises the use of fundamental rather than traditional, empirically based binder testing methods at quantifying the rheological characteristics of unmodified and polymer modified bitumens.

Some of the research work undertaken in the thesis was carried out as part of a Brite Euram research project entitled "Quality Analysis of Polymer Modified Bitumen Products by Microscopy Image Analysis with Fluorescent Light". The aim of the research was to develop a quality control system for the production of polymer modified bitumens (PMB's) using fluorescent microscopy. The partners in the project were Dansk Vejteknologi Ramboll, the University of Nottingham, the Danish Road Institute, Jean Lefebvre, Ooms Avenhorn b.v. and the French Building Research Institute.

## 2 Literature Review

### 2.1 Introduction

This literature review covers specific areas that either influence or are involved in the measurement and modelling of the rheological characteristics of bitumen. The literature review begins by outlining the constitution of bitumen with regard to its elemental, molecular and fractional composition. A number of techniques that are used to determine the chemical composition of bitumen are briefly described. These techniques include liquid chromatographic separation of maltenes after asphaltene precipitation (Corbett analysis), chemical affinity (Rostler analysis), molecular size distribution by gel permeation chromatography (GPC), measurements of polar functionalities by infrared functional group analysis (IR-FGA) and carbon-and-hydrogen-type determination by nuclear magnetic resonance (NMR) methods. In addition to the fractional composition of bitumen, the literature review describes the use of differential scanning calorimetry to characterise the thermal behaviour of bitumen, as well as the colloidal and SHRP microstructural models used to explain bitumen structure.

The second section deals with the measurement of bitumen rheology, from the conventional physical property tests to more fundamental dynamic mechanical analysis. The review gives a brief description of the most commonly used conventional tests, such as Penetration, Softening Point and viscosity and a more detailed description of the viscoelastic behaviour and dynamic testing of bitumen. The equations associated with dynamic mechanical analysis are presented and explained and the Dynamic Shear Rheometer (DSR) is introduced as the preferred means of performing rheological characterisation of bitumen in subsequent chapters. Various means of analysing rheological data are described that range from the use of the time-temperature superposition principle (TTSP) and master curves to isochronal plots and Black diagrams to various rheological models.

The third section of the literature review describes the physical and chemical mechanism associated with the ageing of bitumen. This section forms the basis for understanding the ageing mechanism associated with unmodified and eventually polymer modified bitumens (PMB's). The final section deals with bitumen modification. Various modification mechanisms are briefly described and include the use of reclaimed rubber products, fillers and fibres. A detailed review is then presented for PMB's, concentrating on the use of the semi-crystalline polymer, ethylene vinyl acetate (EVA), and the thermoplastic rubber, styrene butadiene styrene (SBS).

## **2.2 Bitumen Constitution (Chemical Composition)**

### **2.2.1 Elemental Composition of Bitumen**

Bitumen is comprised of a complex mixture of organic molecules which vary widely in their composition. The molecules are comprised predominantly of hydrocarbon molecules (hydrogen and carbon), but also contain minor amounts of structurally analogous heterocyclic species<sup>1</sup> and functional groups (heteroatoms) containing sulphur, nitrogen and oxygen atoms [23,24,25]. Bitumen also contains trace quantities of metals such as vanadium, nickel, iron, magnesium and calcium which occur in the form of inorganic salts and oxides or in porphyrine structures<sup>2</sup>.

The heteroatoms impart functionality and polarity to the molecules and therefore their presence may make a disproportionately large contribution to the differences in the physical properties of bitumens, derived from different sources [26].

---

<sup>1</sup> Heterocyclic species are organic compounds containing a closed ring of atoms, at least one of which is not a carbon atom

<sup>2</sup> Porphyrine structures have a heterocyclic structure

Elementary analysis of bitumens, manufactured from a variety of crude oils with varying physical characteristics, show that most bitumens contain:

- Carbon 82% - 88%
- Hydrogen 8% - 11%
- Sulphur 0% - 6%
- Oxygen 0% - 1.5%
- Nitrogen 0% - 1%

Although, the elemental composition of a bitumen is important to note, it provides little information of how the atoms are assembled into molecules or what types of molecular structure are present in the bitumen. The knowledge of the molecular structure of the bitumen is necessary for a fundamental understanding of how the composition of the bitumen affects the physical properties and chemical reactivity [26].

### 2.2.2 Molecular Structure

The organic molecules found in bitumens vary in composition from non-polar, saturated<sup>3</sup> hydrocarbons to highly polar, highly condensed ring systems [26]. The way in which the elements are incorporated into molecules and the type of molecular structure is far more important than the total amount of each element present in the bitumen.

There are three principal types of molecules found in bitumen:

- Aliphatics,
- Naphthenics, and
- Aromatics.

---

<sup>3</sup> Saturated is defined as the condition where the highest possible hydrogen to carbon ratio is present



The carbon atoms in the aliphatics<sup>4</sup>, or paraffinics, are linked in straight or branched chains. In the naphthenics, or cyclics, they are linked in simple or complex (condensed) saturated rings. Aromatics are materials characterised by the presence of one or more especially stable six-atom rings (e.g. benzene, toluene, etc). The three principal types of molecules are illustrated in Figure 2.1

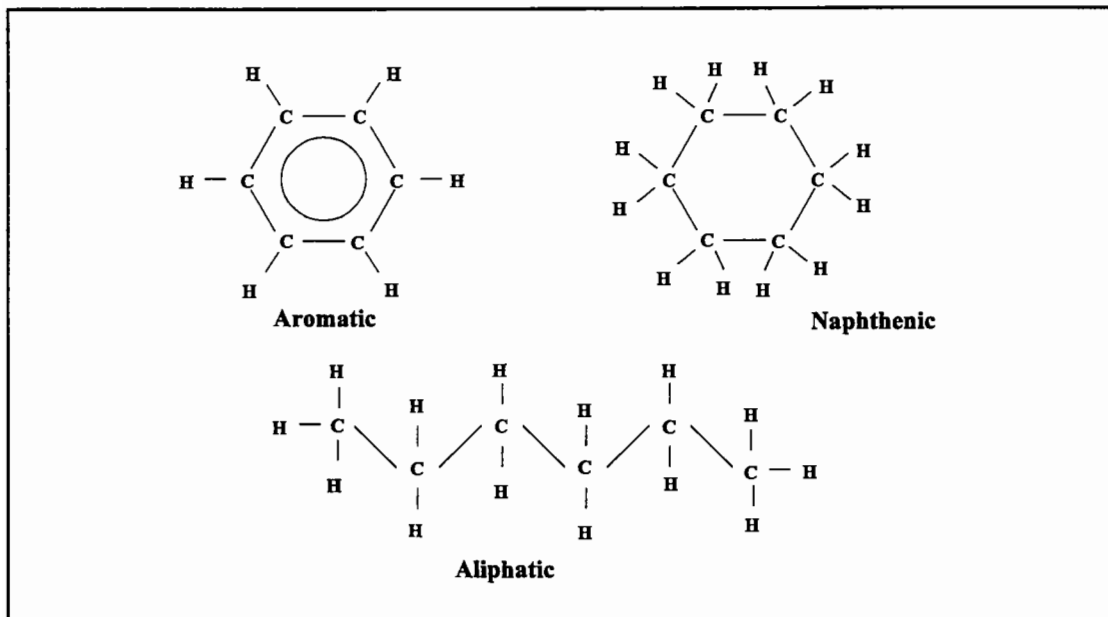


**Figure 2.1: Types of molecules found in bitumen**

The physical and chemical behaviour of bitumens are affected by the various ways in which these compounds interact with one another. The molecules are held together through chemical bonds that are relatively weak and can be broken by heat and/or shear forces.

### 2.2.3 Fractional Composition of Bitumen

The precise composition of a bitumen is dependant on the crude oil source and the

---

<sup>4</sup> Aliphatics are organic compounds that are not aromatic, especially having an open chain structure, such as alkanes (saturated aliphatic hydrocarbon with the general formula  $C_nH_{2n+2}$ , also called paraffin), alkenes (unsaturated aliphatic hydrocarbon with the general formula  $C_nH_{2n}$ , also called olefine) and alkynes (unsaturated aliphatic hydrocarbon with the general formula  $C_nH_{2n-2}$ , also called acetylene)

processes used during the manufacture of the bitumen. Since the chemical composition of bitumen is extremely complex with the number of molecules with different chemical structures being astronomically large, it is not feasible to attempt a complete analysis of bitumen and therefore chemists have not attempted to separate and identify all the different molecules in bitumen [26,27]. Instead, various techniques have been developed to separate bitumen into less complex and more homogenous fractions.

These techniques divide the bitumen into groups or generic fractions based on molecular size, chemical reactivity and/or polarity. Examples of techniques based upon polarity include: Corbett fractionation, SARA (saturates, aromatics, resins and asphaltenes) and Ion Exchange Chromatography (IEC), while High Pressure Gel Permeation Chromatography (HP-GPC) separates bitumen into fractional groups based on molecular sizes. It is important to note that the different separation techniques lead to fractions having different chemical and physical characteristics.

The most common method available for separating bitumen into fractions is by means of various chromatographic techniques. In general bitumen can be divided into two broad chemical groups, called asphaltenes and maltenes. The basis of the chromatographic techniques is to initially precipitate the asphaltenes using hydrocarbon solvents such as n-heptane or n-pentane, followed by chromatographic separation of the remaining maltene material. Using this technique, bitumens can be separated into four groups by subdividing the maltenes into saturates, aromatics and resins, together with the n-heptane insoluble asphaltenes. The main characteristics of the four groups (SARA) are as follows:

### **Asphaltenes**

These are n-heptane insoluble black or brown amorphous solids containing, in addition to carbon and hydrogen, some nitrogen, sulphur and oxygen. They are considered as highly polar, complex aromatic materials with a tendency to interact and associate and have a fairly high molecular weight ranging widely from 600 to 300,000 depending on the separation technique employed. However, the majority of test data indicates a range of 1,000 to 100,000, with a particle size of 5 nm to 30 nm and a hydrogen/carbon (H/C)

atomic ratio of 1.1. [1]

The asphaltene content has a large effect on the rheological characteristics of a bitumen. It has been shown that the asphaltene content can be related to a number of physical parameters such as the glass transition temperature [28,29] and the viscosity of a bitumen [1,27,30,31]. Increasing the asphaltene content produces a harder bitumen with a lower Penetration, higher Ring and Ball Softening Point and consequently higher viscosity. Asphaltenes generally constitute approximately 5% to 25% of the bitumen [1].

### **Resins**

Resins are soluble in n-heptane and, like asphaltenes, are largely composed of hydrogen and carbon with small amounts of oxygen, sulphur and nitrogen. They are dark brown solid or semi-solid and very polar in nature which makes them strongly adhesive. They are dispersing agents or peptisers for the asphaltenes and, therefore, the proportion of resins to asphaltenes governs the degree of solution (SOL) or gelatinous (GEL) character of the bitumen. Resins have molecular weights ranging from 500 to 50,000, a particle size of 1 nm to 5 nm and an H/C atomic ratio of 1.3 to 1.4 [1].

### **Aromatics**

Aromatics are the lowest molecular weight naphthenic aromatic compounds in bitumen and represent the major proportion of the dispersion medium for the peptised asphaltenes. They are dark brown viscous liquids that constitute 40% to 65% of the total bitumen with the average molecular weight ranging from 300 to 2,000 [1]. Aromatics consist of non-polar carbon chains in which the unsaturated ring systems dominate and have a high dissolving ability for other high molecular weight hydrocarbons.

### **Saturates**

Saturates comprise straight and branched-chain aliphatic hydrocarbons together with alkyl-naphthenes and some alkyl-aromatics. They are non-polar viscous oils, straw or white in colour, with a similar molecular weight range to aromatics. The components include both waxy and non-waxy saturates and form 5% to 20% of the bitumen [1].

### **Corbett Fractionality (ASTM D4124)**

One of the most widely used separation techniques is the Corbett's fractionation technique [32]. The method combines the insolubility of asphaltenes in n-heptane, followed by selective adsorption-desorption chromatographic separation of the remaining solution fraction (maltenes) in an alumina column using progressive extraction with increasing polarity solvents. The following four fractions are obtained:

- Asphaltenes - most polar,
- Polar aromatics - strongly polar,
- Naphthene aromatics - weakly polar, and
- Saturates - non-polar.

The polar aromatic fraction is comprised of highly condensed aromatic ring systems and functional groups containing heteroatoms. The polar aromatic fraction serves as the peptisers or dispersing agents for the asphaltenes and is highly polar giving it strong adhesive characteristics.

The naphthene aromatic fraction is a viscous liquid which constitutes the major proportion of the dispersion medium for the asphaltenes. This fraction may contain condensed non-aromatic and aromatic ring systems and possibly sulphur and the heteroatoms oxygen and nitrogen.

The saturate fraction consists of a viscous oil which lacks polar chemical functional groups. The molecules of this fraction are non-polar and may contain saturated normal and branched-chain hydrocarbons (aliphatics), saturated cyclic hydrocarbons and, in addition to sulphur, possibly a small amount of mono-ring aromatic hydrocarbons.

### **Iatroscan Thin Layer Chromatography**

A faster method of fractionating bitumen can be achieved by means of Iatroscan thin layer chromatography using a flame ionization detector (TLC-FID) [33,34]. The separation of the bitumen takes place in silica or alumina lined quartz filaments

(chromarods) by consecutive elution in various solvents.

Using the Iatroscan procedure, a chromatogram is obtained with four separate peaks corresponding to the FID signals from the different fractions, namely:

- Saturates,
- Aromatics,
- Mobile polar Resins, and
- Asphaltenes + Immobile polar Resins.

The percentages of the four fractions is calculated from the chromatogram by means of area normalisation, internal standards or an empirical calibration method [34].

Torres et al [33] have correlated the fractionation of bitumen between Corbett's ASTM D4124 method and the Iatroscan thin layer chromatography method by comparing the asphaltene fractions obtained from the two methods. Due to the different procedures that are used to obtain the asphaltenes (insolubility in n-heptane - ASTM D4124 and non-elution in a silica chromatographic column - Iatroscan), the fractions are not compatible for all bitumens.

In the first case, where there are polar components, different from asphaltenes and normally called immobile polar resins, the Iatroscan method indicates a higher percentage of asphaltenes compared to the ASTM D4124 method. This is because the immobile polar resins are not eluted by any of the solvents used in the thin layer chromatography and are, therefore, incorrectly quantified as asphaltenes. In the ASTM D4124 method these polar components are retained in the alumina column after separation from the asphaltenes by insolubility.

In the second case, the Iatroscan method indicates a lower percentage of asphaltenes compared to the ASTM D4124 method. This occurs when there are asphaltene portions of low or moderate polarity which are precipitated by insolubility in n-heptane, but are

eluted by the solvents used in the Iatroscan procedure.

### **Fractionation by Treatment with Sulphuric Acid (ASTM D2006)**

A third method of determining the fractional composition of bitumen is fractionation by treatment with sulphuric acid - ASTM D2006. This method is known as the Rostler and Sternberg procedure [35,36], where the bitumen is divided into the following chemical compositions:

- Asphaltenes,
- Polar compounds,
- First Acidaffins,
- Second Acidaffins, and
- Saturates.

The asphaltene fraction is the part of the bitumen that is insoluble in n-pentane. The other groups are identified after the separation of the asphaltenes. The polar compounds are the peptising agents for the asphaltene fraction. The first acidaffins act as solvents of the peptised asphaltenes. The second acidaffins correspond approximately to the naphthene aromatic fraction and, finally, the saturates or paraffinic fraction are obtained by elution in a chromatographic column.

### **Index of Colloidal Instability**

Gaestel et al [37] developed an Index of Colloidal Instability based on the proportionality of the basic fractional groups within bitumen. This Index of Colloidal Instability, which is often termed the Colloidal Index (CI) or Gaestel Index, is calculated as:

$$CI = \frac{\text{flocculated constituents}}{\text{dispersing constituents}} = \frac{\text{asphaltenes} + \text{saturates}}{\text{resins} + \text{aromatics}} \quad (1)$$

CI is a representation of the colloidal behaviour of the bitumen. A low CI value means

that the asphaltenes are more peptised in the oil based medium.

### **High Pressure Gel Permeation Chromatography**

High pressure gel permeation chromatography (HP-GPC), also known as size exclusion chromatography (SEC), is a form of liquid chromatography where separation of the molecules is accomplished, in a column of porous gel material, by a simple classification process according to size [34,38]. HP-GPC has been described as essentially a sieve-like analysis of the bitumen components [39]. The gel medium consists of cross-linked polymeric compounds, such as copolymers of styrene and di-vinyl benzene, and contains pores of various sizes. A characteristic of the process is that the smaller molecules enter the pores, gel structure, by diffusion and therefore remaining longer in the column than the larger molecules, which are flushed rapidly through the large interstices. The molecules, which leave the columns at separate times, are detected by ultraviolet (UV) and/or refractive index (RI) detectors. The measured data is recorded in the form of chromatograms of UV absorption or refractive index.

The two parameters that affect the response of HP-GPC are the detection wavelength of the UV detector and the column combination. Depending on the UV wavelength selected, the UV signal shows several aspects of the chemical structure of the bitumen. At the same time, the use of columns with high pore density and small pore width gives more information to the signal. Although the detection sensitivity of the RI detectors is lower than that of the UV detectors, they are non-selective and therefore able to detect all substances, including those that do not absorb UV radiation.

The molecular mass distribution of components, polymer content in polymer modified bitumens (PMB's) and the degradation of polymer in the process of ageing can be studied by HP-GPC [34]. The actual molecular size of the components can be determined by correlation with the UV signals obtained for a standard polystyrene solution of known molecular sizes [38].

The fractionation methods described above generally use liquid chromatography on

stationary phases, such as alumina or silica gel, to determine the bitumen constitution. The first step is usually to remove the most polar components (asphaltenes) by precipitation using hydrocarbon solvents, such as n-heptane or n-pentane. This is followed by chromatographic separation of the remaining material. One of the shortcomings of these methods is that pretreatment, used to remove asphaltenes, may include removal of high molecular weight non-polar molecules in addition to polar species. The use of destructive separation techniques also requires that the specimen are in a solvent phase, which means that the obtained fractions, including insoluble asphaltenes, are highly dependent on testing conditions. It would therefore seem to be desirable to fractionate solutions of whole bitumen without pretreatment and without too much irreversible adsorption onto the solid materials used in separations.

### **Ion Exchange Chromatography**

Ion exchange chromatography (IEC) is a technique used to separate bitumen into distinct chemical fractions based on chemical functionality without the need for initial asphaltene precipitation. IEC accomplishes this fractionation by pumping solutions of bitumen, dissolved in selected solvents, into columns filled with activated cation or anion resins [40]. Bitumen components containing acidic functional groups become adsorbed on anion resins, from which they can be desorbed. Bitumen components having basic functional groups are adsorbed on cation resins. Components containing neither acidic nor basic functional groups will not be adsorbed by either anion or cation columns. Components having both acidic and basic substituents (known as amphoteric) can be adsorbed by both anion and cation resins depending on which resin is contacted first. This process results in five fractions, namely [3,39,40]:

- Strong acids,
- Strong bases,
- Weak acids,
- Weak bases, and
- Neutrals.



The strong acids and bases are the highly aromatic and polar components, while the remainder of the components are either weakly or non-polar. The IEC procedure does not isolate the amphoteric components into a single fraction, but distributes amphoteric components among strong acid, strong base and weak acid fractions [40].

### **Nuclear Magnetic Resonance Analyses**

Nuclear magnetic resonance spectroscopy (NMR) is a non-destructive technique used to characterise the hydrocarbon groups contained in bitumen. NMR analysis of bitumen is undertaken by means of a NMR spectrometer using either  $^1\text{H}$  (proton) and/or  $^{13}\text{C}$  resonance impulses together with Fourier transform analysis and integration of the response signals [34,41].

The NMR method can be used to determine the chemical, generic compositions of bitumen by measuring the main emission peaks or signals that correspond to different generic compositions. Santage et al [41] have used NMR to obtain the percentage compositions of three chemical structural fractions, namely:

- Asphaltenes,
- Saturates + aromatics, and
- Resins.

The three structural NMR fractions that are obtained from NMR peaks are not identical to the fractions obtained from chromatographic columns due to the fact that different chemical and physical methods are used to obtain the fractions [41].

NMR analysis can also be undertaken on polymers by performing the same sort of  $^1\text{H}$  and  $^{13}\text{C}$  analysis on the modifying agents. Mascherpa et al [42] have used  $^1\text{H}$  NMR and  $^{13}\text{C}$  NMR to determine the origin of bitumens, the composition of polymer/bitumen blends and the nature of the polymer.

The main advantage of NMR is that it is possible to perform a chemical analysis on the

neat bitumen, the polymer and the composite bitumen-polymer blend. This allows the possibility of a direct correlation of the chemical composition and physical properties of the PMB, rather than an indirect correlation of the chemical composition of the pure bitumen and the physical properties of the PMB.

#### **2.2.4 Functionality and Polarity**

The heteroatoms, nitrogen, sulphur and oxygen, impart functionality and polarity to the molecules present in bitumens. Although they are present only in small quantities, the heteroatoms significantly affect the physical properties and performance characteristics of bitumens. Functionality refers to the way in which molecules in bitumen interact with each other as well as with the molecules and/or surfaces of other materials, such as aggregates. Polarity refers to the way in which the electrochemical forces in the molecules are imbalanced, producing a dipole.

In brief, molecules composed of carbon and hydrogen tend to associate with one another less strongly than molecules composed of carbon, hydrogen and heteroatoms. These polar compounds form associations, depending on such factors as temperature, shear and solvation, to give bitumen its elastic properties. These compounds coexist with non-polar compounds which, together, give bitumen its viscous properties.

#### **Fourier Transform Infrared Spectroscopy**

Infrared absorption spectroscopy is one of the most powerful means of detecting and identifying organic compounds. It provides information on the vibrational structure of molecules and therefore knowledge of the molecular structure of the various functional groups. Fourier Transform Infrared Spectroscopy (FTIR) is therefore used to characterise the oxygen-containing functionalities (functional groups) found in bitumen and particularly those produced during oxidation [34,40,43,44].

The principle of the FTIR method is that the energy from the IR light source, with wavenumbers of 400 to 4000  $\text{cm}^{-1}$ , is transformed into vibrational energy in the

molecules of the bitumen. It is this vibrational energy that presents a series of adsorption bands which are recorded as transmittance (%) or absorbency against the wavelength ( $\mu\text{m}$ ) or more often wavenumber ( $\text{cm}^{-1}$ ). The position of the peaks along the wavenumber axis are unique to certain chemical bonds and chemical functional groups present in the bitumen.

FTIR is principally used as a means of identifying different bitumens and is often described as the “fingerprint” of the bitumen. FTIR can also be used to evaluate the ageing properties of bitumens by calculating the changes in the spectra associated with particular ageing products within certain frequency ranges, such as:

- S=O, C-H in aromatic - 1020  $\text{cm}^{-1}$
- $\text{SO}_2$  from oxidation - 1108  $\text{cm}^{-1}$
- ester (R-COOR) - 1262  $\text{cm}^{-1}$
- C=C in aromatic - 1618  $\text{cm}^{-1}$
- C=O in carbonyl - 1702  $\text{cm}^{-1}$
- OH in polymers (R-OH) - 3258  $\text{cm}^{-1}$

FTIR can also be used as an appropriate technique for identifying and determining the content of different polymers in PMB's [44]. The characteristics absorption bands for two commonly used polymers are:

- 966 and 698  $\text{cm}^{-1}$  for styrene butadiene styrene (SBS), and
- 1736 and 1242  $\text{cm}^{-1}$  for ethylene vinyl acetate (EVA).

### **Synchronous Ultraviolet Fluorescence**

Another non-destructive spectroscopic method that can be used to determine the chemical composition of bitumen is synchronous ultraviolet fluorescence (SUUVF), which is used to evaluate the aromatic structure content of bitumens [43,45].

Pieri et al [43] have used FTIR and SUUVF spectroscopic methods to determine indices,

defined as ratios of characteristic absorption bands, in order to correlate these indices with the rheological properties of the bitumens. They have shown that there are correlations between the rheological performance of unaged and aged bitumens and various indices, such as the ratio of aliphatic to aromatic structures, the degree of substitution and condensation of aromatics and the ratio of branched to linear aliphatic structures. The work has, however, been limited to unmodified bitumens and the relationships between the FTIR and SF indices and rheological performance may not be applicable to PMB's.

### **2.2.5 Thermochemical Behaviour of Bitumen**

The thermal properties of bitumen can be analysed by differential scanning calorimetry (DSC) and thermomicroscopy methods such as polarized light and phase contrast.

#### **Optical Thermomicroscopy Techniques**

Phase contrast microscopy (PCM) and polarised light microscopy (PLM) have been used to directly observe solid-liquid transitions in neat bitumen as well as the morphology of semi-crystalline PMB's [46,47]. Polarised light microscopy (in crossed polar mode) detects anisotropic structures, within substances that exhibit more than one refractive index, such as waxes in bitumen and the crystalline domains of semi-crystalline polymers. Phase contrast microscopy is used to increase the contrast between a region of interest and the surrounding matrix when the refractive index of both is very similar, such as in polymeric and asphaltene-rich phases. Together these two methods can observe both crystalline domains (polarised light) and amorphous fractions (phase contrast) in neat bitumen and semi-crystalline PMB's.

#### **Differential Scanning Calorimetry**

Differential scanning calorimetry (DSC) is a technique used to characterise the thermal behaviour of pure bitumens [47].

The technique provides the values of temperature ( $^{\circ}\text{C}$ ) and enthalpy ( $\text{kJ/kg}$ ) corresponding to the following transitions:

- Glass transition (2nd order transition),
- Melting (fusion) (1st order transition), and
- Crystallisation (1st order transition).

Second-order transitions are associated with amorphous material (structures) such as the glass transition of bitumen and the melting of SBS copolymers in SBS PMB's, while first-order transitions are associated with crystalline structures.

The DSC test can be performed in either a heating mode, to obtain melting (fusion) peaks, or in a cooling mode, to obtain crystallisation peaks. In the first mode, the DSC data is obtained by heating the bitumen sample at a constant rate ( $5^{\circ}\text{C}/\text{min}$ ,  $10^{\circ}\text{C}/\text{min}$  or  $20^{\circ}\text{C}/\text{min}$ ) from a low temperature ( $-60^{\circ}\text{C}$ ) to a high temperature ( $120^{\circ}\text{C}$ ) and measuring the absorbed heat peaks (endothermic reactions). In the second mode, the DSC data is obtained by cooling the bitumen sample at a constant rate ( $-5^{\circ}\text{C}/\text{min}$  or  $10^{\circ}\text{C}/\text{min}$ ) from a high temperature ( $100^{\circ}\text{C}$ ) to a low temperature ( $-40^{\circ}\text{C}$ ) and measuring the expelled heat peaks (exothermic reactions). Using the heating mode, melting zones can be identified for crystalline waxes and for organised bitumen components such as the long alkyl side-chains of asphaltenes in pure bitumens.

DSC can also be used to characterise the thermal behaviour of ethylene copolymer modified bitumens by indicating the presence of specific crystalline components in the PMB's [47,48,49]. Using the heating mode of testing, the first-order transition, associated with the melting of the crystallised fractions of the copolymer, are accompanied by endothermic signals which are easily characterised by DSC analysis.

The temperature region in which the first-order transition occurs depends on the type of ethylene copolymer and the type of base bitumen but proves to be insensitive to the copolymer content [47,48]. However, the copolymer content does have an effect on the

enthalpy associated with the endothermic reaction, there being an increase in enthalpy with an increase in polymer content [48]. The melting peak, for ethylene copolymer modified bitumens, usually lies within the temperature range of 60°C to 75°C [47].

The thermal treatment of the sample is an important parameter that must be recognised during DSC testing. Some organised structures, such as bitumen waxes and ethylene copolymers which are destroyed during a heating cycle, may not immediately recover on cooling and therefore may not be present as melting peaks during a second heat cycle. It is also important to appreciate that the thermal treatment of the sample can entail changes in the crystallite size [47].

## **2.3 Bitumen Structure**

### **2.3.1 Colloidal Model**

Bitumen is traditionally regarded as a colloidal system consisting of high molecular weight asphaltene micelles dispersed or dissolved in a lower molecular weight oily medium (maltenes) [26,27,50,51,52,53,54,55]. The colloidal model for bitumen was first introduced by Nellensteyn [50], and later developed and refined by other researchers [51,52]. In the model, the micelles are considered to be asphaltenes together with an absorbed sheath of high molecular weight aromatic resins, which act as a stabilising solvating layer to peptise the asphaltenes within the solvent maltenes phase. Away from the centre of the micelle there is a gradual transition to less polar aromatic resins and, finally, to the less aromatic oily dispersion medium.

Pfeiffer and Saal [52] suggested that the bitumen dispersed phases are composed of an aromatic core surrounded by layers of less aromatic molecules and dispersed in a relatively aliphatic solvent solution. In their colloidal model there are no distinct boundaries between the dispersed and solvent phases, but a continuum from low to high aromaticity from the solvent phase to the centre of the entities making up the dispersed phase. They found that asphaltenes, which are the core constituents of the dispersed

phases, attract smaller aromatic components of the maltenes, which surround and peptise the asphaltenes. These smaller aromatic molecules are compatible with the naphthenic and aliphatic components of the remainder of the maltene phase. Therefore, there is no contact between materials having greatly different surface tensions anywhere in the system, although the differences in surface tension between the aromatic asphaltenes cores and the more naphthenic and aliphatic solvents may be fairly large.

In bitumens having sufficient quantities of resins and aromatics of adequate solvating power, the asphaltenes are fully peptised, well dispersed and do not form extensive associations. These bitumens are known as solution or 'SOL' type bitumens [53]. If the quantity of the aromatic/resin fraction is insufficient to peptise the micelles or has insufficient solvating power, the asphaltenes can associate to form large agglomerations or even a continuous network throughout the bitumen. These bitumens are known as gelatinous or 'GEL' type bitumens. In practice most bitumens are of intermediate character.

### **2.3.2 SHRP Microstructural Model**

As part of the A-002A contract of the recently completed Strategic Highways Research Program (SHRP) in the United States, a conceptual model, referred to as the 'microstructural model' was developed [3]. The microstructural model states that the bitumen structure consists of microstructures (comprised of polar, aromatic, asphaltene-like molecules that tend to form associations) dispersed in a bulk solvent moiety consisting of relatively non-polar, aliphatic molecules [3,40]. Many of the molecules comprising the dispersed phase (dispersed moiety) are assumed to be polyfunctional and capable of associating through hydrogen bonds, dipole interactions and  $\pi$ - $\pi$  interactions to form primary microstructures. Under proper conditions, the primary microstructures can associate into three dimensional networks, which may be broken, together with the microstructures, by heat and shear stress. According to the model, bitumen physical properties are described by the effectiveness with which the polar, associated materials are dispersed by the solvent moiety rather than being described by global chemical

parameters such as elemental composition.

The model requires that the dispersed moiety of a bitumen has a larger overall molecular size than the solvent moiety and that the two moieties differ chemically. Separation of the bitumen by SEC (also known as GPC or HP-GPC) and by IEC fractional procedures was undertaken to validate the microstructural model. SEC was used to separate bitumens into fractions comprised of associating and non-associating components according to molecular size. IEC was used to separate bitumen into polar components (comprised of strong and weak acids, strong and weak bases and amphoteric) and non-polar (neutral) components in order to demonstrate the existence of the solvent and dispersed moieties as postulated in the model.

## **2.4 Bitumen Rheology**

### **2.4.1 Definition of Rheology**

Bitumen is a thermoplastic, viscoelastic liquid that behaves as a glass-like elastic solid at low temperatures and/or during rapid loading (short loading times - high loading frequencies) and as a viscous fluid at high temperatures and/or during slow loading (long loading times - low loading frequencies). The response of bitumen to stress is therefore dependent on both temperature and loading time and consequently the rheology of bitumen is defined by its stress-strain-time-temperature response.

In the measurement of the physical properties of bitumen, primary emphasis is given to the characterisation of the rheological behaviour of bitumen. Rheology is a fundamental interdisciplinary science which is concerned with the study of the internal response of real materials to stresses. The word *rheology* is derived from the Greek words " $\rho\epsilon\omega$ ", which translates literally as "to flow" and " $\lambda\omicron\gamma\omicron\sigma$ " meaning "word, science" and therefore literally means "the study of the flow" [56]. Bitumen rheology can therefore broadly be defined as the fundamental measurements associated with the flow and deformation characteristics of bitumen.



The stiffness of bituminous binders is time dependent, which means that they flow with time. The properties of rheological materials are also temperature dependent and therefore both time of loading and temperature of loading need to be considered when characterising the flow properties of rheological materials such as bitumen.

#### 2.4.2 Conventional Physical Property Tests

The two most common bitumen specifications are the penetration-graded and viscosity-graded specifications. The primary purpose of these specifications is to grade bitumen according to its consistency, so do not address specific distress modes or ensure long term field performance. Examples of bitumens as graded by the Penetration and viscosity specifications are presented in Table 2.1.

**Table 2.1: Penetration and viscosity graded bitumens [57]**

Penetration grade	Penetration @ 25°C (dmm)	Viscosity grade	Viscosity @ 60°C (Pa.s)
40/50	40-50	B24	170-300
60/70	60-70	B12	105-165
80/100	80-100	B8	55-100
150/200	150-200	B4	25-50

These specifications have at times been modified to relate the specification criteria to field performance, but these modified specifications still tended to be largely based on empirical parameters, such as Penetration, ductility and Fraass breaking point. The result was that it was still difficult to reliably relate the specification criteria to pavement performance.

The traditional empirical tests that are used to characterise bitumen are conducted at different regions of the temperature response of bitumen:

- Fraass breaking point:- brittleness range,
- Penetration:- semi-solid range,

- Softening point:- beginning of fluidity range, and
- Viscosity:- fluidity range.

Penetration grade bitumens are traditionally specified by the consistency tests of Penetration and Softening Point [1].

#### **Penetration test [58]**

The Penetration is a measure of the consistency of the bitumen expressed as the distance in tenths of a millimetre (decimillimetre) that a standard needle is allowed to penetrate vertically into a sample of the bitumen, under a specified load and loading time, at a fixed temperature of 25°C. Therefore the greater the penetration of the needle the softer the bitumen and vice versa [1]. The Penetration test can be considered as an indirect measurement of the viscosity of the bitumen at a temperature of 25°C.

#### **Ring and Ball Softening Point test [59]**

The Ring and Ball Softening Point test is an empirical test used to determine the consistency of a bitumen by measuring the equiviscous temperature at which the consistency of the bitumen is between solid and liquid behaviour. Therefore, regardless of the grade of the bitumen, the consistency will be the same for different grade bitumens at their respective Softening Point temperatures. The American Society for Testing Materials (ASTM) also specifies a similar Softening Point test but unlike the BS 2000, Part 58, 1983 method no stirrer is used in the liquid bath and, consequently, the ASTM Softening Point is 1.5°C higher than the BS method.

The viscosity tests are used either as an addition to the Penetration and Softening Point data, in the penetration-grade specification, or as the basis for the viscosity-grade specification.

#### **Viscosity measurements**

Viscosity is the measure of the resistance to flow of a liquid and is defined as the ratio between the applied shear stress and the rate of shear strain. The rotational viscometer

test method is presently considered to be the most practical means of determining the viscosity of bitumen, since the instrument allows the testing of a wide range of bitumens over a wide range of temperatures, more so than most other viscosity measurement systems [60].

Rotational viscometers consist of one cylinder rotating coaxially inside a second (static) cylinder containing the bitumen sample. The material between the inner cylinder and the outer cylinder is therefore analogous to the thin bitumen film found in the sliding plate viscometer. The torque on the rotating cylinder or spindle is used to measure the relative resistance to rotation of the bitumen at a particular temperature. The torque value is then altered by means of calibration factors to yield the viscosity of the bitumen.

The viscosity tests are conducted in a high temperature range (above 60°C), whereas the Penetration and Softening Point tests are conducted in the intermediate to low temperature range (below 60°C) [61]. Unfortunately, the rheological properties of bitumen vary in a bitumen-specific fashion as a function of both temperature and loading time at temperatures below 60°C, for unmodified bitumens, and below slightly higher temperatures for polymer modified bitumens. This behaviour is illustrated in Figure 2.2 and, therefore, measurements above these temperatures cannot adequately be extrapolated to describe the behaviour of bitumen at lower temperatures. Consequently, this results in problems when attempting to predict high and low temperature performance, from the penetration-grade specifications, and low and intermediate temperature performance, from the viscosity-grade specifications.

The increasing use of polymer modified binders required the development of new technology as the conventional bitumen test procedures were proving to be inadequate [62]. One of the reasons for this is that many polymer modified bitumens tend to behave more as a polymer than as a bitumen. The ductility, elastic recovery and toughness-tenacity tests are modifications that have been added to the penetration-grade or viscosity-grade specifications in an attempt to relate the specification criteria to field performance, particularly for modified bitumens [62]. However, there are still problems

with the use of a modified penetration-ductility specification, since both tests are inappropriate as fundamental measurements of low temperature rheology. This is because the stress fields within the test specimens cannot be defined, the strains developed during the test are very large and vary within the specimen and the stress-strain field cannot be easily modelled or calculated.

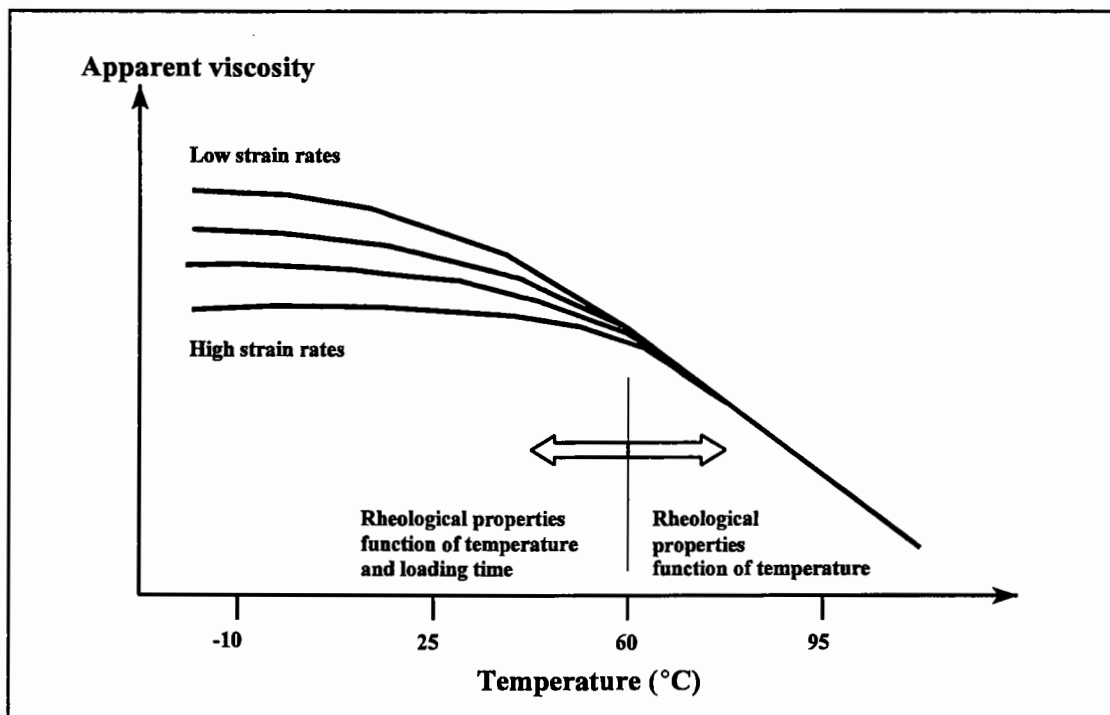


**Figure 2.2: Rheological behaviour of bitumen**

The conventional methods of characterising the rheological properties of bitumen cannot therefore completely describe the viscoelastic properties, which are needed to relate fundamental physical binder properties to performance. The Penetration and Softening Point tests are almost completely empirical and hence unsuitable for characterising the viscoelastic behaviour of bitumen. Viscosity testing, although a more fundamental method of determining the rheological performance of a bitumen, does not provide information on the time dependence of bitumen. These measurements are consequently not adequate for describing the viscoelastic properties needed for the complete rheological evaluation of a bitumen [63].

### 2.4.3 Viscoelastic Behaviour of Bitumen

Bitumen is a thermoplastic liquid that behaves as a viscoelastic material as shown in Figure 2.3. The term "viscoelastic behaviour" refers to the mechanical properties of the bitumen, which, in two limiting extremes, can result in the bitumen behaving either as an elastic solid or a viscous fluid, depending on temperature and time of loading. At low temperatures the elastic properties dominate, while at high temperatures the bitumen behaves like a liquid, usually with Newtonian viscous flow properties. At normal pavement temperatures, the bitumen has properties that are in the viscoelastic region [64]. At these temperatures the bitumen therefore exhibits both viscous and elastic behaviour and displays a time dependent relationship between applied stress or strain and resultant strain or stress [19]. The intermediate range of temperatures and loading times, at which the viscoelastic behaviour occurs, is indicative of the typical conditions experienced in service.

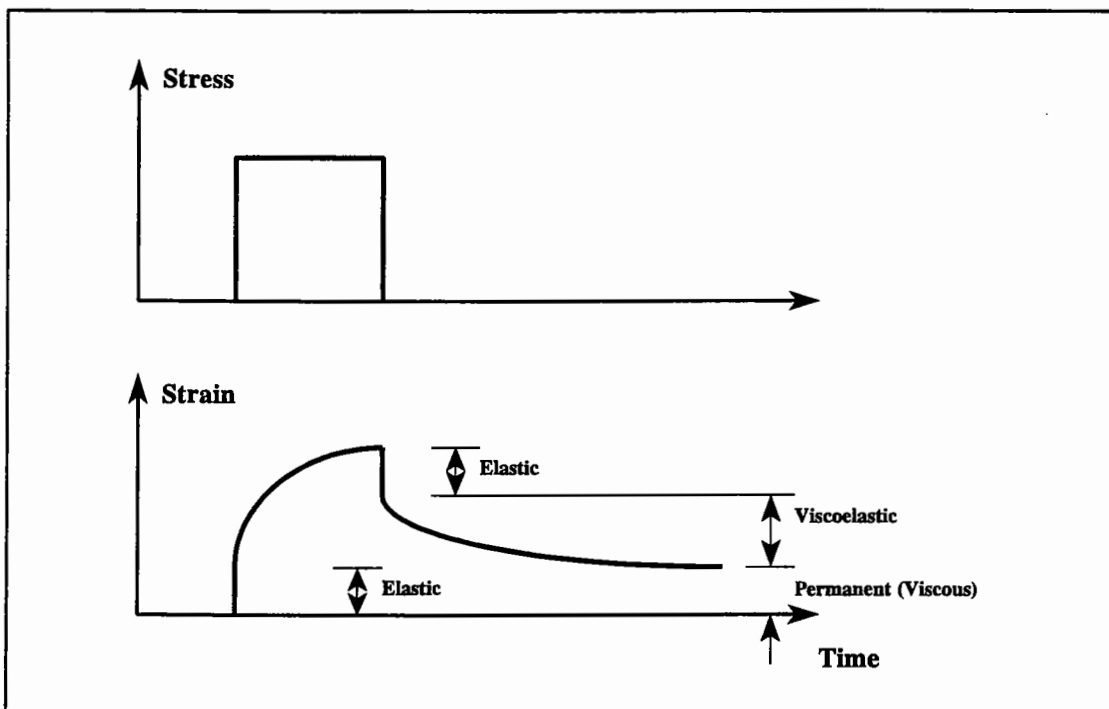
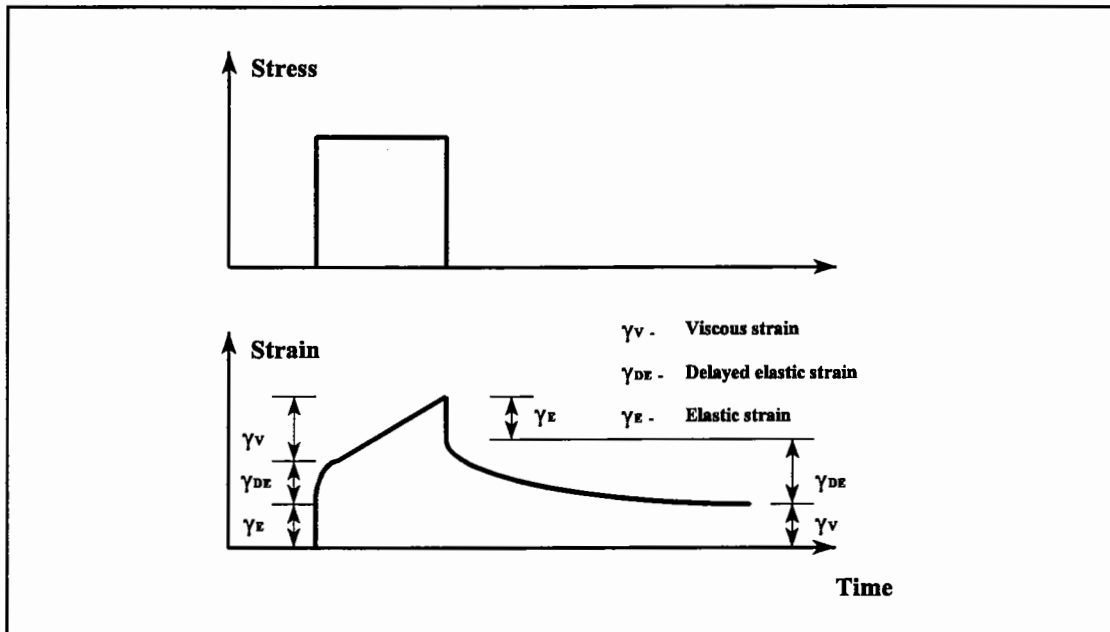


Figure 2.3: Viscoelastic response to an applied load

Another viscoelastic representation of the behaviour of bitumen is represented in Figure 2.4, where three regions of behaviour are observed, namely:

- linear elastic,
- delayed elastic, and
- viscous.



**Figure 2.4: Viscoelastic response of bitumen under creep loading**

The viscous portion is solely responsible for the non-recoverable deformation experienced when the bitumen or asphalt mixture incorporating the bitumen is loaded. However, the elastic and delayed elastic strain are totally recoverable once the load and applied stress are released. The elastic response of the bitumen dominates at short loading times and/or low temperatures, while the viscous response dominates at long loading times and/or high temperatures. The delayed elastic response dominates at intermediate loading times and temperatures. The purely viscous component and the delayed elastic component constitute the time dependent deformation of the viscoelastic material. Although none of the viscous deformation is recovered once the load is removed, the delayed elastic deformation is recovered but not immediately as with the purely elastic deformation. Because the relative magnitude of the three components change with

loading time and temperature, both the magnitude and the shape of the creep curve in Figure 2.4 will change with loading time and temperature [63].

The descriptions given above of elastic, viscous and viscoelastic response are for a linear response, meaning that the deformation at any time and temperature is directly proportional to the applied load. Nonlinear response, especially for viscoelastic materials, is extremely difficult to characterise in the laboratory or to model in practical engineering applications [65]. Fortunately, linear methods of characterisation and analysis are generally more than adequate for engineering design problems. Therefore, within the linear viscoelastic region of a bitumen, the interrelation of stress and strain, and therefore stiffness, is influence by time only and not by the magnitude of the stress. To ensure the bitumen remains within this linear viscoelastic region, the strain, or deformation, that is applied to the bitumen must remain within certain strain boundaries [22].

Linear behaviour is fulfilled at low temperatures and short loading times (high frequencies), where the material behaves as an elastic solid. The linearity is also maintained at high temperatures and long loading times (low frequencies) where the material behaves almost entirely as a Newtonian fluid. The area where non-linearity is prominent is therefore in the range of moderate temperatures and loading times [22]. This range of temperatures and loading times corresponds to the conditions experienced in the field.

According to Ferry [66], the shape of the linear viscoelastic (LVE) response of a bitumen, including polymer modified bitumens, can be sub-divided into four zones:

- a terminal or flow zone,
- a plateau zone (only present in the case of a network),
- a transition zone, and
- a glassy zone.

The LVE response of bitumen and therefore the shape of the master curve can more

generally be divided up or separated into three regions or zones of behaviour:

- At low temperatures or short loading times (high frequencies), bitumen behaves as glassy solid. The stiffness therefore approaches a limiting value of approximately 1 GPa in shear and 3 GPa in tension-compression or bending. In this region the stiffness is only slightly dependent on temperature and/or time of loading.
- At intermediate temperatures or loading times (frequencies), bitumen undergoes a gradual transition from glassy to fluid behaviour. This transition is characterised by large amounts of delayed elasticity. The stiffness modulus changes dramatically in this region as a function of temperature and/or loading time.
- At high temperatures or long loading times (low frequencies), bitumen behaves as a viscous fluid. The bitumen is considered to behave as a Newtonian fluid and for low to moderate stresses and strains the shear strain rate is proportional to the shear stress.

The general shape of the master curve of a bitumen is shown in Figure 2.5.

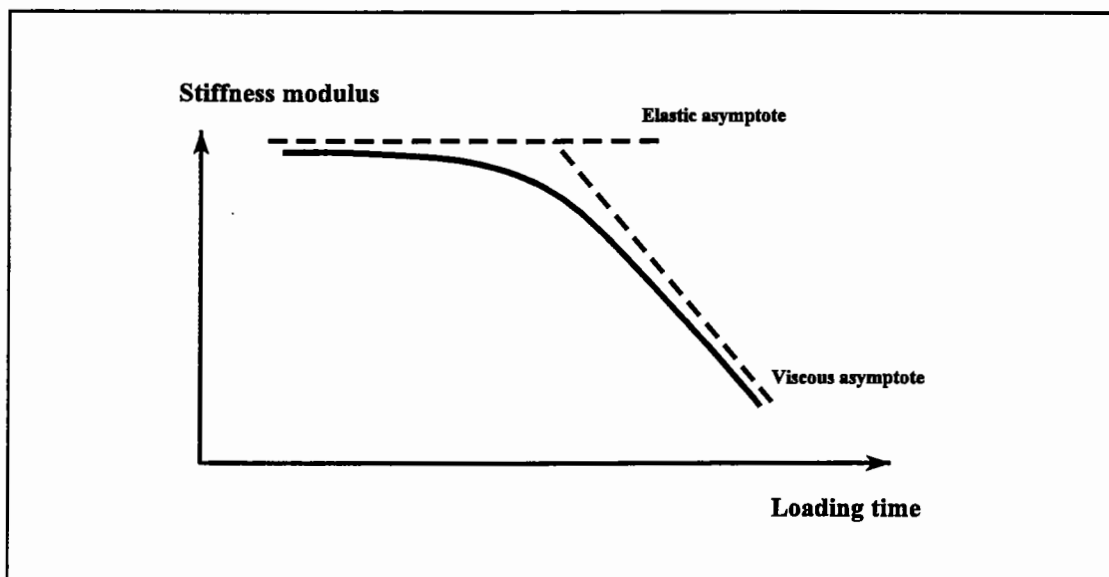


**Figure 2.5: Linear viscoelastic response of bitumen**



### Shear Susceptibility

The shear susceptibility, or shear rate dependency of a bitumen, is defined as the change in rheological properties of the bitumen as a function of loading time. The shear susceptibility of bitumen can be represented by modelling the flow properties using a power law model in which the logarithms of the shear stress and shear strain rate are linearly related [67]:

$$\log \tau = c(\log \dot{\gamma}) + B \quad (2)$$

where:

$\tau$	=	shear stress
$\dot{\gamma}$	=	$d\gamma(t)/dt$ shear strain rate
$c$	=	degree of complex flow
$B$	=	constant

A more common representation of shear-rate dependency is the following function:

$$\eta = \frac{\tau}{\dot{\gamma}^c} \quad (3)$$

where:  $\eta$  = apparent viscosity

For Newtonian materials,  $c$  is, by definition, equal to unity and for non-Newtonian behaviour,  $c$  is a measure of the degree of non-Newtonian complex flow. At very low shear rates or very low stress levels, almost all bitumens exhibit Newtonian behaviour. Non-Newtonian behaviour appears gradually as the shear-rate or stress level increases [68].

Generally, unmodified bitumens tend to exhibit Newtonian behaviour at temperatures greater than approximately 60°C. However, polymer modified bitumens tend to be shear susceptible at 60°C and sometimes at mixing and compaction temperatures and therefore exhibit non-Newtonian behaviour at higher temperatures than those associated with

unmodified bitumens [63].

Steady state creep measurements can be used to calculate an apparent viscosity at intermediate pavement service temperatures, ranging from 0°C to 25°C [69,70,71]. To conduct such measurements, it is necessary to apply a shear stress to the bitumen until the strain rate becomes constant. At low temperatures longer times are required for delayed elasticity to be expended and steady state flow to occur. This results in the bitumen being subjected to very large strains causing geometric non-linearity. The delayed elasticity and geometric non-linearity can be overcome by assuming that the steady state strain rate has been attained at a series of shear stress levels and extrapolating the calculated apparent viscosities to a zero shear rate. This apparent viscosity at zero shear rate is known as the zero shear rate viscosity,  $\eta_0$ , and is equivalent to the maximum Newtonian viscosity of the bitumen at the test temperature.

### **Temperature Susceptibility**

Temperature susceptibility is defined as the change in consistency, stiffness or viscosity of a material as a function of temperature and is usually quantified through parameters calculated from consistency measurements made at two different temperatures. Because the rheological properties of bitumen are functions of both loading time and temperature, rheological parameters, used to characterise bitumen, should completely separate time and temperature effects. Temperature susceptibility parameters should be based on measurements at different temperatures but similar loading times. Unfortunately, no commonly used temperature susceptibility parameter meets these criteria.

The viscosity-temperature susceptibility (VTS) was defined using capillary viscosity measurements at 60°C and 135°C [72]. Since the flow behaviour of unaged, unmodified bitumen at temperatures above 60°C is essentially Newtonian and independent of loading, this parameter can be used in many cases to characterise the temperature susceptibility above 60°C. However, the VTS parameter cannot be extrapolated to describe behaviour below 60°C where delayed elastic properties of bitumen become significant. The VTS parameter is also not applicable to polymer modified bitumens as

they exhibit significant shear-rate dependence when tested in capillary viscometers [63].

The temperature susceptibility of conventional bitumens is often characterised by the empirical methods of Penetration Indexes (PI's) or penetration-viscosity numbers (PVN's). The Penetration Index can be obtained from the following equation [73]:

$$\frac{\log 800 - \log \textit{penetration}}{T_{RB} - T} = \frac{20 - P.I.}{50(10 + P.I.)} \quad (4)$$

where:  $T_{RB}$  = ASTM Ring and Ball Softening Point temperature, °C  
 $T$  = Penetration temperature, usually 25°C  
 $P.I.$  = Penetration Index

The Penetration value of 800 corresponds to the Penetration at Softening Point temperature for low wax content bitumens (maximum wax content of 2 percent) [73]. Assuming that the Penetration test temperature will be 25°C, equation 4 can be rearranged to calculate the PI value of the bitumen as:

$$P.I. = \frac{1952 - 500 \log \textit{pen} - 20 T_{RB}}{50 \log \textit{pen} - T_{R.B} - 120} \quad (5)$$

The PI was later used by Van der Poel in the development of a nomograph for predicting stiffness of bitumen using routine test data [22]. Pfeiffer, van Doormaal and Van der Poel recognised the confounding of time and temperature effects in the calculation of PI and found that in most cases the time dependence, or the rheological type of the bitumen, was the dominant effect. They concluded that PI was therefore a reasonable estimate of the rheological type of bitumen, rather than purely a temperature susceptibility parameter. However, recent research has shown that the relationship between PI and rheological type, as measured by more rigorous means, is relatively poor [3]. This is probably a result of the confounding of time and temperature effects in the determination of PI.

The PVN is based on the Penetration of a bitumen at 25°C and its viscosity measured either in centistokes at 135°C or in poises at 60°C [74]. The PVN values are also unsuitable for describing the temperature susceptibility of bitumen since these values appear to remain unchanged with ageing, whereas the rheological type and temperature dependency change with ageing [68].

It can therefore be concluded that temperature susceptibility parameters are not rational indicators of rheological behaviour since they are calculated from Penetration, Softening Point and viscosity data. These parameters also have the problem of confounding time and temperature effects and are therefore unable to make a complete and accurate description of the viscoelastic behaviour of bitumens.

In the late sixties, Heukelom [75,76] developed a system that enabled Penetration, Softening Point, Fraass breaking point and viscosity data to be described as a function of temperature on one chart. This chart is known as the bitumen test data chart (BTDC). The chart enables the temperature/viscosity characteristics of a penetration grade bitumen to be determined over wide range of temperatures from only the Penetration and Softening Point of the bitumen and is therefore a refinement of the PI method developed by Pfeiffer and van Doormaal [73]. Using the BTDC, bitumen is grouped into three categories, "S" or normal bitumens, "B" or blown bitumens and "W" or waxy bitumens. The BTDC therefore is able to show how the viscosity of a bitumen depends on temperature but the chart cannot take into account the effect of loading time. Therefore the BTDC cannot fully characterise the rheological properties of a bitumen.

### **Van der Poel's Nomograph**

The modulus that relates stress to strain for bitumen is referred to as the stiffness modulus, or simply stiffness and is written as  $S(T,t)$ , where  $T$  indicates temperature dependency and  $t$  indicates time dependency. The term "stiffness modulus" was first coined by Van der Poel [22] and is widely used among bitumen and asphalt technologists.

Van der Poel [22] developed a simple system, in the form of a nomograph, that could be used to predict or estimate the stiffness of a bitumen using routine, empirical binder tests such as Penetration and the ASTM Softening Point. Van der Poel assumed a more or less hyperbolic shape for stiffness as a function of time. The shape of the master curve is estimated from the Penetration Index and the Ring-and-Ball temperature. Van der Poel concluded that the stiffness of a bitumen depended on:

- Time of loading or frequency,
- Temperature,
- Hardness of the bitumen, and
- Rheological type of bitumen.

The rheological stiffness property of a bitumen could therefore be estimated by entering the following information into the nomograph:

- Temperature,
- ASTM Softening point,
- Loading time, and
- Penetration Index, PI.

The hardness of the bitumen was characterised by the Ring and Ball Softening Point and the rheological type by the Penetration Index. Van der Poel's nomograph for the prediction of bitumen stiffness is shown in Figure 2.6.

Several researchers have attempted to modify Van der Poel's nomograph including McLeod [74] and Heukelom [77]. These latter modifications were largely minor and only cosmetic, although the suggestion of using viscosity deviates from Van der Poel's approach.

Although the Van der Poel nomograph has been successfully used as a means of predicting the stiffness of bitumens, it does have a number of shortcomings. The stiffness

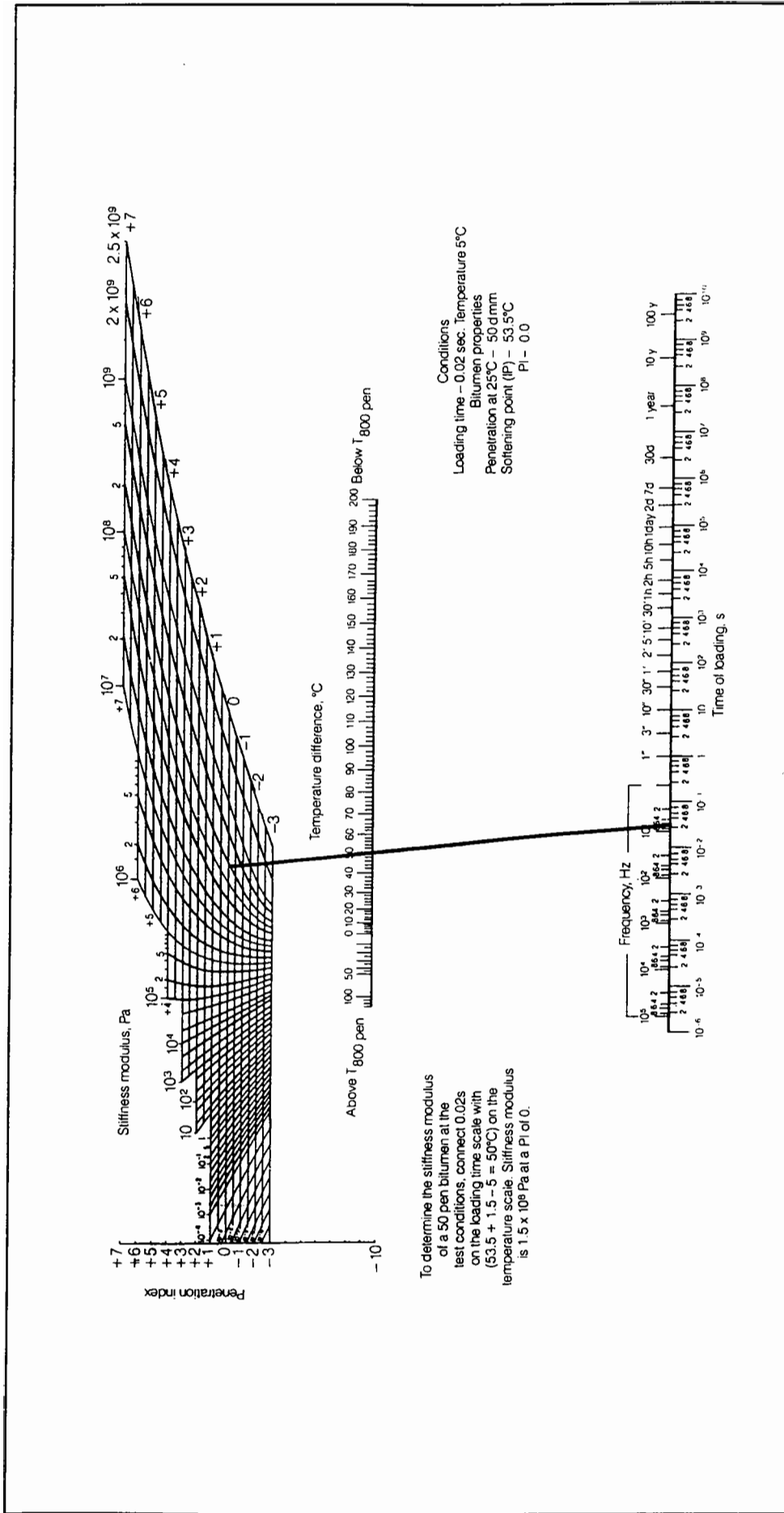


Figure 2.6: Nomograph for determining the stiffness modulus of bitumens [22]

obtained from the nomograph requires that the bitumen satisfies time-temperature equivalency and is therefore not valid for certain bitumens with a high wax contents [21]. Van der Poel's nomograph provides only an estimate of the stiffness of the bitumen within an accuracy factor of two and, since it is based on unmodified bitumens, is unable to give a realistic stiffness value for modified binders. The stiffness estimates obtained from the nomograph may also be in considerable error at low temperatures and long loading times [3]. The method is therefore useful for approximate calculations but is not capable of sufficient accuracy for exact work.

#### **2.4.4 Dynamic Mechanical Analysis**

The rheology of bitumen can be measured by dynamic mechanical analysis (DMA) using oscillatory-type testing, generally conducted within the region of linear viscoelastic response. DMA allows the viscous and elastic (viscoelastic) nature of the bitumen to be determined over a wide range of temperatures and loading times [19,65,78].

During DMA, a sample of bitumen, that is sandwiched between two parallel disks or plates, is subjected to alternating shear stresses and strains. The test can be either stress-controlled or strain-controlled, depending on which of these variables is controlled by the test apparatus. The test condition usually used to determine the dynamic rheological properties of the bitumen is the controlled-strain condition [19,79]. The use of the controlled-strain condition ensures that the strains are kept small and therefore within the linear viscoelastic region.

In the dynamic test, the material is subjected to a sinusoidal strain with a loading frequency  $\omega$  (rad/sec) represented by the following complex notation [79]:

$$\gamma^* = \gamma_0 e^{i\omega t} \quad (6)$$

where:  $\gamma^*$  = dynamic oscillating shear strain  
 $\gamma_0$  = peak shear strain  
 $\omega$  = angular frequency, rad/sec

and where:

$$i = \sqrt{-1} \quad (7)$$

The sinusoidal strain can also be represented in the following notation:

$$\gamma^* = \gamma_0 \sin \omega t \quad (8)$$

The loading frequency,  $\omega$ , is known as the angular frequency, rotational frequency or radian frequency and is defined as [22,56]:

$$\omega = 2\pi f \quad (9)$$

where:  $\omega$  = angular frequency, rad/sec  
 $f$  = frequency, Hz

The response of the applied strain is the development of a stress which, for linear viscoelasticity (small strains), is sinusoidal and out of phase with the applied strain by an amount  $\delta$ . The response stress is represented by the following complex notation:

$$\sigma^* = \sigma_0 e^{i(\omega t - \delta)} \quad (10)$$

where:  $\sigma^*$  = dynamic oscillating shear stress, Pa  
 $\sigma_0$  = peak stress, Pa  
 $\delta$  = phase angle, degrees



The response sinusoidal stress can also be represented in the following notation:

$$\sigma^* = \sigma_0 \sin (\omega t - \delta) \quad (11)$$

The phase angle,  $\delta$ , is defined as the phase difference between stress and strain and is also called the loss angle or the phase lag. An alternative symbol,  $\phi$ , can also be used for the phase angle. For purely elastic materials, the phase angle will be zero, whereas for purely viscous materials, the phase angle will be  $90^\circ$ . The phase angle is therefore important in describing the viscoelastic properties of a material such as bitumen.

The sinusoidal, oscillatory, stress and strain waveforms and the resulting dynamic test outputs are shown in Figures 2.7 and 2.8. The ratio of the resulting stress to the applied strain is called the complex shear modulus and defined by:

$$G^*(\omega) = \frac{\sigma^*}{\gamma^*} = \frac{\sigma_0}{\gamma_0} e^{i\delta} \quad (12)$$

where:  $G^*(\omega) =$  complex shear modulus, Pa, as a function of rotational frequency,  $\omega$

and whose absolute value, or the norm of the complex shear modulus, is the ratio of the peak stress to the peak strain:

$$|G^*(\omega)| = \frac{\sigma_0}{\gamma_0} \quad (13)$$

Equation 12 can be written as:

$$G^*(\omega) = \left(\frac{\sigma_0}{\gamma_0}\right) \cos \delta + i \left(\frac{\sigma_0}{\gamma_0}\right) \sin \delta = G'(\omega) + i G''(\omega) \quad (14)$$

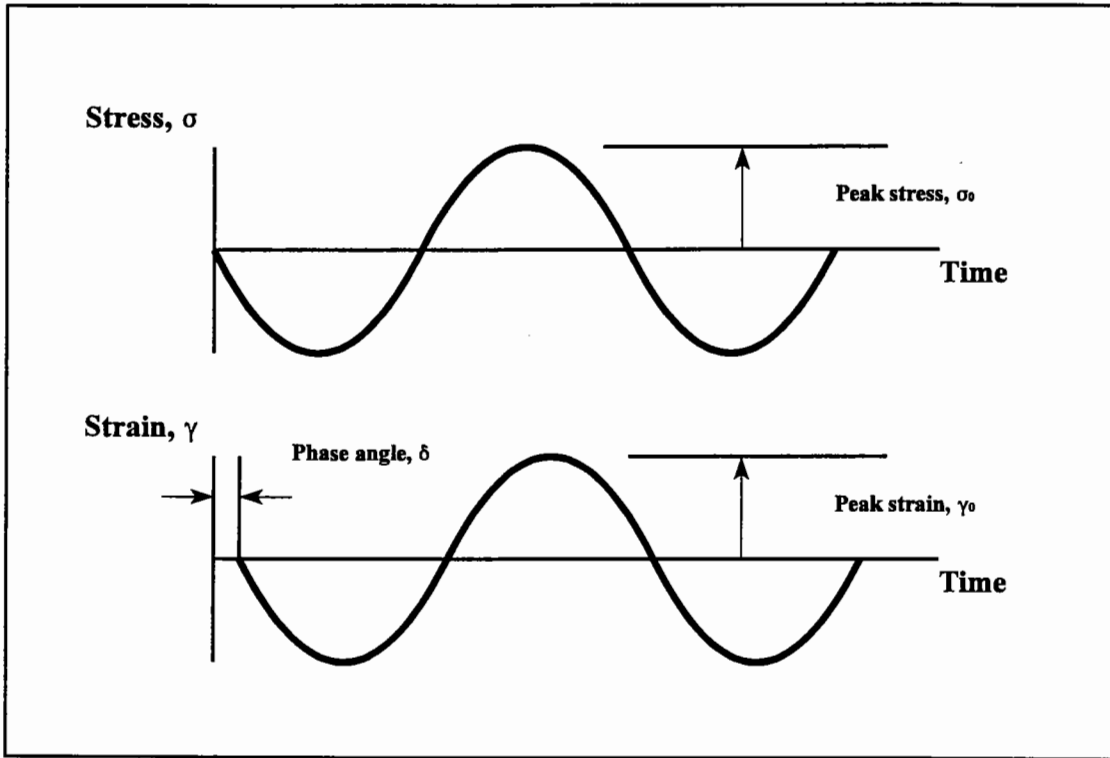


Figure 2.7: Dynamic oscillatory stress-strain functions

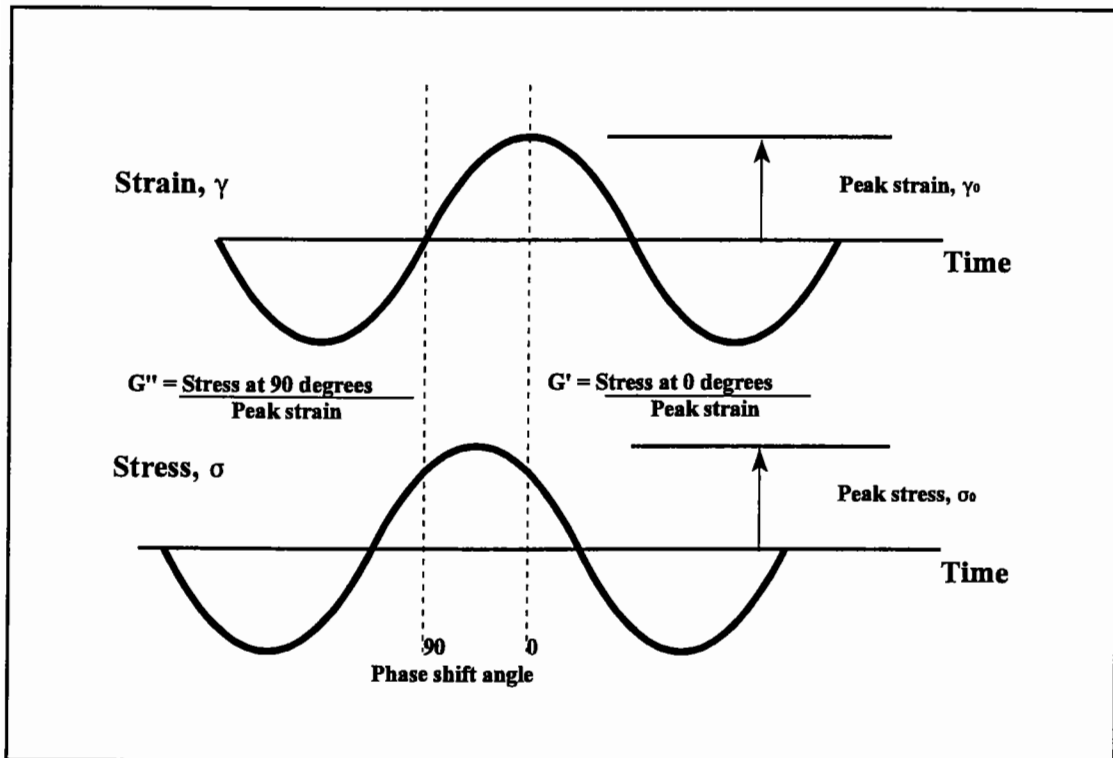


Figure 2.8: Dynamic test outputs from dynamic mechanical analysis (DMA)

where:  $G^*(\omega)$  = complex shear modulus, Pa  
 $\sigma_0$  = peak stress, Pa  
 $\gamma_0$  = peak strain  
 $\delta$  = phase angle, degrees  
 $G'(\omega)$  = storage modulus, Pa  
 $G''(\omega)$  = loss modulus, Pa

which corresponds to the definition for complex shear modulus,  $G^*$ , given in the Eurobitume glossary of rheological terms [56]:

$$G^* = G' + iG'' \quad (15)$$

where:  $G^*$  = complex shear modulus, Pa  
 $G'$  = storage modulus, Pa  
 $G''$  = loss modulus, Pa

The norm of the complex modulus is analogous to the magnitude of a vector, Figure 2.9, as the value is calculated from the square root of the sum of the squares of the components:

$$|G^*| = \sqrt{[(G')^2 + (G'')^2]} \quad (16)$$

The complex shear modulus is also referred to as the complex modulus, shear modulus or simply stiffness.

The in-phase component of  $G^*$  is called the shear storage modulus or commonly the storage modulus. The storage modulus is the real part of the complex modulus and equals the stress that is in phase with the strain divided by the strain, or:

$$G' = G^* \cos \delta \quad (17)$$

The storage modulus describes the amount of energy that is stored and released elastically in each oscillation and is therefore also known as the elastic modulus, or the elastic component of the complex modulus.

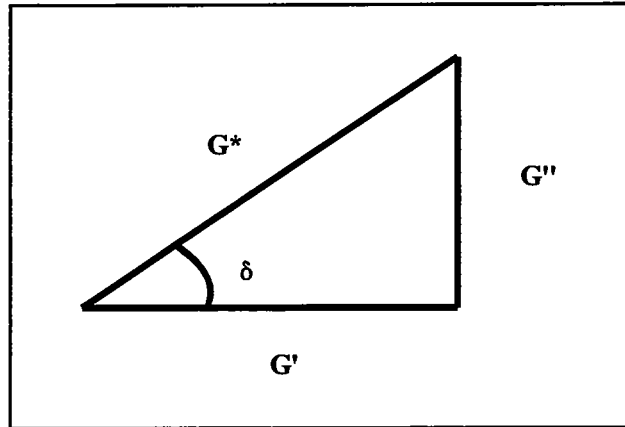


**Figure 2.9: Relationship between complex modulus, storage modulus, loss modulus and phase angle**

The shear loss modulus, or simply the loss modulus, is the out-of-phase component of  $G^*$ . The loss modulus is the imaginary part of the complex modulus and equals the stress  $90^\circ$  out of phase with the strain divided by the strain, or:

$$G'' = G^* \sin \delta \quad (18)$$

The loss modulus describes the average energy dissipation rate in the continuous steady oscillation found in the dynamic test. The loss modulus is also referred to as the viscous modulus or the viscous component of the complex modulus.

At low temperatures, or short loading times, bitumen behaves as a nearly ideal solid and the resulting stress will exactly follow the input strain [19]. At elevated temperatures bitumen will approach ideal liquid (Newtonian) behaviour where the maximum stress will occur when the strain rate is a maximum and therefore  $90^\circ$  out-of-phase with the peak strain.

The storage and loss modulus,  $G'$  and  $G''$ , are sometimes misinterpreted as the elastic and viscous modulus respectively. In reality the elastic component of the response only represents part of the storage modulus and the viscous response only part of the loss modulus. In addition viscoelastic materials exhibit a significant amount of delayed elastic response that is time dependent but completely recoverable. The storage and loss modulus both reflect a portion of the delayed elastic response.

The loss tangent is defined as the ratio of the viscous and elastic components of the complex modulus or simply the tangent of the phase angle:

$$\tan \delta = \frac{G''}{G'} \quad (19)$$

A viscosity value for the bitumen can also be obtained from the dynamic oscillatory test. This viscosity is known as the complex viscosity and is defined as the ratio of the complex modulus and the angular frequency:

$$\eta^* = \frac{G^*}{\omega} \quad (20)$$

where:  $\eta^*$  = complex viscosity, Pa.s or P

The complex viscosity can also be termed the complex dynamic shear viscosity.

Since the complex viscosity is a function of a complex number pair, a real part and an imaginary part of the complex viscosity can also be defined.

The real part of the complex viscosity is termed the dynamic viscosity and defined as:

$$\eta' = \frac{G''}{\omega} \quad (21)$$

where:  $\eta'$  = dynamic viscosity, Pa.s or P

The imaginary part of the complex viscosity is called the out of phase component of  $\eta^*$  and defined as:

$$\eta'' = \frac{G''}{\omega} \quad (22)$$

where:  $\eta''$  = out of phase component of  $\eta^*$ , Pa.s or P

The two most common means of determining the stiffness of bitumen are by creep measurements (constant stress experiments) and dynamic oscillatory measurements (alternating stress and strain of constant amplitude and frequency). Dynamic shear rheometers are used to measure the linear viscoelastic moduli of bitumen in the sinusoidal (oscillatory) loading mode. Measurements can be made at different temperatures, strain and stress levels and test frequencies. They provide the only practical means of obtaining data at short loading times of less than 1 second [79]. However, in the range of intermediate loading times, such as 1 second to 100 seconds, dynamic instruments also provide data that are equivalent to those obtained from transient instruments, such as the sliding plate rheometer. The dynamic data can additionally be transformed by means of time-temperature superposition principles to long loading time data that are relevant to thermal cracking.

It is important that strain sweeps are carried out to ensure that the dynamic tests are conducted in the linear viscoelastic range so that the material functions, such as  $G^*$  and  $\eta^*$ , are independent of the applied strain levels.

The dynamic measurements can be compared to the transient (creep) measurements that are made with the sliding plate rheometer. The transient response is complex because the elastic and viscous components are superimposed in the creep compliance and the creep stiffness [79]. The transient and the dynamic viscoelastic functions can be related mathematically, although the exact relationships are complicated. However, approximate

relationships exist which are frequently accurate enough for practical purposes [66].

Van der Poel [22] defined stiffness as either the inverse of the creep compliance at loading time  $t$ , or the uniaxial dynamic modulus at loading frequency  $1/t$ . Therefore a simple approximation between creep compliance and dynamic complex modulus can be defined as:

$$G^*(\omega) \approx 1 / J(t) \text{ as } t \rightarrow 1/\omega \quad (23)$$

The reciprocal of the shear compliance,  $J(t)$ , obtained at time  $t_i$  is approximately equal numerically to the complex shear modulus,  $G^*(\omega)$  at a frequency  $\omega_i$  where  $t_i = 1/\omega_i$ .

### **Dynamic Shear Rheometer**

The dynamic shear rheometer (DSR) is used to conduct dynamic mechanical analysis (DMA) of bitumen test specimens [19,65,78]. In DMA, a sinusoidal strain is applied to a specimen and the resulting stress is monitored as a function of frequency. This is termed strain-controlled testing and is more common than the stress-controlled dynamic mechanical analysis in which a sinusoidal varying stress is applied and the strain response measured. The DSR is therefore used to measure the linear viscoelastic properties of bituminous binders using a sinusoidal (oscillatory) loading mode. Measurements of stiffness and viscosity can be obtained at different temperatures, stress and strain levels, and test frequencies.

The operational procedure used in dynamic mechanical testing is to impose sinusoidal strains, as an oscillatory shear, on samples of bitumen sandwiched between the parallel disks of the DSR as shown in Figure 2.10 [19]. The amplitude of the responding stress is measured by determining the torque transmitted through the sample in response to the applied strain. The stress and strain parameters are therefore calculated as:

$$\sigma = \frac{2 T}{\pi r^3} \quad (24)$$

where:  $\sigma$  = shear stress  
 $T$  = torque  
 $r$  = radius of parallel disks

$$\gamma = \frac{\theta r}{h} \quad (25)$$

where:  $\gamma$  = shear strain  
 $\theta$  = deflection angle  
 $h$  = gap between parallel disks

The shear stress and strain in equations 24 and 25 are dependent on the radius of the parallel disks and vary in magnitude from the centre to the perimeter of the disk. The shear stress, shear strain and complex modulus, which is a function of the radius to the fourth power, are calculated for the maximum value of radius. The phase angle,  $\delta$ , is measured by the instrument by accurately determining the sine wave forms of the strain and torque.

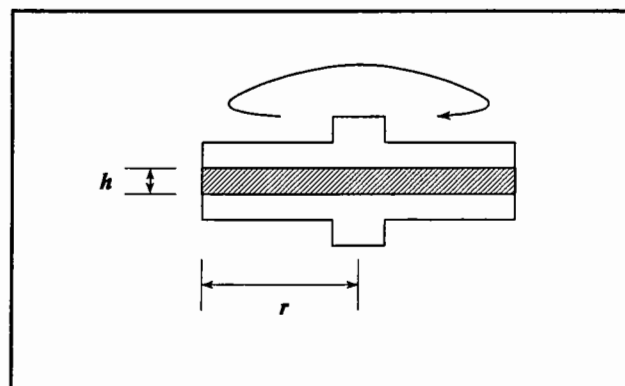


**Figure 2.10: Dynamic Shear Rheometer testing geometry**

The strains that are applied during the dynamic mechanical testing must be kept small to ensure that the test remains in the linear viscoelastic region. Strain sweeps can be used to verify that testing occurs in the linear viscoelastic region. The strain must generally be less than 0.5 percent at low temperatures but can be increased at higher temperatures [19].



Various parallel disk sizes can be used during dynamic mechanical testing. The size of the disk that should be used to test the bitumen decreases as the expected stiffness of the bitumen increases. In other words, the lower the testing temperature, the smaller the diameter of the disk that needs to be used to accurately determine the dynamic properties of the bitumen [19,62].

#### **2.4.5 Time-Temperature Superposition Principle**

One of the primary analytical techniques used in analysing dynamic mechanical data involves the construction of master curves. Work done by various researchers, have found that there is an interrelationship between temperature and frequency (or temperature and loading time) which, through shifting factors, can bring measurements done at different temperatures to fit one overall continuous curve at a reduced frequency or time scale. This continuous curve represents the binder behaviour at a given temperature for a large range of frequencies. The principle that is used to relate the equivalency between time and temperature and thereby produce the master curve is known as the time-temperature superposition principle or the method of reduced variables [66].

Modulus curves at low temperatures crowd together at high frequency values and at very high frequencies they nearly all coincide with one horizontal asymptote. The limiting elastic behaviour is therefore not only independent of frequency, but also nearly independent of temperature. The elastic modulus corresponding with this asymptote is called the glassy modulus,  $G_g$ . However, under viscous conditions, there is no convergence to a single viscous asymptote as viscosity strongly depends on temperature and therefore each temperature gives rise to a separate viscous flow asymptote (Figure 2.5).

Because the limiting viscous behaviour is strongly temperature dependent and the elastic behaviour is not, it is possible to separate the influence of frequency and temperature. The concept of frequency-temperature superposition or time-temperature superposition

is shown in Figure 2.11 which shows an asymptote pair for an arbitrary reference temperature  $T_r$ . If the temperature is increased from  $T_r$  to  $T$  there is a decrease in viscosity by a factor  $a(T)$ . The viscous asymptote at  $T$  therefore lies an amount  $\log a(T)$  below that of  $T_r$ . However, the elastic asymptote is negligibly changed during the temperature rise. The result is that the asymptote pair appears to be shifted a distance  $\log a(T)$  along the  $\log \omega$  axis, because the viscous asymptote has unit slope.

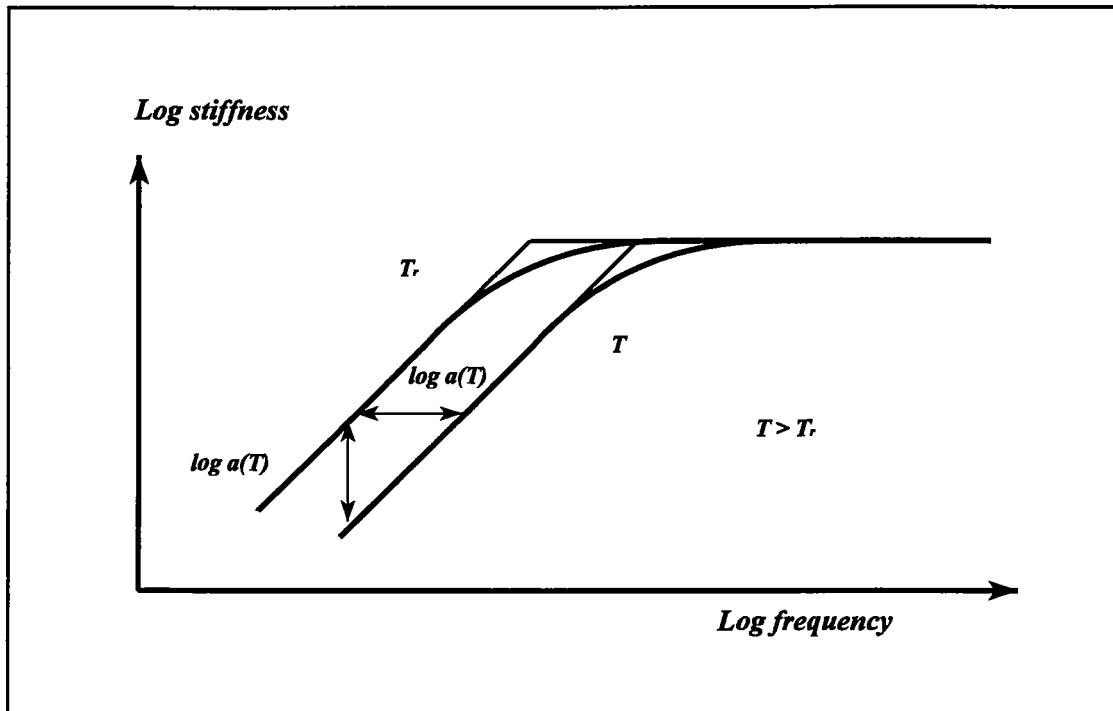


**Figure 2.11: Time-temperature superposition principle**

The viscoelastic response of a bitumen is a transition between the asymptotic viscous and elastic responses and is represented by the curve for  $T_r$ . If a change in temperature causes the modulus curve to shift together with its asymptotes over the same distance  $\log a(T)$ , the material is called “thermorheologically simple”. A reference temperature can be chosen and the next higher modulus curve shifted to coincide with the reference temperature curve to obtain a value for the horizontal shift factor  $\log a(T)$  and a more extended modulus curve. This procedure is repeated for all the other curves in succession to obtain the continuous modulus curve called a master curve. The effect of temperature on complex modulus is, therefore, to shift the curve of  $\log |G^*|$  versus  $\log \omega$  along the  $\log \omega$  axis without changing its shape. This permits the reduction of isotherms of  $\log$

$|G^*|$  versus  $\log \omega$  measured over a wide range of temperatures to a single master curve [66].

The extended time or frequency scale used in a master curve is referred to as the reduced time or reduced frequency scale, where reduced frequency scale is defined as:

$$\log f_r = \log f + \log a(T) \quad (26)$$

where:  $f_r$  = reduced frequency, Hz  
 $f$  = frequency, Hz  
 $a(T)$  = shift factor

The amount of shifting required at each temperature to form the master curve is of special importance and is called the shift factor,  $a(T)$ . A plot of  $\log a(T)$  versus temperature with respect to the reference temperature curve is generally prepared in conjunction with a master curve. These values can be considered to be viscosity changes with respect to the viscosity at the reference temperature and give a visual indication of how the properties of a viscoelastic material change with temperature. The viscoelastic behaviour of a bitumen is therefore represented by two curves, namely viscosity as a function of temperature (shift factor versus temperature), and modulus as a function of frequency at a fixed temperature (master curve).

The time-temperature superposition principle can be expressed as [80]:

$$G(\omega, T) = G(\omega a(T), T_r) \quad (27)$$

where:  $G$  = modulus and may be  $G'$ ,  $G''$  or  $|G^*|$   
 $a(T)$  = shift factor  
 $\omega$  = loading frequency  
 $T$  = temperature  
 $T_r$  = reference temperature

The phase angle can be shifted together with its modulus value, to obtain a curve of phase angle versus the logarithm of reduced frequency.

Because bituminous binders are linear viscoelastic in a wide range of their applications and because they are found to be “thermorheologically simple”, the time-temperature superposition principle can be used to determine master curves and shift factors using the following procedure:

- Dynamic data are first collected over a range of temperatures and frequencies,
- A standard reference temperature must then be selected which is usually 25°C or 0°C,
- The data at all the other temperatures are then shifted with respect to time until the curves merge into a single smooth function.

The shifting may be done based on any of the viscoelastic functions, such as  $G^*$ , and if time-temperature superposition is valid the other viscoelastic functions will all form continuous functions after shifting.

The time-temperature superposition principle can also be applied to creep test data to produce a master curve from the creep data. The horizontal shift factor,  $a(T)$ , needed for the production of the master curve, can be produced for each creep curve determined at a particular test temperature. These shift factors can be plotted against temperature to form, together with the master curve, a complete characterisation of the linear stress-strain-time-temperature response of the bitumen. The time dependency of the bitumen is reflected in the master curve whereas the temperature dependency is reflected in the temperature shift factors,  $\log a(T)$ . The time and temperature dependency of the stress-strain response of the bitumen are therefore separated and characterised by separate parameters as shown in Figure 2.12.

### **Master curves**

Master curves are only valid for the reference temperature used in the master curve plot.

Time-temperature superposition must be applied to calculate the rheological properties at other temperatures. It must be remembered that in interpreting the master curve both the time dependency, as indicated by the master curve, and the temperature dependency, as indicated by the shift factors, must be considered in evaluating the rheological properties of the viscoelastic material. For this reason, isochronal plots are probably more informative and easily interpreted when characterising the rheological properties of bitumen [81].

The shape of the master curve of the complex modulus as a function of the reduced frequency, on a log-log scale, resembles the shape of a hyperbola. The curve has a horizontal asymptote (glassy modulus) at high frequencies and an asymptote at an angle of 45° (viscous part) at low frequencies with a transition range in between. The typical shape of a master curve for an unmodified bitumen is shown in Figure 2.13.

Master curves can also be determined from creep test data. The individual creep curves can be combined into a single master curve by translating the curves along the time axis to obtain a creep curve at a single reference temperature.

### **Shift Factors**

The temperature dependency of the viscoelastic behaviour of bitumen is indicated by means of shift factors and expressed as:

$$a_T = a_T(T, T_{ref}) \quad (28)$$

and therefore depends, for a given system, only on the temperature.

Temperature dependency, as indicated by shift factors, should not be confused with temperature susceptibility, which is an empirical concept based on the change of consistency or hardness of a bitumen with temperature. Temperature dependency is a fundamental concept that indicates how the relaxation processes, within a bitumen, change with temperature.

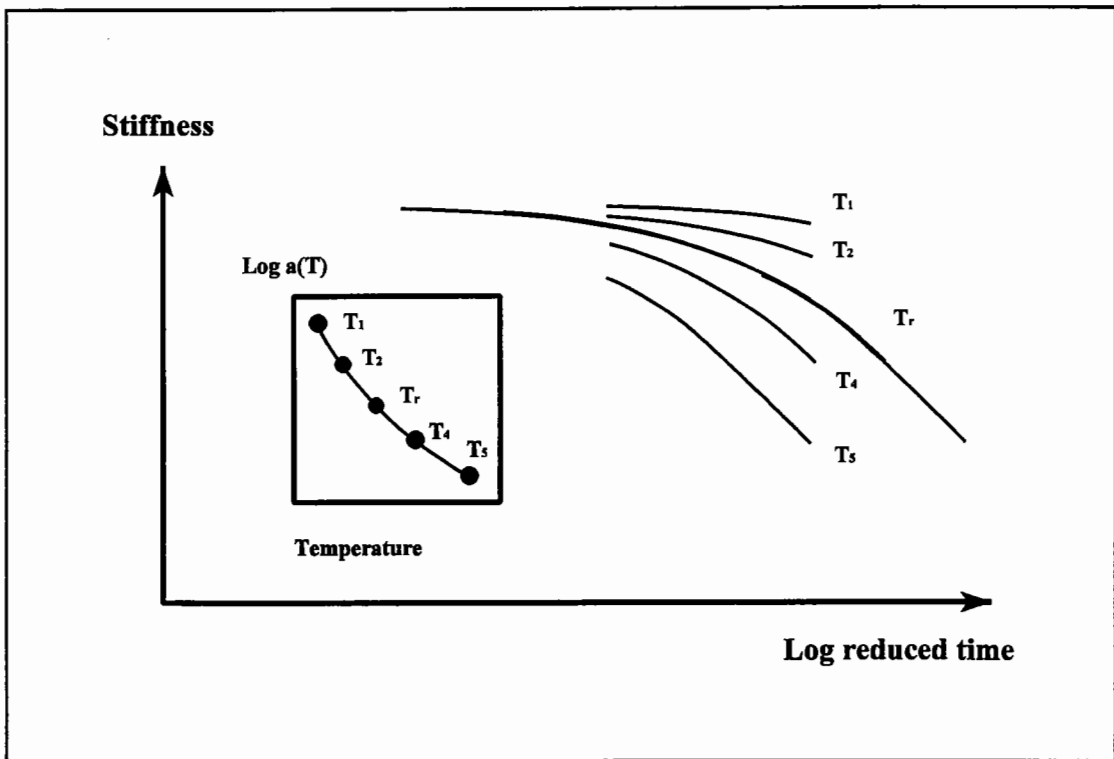


Figure 2.12: Time-temperature superposition in the construction of a master curve

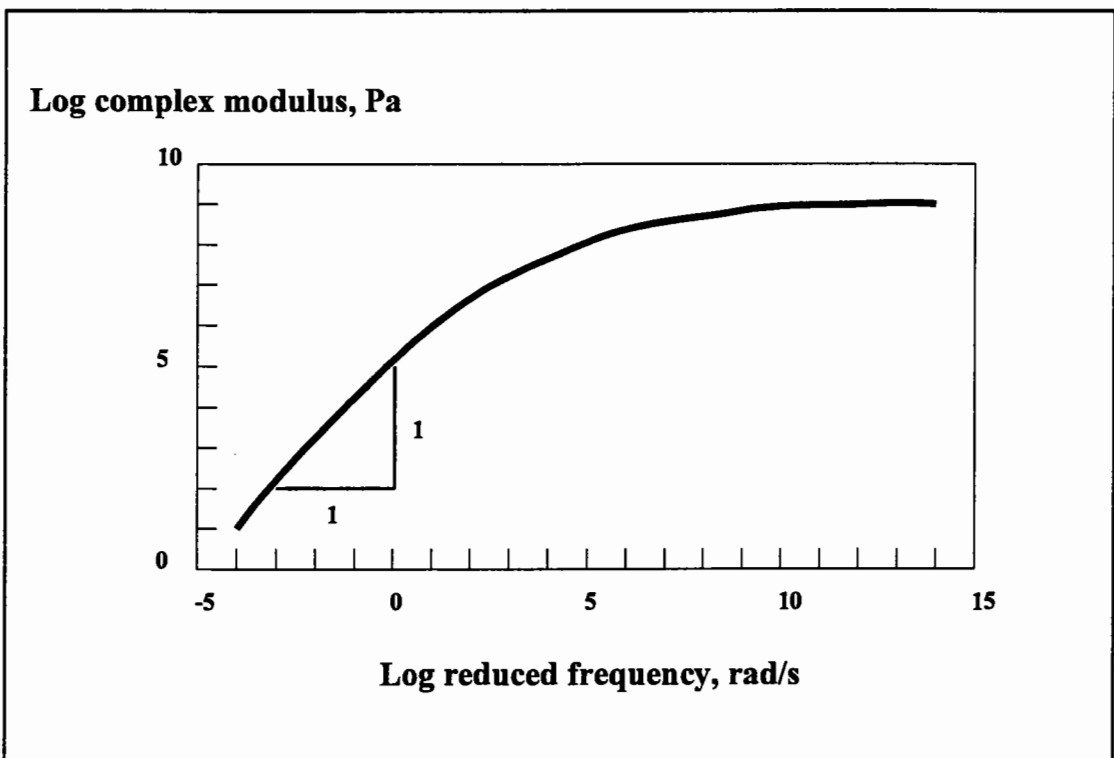


Figure 2.13: Typical complex modulus master curve for bitumen

Viscosity-temperature equations are used to characterise the temperature dependency of bitumens and therefore determine the shift factors needed for the time-temperature superposition principle. The shift factor,  $a(T)$ , can be defined in several ways depending on the mathematical expression used to determine the shift factor.

The Williams Landel and Ferry (WLF) equation [82] has been widely used to describe the relationship between the shift factors and temperature and thereby determine the shift factors of bitumens. The equation is theoretical based on the free volume theory [66] and makes use of temperature differences which makes it suitable for practical manipulations. The equation has also been found to be applicable to bitumen results. The WLF equation is:

$$\log a(T) = \log \frac{\eta_0(T)}{\eta_0(T_r)} = - \frac{C_1(T - T_r)}{C_2 + (T - T_r)} \quad (29)$$

where:

- $a(T)$  = shift factor at temperature T
- $\eta_0(T)$  = Newtonian viscosity at temperature T
- $\eta_0(T_r)$  = Newtonian viscosity at the reference temperature  $T_r$
- $C_1, C_2$  = empirically determined coefficients

The WLF equation requires three constants to be determined, namely  $C_1$ ,  $C_2$ , and  $T_r$ . The constants  $C_1$  and  $C_2$  can be calculated with respect to the reference temperature,  $T_r$ , from the slope and intercept of the linear form of the WLF equation:

$$- \frac{T - T_r}{\log a(T)} = \frac{C_2}{C_1} + \frac{1}{C_1} (T - T_r) \quad (30)$$

The temperature dependency of bitumens can be described by one parameter  $T_r$  if universal constants are used for  $C_1$  and  $C_2$  in the WLF equation. Williams et al [82] proposed that if  $T_r$  is suitably chosen for each materials then  $C_1$  and  $C_2$  could be allotted universal values of 8.86 and 101.6 respectively. Brodnyan et al [83] showed that for

bitumens the universal parameters fitted the data for  $T - T_r > -20^\circ\text{C}$ , but at lower temperatures the predicted shift factors were too great.

Anderson et al [63] have found that for aged and unaged bitumen the constants in the WLF equation are all essentially the same value, with  $C_1$  equal to 19 and  $C_2$  equal to 92 based on a defining temperature,  $T_d$ , which is bitumen specific. These values have also be obtained by Jongepier and Kuilman [84].

Unfortunately  $T_r$ , also known as standard reference temperature,  $T_s$ , or the defining temperature,  $T_d$ , is difficult to determine. Brodnyan et al [83] suggested that  $T_r$  is very similar to the Softening Point. Williams et al [82] proposed that  $T_r$  was related to the glass transition temperature  $T_g$  by the relationship:

$$T_r - T_g = 50^\circ\text{C} \quad (31)$$

Nielsen [85] states that due to the nature of the WLF expression the reference temperature,  $T_r$ , cannot be chosen arbitrarily but must be determined by iteration.

Another equation that can be used to describe the relationship between the shift factors and temperature is the Arrhenius equation:

$$\log a(T) = \frac{\Delta H_a}{2.303R} \left( \frac{1}{T} - \frac{1}{T_{rd}} \right) \quad (32)$$

where:

$a(T)$	=	horizontal shift factor
$\Delta H_a$	=	activation energy, typically 250 kJ/mol
$R$	=	universal gas constant (8.314 J/°K-mol)
$T$	=	temperature, °C
$T_r$	=	the reference temperature, °C

The Arrhenius expression or function requires only one constant to be determined,



namely the activation energy. The reference temperature,  $T_r$ , can be arbitrary chosen [85].

Anderson et al [63] found that for aged and unaged bitumen, the Arrhenius expression is better than the WLF equation at relating shift factors to temperature at low temperatures, below a bitumen specific defining temperature,  $T_d$ .

Both the Arrhenius and WLF equations are based on theoretical considerations and therefore their parameters provide some insight into the molecular structure of bitumen [86].

### **Glass Transition Temperature**

The glass transition temperature,  $T_g$ , is defined as the temperature range at which amorphous polymers change from a glassy to a fluid condition [87]. Bitumens have similar characteristics to amorphous polymers and therefore the glass transition temperature of a bitumen can also be determined.

The dilatometric method has been commonly used to determine the glass transition temperature of a bitumen. Using volume dilatometry,  $T_g$  is defined as the temperature at which there is a change in the sample's cubic thermal expansion coefficient [28,87]. The common approach of obtaining the  $T_g$  value is to manually fit two tangents to the two ends of the measured volume-temperature relationship and take the temperature where the two tangents intersect as the  $T_g$  value.

Volume dilatometry has now been replaced by differential scanning calorimetry (DSC) as the method used to determine the  $T_g$  of bitumen [88]. Using the heating mode, a clearly defined increase in heat capacity, at temperature well below 0°C, corresponds to the glass transition within the hydrocarbon matrix. The  $T_g$  is assumed to be the midpoint of this temperature range [46].

### **Crystallised Fraction (Waxes)**

Certain molecular associations within bitumen, identified by DSC and thermomicroscopy

methods (polarised light and phase contrast), have been defined as "crystallised fraction" or "waxes" [46,88]. These associated species are found mainly in the saturates fraction of bitumen and are thought to be long aliphatic chains held together by weak Van der Waals forces. These aliphatic associations do not necessarily form clearly defined crystalline regions, but agglomerate into small amorphous zones through a precipitation mechanism called spinodal decomposition [46].

The TTSP can be applied to materials that undergo a transition, such as the glass transition, as well as to heterogeneous materials, providing the dispersed phase undergoes no structural change in the transition zone [52]. However, time-temperature equivalency or TTSP does not hold across phase transitions, as found in highly crystalline bitumens (wax contents > 7%), structured bitumen with high asphaltene contents and highly polymer modified bitumens [3,21,86,89,90].

#### **2.4.6 Rheological Data Representation**

In order to study the rheological characteristics of bitumens, including polymer modified bitumens, the data obtained from DMA need to be represented in a useful form. The most common data representation diagram and curves are discussed below.

##### **Isochronal Plots**

An isochronal plot or isochrone is an equation, or a curve on a graph, representing the behaviour of a system at a constant frequency or loading time. In a dynamic test, such as the DSR test, curves of the complex modulus,  $G^*$ , or other viscoelastic functions, versus temperature at constant frequencies are isochrones [56].

##### **Isothermal Plots**

An isothermal plot or isotherm is an equation, or a curve on a graph, representing the behaviour of a system at a constant temperature. In a dynamic test, curves of the complex modulus,  $G^*$ , as a function of frequency at constant temperatures are isotherms [56].

### **Master curves**

In their simplest form, master curves are produced by manually shifting modulus versus frequency plots (isotherms) at different temperatures along the logarithmic frequency axis to produce a smooth master curve [86]. The shift factors may simply be reported in a graphical or tabular format, or they may be regressed or forced to fit some predetermined function such as an Arrhenius function or the WLF equation [86]. Breaks in the smoothness of the master curve indicate the presence of structural changes with temperature within the bitumen, as would be found for waxy bitumens, highly structured 'GEL' type bitumens and polymer modified bitumens.

### **Black Diagrams**

A black diagram is a graph of the magnitude (norm) of the complex modulus,  $|G^*|$ , versus the phase angle,  $\delta$ , obtained from a dynamic test [56]. The frequency and the temperature are therefore eliminated from the plot, which allows all the dynamic data to be presented in one plot without the need to perform TTSP manipulations of the raw data. A smooth curve in a black diagram is a useful indicator of time-temperature equivalency, while a disjointed curve indicates the breakdown on the TTSP and the presence of a high wax content bitumen, a high asphaltene structured bitumen or a highly polymer modified bitumen [89,90].

### **Cole-Cole Diagrams**

A Cole-Cole diagram is a graph of the loss (viscous) modulus,  $G''$ , as a function of the storage (elastic) modulus,  $G'$ . The plot provides a means of representing the viscoelastic balance of the bitumen without incorporating frequency and/or temperature as one of the axes [56].

#### **2.4.7 Rheological Models**

In general all bitumens exhibit a glasslike behaviour at very low temperatures and a relatively fluid behaviour at high temperatures. However, the transition from the glassy to the fluid state, or vice versa, varies substantially from one bitumen to another. This

variation is not a single temperature susceptibility constant and hence no two-point measurement can describe the variation in viscoelastic properties of bitumen and, therefore, bitumens require the time consuming process of determining rheological master curves.

The aim or purpose of a rheological model is to provide a means of calculating the viscoelastic properties of a bitumen, over a full range of frequencies and temperatures, using only a limited amount of experimental data and thereby simulate the master curve. The complex mechanical behaviour of viscoelastic materials, such as bitumen, is a result of the interaction of both time and temperature dependency. In the mathematical modelling of the LVE behaviour of bitumen, these effects must be treated separately. The two effects are known as time dependency and temperature dependency [54]. Time dependency is reflected on the location and shape of the master curve and temperature dependency is indicated by the plot of  $\log a(T)$  versus temperature.

Various researchers have used mathematical models to characterise the master curves of stiffness of bituminous binders. These models include a hyperbolic model proposed by Dickinson and Witt [91], a mathematical model based on empirical observations concerning the shape of master curves of complex modulus,  $G^*$ , versus frequency developed by Dobson [80,92] and a model developed by Jongepier and Kuilman [84] using the relaxation times of bitumen. The latest model has been developed by the Penn State SHRP research team [63,93]. This model has the general hyperbolic shape used in previous models but is simpler in application.

Although all of these models are reasonable accurate, they have their shortcomings. Jongepier and Kuilman's model makes use of integral equations which means that practical calculations with this model are impossible. Dickinson and Witt's model is more practical than Jongepier and Kuilman's model, but the glassy modulus and viscosity in the model are determined statistically and in many cases overestimated. Additionally the mathematics of the model are such that useful manipulation of the various equations is difficult, thus making engineering calculations cumbersome. Christensen and Anderson's

model was found to be reasonably accurate and mathematically simple enough, compared to the other mathematical models, to allow direct engineering calculations. However, the model is not able to model the rheological behaviour of polymer modified bitumens.

It should be recognised that these models are only a reliable simulation of the master curve or viscoelastic properties of a bitumen and further development is needed to account for bitumens that develop structural changes with temperature, such waxy bitumens and PMB's that exhibit a plateau zone in the master curve.

#### **2.4.8 SHRP Binder Specifications**

The Asphalt Research Program of the Strategic Highway Research Program (SHRP) has developed and implemented a number of binder rheological and fracture (failure) tests that measure the physical properties of bitumen. The fundamental properties, obtained from these new or improved test methods have been used to develop a performance related specification as part of Project A-002A [94]. The two criteria that will be of most interest within the climatic conditions of the U.K. are the rutting and fatigue parameters.

##### **SHRP Rutting Parameter**

Although rutting of asphalt mixtures is influenced primarily by mixture properties, the properties of the binder are also important. This is particularly true for PMB's, which are claimed to enhance the rutting resistance of asphalt pavements. As rutting is more prevalent at high temperatures, the properties relating to rutting should be measured at high temperatures. Ageing of the bitumen also increases the stiffness and therefore the resistance to rutting and consequently the rutting criteria should be measured on unaged or RTFOT aged bitumen [3].

Based on these observation, a measurement of the non-recoverable deformation of bitumen at high temperatures, was established as a suitable rutting parameter for bitumen. A loading time of 0.1 seconds was chosen to represent the loading time within the pavement, which can be attributed to a truck tyre travelling at 80 km/h [3]. Using DMA,

this 0.1 second loading time is equivalent to sinusoidal loading at 10 rad/sec (1.59 Hz).

The specification criterion for rutting was taken as the inverse of the loss compliance,  $1/J''$ , which is numerically equal to the complex modulus divided by the sine of the phase angle,  $G^*/\sin\delta$  [94]. The SHRP specification states that at the maximum pavement design temperature,  $G^*/\sin\delta$  for the unaged bitumen must be greater than 1.0 kPa and for the RTFOT aged bitumen greater than 2.2 kPa [3,94].

### **SHRP Fatigue Parameter**

Fatigue cracking generally occurs late in the life of the pavement and therefore the bitumen needs to be tested after appropriate long term ageing. The fatigue parameter was chosen to reflect the energy dissipated per load cycle, which can be calculated as  $G^*\sin\delta$  in a dynamic shear test [66]. The SHRP specification requires that at the intermediate pavement design temperature, the  $G^*\sin\delta$  at 10 rad/s must be less than 5.0 MPa [3,94].

One of the main advantages of the research undertaken during the SHRP study is the measurement of fundamental properties, such as  $G^*$  and  $\delta$ , at various temperatures and loading times compared to the single point measurements obtained from empirical tests, such as Penetration and Softening Point. However, this advantage may be lost through the selection of the basically empirical parameters of  $G^*/\sin\delta$  and  $G^*\sin\delta$  from the available DSR rheological data to describe the performance of bituminous binders. This is particularly relevant for modified binders, such as PMB's, which, due to their complex rheological behaviour, require greater quantities of data for their complete characterisation.

## **2.5 Bitumen Ageing**

Bitumen, like many other organic substances, is affected by the presence of oxygen, ultraviolet radiation and by changes in temperature. These external influences cause bitumen to harden, resulting in a decrease in Penetration and an increase in Softening Point and viscosity [1].

There are four principal mechanisms of bitumen hardening:

- Oxidation,
- Loss of volatiles,
- Steric hardening, and
- Exudative hardening (loss of lighter bitumen fractions by absorption into the mixture aggregate).

Of the four mechanisms, oxidative hardening is considered to be the main cause of bitumen ageing. Bitumen slowly oxidises when in contact with air, with atmospheric oxygen reacting with the more reactive components of bitumen, producing compounds of high polarity through oxidation, dehydrogenation, condensation and polymerisation reactions. The formation of these highly polar compounds produce forces of molecular interaction, that cause the polar oxygen-containing groups to associate into micelles of higher molecular weight, causing gelification and hardening of bitumen thereby increasing the viscosity of the bitumen. The chemical functional groups that are formed during oxidative ageing include polar hydroxyl, carbonyl and carboxylic groups, which result in the formation of larger more complex molecules, which make the bitumen harder and less flexible (embrittlement).

The evaporation of the more volatile components of the bitumen can also be significant, although penetration grade bitumens are relatively involatile and, therefore, hardening resulting from loss of volatiles is usually fairly small. Steric hardening occurs at ambient temperatures and is attributed to reorientation of bitumen molecules and the slow crystallisation of waxes. However, the process is reversible and the unaged properties can be achieved with reheating and cooling. Exudation hardening is a function of both the exudation tendency of the bitumen and porosity of the aggregate.

The changes in fractional chemical composition of bitumen associated with ageing are shown in Figure 2.14, where there is, firstly, a continued increase in asphaltenes after progressively longer ageing, oxidation times. Elemental analysis of the asphaltenes shows

that there is also an increase in the oxygen content during ageing [35]. Secondly, Figure 2.14 shows that the naphthene aromatics content decreases throughout the oxidation period. The decrease in the naphthene aromatics fraction occurs at a relatively high rate in the initial stages of oxidative ageing and then decreases to a more uniform, slower rate at longer oxidation times. The sulphur content of the naphthene aromatics decreases during ageing as the molecules, with this heteroatom, become polar and are therefore excluded from this fraction [35].

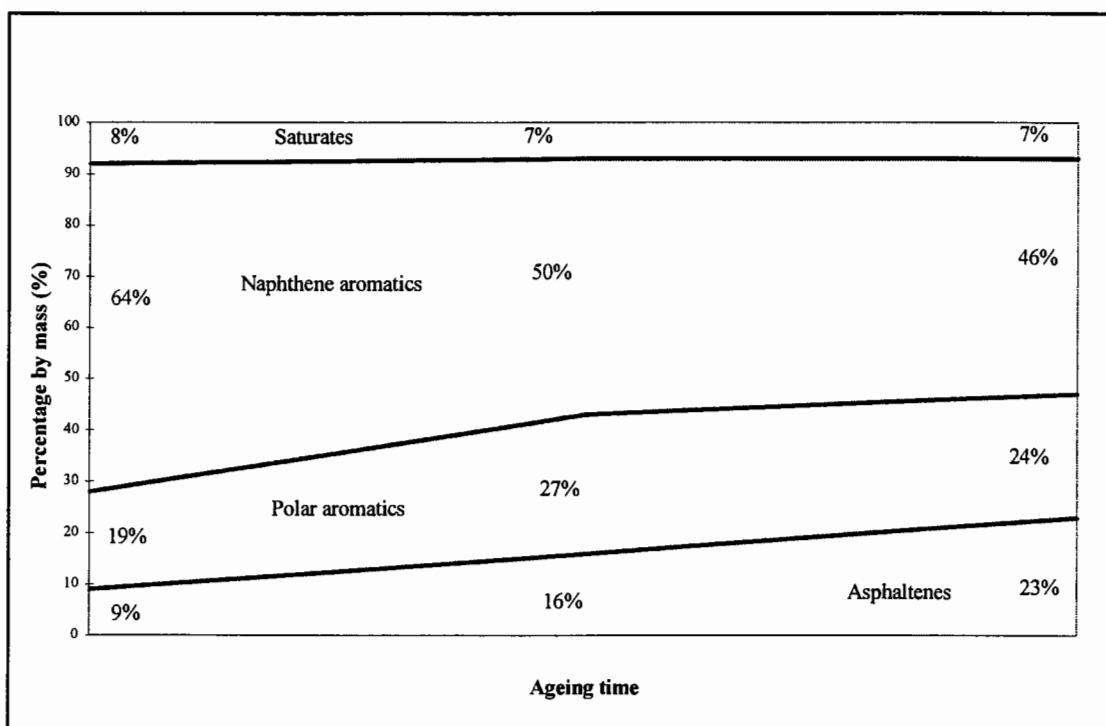


**Figure 2.14: Changes in fractional chemical composition as a function of ageing**

The polar aromatics, as shown in Figure 2.14, increase during the initial stages of oxidation, up to a maximum and then decrease in content. The increase in this fraction coincides with the rapid reduction in the naphthene aromatics content and starts to decrease at the point where the decrease in naphthene aromatics is considerably slower than during the initial stages of ageing. The increase in polar aromatics, during the initial stages of ageing, results from the contribution from the naphthene aromatics being greater than the loss suffered by transformation to asphaltenes. Once the rate of decrease of the naphthene aromatics has slowed down, the loss suffered by transformation to asphaltenes is greater and therefore there is a decrease in polar aromatics.



The polar aromatics therefore either increase or decrease during oxidative ageing, depending on the equilibrium between its transformation into asphaltenes and its formulation from naphthene aromatics. However, the total sum of the aromatics (naphthene and polar) decrease during oxidation. This is expected since they do not receive any contributions and have to feed the asphaltenes fraction.

The saturates fraction decreases slightly during oxidation, as seen in Figure 2.14, and is probably a result of volatilisation of some of the saturate components.

The process of bitumen ageing or hardening occurs in three stages:

- Hardening of bitumen during mixing with aggregate,
- Hardening of bitumen in a mixture during storage, transport and laying, and
- Hardening of bitumen in the road.

The majority of bitumen hardening occurs during mixing and to a lesser extent during storage, transport and laying. However, hardening of the bitumen can also occur on the road, with the main factor influencing the degree of hardening being the void content of the asphalt mixture.

Laboratory test methods have been designed to simulate both short term and long term ageing. Most of these laboratory tests utilise thin film ovens to age the bitumen in an accelerated manner.

### **Thin Film Oven Test**

The Thin Film Oven Test (TFOT) was introduced by Lewis and Welborn [95] to simulate the short term ageing which a bitumen undergoes during mixing in an asphalt mixing plant. In the test 50 g of bitumen is placed to a depth of 3.2 mm in a flat, 140 mm diameter container and stored at 163°C for 5 hours. The residue is then tested for Penetration, ductility and Softening Point. The test was adopted by the American Society for Testing and Material (ASTM) in 1969 as test method ASTM D1754 [96].

### **Rolling Thin Film Oven Test**

The most significant modification to the TFOT involves placing bitumen in a glass jar and rotating it such that thinner films than the 3.2 mm used in the TFOT can be aged. The Rolling Thin Film Oven Test (RTFOT) test therefore simulates far better the hardening which a bitumen undergoes during mixing [97,98].

In the RTFOT eight glass cylinders each containing 35 g of bitumen are fixed in a vertically rotating shelf. During the test, the bitumen flows continuously around the inner surface of each container in relatively thin films of 1.25 mm. The method ensures that all the bitumen is exposed to heat and air and the continuous movement ensures that no skin develops to protect the bitumen. The conditions in the test are not identical to those found in practice but experience has shown that the amount of hardening in the RTFOT correlates reasonably well with that observed in a conventional batch mixer [1]. The RTFOT was adopted by ASTM in 1970 as ASTM D2872 [96].

### **Pressure Ageing Vessel**

The SHRP A-002A research team developed a method involving the use of the Pressure Ageing Vessel (PAV) which is used to simulate the physical and chemical property changes that occur in bitumens as a result of long term, in-service oxidative ageing in the field [93].

The method involves oxidation of bitumen in the RTFOT - ASTM D2872 [96] or the TFOT - ASTM D1754 [96] followed by oxidation of the residue in a pressurised ageing vessel (PAV) [14,65]. The PAV test consists of ageing 50 g of bitumen placed in a pan within a heated vessel pressurised with air to 2.1 MPa for 20 hours at temperatures between 90 and 110°C. The particular ageing temperature is dependent on the climatic region where the binder will be put into service and is selected from the SHRP performance graded binder specification [14]. The test accounts for temperature effects but is not intended to account for mixture variables such as air voids, aggregate type and aggregate adsorption [65,78].

The ageing of bitumen is commonly evaluated by means of an ageing index. The generic form of the ageing index can be expressed in the following equation:

$$\textit{Ageing Index} = \frac{P_{\textit{AGED}}}{P_{\textit{UNAGED}}} \quad (33)$$

where:  $P_{\textit{UNAGED}}$  = some physical property (e.g. Penetration, viscosity, Softening Point, etc) measured on the unaged bitumen)

$P_{\textit{AGED}}$  = the same physical property as measured on the unaged bitumen but performed after the bitumen has been aged in some fashion (e.g. RTFOT, PAV, etc)

## 2.6 Bitumen Modification

Conventional bituminous material have tended to perform satisfactorily in most highway pavement and airfield runway applications. However, in recent years, increased traffic levels, larger and heavier trucks, new axle designs and increased type pressures, have added to the already severe demands of load and environment on the highway system, resulting in the need for enhancement of the properties of existing asphalt material [99].

As bitumen is responsible for the viscoelastic behaviour characteristic of the asphalt mixture, it plays an important part in road performance aspects such as permanent deformation resistance and cracking resistance. In general, the non-recoverable induced strain in an asphalt mixture is attributed to viscous flow and increases with both loading time and temperature [1]. Bitumen modification offers one solution to overcome the deficiencies of bitumen and thereby improve the performance of asphalt mixtures.

One of the primary roles of a bitumen modifier is to increase the resistance of the asphalt to permanent deformation at high service temperatures, without adversely affecting the properties of the asphalt at other temperatures. This is achieved by either stiffening the bitumen so that the total viscoelastic response of the asphalt is reduced, with a corresponding reduction in permanent strain (deformation), or by increasing the elastic component of the bitumen, thereby, reducing the viscous component again with a reduction in permanent strain.

Increasing the stiffness of the bitumen will also increase the dynamic stiffness of the asphalt and, thereby, improve the load spreading ability of the material and reduce critical strains. This will increase the expected design life for a given asphalt layer thickness. Increasing the elastic component of the bitumen response will improve the flexibility of the asphalt which is important where high tensile strains are present.

The modifiers which are currently available fall into various categories, including naturally occurring materials, industrial by-products and waste materials as well as carefully engineered products. Some of the more common categories include, reclaimed rubber products, fillers, fibres, catalysts, extenders and finally polymers.

### **2.6.1 Reclaimed Rubber Products**

Reclaimed rubber is generally obtained from grinding down old vehicle tyres to a desired gradation and then modifying by the addition of plasticisers, by chemical devulcanisation or by the addition of natural or synthetic rubbers [99]. There are two reclaimed rubber modifying processes, known as the “wet” process and the “dry” process. The “wet” entails the bitumen being preblended with the ground rubber resulting in a modified binder known as “bitumen rubber”. The “dry” process consists of a rubber-filled system in which the scrap rubber is added during the mixing process to produce the modified asphalt mixture.

In the “wet” system, the process of dispersing the rubber into the bitumen can be

difficult, requiring high temperatures and long digestion times and can result in a heterogeneous binder, with the rubber acting mainly as a flexible filler [1]. During the “wet” process, the rubber particles are known to swell to at least twice their original volume. This swelling results in an increase in viscosity of the bitumen-rubber blend and the establishment of a three dimensional network lattice [99].

### **2.6.2 Fillers**

Fillers are generally added to asphalt mixtures to improve the stiffness and load carrying capabilities of the material. They are normally inert, but their physical properties can influence the performance of the asphalt mixture. These properties include surface area, particle shape, particle size, packing arrangement and void volume. Typical fillers that have been used as modifiers are carbon black, lime and hydrated lime [34,99].

### **2.6.3 Fibres**

Fibres have been used to improve the cohesive and tensile strengths of asphalt mixtures. They are used to reinforce and toughen the material and thereby increase the amount of strain energy that can be absorbed during fatigue and fracture of the asphalt mixture [100].

Finely divided fibres, with a high surface area per unit weight, can also act as filler materials with the ability to prevent binder run-off during mixing, transportation and construction operations. This form of modification is used extensively to ensure the formation of thick binder films in porous asphalt mixtures.

### **2.6.4 Catalysts (Organo-Manganese Compounds)**

Catalysts are used to accelerate the stiffening of bitumen and improve the temperature susceptibility of modified asphalt mixtures. Catalyst modified mixtures not only have reduced temperature susceptibility and increased stiffness, but show an increase in

deformation resistance with time [101,102]. However, the fatigue resistance of the modified asphalt mixture is inferior when compared to conventional asphalt mixtures [99]. This can be compensated for by the lower tensile strains that will be obtained from the stiffer asphalt mixture, but the modified mixtures will still be susceptible to cracking.

#### **2.6.5. Extenders (Sulphur Addition)**

The addition of sulphur to an asphalt mixture improves both workability and eventually the stiffness of the compacted mixture [103]. The stiffening mechanism is, however, time dependent due to a possible retardation of the crystallisation of the sulphur and initially the stiffness of the mixture may be lower than that of an unmodified mixture.

#### **2.6.6 Polymer Modified Bitumens**

Polymers have traditionally been used to improve the temperature susceptibility of bitumens by increasing binder stiffness at high service temperatures and reducing stiffness at low service temperatures. In addition, the PMB should possess improved resistance to permanent deformation, thermal and fatigue cracking [99]. The degree of modification depends on the polymer properties, polymer content and the nature of the base bitumen.

Polymers can generally be separated into two broad categories, namely:

- Plastomers, and
- Elastomers.

Plastomers form a tough, rigid, three dimensional network to resist deformation, while elastomers have a characteristically high elastic response and, therefore, resist permanent deformation by stretching and recovering their initial shape. Plastomers can be further subdivided into thermoplastics and thermosets (thermosetting resins), and elastomers into natural and synthetic rubber.

## Thermoplastic Polymers

Thermoplastics are characterised by softening on heating and hardening on cooling. Polyethylene (PE), polypropylene (PP), polyvinyl chloride (PVC), polystyrene (PS) and various ethylene copolymers (semi-crystalline polymers), such as ethylene vinyl acetate (EVA), ethylene methyl acrylate (EMA) and ethylene butyl acrylate (EBA), are the principal thermoplastic polymers. These polymers increase the viscosity and stiffness of bitumen at normal service temperatures.

EVA polymers have been widely used in the road construction industry for more than 20 years, where they improve both the workability of the asphalt during compaction and its deformation resistance in service [104]. EVA polymers significantly improve the bitumen properties but to a different extent depending on the bitumen source and the polymer characteristics [105]. For this reason manufacturers have needed to identify suitable bitumen sources and appropriate polymers to ensure the production of superior quality PMB's. Bitumen fluxing with compatibilising oils or polymer "over-addition" can be used to improve the performance of poorly produced PMB's, but these solutions are obviously less cost effective.

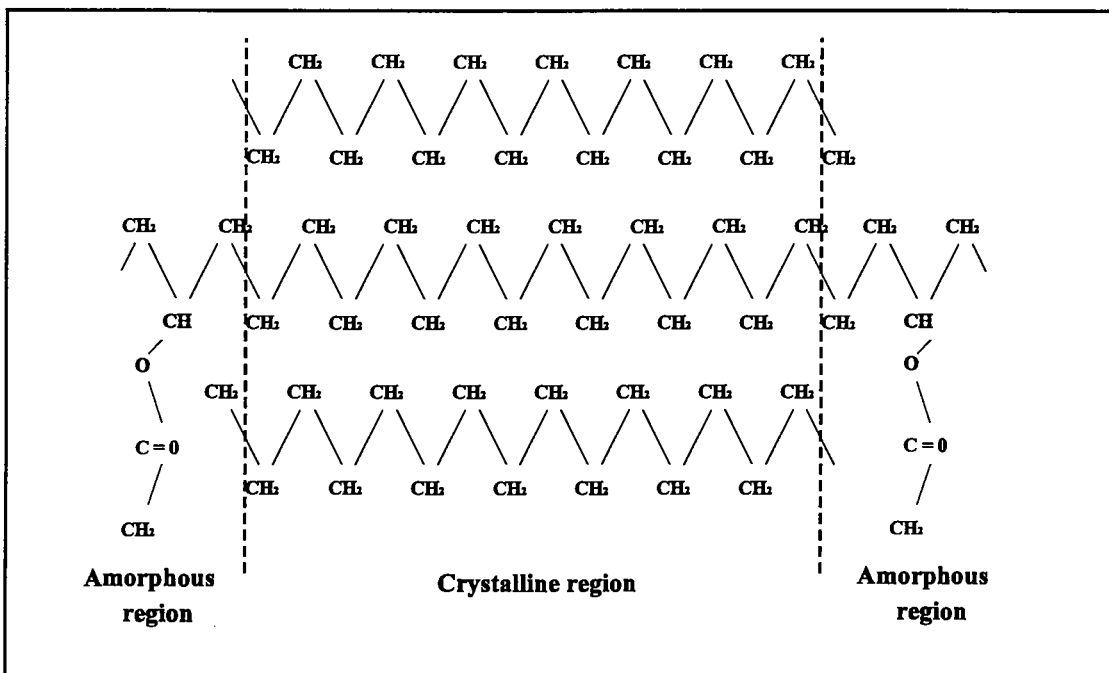


Figure 2.15: EVA copolymer structure

EVA copolymers consist of a random structure produced by the copolymerisation of ethylene and vinyl acetate. The structure of the EVA copolymer is shown in Figure 2.15 and consists of the closely packed, regular polyethylene segments of the chain, that form the crystalline regions, and the bulky vinyl acetate groups, that form the non-crystalline or amorphous rubbery regions. The properties of EVA copolymers are controlled by the molecular weight and vinyl acetate content of the polymer. The molecular weight of the polymer is measured by its melt flow index (MFI), which is inversely related to molecular weight and is analogous to the Penetration test for bitumen [1]. The proportion of vinyl acetate in the copolymer determines whether the behaviour of the EVA will be more crystalline, stiff and reinforcing in character or more amorphous and rubbery.

EVA copolymers are easily dispersed in and have good compatibility with most available bitumens and are thermally stable at normal mixing and handling temperatures [1,34]. When the EVA copolymer is blended with the base bitumen, portions of the “oil fraction<sup>5</sup>” of the bitumen are absorbed by the amorphous phase causing the polymer to swell [106,107,108]. Only the amorphous, low molecular weight fractions of the polymer are involved in this dissolution reaction between the bitumen and the polymer. EVA copolymers with a low vinyl acetate content and high molecular weight, therefore do not absorb “oil” significantly, due to their high crystallinity [106,108].

The quantity and chemical composition of the “oil fraction” of the bitumen and the crystallinity of the semi-crystalline polymer are critical in determining the rheological character of ethylene copolymer modified bitumen. Highly crystalline polymers, that do not absorb sufficient quantities of oil, do not swell and therefore tend to behave simply as fillers in the modified bitumen, therefore reproducing a generally bitumen-like rheological character. At the same time, polymers that dissolve too easily in the PMB matrix, lose their mechanical characteristics resulting in a blend that again shows a bitumen-like behaviour [108]. Too high a degree of compatibility will therefore mask the properties of the EVA copolymer, and hence a certain degree of incompatibility is

---

<sup>5</sup> Oil fraction consists of the aromatic oils and saturates of the bitumen



required to produce an optimum blend.

### Elastomers

Elastomers such as natural rubber (NR), polybutadiene (BR), polyisoprene (IR), isobutene isoprene copolymer (IIR), polychloroprene (CR), styrene butadiene rubber (SBR) and styrenic block copolymers have been used to modify bitumen. Of these groups, the styrenic block copolymers have the greatest potential when blended with bitumen [109]

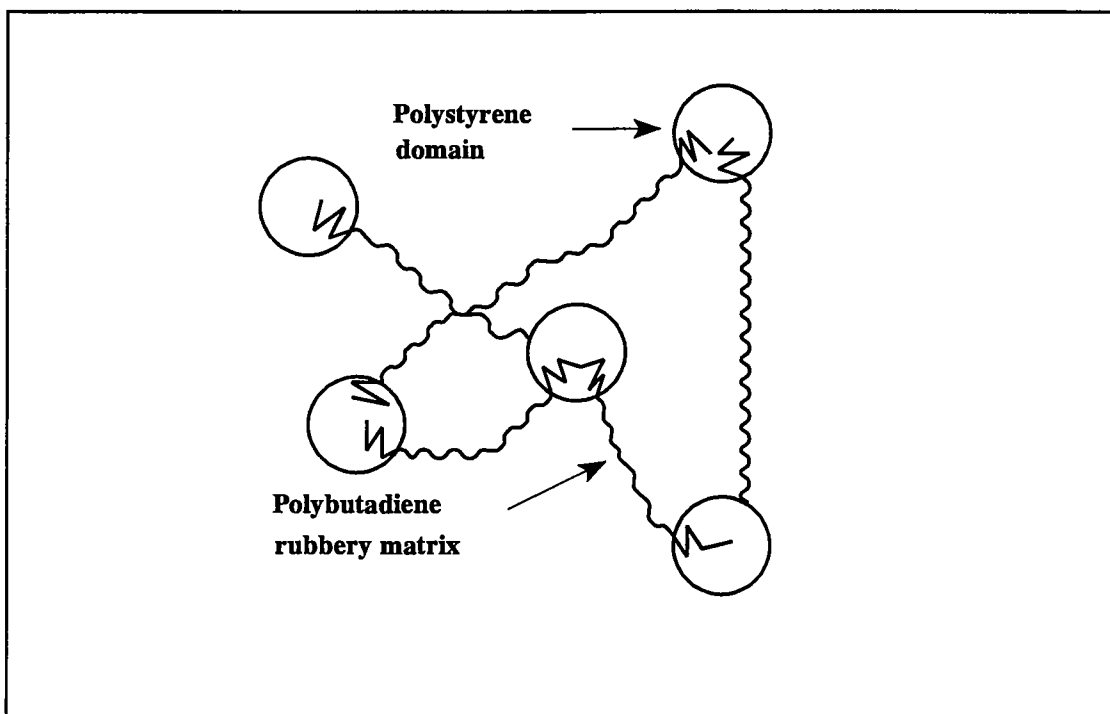


**Figure 2.16: SBS copolymer structure**

Styrenic block copolymers, commonly termed thermoplastic rubbers (TR) due to their ability to combine both elastic and thermoplastic properties, may be produced by a sequential operation of successive polymerisation of styrene-butadiene-styrene (SBS) or styrene-isoprene-styrene (SIS). Alternatively, a di-block precursor can be produced by successive polymerisation of styrene and mid-block monomer, followed by a reaction with a coupling agent [1]. Therefore, not only linear copolymers but multi-armed copolymers, known as star-shaped, radial or branched copolymers, can be produced. The structure of a SBS copolymer is shown in Figure 2.16 and consists of styrene-butadiene-

styrene tri-block chains, having a two phase morphology of spherical polystyrene block domains within a matrix of polybutadiene [1,34].

SBS copolymers derive their strength and elasticity from physical cross-linking of the molecules into a three-dimensional network. The polystyrene end-blocks impart the strength to the polymer and the polybutadiene or polyisoprene rubbery matrix mid-blocks give the material its exceptional elasticity. The effectiveness of these cross-links diminishes rapidly above the glass transition temperature of polystyrene of approximately 100°C, but the polystyrene domains will reform, and the strength and elasticity will be restored on cooling [1,34].

When SBS is blended with the base bitumen, the elastomeric phase of the SBS copolymer absorbs maltenes (oil fractions) from the bitumen and swells up to nine times its initial volume [34,106]. At suitable SBS concentrations (commonly 5% to 6% by mass), a continuous polymer network (phase) is formed throughout the PMB, significantly modifying the bitumen properties. As thermoplastic rubbers have molecular weights similar to or higher than that of asphaltenes, they compete for the solvency power of the maltene phase and phase separation can occur if insufficient maltenes are available. This phase separation is an indication of the incompatibility of the base bitumen and the polymer and care should be taken when blending thermoplastic rubber PMB's. The compatibility of the SBS - bitumen blend can be improved through the addition of aromatic oils. However, too high an aromatic content in the blend will dissolve the polystyrene blocks and destroy the benefits of the SBS copolymer in the PMB.

#### **2.6.7 Fluorescent Microscopy**

A first approach to obtaining information on the structural changes associated with polymer modification is by fluorescent microscopy (UV reflection microscopy), which permits the characterisation of the PMB blend from a microstructural standpoint. The morphology of the PMB mixture is generally seen as a two-phase system with a bitumen-

rich phase and a polymer-rich phase. The polymer-rich phase results from the selective absorption of part of the low molecular weight components, oils, which are initially present in the base bitumen or which are added to the PMB blend.

With the fluorescent microscopy technique, the bitumen-rich phase appears dark while the polymer-rich phase appears light. However, when bitumen is broken down into its broad fractional components, the asphaltenes and saturates appear dark, but the naphthenic and polar aromatics appear light [62]. It is the aromatic oils, absorbed to swell the polymer, that result in the light appearance of the polymer-rich phase.

In the two phase system, one of the phases is generally the continuous phase with the other phase being dispersed within the continuous phase. The selection of the continuous phase and the dispersed phase and therefore the morphology of the PMB is a function of the composition of the base bitumen, the polymer concentration and the nature of the polymer [106].

An effective bitumen modification is obtained when the polymer can build up a continuous phase containing the bitumen in the form of finely dispersed droplets composed of an assembly of precipitated asphaltene particles [105]. The oil fractions of the bitumen swell the elastomeric phase of the SBS copolymer and the amorphous phase of the EVA copolymer, while the incompatible fractions will be present as discrete domains dispersed in the polymeric matrix [106]. Under these conditions, the rheological performance of a PMB should reflect the overall behaviour of the polymer that is incorporated in the PMB.

In the case where the polymer is dispersed in a continuous bitumen-rich phase, the rheological behaviour of the PMB blend should reproduce that of the bitumen. The analysis of the morphology of the PMB's can, therefore, be considered as the first step in estimating the rheological behaviour of the polymer-bitumen blends. However, the fluorescent image is limited in its ability to accurately describe the complex rheological characteristics of PMB's and, therefore, is limited to production control of PMB's.

## 2.7 Summary

The chemistry of bitumen has been briefly described in order to provide a background to understanding the rheological characteristics of penetration grade bitumens and polymer modified bitumens (PMB's). High pressure gel permeation chromatography (HP-GPC) has the ability to measure the molecular mass distribution of both penetration grade bitumens and PMB's as well as the degradation of SBS polymers during ageing. Differential scanning calorimetry (DSC) can be used to measure the changes in enthalpy associated with different polymer contents and ageing conditions of EVA PMB's. Infrared spectroscopy (IR) provides an explanation of the oxidative ageing process by calculating the changes in the spectra associated with particular ageing products for penetration grade bitumens and PMB's. These three chemistry tests will be used in the following chapters to explain the rheological characteristics of aged and unaged PMB's. Other chemistry tests, such as nuclear magnetic resonance (NMR) spectroscopy and optical thermomicroscopy techniques, such as phase contrast microscopy (PCM) and polarised light microscopy (PLM), have great potential for the chemical analysis of PMB's, but unfortunately could not be used in this thesis.

The literature review has explained in detail the dynamic mechanical analysis (DMA) technique, that will be used in the following chapters, and described the most useful rheological presentation methods for bitumen rheological characterisation. Dynamic shear rheological testing using the Dynamic Shear Rheometer (DSR) provides a practical and relatively simple method of obtaining the large quantities of rheological data, at various temperatures and loading frequencies, required for the complete characterisation of PMB's. Combinations of isochronal plots, master curves, Black diagrams and Cole-Cole diagrams provide the means of representing this rheological data in a convenient and useful form.

The various rheological models, derived by Jongepier and Kuilman, Dobson, Dickinson and Witt, and Christensen and Anderson, allow the rheological characteristics of a bitumen to be calculated using only a limited amount of experimental data. However, no

matter how accurate and mathematically sound, they are still only simulations of the viscoelastic properties of the bitumen. Factors such as wax crystallisation, asphaltene structuring and more importantly polymer modification lead to a breakdown of the time-temperature equivalency of bitumen and, therefore, a nullification of these models. These models are, therefore, not recommended for research purposes and will not be used to investigate the rheological characteristics of PMB's in this thesis.

The chemical and physical consequences of oxidative ageing, as pertaining to unmodified, penetration grade bitumens, have been described as well as the currently used methods of laboratory simulation of short and long-term ageing. The oxidative ageing of unmodified bitumens results in a chemical transition of the light, non-polar components to heavier, polar components and a consequential hardening of the bitumen. The rolling thin film oven test (RTFOT) and the pressure ageing vessel (PAV) have been chosen as the short and long-term laboratory ageing methods that will be used in the work described in Chapter 5.

Two of the most commonly used polymers in bitumen modification are the semi-crystalline polymer, ethylene vinyl acetate (EVA), and the thermoplastic rubber, styrene butadiene styrene (SBS). These two polymers were chosen to produce the polymer modified bitumens (PMB's) that were used in this research.

The rheological characteristics of the different PMB's depend on the nature of the polymer, the polymer content and the nature of the base bitumen. The compatibility of the different bitumen-polymer blends dictates whether the modification will be dominated by the polymer (polymeric-type modification) or simply a filler-type modification. With regard to EVA PMB's, a degree of incompatibility is required to obtain a polymeric-type modification and, therefore, rheological behaviour. Highly compatible blends dissolve the EVA copolymer so that the polymeric nature of the copolymer is lost resulting in a filler-type modification and rheological behaviour. At the other extreme, EVA copolymers that cannot absorb sufficient quantities of "oil fraction" to dissolve the copolymer will also result in filler-type modification and rheological

behaviour. The compatibility requirements (chemistry) for SBS PMB's are considerably more complicated but still dictate the creation of a polymeric or filler-type modification and rheological behaviour.

# 3 Bitumen Rheology Testing Procedure

## 3.1 Introduction

Currently, different activities in standardisation and testing of bituminous binders are under way in Europe and the United States. Most of them are related to the standardisation and characterisation of bitumen and polymer modified bitumen (PMB) as proposed by the Technical Committee TC 19 on "Petroleum Products" of the European Committee for Standardisation (CEN), the Strategic Highway Research Program (SHRP), and the RILEM Technical Committee TC 152 PBM on "Performance of Bituminous Materials".

These activities have shown an increasing interest in the use of fundamental rheological parameters to specify bituminous binders. The rheological properties of bitumen are important for conducting research to correlate the physical and chemical properties of binders, correlating binder physical properties with pavement performance and specifications, and accepting bitumen for construction purposes. In the USA, SHRP has developed specifications which classify the grade of bitumen on the basis of its performance in a number of rheological tests. The parameters are based on both the complex shear modulus,  $G^*$ , and phase angle,  $\delta$ .

In the UK, new specifications for modified binders in both hot rolled asphalt (HRA) wearing course and surface dressing also require rheological measurements and it is proposed that rheological data will be required for all road applications. The specification (Highways Agency Clause 943) is still in draft but some contracts already request rheological information for both applications. The draft specifications, once finalised, will eventually be adopted in the Specifications for Highways Works [15]. Data required will consist of either isotherms of complex modulus as a function of frequency at a number of temperatures or master curves.

The Dynamic Shear Rheometer (DSR) has become accepted as a test method for the new binder test methods and specifications developed during SHRP [78,94,110]. DSR's are able to characterise the viscoelastic properties of bitumen by measurements of complex modulus and phase angle at different temperatures, frequencies, strain and stress levels. In addition, the ability of the DSR to determine the rheological characteristics of bitumens over a wide range of temperature and loading rate conditions allows it to be used extensively, in many parts of the world, for various research studies on bitumen. However, the use of the DSR is still in its infancy when compared with well established measurements such as Penetration, Softening Point and viscosity. These conventional tests have long recognised the importance of closely controlled conditions and appropriate calibration to obtain repeatable and reproducible results, particularly for specification purposes. In contrast, the rheological properties obtained with the DSR, still require detailed evaluation with regard to precision and testing configuration.

This chapter looks at the test methodology used with the Bohlin Model DSR50 Dynamic Shear Rheometer by evaluating the main parameters affecting the DSR rheological testing of bitumen, such as temperature control, strain amplitudes and sample geometry. Although these parameters are addressed in the AASHTO testing standard [110], the practical limitations of strain amplitudes and sample geometry, associated with the Bohlin DSR50, have needed to be quantified in more detail in this chapter.

The chapter also investigates the precision of the DSR by conducting repeatability tests of complex modulus and phase angle for various penetration grade and polymer modified bitumens (PMB's). The variability of the rheological testing procedure used with the Bohlin DSR50 has been compared to that of other dynamic shear rheometers and testing procedures used in the RILEM interlaboratory precision study [111,112].



## 3.2 Dynamic Shear Rheometry

Dynamic Shear Rheometers (DSR's) are used to measure the rheological characteristics of bitumen. The principles involved in dynamic shear rheometry testing are illustrated in Figure 3.1, where the bitumen is sandwiched between a spindle and a base plate. The spindle, which can be either a disc-shaped plate or a cone, is allowed to rotate while the base plate remains fixed during testing. The test is performed by oscillating the spindle about its own axis such that a radial line through Point A moves to Point B, then reverses direction and moves past Point A to Point C, followed by a further reversal and movement back to Point A. This oscillation comprises one smooth, continuous cycle which can be continuously repeated during the test. Normally DSR tests are carried out over a range of frequencies (number of cycles per second) and temperatures.

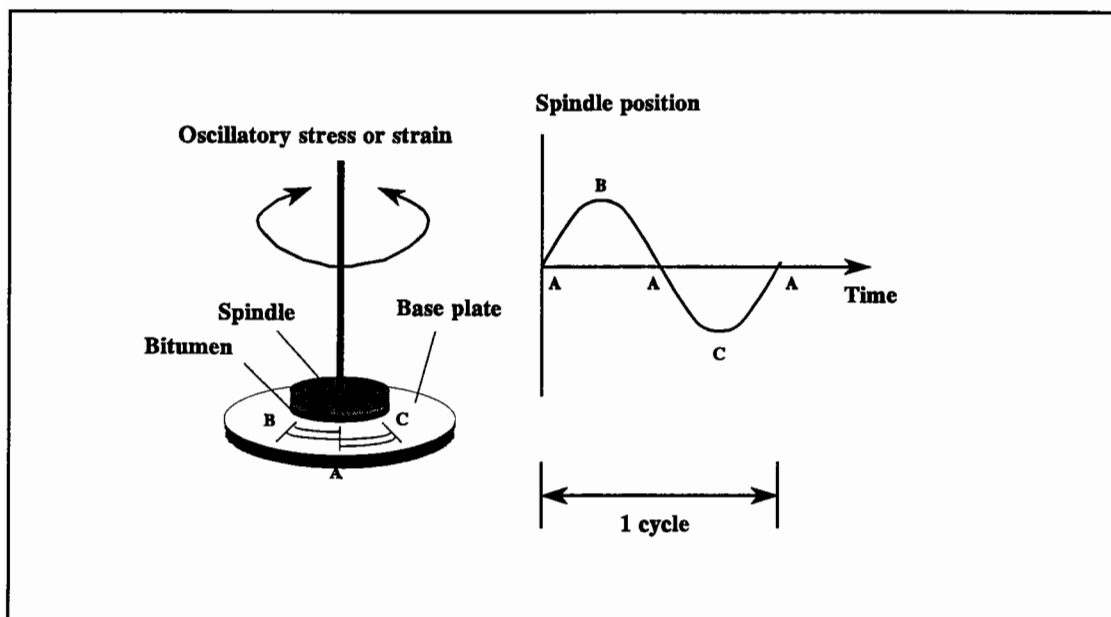


**Figure 3.1: Principles of operation of torsional-type Dynamic Shear Rheometers**

DSR tests can be carried out in either controlled stress or controlled strain testing modes. In the controlled stress mode, a specified magnitude of shear stress is applied to the bitumen by application of a torque to the spindle and the resultant spindle rotation is measured, from which the magnitude of shear strain is calculated. In the controlled strain mode, the magnitude of spindle rotation is specified and the required torque to achieve this is measured, from which the magnitude of shear stress is calculated.

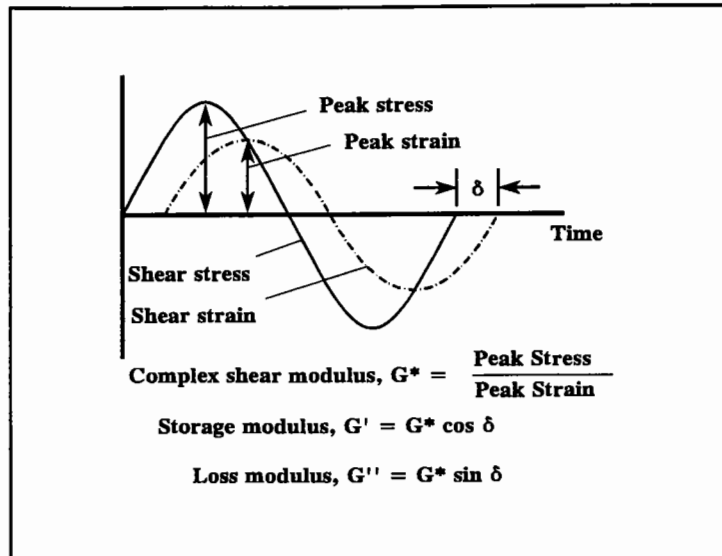


**Figure 3.2: Definitions of stiffness moduli from dynamic shear rheometry tests**

In either mode of testing, the complex modulus,  $G^*$ , is calculated as the ratio of shear stress to shear strain as shown in Figure 3.2. The complex shear modulus, which provides a measure of the total resistance to deformation when the bitumen is subjected to shear loading, is comprised of elastic and viscous components. These components are known as the storage modulus,  $G'$ , and loss modulus,  $G''$ , respectively, and are related to the complex modulus and to each other by means of the phase angle,  $\delta$ , which is the phase lag between the shear stress and shear strain responses during the test.

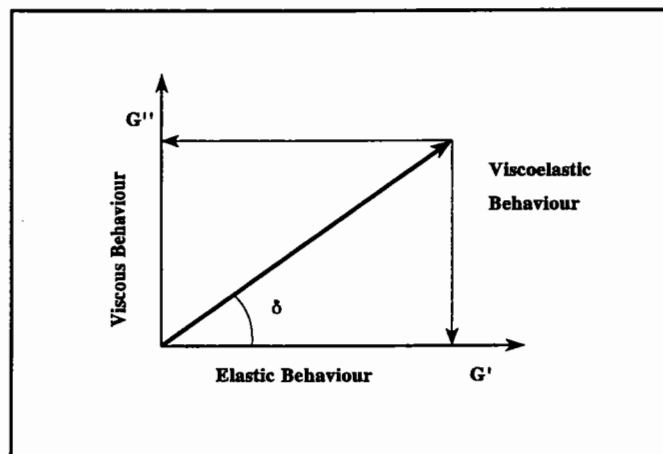


**Figure 3.3: Viscoelastic behaviour of bitumen**

The relationships amongst the moduli can be represented graphically on a plane Cartesian

coordinate system such as that shown in Figure 3.3. The axes of the graph represent the extrema of the continuum of bitumen behaviour. This means that the vertical axis represents completely viscous or fluid-like behaviour, whereas, the horizontal axis represents completely elastic or glass-like behaviour. At moderate to low temperatures, viscous behaviour can be achieved through long-term or very slow shear loading and at moderate to high temperatures, elastic behaviour can be realised through very rapid shear loading. Under normal conditions experienced for bituminous mixtures, the temperature and loading conditions are such that the behaviour of bitumen lies somewhere between the two axes, represented by a vector with a magnitude  $G^*$  and direction  $\delta$  degrees anti-clockwise from the horizontal axis. The phase angle indicates how much of the total complex modulus,  $G^*$ , is attributable to viscous behaviour and how much is attributable to elastic behaviour.

### **3.3 Factors Affecting DSR Rheological Testing**

#### **3.3.1 Temperature**

Bitumen is a good thermal insulator and is also highly temperature susceptible. In order to make accurate measurements it is important, firstly, that the whole sample is at the same temperature and secondly, that the temperature is accurately controlled. Temperature gradients in the bitumen sample lead to a reduction in the precision and accuracy of the measured rheological data.

Various temperature control systems can be used with dynamic shear rheometry, such as the:

- Peltier system,
- Extended temperature module (ETM) system, and
- Fluid (water) bath system.

The Peltier system uses a thermo-electric effect, with a particularly quick response time,

to control temperature. A drawback of the system is that only the lower, fixed plate is heated. The ETM system operates by electromagnetic induction heating of both the upper and lower plates. The system were the sample is submerged in a fluid (water) bath consists of a circulating fluid bath so that the test specimen can be flooded with fluid. The fluid provides rapid heat transfer and is very reliable with respect to temperature control.

Both the Peltier and ETM systems produce temperature gradients in samples which are strongly related to the sample geometry, especially gap width [113]. The temperature gradients found with the Peltier system result from the heating of the sample from only one side. The ETM reduces this problem by heating the sample from both top and bottom but does cause problems with the trimming of the sample [114]. Teugels and Nilsson [115] have found that the ETM system is more accurate at higher temperatures (above 80°C - 100°C) whereas the Peltier system should be used at lower temperatures.

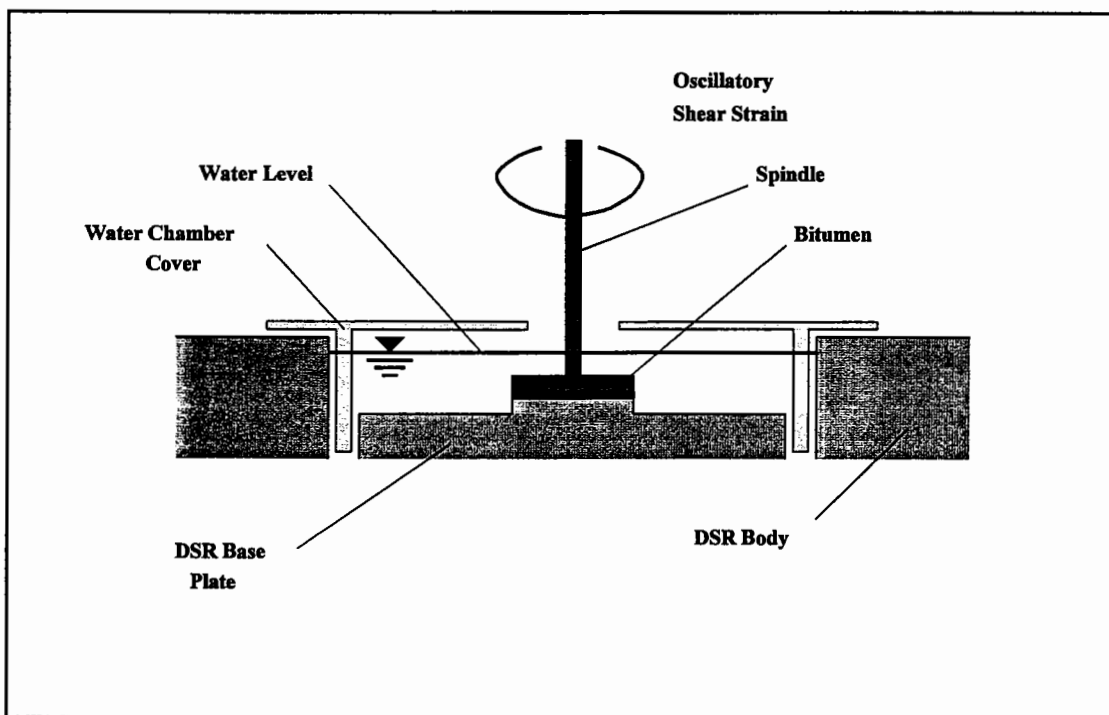


**Figure 3.4: Testing arrangement in Dynamic Shear Rheometer**

Small variations between the set temperature and the actual binder temperature can cause large variations in results. Accurate temperature control of the whole environment around the bitumen by means of a fluid bath is, therefore, essential. The temperature control of

the specimen in the Bohlin DSR50 is accomplished through submersion of the specimen in a fluid as shown in Figure 3.4. Cointe and Monnoye [116] have found that the fluid bath system allows the temperature of the sample to be kept uniform and constant over a temperature range of 5°C to 90°C. The temperature control unit, used with the Bohlin DSR50, is capable of maintaining a temperature to within  $\pm 0.1^\circ\text{C}$ , as recommended by Petersen et al [78]. This  $\pm 0.1^\circ\text{C}$  change in temperature has been found to correspond to only a  $\pm 2$  percent error in measured complex modulus [117].

### **3.3.2 Strain Amplitude, Stress Level and Frequency of Oscillation**

Viscoelastic materials, such as bitumen, do not behave linearly in terms of their stiffness as a function of stress or strain. The dynamic shear modulus and phase angle therefore depend upon the magnitude of the shear strain with both decreasing with increasing shear strain. However, a linear region may be defined at small strains where the shear modulus is relatively independent of shear strain. This region will vary with the magnitude of the complex modulus and, therefore, the strains have been kept small at low temperatures (0.5% at 10°C) and increased at higher temperatures (10% at 75°C).

The limit of the linear viscoelastic<sup>1</sup> behaviour has been defined as the point beyond which the measured value of  $G^*$  decreases to 95% of its zero-strain value [78]. In order to ensure that the rheological tests are conducted within the linear viscoelastic region of bitumen behaviour, a set of strain sweeps were conducted at 20°C, 40°C and 60°C, as shown in Figure 3.5, for one penetration grade bitumen and one PMB.

The shear strain varies linearly from zero at the centre of the plates to a maximum at the extremities of the plate perimeter. The shear stress is calculated from the applied or measured torque and the geometry of the test sample.

---

<sup>1</sup>Linear viscoelasticity refers to the region of behaviour in which the dynamic shear modulus is independent of shear stress or strain

The dynamic shear tests were conducted by means of frequency sweeps at various temperatures. The combination of frequencies and temperatures are:

- 14 frequencies (0.01, 0.015, 0.02, 0.05, 0.1, 0.15, 0.2, 0.5, 1, 1.5, 2, 5, 10 and 15 Hz), and
- 8 temperatures (10, 15, 25, 35, 45, 55, 65 and 75°C).

As well as being dictated by the linear viscoelasticity of the bitumen, the strain amplitudes are also affected by the torque range of the DSR. At low temperatures and high loading frequencies, the DSR is not capable of applying sufficient torque to achieve target strains above 2%. At high temperatures and low loading frequencies, the DSR cannot apply a small enough torque to achieve target strain amplitudes below 10%.

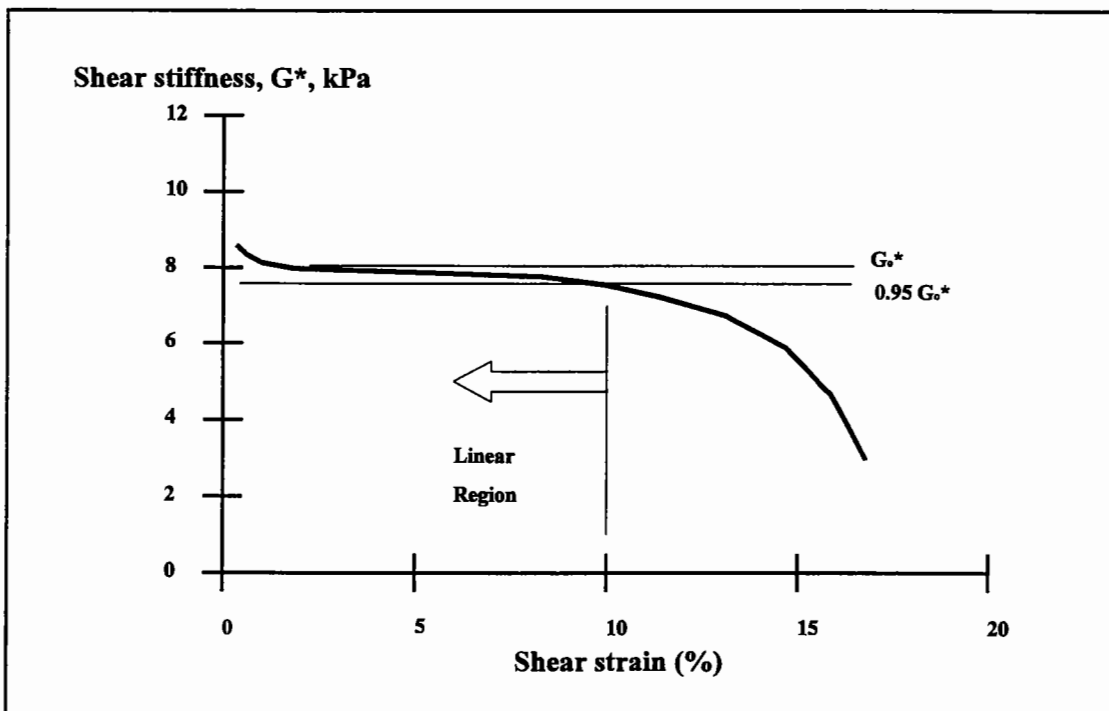


Figure 3.5: Strain sweeps used to determine linear region

### 3.3.3 Sample Preparation and Geometry

The bitumen samples for the DSR rheology testing were prepared according to the test method described in Appendix A, which is similar to the AASHTO method [110].

The sample geometry of the test sample consists of two parameters:

- Plate (disk) diameter, and
- Gap width (sample height).

The testing configuration of the DSR consists of a number of different parallel plate and cone/plate geometries to measure a wide range of bitumen stiffness. However, in the UK there are no clear guidelines on the choice of a suitable sample geometry (plate diameter and gap setting) and it is usually left to the individual to determine the most appropriate for the particular bitumen. As a result, there are no standard geometries which have been identified as suitable for specific ranges of binder stiffness.

Different disk sizes and suggested testing temperatures have been proposed by various researchers based on different sample types. The disk diameters suggested by Goodrich [19,20] are given in Table 3.1.

**Table 3.1: Suggested disk diameters for DSR rheology testing [19,20]**

Sample Type	Disk Diameter	Test Temperature Range
RTFOT residue	8 mm	-40°C to +10°C
RTFOT residue	25 mm	+10°C to +50°C
RTFOT residue	40 mm	+50°C to +80°C

The researchers involved with the SHRP Project A-002A [65] have suggested slightly different disk diameters as presented in Table 3.2.

**Table 3.2: SHRP suggested disk diameters for DSR rheology testing [65]**

Disk Diameter	Test Temperature Range	Typical G* Range
8 mm	0°C to +40°C	10 <sup>5</sup> Pa to 10 <sup>7</sup> Pa
25 mm	+40°C to +80°C	10 <sup>3</sup> Pa to 10 <sup>5</sup> Pa
40 mm	> 80°C	< 10 <sup>3</sup> Pa

The proper choice of disk (plate) size or specimen geometry should not be dictated by the

temperature of the test specimen, but rather by the stiffness of the test specimen. The use of a larger diameter at temperatures more appropriate to a smaller diameter results in the dynamic shear instrument reaching its torque limit and, therefore, the resulting stresses obtained from the equipment are below their true value. This results in a lower binder stiffness being measured at that particular temperature. Another factor that needs to be taken into account is that the larger disks tend to give smaller values of  $G'$  due to slippage [62].

The gap height between the two parallel disks is generally in the range between 0.5 to 1.0 mm, although thicker samples of bitumen of between 1.5 to 2.2 mm have been used in the dynamic oscillatory tests [62] and between 1 to 2.5 mm by Goodrich [20]. It is also recommended that when the complex shear modulus of the bitumen is greater than approximately 30 MPa, parallel plate geometry should not be used because the compliance of the rheometer can be sufficient to cause errors in the measurements [78]. The SHRP research team suggest that the following guidelines should be used [78]:

- Use Bending Beam Rheometer (BBR) or torsional bar geometry when  $G^* > 30$  MPa.
- Use 8 mm parallel plates with a 2 mm gap when  $0.1 \text{ MPa} < G^* < 30 \text{ MPa}$ .
- Use 25 mm parallel plates with a 1 mm gap when  $1.0 \text{ kPa} < G^* < 100 \text{ kPa}$ .
- Use 50 mm parallel plates when  $G^* < 1 \text{ kPa}$ .

Although these recommended guidelines provide a useful indication of plate and gap geometry, care should be taken when using them over wide frequency sweeps and for different bitumens. This is particularly relevant at the transitions between the different sample geometries and, therefore, it is recommended that there should be an overlap of rheological testing with two disk and gap configurations being used at the transition points.

The complex modulus and phase angle were, therefore, measured under different temperature and frequency conditions for different plate diameters and gap widths as



shown in Table 3.3.

**Table 3.3: DSR test conditions for sample geometry**

Parameter	Testing configuration one	Testing configuration two
Temperature	10°C to 35°C <sup>1</sup>	25°C to 75°C
Frequency	0.01 Hz to 15 Hz	0.01 Hz to 15 Hz
Plate diameter	8 mm	25 mm
Gap width	2 mm	1 mm

<sup>1</sup>Temperature was varied from 35°C to 55°C depending on the bitumen

The  $G^*$  and  $\delta$  results for a Middle East 80/100 pen bitumen are shown in Figures 3.6 and 3.7, which is the current format required by the UK Highways Agency. The behaviour seems to be as would be expected with an increase in  $G^*$  and a decrease in  $\delta$  as the binder becomes more elastic at higher frequencies and lower temperatures. However, in Figure 3.6, the isotherms at 25°C and 35°C are different for the 25 mm and 8 mm diameter plates, with the 25 mm diameter isotherms suggesting that the limiting stiffness of the bitumen is not approximately  $10^9$  Pa, but a value closer to  $10^7$  Pa. With regard to the phase angle, the 25 mm diameter disk configuration overestimates the degree of elasticity of the bitumen at 25°C and 35°C.

The effect of using the 25 mm rather than the 8 mm diameter disk configuration is shown in Table 3.4 with regard to the SHRP fatigue parameter,  $G^*\sin\delta$ .

**Table 3.4: SHRP fatigue parameter,  $G^*\sin\delta$  for the 25 mm and 8 mm configurations**

Temperature (°C)	25 mm diameter disk	8 mm diameter disk
25	$1.058 \times 10^6$ Pa	$3.014 \times 10^6$ Pa
35	$0.546 \times 10^6$ Pa	$0.681 \times 10^6$ Pa

The fatigue criterion is defined as the temperature at which the binder has a value of  $G^*\sin\delta$  equal to 5,000 kPa. The use of the 25 mm compared to the 8 mm configuration results in a considerably lower value of  $G^*\sin\delta$ , particularly as the temperature decreases

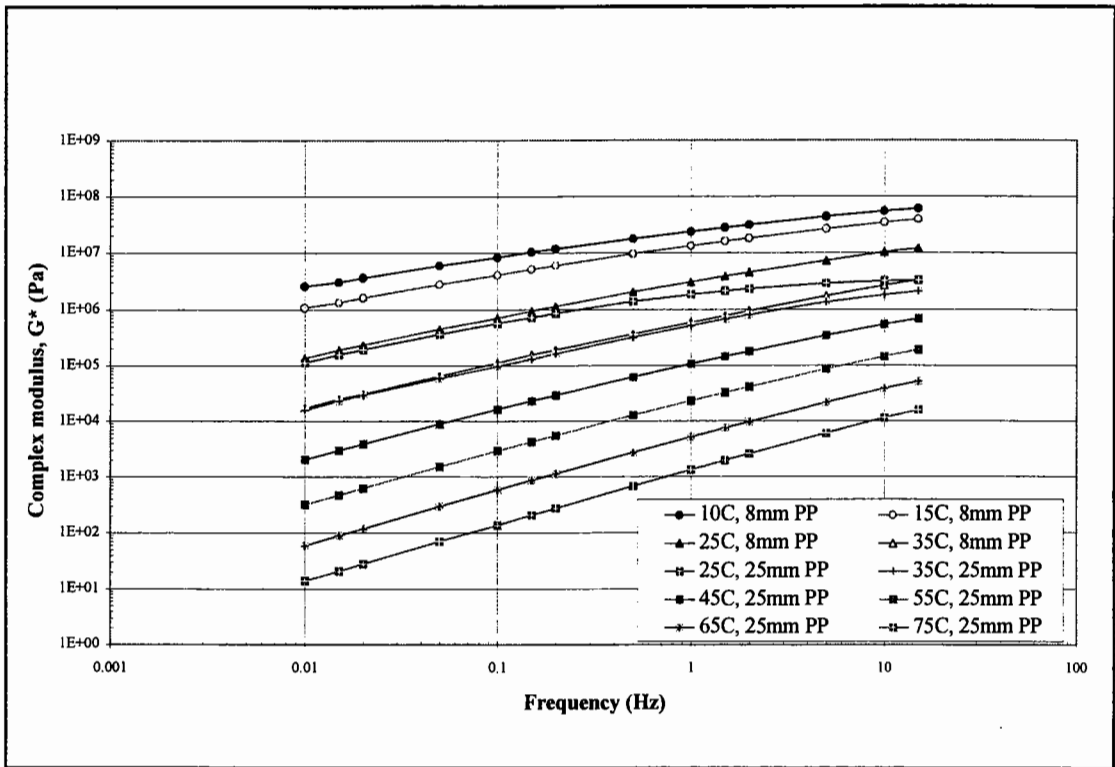


Figure 3.6: Isothermal plot of complex modulus for Middle East 80/100 pen

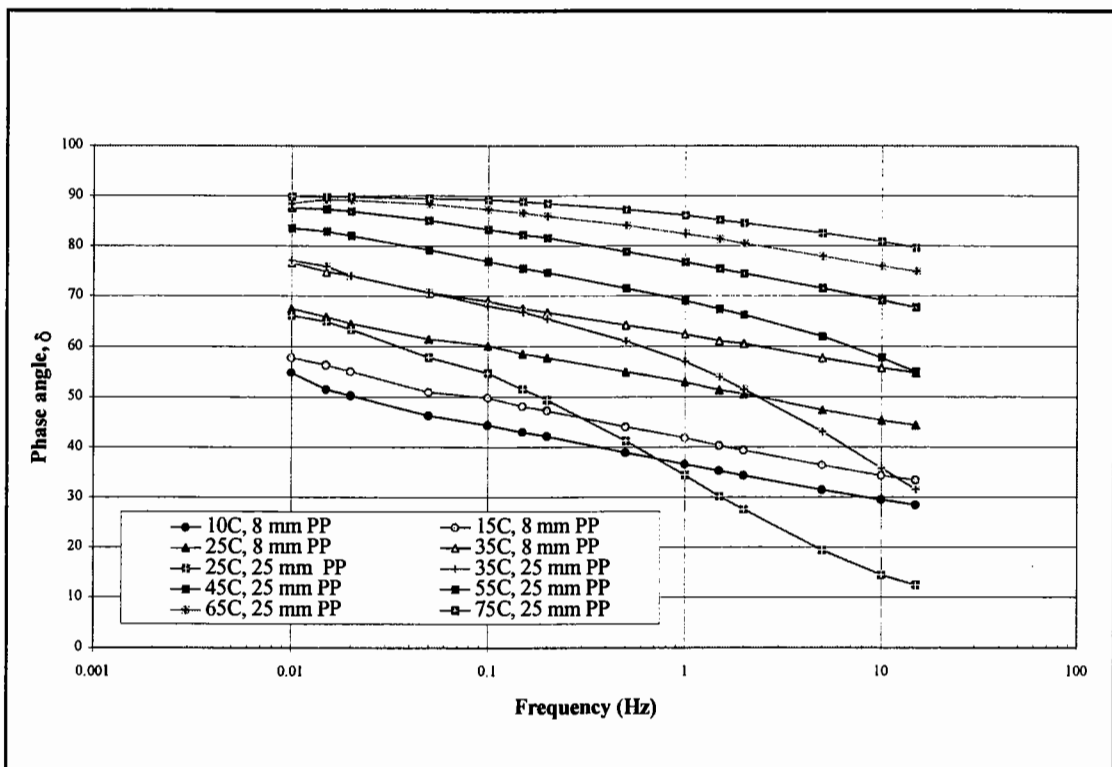


Figure 3.7: Isothermal plot of phase angle for Middle East 80/100 pen

and the stiffness of the bitumen increases. This results in a lower temperature specification grade being ascribed for the bitumen for the 25 mm configuration and, therefore, an overestimation of the fatigue performance of the bitumen compared to the more appropriate grade determined with the 8 mm configuration.

The complex modulus and phase angle are also presented in the form of isochronal plots at a low frequency of 0.02 Hz in Figure 3.8 and at a higher frequency of 10 Hz in Figure 3.9. At the lower frequency, the  $G^*$  and  $\delta$  values differ only slightly at 25°C. However, at the higher frequency and, therefore, greater stiffness, there are large differences in the values of  $G^*$  and  $\delta$  at both 25°C and 35°C.

The values of  $G^*$  and  $\delta$  measured by the different sample geometries have also been plotted in the form of Black diagrams, in Figure 3.10, in order to eliminate the effect of temperature and frequency from the results. The Black diagram provides a suitable means of evaluating the suitability of the DSR testing configurations. Extrapolating lines to the y-axis indicate different values of limiting stiffness for the 25 mm and 8 mm configurations. The 25 mm configuration indicates a limiting stiffness of approximately  $5 \times 10^6$  Pa which is considerably lower than the traditionally recognised value of  $10^9$  Pa indicated by the 8 mm configuration.

The upper limit of stiffness can be more accurately estimated by using a linear relationship between the logarithm of  $(1 + \tan\delta)$  and the logarithm of  $G^*$  within the range of 0 to 1 for  $\log(1 + \tan\delta)$  [80,118]. This plot for the Middle East bitumen is shown in Figure 3.11, where, firstly, the limiting stiffness may be more readily extrapolated and secondly, the point of departure from linearity, where lower than expected values of  $G^*$  are obtained, can be identified. The 8 mm configuration can be extrapolated to a limiting stiffness of approximately  $2 \times 10^9$  Pa, but the value for the 25 mm configuration is limited to  $2.5 \times 10^7$  Pa. The point of departure from the extrapolated line, for the 25 mm configuration, occurs at approximately  $10^6$  Pa.

The complex modulus and phase angle, under different temperature and frequency

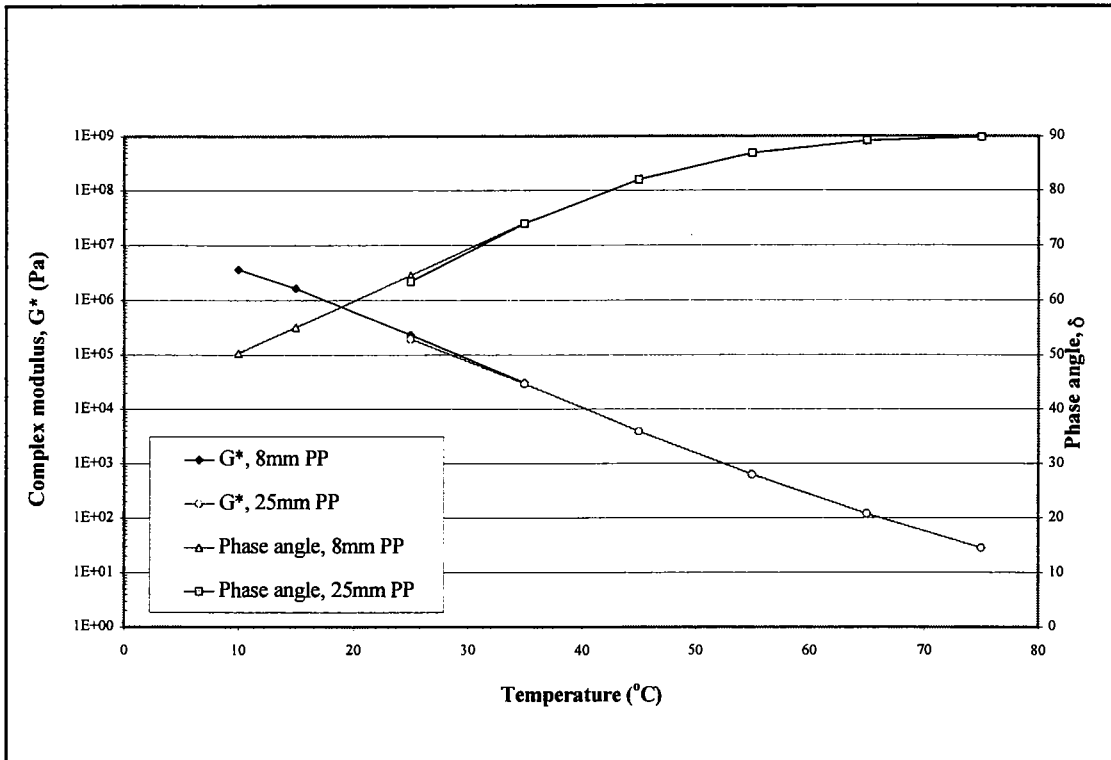


Figure 3.8: Isochronal plot at 0.02 Hz for Middle East 80/100 pen

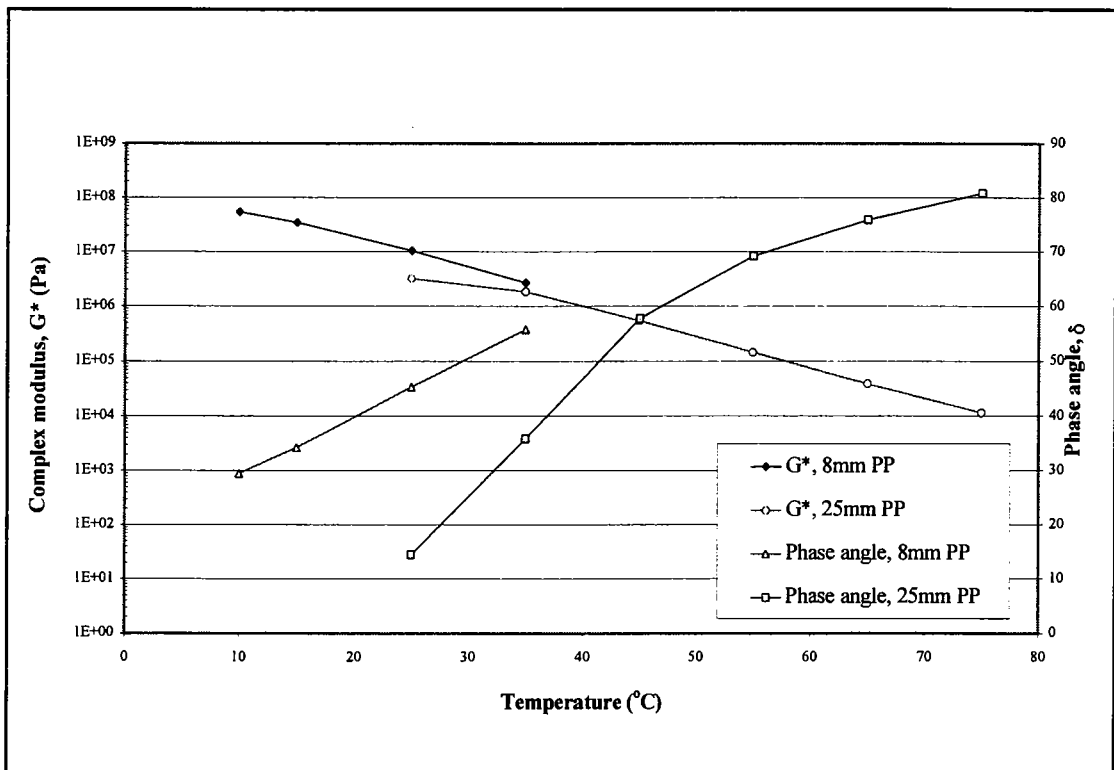


Figure 3.9: Isochronal plot at 10 Hz for Middle East 80/100 pen

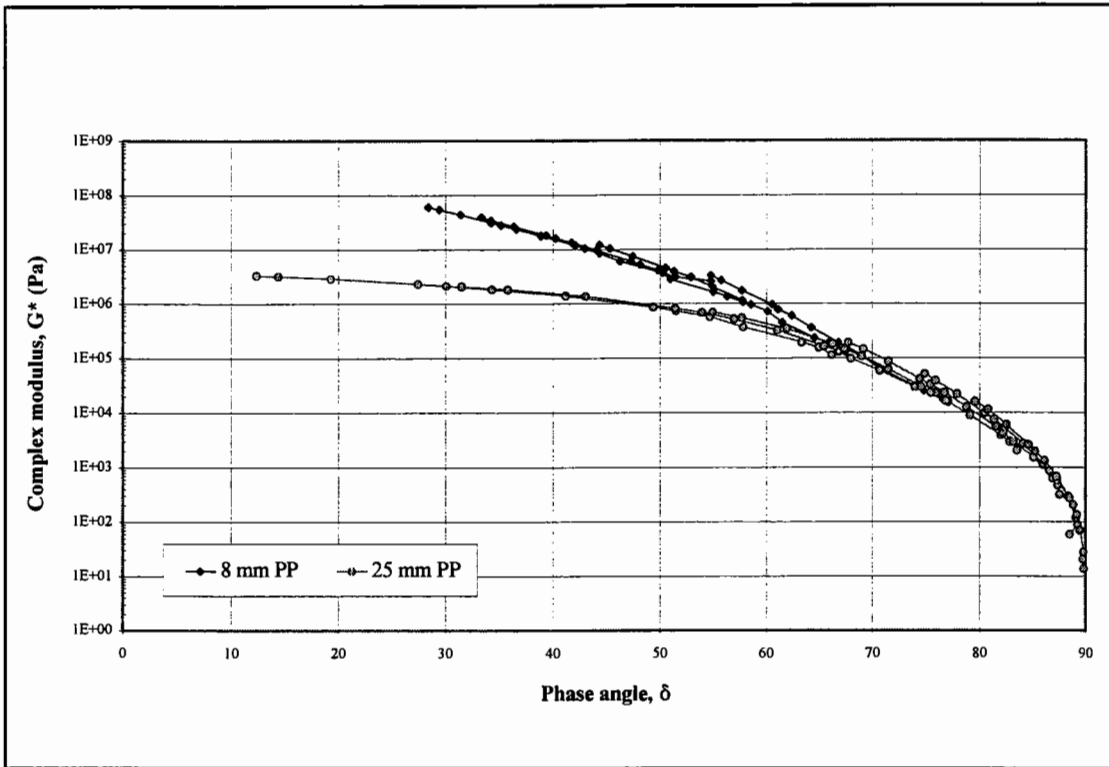


Figure 3.10: Black diagram for Middle East 80/100 pen

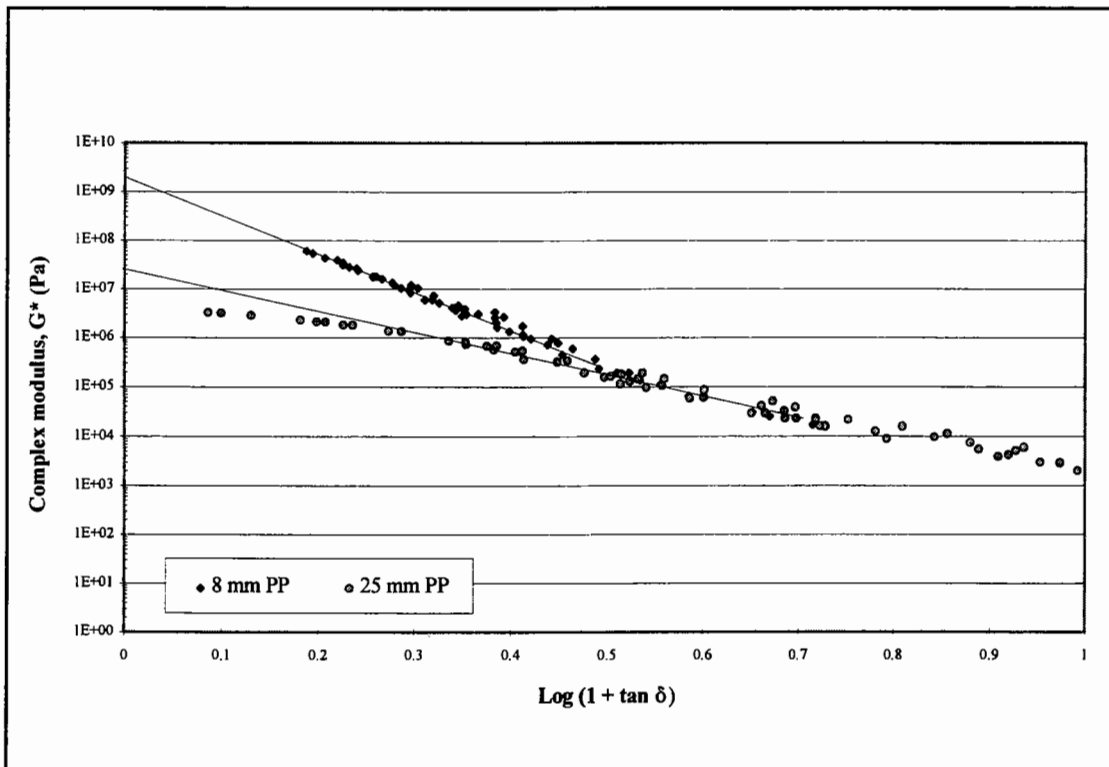


Figure 3.11: Complex modulus versus  $\log(1 + \tan\delta)$  for Middle East 80/100 pen

conditions for the two plate diameters and gap widths, have also been measured for a 7% EVA PMB and a 7% SBS PMB. The isochronal plot at 10 Hz for the 7% EVA PMB is shown in Figure 3.12. As with the penetration grade bitumen,  $G^*$  and  $\delta$  differ between the two measuring configurations at high stiffness values. The 25 mm configuration underestimates the stiffness of the bitumen and overestimates its elastic component as the stiffness of the bitumen increases. The Black diagram for the EVA PMB, in Figure 3.13, shows the limits of the 25 mm configuration at testing the bitumen in the high stiffness modulus domain. The figure also illustrates that at slightly lower stiffness values, corresponding to measurements at lower frequencies at 25°C and 35°C, there is good agreement of the measured rheological data for both the 25 mm and 8 mm configurations.

The isochronal plot at 10 Hz for the SBS PMB is shown in Figure 3.14 where the difference between the two configurations is not as marked as that seen for the EVA PMB due to the lower  $G^*$  values for the elastomeric PMB compared to that of the plastomeric PMB. However, the Black diagram, in Figure 3.15, again gives a clear indication of the necessity of using the 8 mm configuration at stiffness values greater than approximately  $10^5$  Pa.

### **3.4 Repeatability of DSR Rheological Testing**

The factors affecting the precision (repeatability and reproducibility) of measurements made with the DSR can be grouped as follows:

- Measuring equipment and transducers,
- Handling and sample preparation, and
- Temperature control.

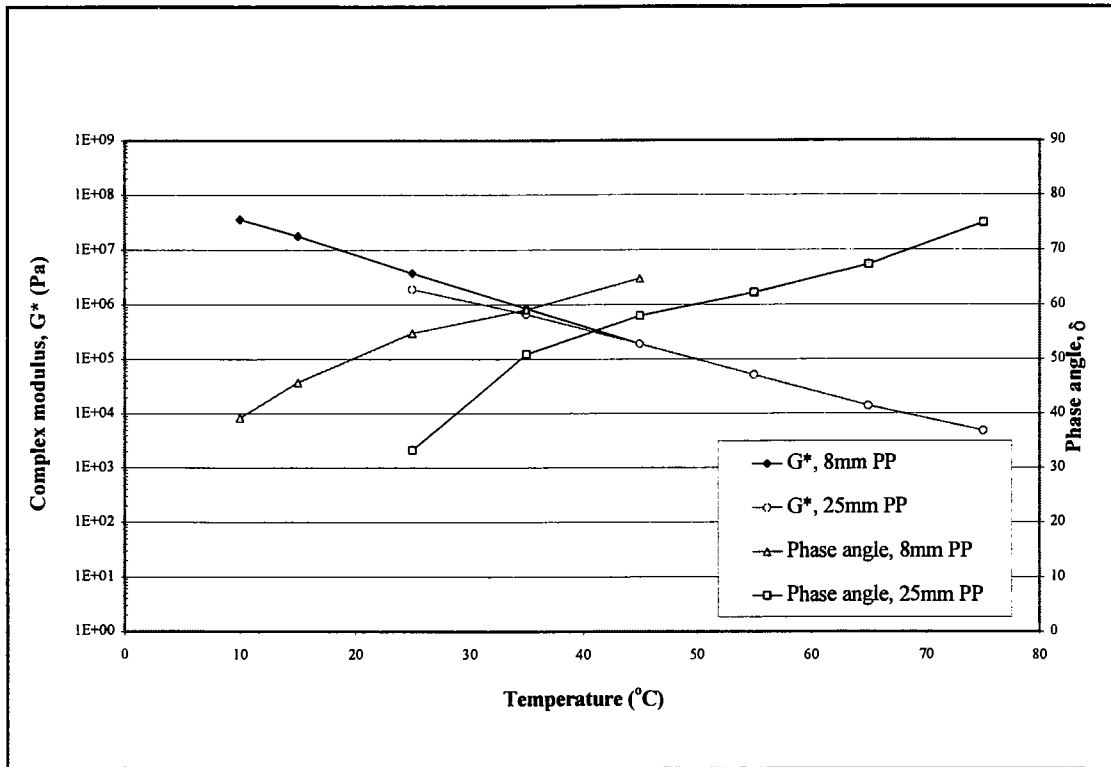


Figure 3.12: Isochronal plot at 10 Hz for 7% EVA - Russian 80 pen

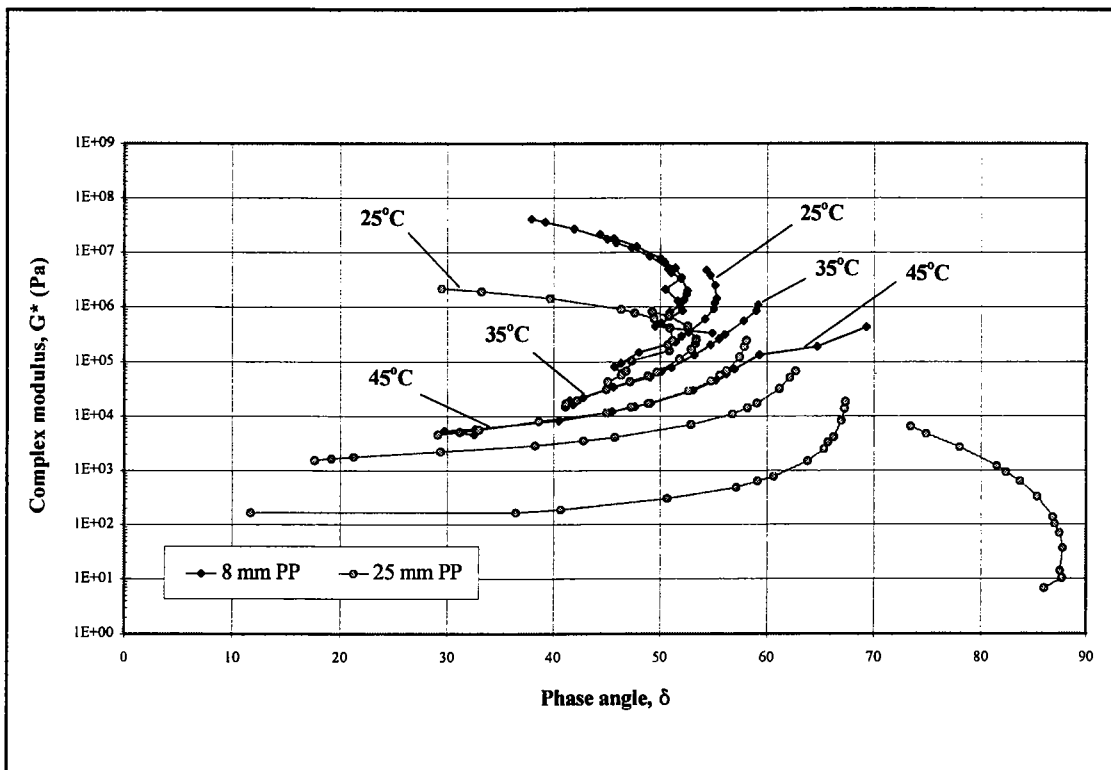


Figure 3.13: Black diagram for 7% EVA - Russian 80 pen

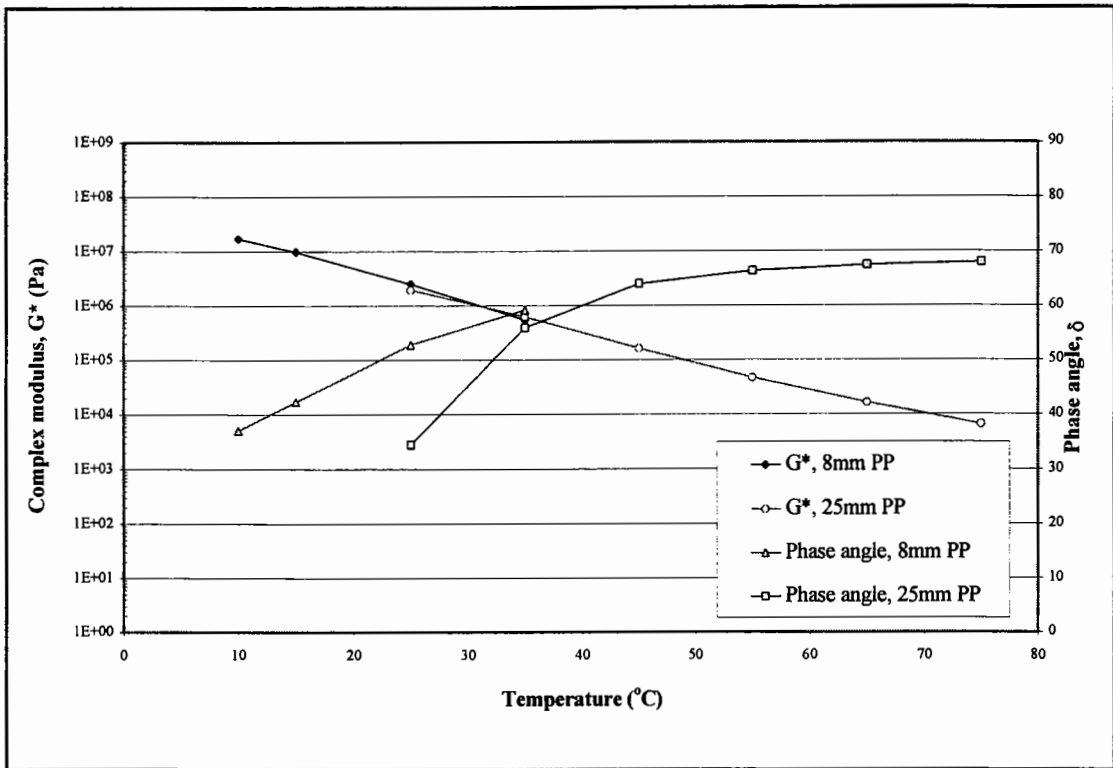


Figure 3.14: Isochronal plot at 10 Hz for 7% SBS - Russian 80 pen

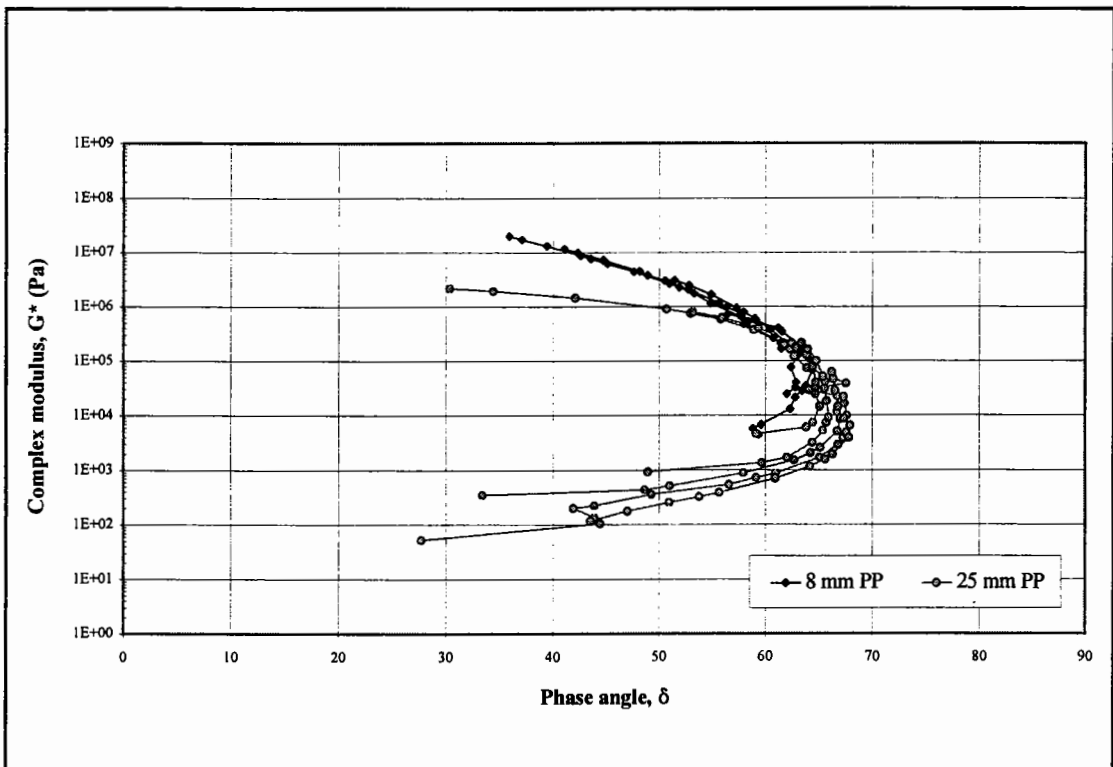


Figure 3.15: Black diagram for 7% SBS - Russian 80 pen



The precision of the Bohlin DSR50, with regard to the repeatability of the measuring equipment and transducers, was determined by conducting five test repeats of a bitumen sample at 28 reference conditions resulting from the combination of:

- 7 frequencies (0.1, 0.2, 0.5, 1, 2, 5 and 10 Hz), and
- 4 temperatures (25, 35, 45 and 60°C).

The isotherms of complex modulus and phase angle versus frequency, for the bitumen used in the repeatability study, are shown in Figures 3.16 and 3.17.

The rheological data in the figures, which consist of the five repeats and the average isochronal plots, indicate the high degree of repeatability for both the stiffness and phase angle measurements. The average, standard deviation and coefficient of variation<sup>2</sup> (CV) of the five single test results at each of the 28 reference conditions have been calculated and the CV values presented in Tables 3.5 and 3.6.

**Table 3.5: Percentage variation of complex modulus with regard to DSR measuring equipment and transducers**

Temperature (°C)	Coefficient of variation (%)						
	0.1 Hz	0.2 Hz	0.5 Hz	1 Hz	2 Hz	5 Hz	10 Hz
25	1.6	2.4	2.3	2.5	2.7	2.7	2.4
35	1.3	1.6	1.3	1.4	1.7	2.4	2.4
45	3.1	3.1	3.2	3.1	3.1	3.3	3.2
60	2.8	2.3	2.1	2.4	2.1	1.5	1.9

---

<sup>2</sup>Ratio of standard deviation to average value expressed as a percentage

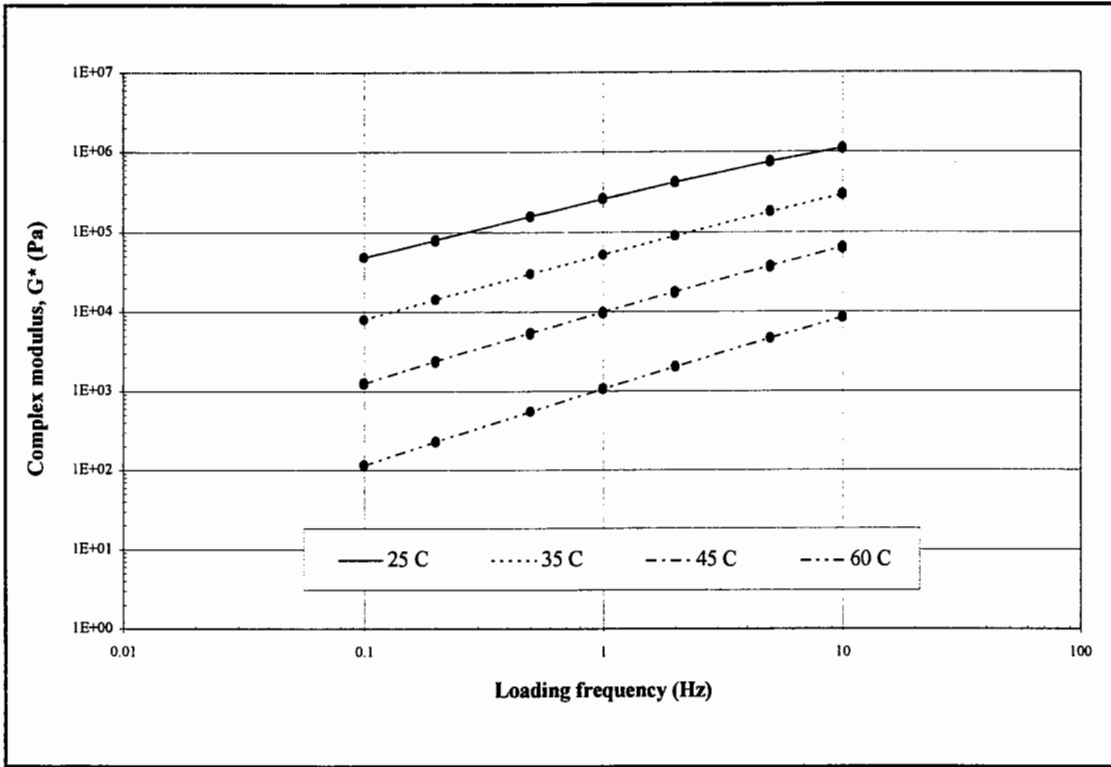


Figure 3.16: Isothermal plot of complex modulus for repeatability study

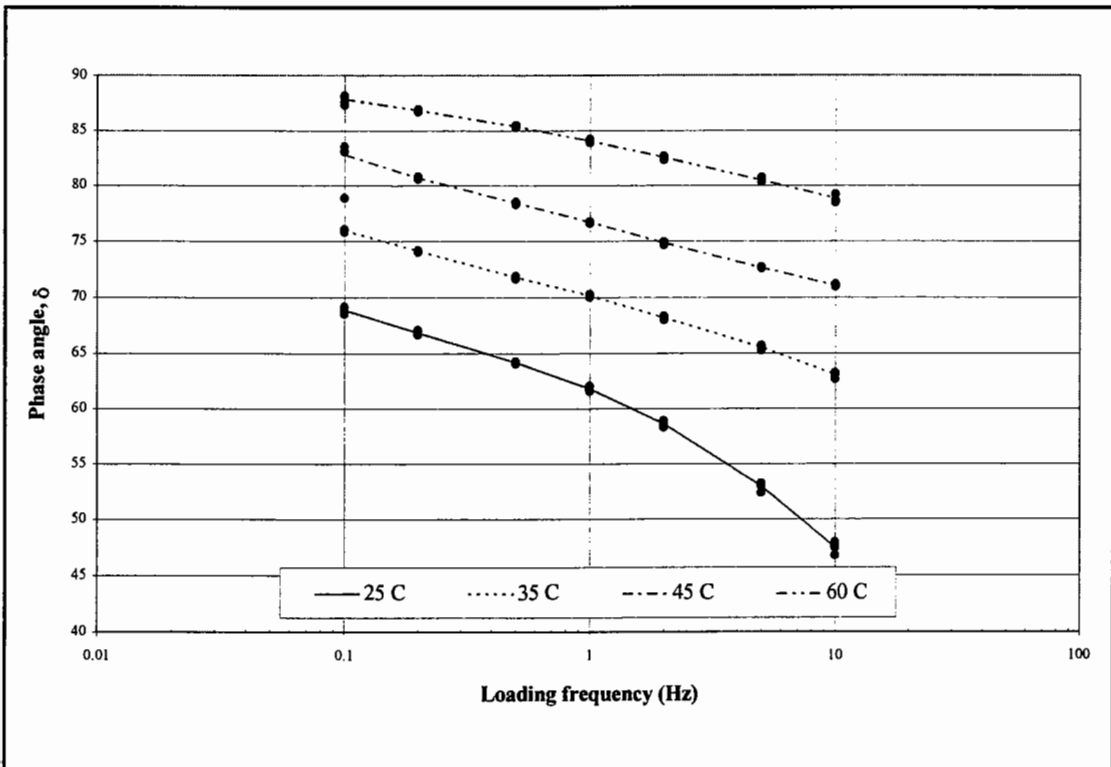


Figure 3.17: Isothermal plot of phase angle for repeatability study

**Table 3.6: Percentage variation of phase angle with regard to DSR measuring equipment and transducers**

Temperature (°C)	Coefficient of variation (%)						
	0.1 Hz	0.2 Hz	0.5 Hz	1 Hz	2 Hz	5 Hz	10 Hz
25	0.4	0.2	0.1	0.3	0.5	0.7	0.9
35	0.2	0.1	0.1	0.2	0.2	0.3	0.4
45	1.5	0.1	0.1	0.1	0.2	0.1	0.1
60	0.4	0.1	0.1	0.2	0.2	0.2	0.4

The CV results in Tables 3.5 and 3.6 indicate a high degree of repeatability for the DSR measurement equipment and transducers. However, this precision test does not include the additional sources of error found during DSR testing, which are can be classified as:

- Handling and sample preparation, and
- Temperature control.

Therefore, additional precision testing, with regard to the total repeatability of the Bohlin DSR50, was undertaken by testing five samples each of one penetration grade bitumen and three PMB's at 112 reference conditions resulting from the combination of:

- 14 frequencies (0.01, 0.015, 0.02, 0.05, 0.1, 0.15, 0.2, 0.5, 1, 1.5, 2, 5, 10 and 15 Hz), and
- 8 temperatures (10, 15, 25, 35, 45, 55, 65 and 75°C).

The CV values, at the 28 reference conditions used in the initial precision test, for one of the four binders are presented in Tables 3.7 and 3.8. The CV values for complex modulus and phase angle for all four binders are also shown in the form of histograms in Figures 3.18 and 3.19.

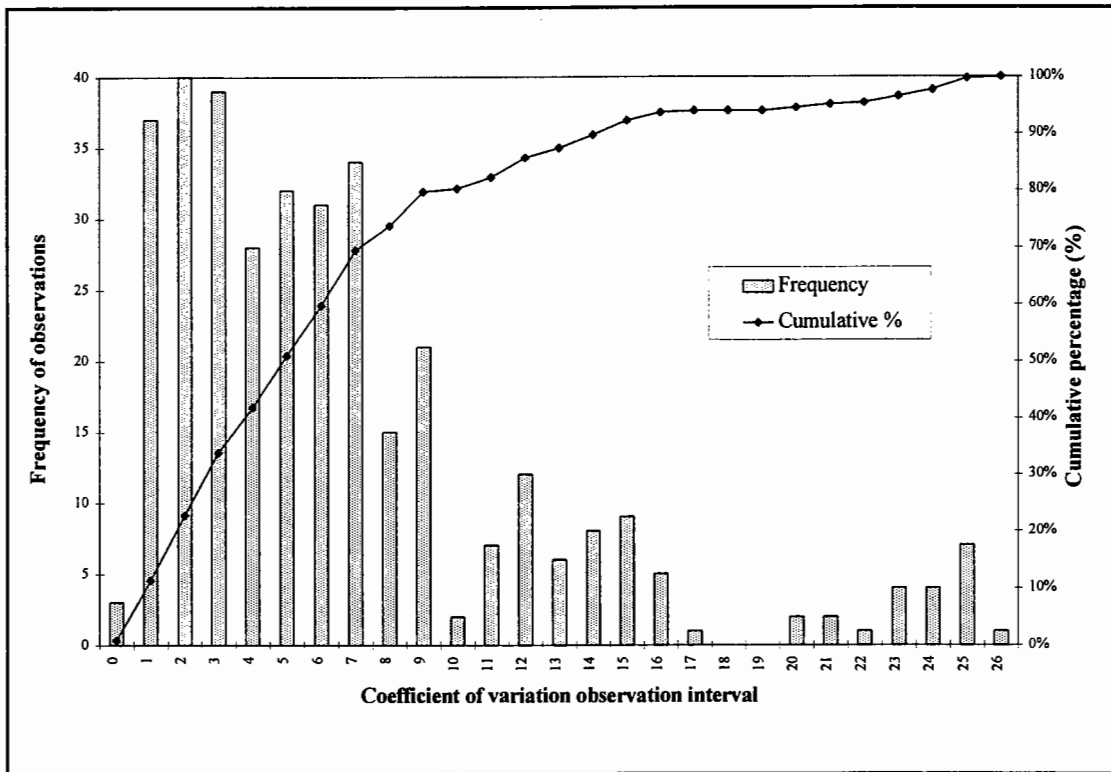


Figure 3.18: Histogram of repeatability study for complex modulus

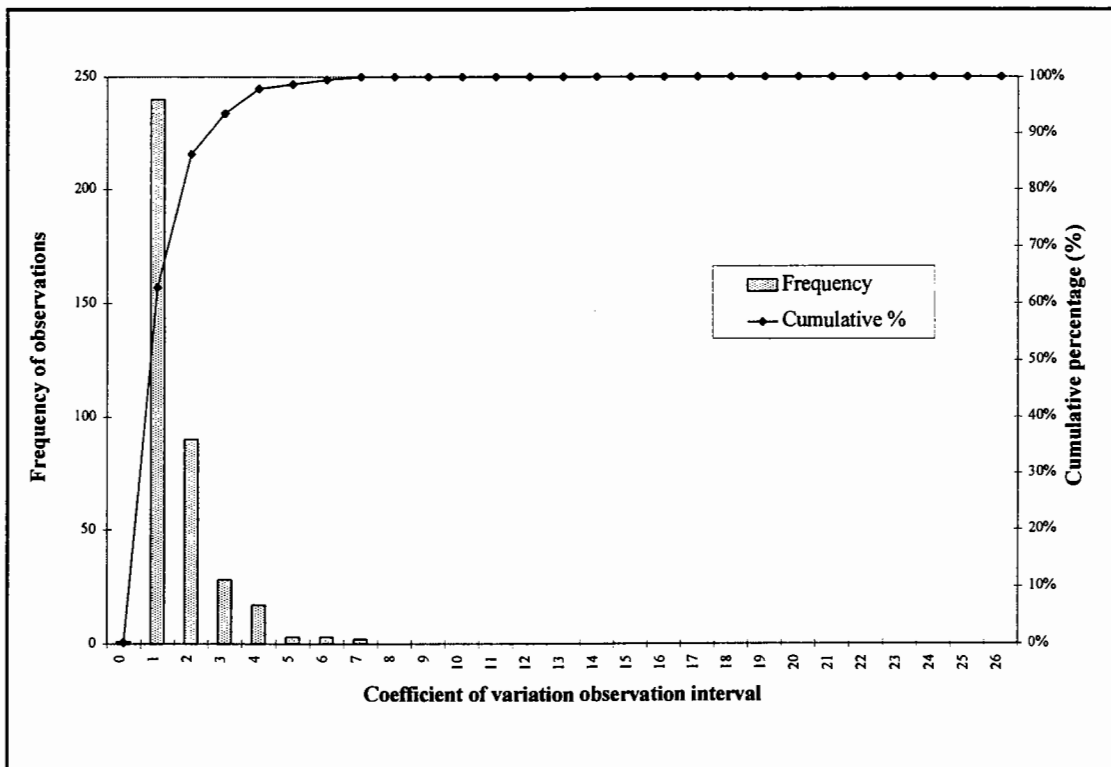


Figure 3.19: Histogram of repeatability study for phase angle

**Table 3.7: Percentage variation of complex modulus for Bohlin DSR50**

Temperature (°C)	Coefficient of variation (%)						
	0.1 Hz	0.2 Hz	0.5 Hz	1 Hz	2 Hz	5 Hz	10 Hz
25	1.2	0.6	0.9	2.4	2.7	3.5	3.6
35	0.6	6.2	6.1	5.5	3.7	2.0	0.8
45	2.8	1.7	1.4	1.1	1.0	0.7	0.5
65	4.9	6.2	5.2	4.9	4.2	3.3	4.1

**Table 3.8: Percentage variation of phase angle for Bohlin DSR50**

Temperature (°C)	Coefficient of variation (%)						
	0.1 Hz	0.2 Hz	0.5 Hz	1 Hz	2 Hz	5 Hz	10 Hz
25	0.1	0.1	0.4	0.4	0.2	0.3	0.3
35	0.4	0.1	0.1	0.1	0.1	0.2	0.1
45	1.4	1.1	0.4	0.1	0.1	0.2	0.3
65	0.1	0.4	0.5	0.6	0.9	0.5	0.1

The CV values in Tables 3.7 and 3.8 vary depending on the testing frequency and temperature and are on average greater than those found simply for the measurement equipment and transducers. This is understandable due to the increased variability associated with sample preparation and the inherent variability associated with different bitumen samples.

The histogram for complex modulus, in Figure 3.18, shows that 80 percent of the CV values are less than 10%, with a maximum CV value of 26%. The histogram for  $\delta$ , in Figure 3.19, shows that the phase angle measurements are less sensitive to variations in operating conditions than stiffness measurements with 80 percent of the values being less than 2% with a maximum of 7%.

The RILEM Technical Committee 152 PBM “Performance of bituminous materials” initiated in 1994 an interlaboratory test programme on the rheology of bituminous binders. The results of the reproducibility study showed that the percentage variations

ranges from 23% to 39% in the determination of complex modulus and 1% to 12% for phase angle [111,112]. The variance found for the Bohlin DSR50, therefore, compares favourably with that found for the RILEM reproducibility study. It is important to note that, although precise and accurate measurements are required for both research and specification purposes, the tolerable levels of precision and accuracy are more restrictive for specification purposes than for research purposes.

### **3.5 Discussion**

Accurate temperature control during DSR testing is essential in order to obtain accurate rheological measurements. The use of a fluid bath system, with the Bohlin Model DSR50, can be considered to provide the most practical and effective means of providing this temperature control. Other systems, such as the Peltier and extended temperature module (ETM) systems, are not as efficient at maintaining a constant and uniform temperature within the bitumen sample and tend to produce temperature gradients.

In addition, the choice of sample geometry has a large influence on the rheological results. The influence can be considered to be due to machine compliance, the extent of which depends on the rheometer, the plate diameter and sample thickness (plate gap). As the stiffness of the bitumen increases, the strain (displacement) in the bitumen decreases until a point is reached where the torsional movements in the DSR become significant. The instrument and software assumes that the torsional movement is entirely due to the bitumen and, therefore, when this is not the case, results in a lower measured stiffness as seen for the 25 mm diameter plate configuration at low temperatures and high loading frequencies.

Another explanation for the lower measured stiffness is that at low temperatures, where the bitumen becomes increasingly stiffer, it is possible that the stiffness of the sample may be equal to or greater than the effective stiffness of the drive-shaft [119]. This can be readily seen where the limiting stiffness of the bitumen is not approximately 1 GPa. In order to measure higher stiffness values, it is necessary to consider either an alternative

geometry, for example tension-compression, or an alternative instrument, such as the bending beam rheometer.

The DSR experiments with the 25 mm and 8 mm disk configurations have shown that with wide frequency sweeps at different temperatures it is necessary to overlap the dynamic shear testing, using the two configurations, at the transitional stiffness regions of the bitumen. This overlapping allows the differences in  $G^*$  and  $\delta$ , as measured by the two configurations, to be identified and the appropriate values to be selected for the rheological characterisation of the bitumen. Black diagrams of  $G^*$  versus  $\delta$  provide a useful means of identifying these appropriate values and, therefore, aid the selection of suitable disk configurations.

The combination of the 8 mm diameter disk with a 2 mm gap width at low temperatures, and at high frequencies in the transition stiffness region of approximately 100 kPa, and the 25 mm diameter disk with a 1 mm gap width at high temperatures, and at low frequencies in the stiffness region of approximately 100 kPa, has been used to produce the rheological data for the different penetration grade bitumens and PMB's tested in the subsequent chapters of this thesis.

### **3.6 Conclusions**

The following conclusions can be drawn from this chapter:

- The circulating fluid bath used with the Bohlin DSR50 provides a reliable and accurate means of controlling the test temperature during rheological tests within  $\pm 0.1^\circ\text{C}$ .
- The strain amplitudes used with the Bohlin DSR50 vary from 0.5% at  $10^\circ\text{C}$  to 10% at  $75^\circ\text{C}$  and depend on rheological testing temperature and the stiffness of the bitumen.

- Representative rheological results for penetration grade bitumens and PMB's can be produced by means of the Bohlin DSR50 using a combination of the 8 mm and 25 mm diameter disk configurations. The combination of the two configurations is governed by the stiffness and composition of the unmodified and polymer modified bitumens.
- The repeatability of the Bohlin DSR50 was found to be well within the repeatability and reproducibility findings of the RILEM interlaboratory study. As with the RILEM study, the variability was found to be greater for complex modulus than phase angle.



# **4 The Rheological Characteristics of Polymer Modified Bitumens**

## **4.1 Introduction**

Polymer modification of bitumen results in a product that under certain loading conditions and temperatures tends to behave more as a polymer than as a bitumen. It is accepted that polymer modification improves the temperature susceptibility of bitumens and, in addition, its resistance to permanent deformation, thermal and fatigue cracking [99]. It is also accepted that a polymer modified bitumen (PMB) with a dominant polymer-rich phase disrupts the traditional viscoelastic behaviour of a bitumen as well as rheological principles such as time-temperature superposition (TTSP) and, therefore, the ability to produce smooth, continuous master curves [3,21,86,89,90].

This chapter looks at the effect of polymer modification on the physical and rheological properties of various EVA and SBS PMB's as measured by conventional methods and more fundamental rheological methods, such as the Dynamic Shear Rheometer (DSR). Although Penetration and Softening Point are empirically based tests, specifically used to determine the consistency of unmodified bitumens, they are still being used in practice to quantify the effects of polymer modification of bitumens. The aims of the tests conducted in this chapter are, therefore, to quantify the effect of polymer modification on the rheological character of PMB's, as well as to produce a critical analysis of the suitability of different test methods for describing the effect of polymer modification, highlighting their advantages and disadvantages.

## 4.2 Experimental Design

### 4.2.1 Materials

Three base bitumens, from different crude sources, were used to produce the EVA and SBS PMB's. The three base bitumens all have similar consistencies and differ only slightly in their chemical composition.

The three base bitumens are:

- Middle East, 80/100 penetration (Paraffinic),
- Russian, 80 penetration (Paraffinic), and
- Venezuelan, 70/100 penetration (Naphthenic).

The chemical compositions of the three base bitumens were determined by means of Iatroscan thin film chromatography analysis to divide the bitumens into SARA chemical fractions as presented in Table 4.1.

**Table 4.1: SARA analysis of base bitumens**

Bitumen	Saturates (%)	Aromatics (%)	Resins (%)	Asphaltenes (%)	Colloidal Index
Middle East 80/100	5	69	15	11	0.190
Russian 80	4	68	19	9	0.149
Venezuelan 70/100	11	58	17	14	0.333

Although the percentages of the different fractions are similar for all three bitumens, the naphthenic Venezuelan bitumen has a higher proportion of high molecular weight asphaltenes and a lower proportion of low molecular weight aromatics compared to the two paraffinic bitumens.

The Colloidal Indices (CI) of the three bitumens were calculated in order to determine the potential compatibility of the base bitumens to polymer modification. Serfass et al [120] are of the opinion that no precise CI borderline exists between what will be a "compatible" and what will be an "incompatible" bitumen. Therefore, although the two paraffinic bitumens have similar SARA and CI values, other factors governing compatibility, such as maltenes solvency power and molecular weight, may differ between the bitumens resulting in different potential compatibilities to polymer modification. Additionally, the use of a chemical composition parameter, such as CI, which is calculated for an unmodified bitumen and used as a means of evaluating the physical compatibility of a polymer-bitumen blend is questionable.

The base bitumens were further characterised by means of their Penetration and Ring and Ball Softening Point as presented in Table 4.2.

**Table 4.2: Empirical test data for base bitumens**

Bitumen	Penetration (dmm)	Softening Point (°C)	Penetration Index (PI)
Middle East 80/100	60	48.8	-1.08
Russian 80	73	47.0	-1.08
Venezuelan 70/100	81	46.8	-0.86

Of the three base bitumens, the Middle East can be graded as the "hardest" and the Venezuelan as the "softest". The temperature susceptibility, as determined by the Penetration Index (PI), indicates that the Middle East and Russian bitumens have identical temperature susceptibilities, with the Venezuelan bitumen having a higher PI value and, therefore, a lower temperature susceptibility.

The two polymers that were used to modify the base bitumens are:

- EVA 20/20 (semi-crystalline polymer), and
- SBS Cariflex linear (thermoplastic rubber).

The EVA copolymer was blended with all three base bitumens, while the SBS copolymer was only blended with the Russian and Venezuelan bitumens, to produce a total of five PMB groups.

The polymer contents of the PMB's are:

- 3% by mass,
- 5% by mass, and
- 7% by mass.

resulting in a total of 15 PMB's. These PMB's are physical blends produced in a laboratory without the addition of compatibilising oils and chemical blending methods.

#### **4.2.2 Testing Programme**

The 15 PMB and three base bitumens were subjected to the following testing programme:

- Chemical analysis (performed by Jean Lefebvre in France),
- Conventional, empirically based testing,
- Viscosity testing, and
- Dynamic mechanical analysis (DMA).

The chemical analysis consisted of DSC evaluation of the thermal behaviour of the semi-crystalline EVA PMB's and HP-GPC analysis of the molecular size distribution of the thermoplastic rubber SBS PMB's.

The DSC analysis was conducted in a heating mode at a constant heating rate of 5°C/min from a temperature of 0°C to 120°C to obtain the fusion temperature parameters and enthalpy associated with the melting of the EVA copolymer. The molecular size distribution of the SBS PMB's was obtained from the refractive index chromatograms of the HP-GPC analysis.

The conventional tests consisted of Penetration and Softening Point, while the viscosity testing was conducted using a rotational viscometry method in a temperature range of 60°C to 160°C for the unmodified bitumens and 100°C to 200°C for the PMB's.

The DMA was performed using a Bohlin Model DSR50 Dynamic Shear Rheometer with the following test conditions:

- Mode of loading: Controlled-strain,
- Temperatures: 10, 15, 25, 35, 45, 55, 65 and 75°C,
- Frequencies: 0.01, 0.015, 0.02, 0.05, 0.1, 0.15, 0.2, 0.5, 1, 1.5, 2, 5, 10 and 15 Hz, and
- Strain amplitude: 0.5% to 10%, depending on temperature.

To appreciate the effect of polymer modification, DMA was also conducted on the semi-crystalline EVA copolymer.

The conventional tests, Penetration and Softening Point, were used to evaluate the temperature susceptibility, as measured by Penetration Index (PI) [73], of the PMB's. The Penetration, Softening Point and viscosity were also incorporated in Heukelom's BTDC [76,77] to evaluate the suitability of the chart at describing the rheological characteristics of PMB's.

The modification of the base bitumens was evaluated by means of an modification index, expressed as:

$$\text{Modification Index} = \frac{P_{\text{MODIFIED}}}{P_{\text{UNMODIFIED}}} \quad (1)$$

where:  $P_{\text{UNMODIFIED}}$  = some rheological property measured on the unmodified bitumen (Softening Point, complex modulus, etc)

$P_{\text{MODIFIED}}$  = the same rheological property as measured on the unmodified bitumen, but performed after bitumen polymer modification

The stiffness values, obtained from the DSR testing, were plotted against the predicted stiffness from Van der Poel's nomograph, to evaluate the suitability of this method at describing the rheological characteristics of PMB's. The rheological data, obtained from rotational viscosity testing and DMA was also analysed in the form of:

- Viscosity-temperature plots,
- Complex modulus and phase angle isochronal plots,
- Complex modulus and phase angle master curves at a reference temperature of 25°C,
- Black diagrams, and
- Cole-Cole diagrams.

The dynamic mechanical data obtained from the DSR was presented in the form of isochronal plots of complex modulus,  $G^*$ , and phase angle,  $\delta$ , at two frequencies of 0.02 Hz and 1 Hz. The lower loading frequency of 0.02 Hz allows the benefits of polymer modification to be more readily identified than is possible at the higher frequency of 1 Hz.

## **4.3 Chemical Analysis of Polymer Modified Bitumens**

### **4.3.1 Differential Scanning Calorimetry of EVA PMB's**

Differential scanning calorimetry (DSC) was performed on the nine EVA PMB's in order to characterise their thermal behaviour. The DSC plots for the 3%, 5% and 7% Venezuelan - EVA PMB's are shown in Figure 4.1. The DSC parameters for all nine PMB's are presented in Table 4.3.

**Table 4.3: Variations in DSC parameters due to modification of EVA PMB's**

Bitumen	Polymer Content	Enthalpy (J/g)	Temperature Fusion Range		
			Peak Temp (°C)	Low Temp (°C)	High Temp (°C)
Middle East 80/100	3%	2.4	69.7	41	81
	5%	3.0	69.9	46	82
	7%	3.2	69.9	47	86
Russian 80	3%	2.7	66.7	44	80
	5%	3.4	69.6	44	83
	7%	4.3	69.9	43	85
Venezuelan 70/100	3%	2.5	61.9	43	77
	5%	3.1	61.5	42	81
	7%	4.4	65.4	42	82

The temperature fusion range, including the peak temperature, differ only slightly between the three EVA PMB groups. The two paraffinic bitumen - EVA combinations both have a peak temperature of just less than 70°C, while the Venezuelan - EVA PMB's have a peak temperature of approximately 65°C. The DSC results are therefore consistent with those of other researchers [47,48].

The enthalpy values, within each bitumen - EVA group increase with polymer content, and also differ between the three groups. Therefore, the use of the same EVA copolymer, combined with different bitumens, but with the same SARA proportions (paraffinic bitumens), does not guarantee an identical behaviour for the different PMB combinations. Although, the differences in enthalpy between the three groups are not large, on average it can be seen that the Middle East - EVA PMB's have the lowest enthalpy values, followed by the Venezuelan - EVA group with the Russian - EVA PMB's been highest. Lower enthalpy values correspond to bitumen - EVA blends that have a high compatibility, while high enthalpy values are found for blends will poor compatibility [121]. The Russian - EVA PMB's will, therefore, be considered to be less compatible than the Middle East and Venezuelan - EVA PMB's.

The ability of the different rheological characterisation methods at demonstrating the

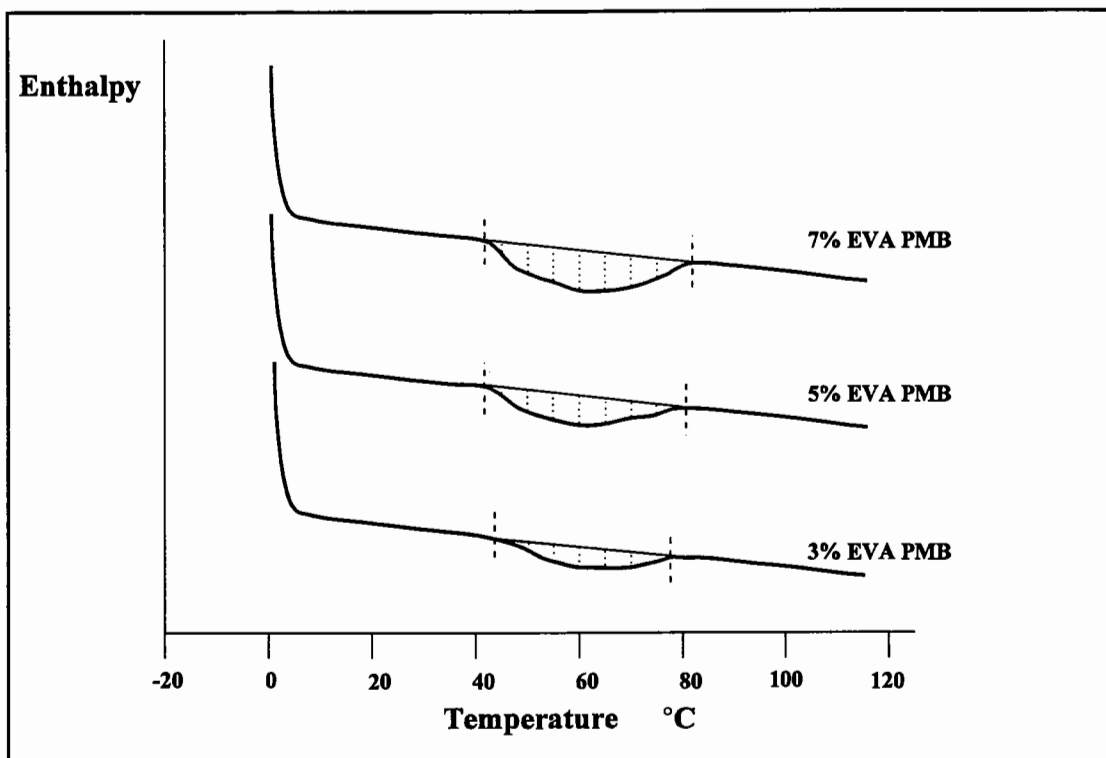


Figure 4.1: DSC plot for Venezuelan - EVA PMB's

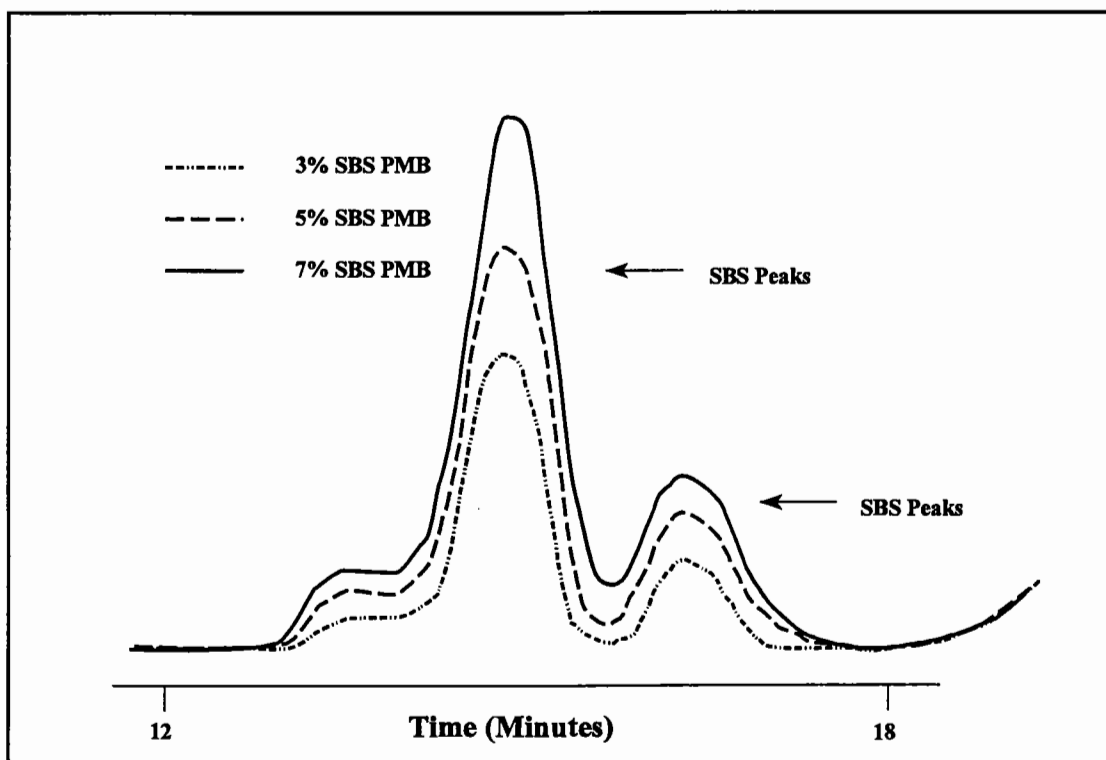


Figure 4.2: HP-GPC plot for Venezuelan - SBS PMB's



differences in behaviour of the EVA PMB's, as shown by their differences in thermal behaviour and compatibility, will be investigated in the subsequent sections of this chapter.

### **4.3.2 High Performance Gel Permeation Chromatography of SBS PMB's**

The chromatogram of the 3%, 5% and 7% Venezuelan - SBS PMB's are shown in Figure 4.2. The chromatograms show an increase in the peaks, corresponding to the molecular weights of the SBS copolymer, as the polymer content increases. Although the HP-GPC analysis has enabled the SBS copolymer to be identified and the increase in polymer content to be verified, its ability, in its present form, to quantify any particular rheological characteristic is limited.

## **4.4 Conventional Physical Property Tests**

### **4.4.1 Penetration and Softening Point**

The Penetrations and Softening Points for the five PMB groups are presented in Table 4.4 and indicate that for all five PMB groups there is a decrease in Penetration with increasing polymer content and therefore modification. The increase in binder hardness, as indicated by the decrease in penetration, can be attributed to a hardening effect caused by the addition of the EVA and SBS copolymers to the base bitumens.

The Softening Points, in Table 4.4, increased after polymer modification indicating the same increase in hardness or stiffness of the PMB's as seen for the Penetrations. Relying on the results from these two empirical tests, the mechanism of modification for the EVA and SBS copolymer PMB's would seem to consist simply of a stiffening of the base bitumen.

**Table 4.4: Penetration and Softening Point for PMB's**

Bitumen	Modification	Penetration (dmm)	Softening Point (°C)
Middle East 80/100	0% EVA	60	48.8
	3% EVA	53	54.8
	5% EVA	43	61.0
	7% EVA	37	69.4
Russian 80	0% EVA	73	47.0
	3% EVA	61	59.5
	5% EVA	51	66.6
	7% EVA	47	69.2
Venezuelan 80/100	0% EVA	81	46.8
	3% EVA	65	53.7
	5% EVA	58	63.8
	7% EVA	53	69.2
Russian 80	0% SBS	73	47.0
	3% SBS	63	52.4
	5% SBS	57	78.0
	7% SBS	50	95.0
Venezuelan 70/100	0% SBS	81	46.8
	3% SBS	63	52.2
	5% SBS	54	74.0
	7% SBS	49	88.0

**Modification Indices**

The modification indices for Penetration and Softening Point, determined using Equation 1, are presented in Figures 4.3 and 4.4. The data presented in these figures is not intended to present a modification versus polymer content relationship, but merely to improve the understanding of the modification process.

Figure 4.3 illustrates that, although there are variations in the magnitude of the modification index between the five PMB groups, no distinctive trends could be identified. The Penetration test therefore seems to be relatively insensitive to the morphology of the EVA and SBS PMB's, indicating a stiffening effect that could be accomplished through the addition of any 'filler' type material, or even ageing of the base

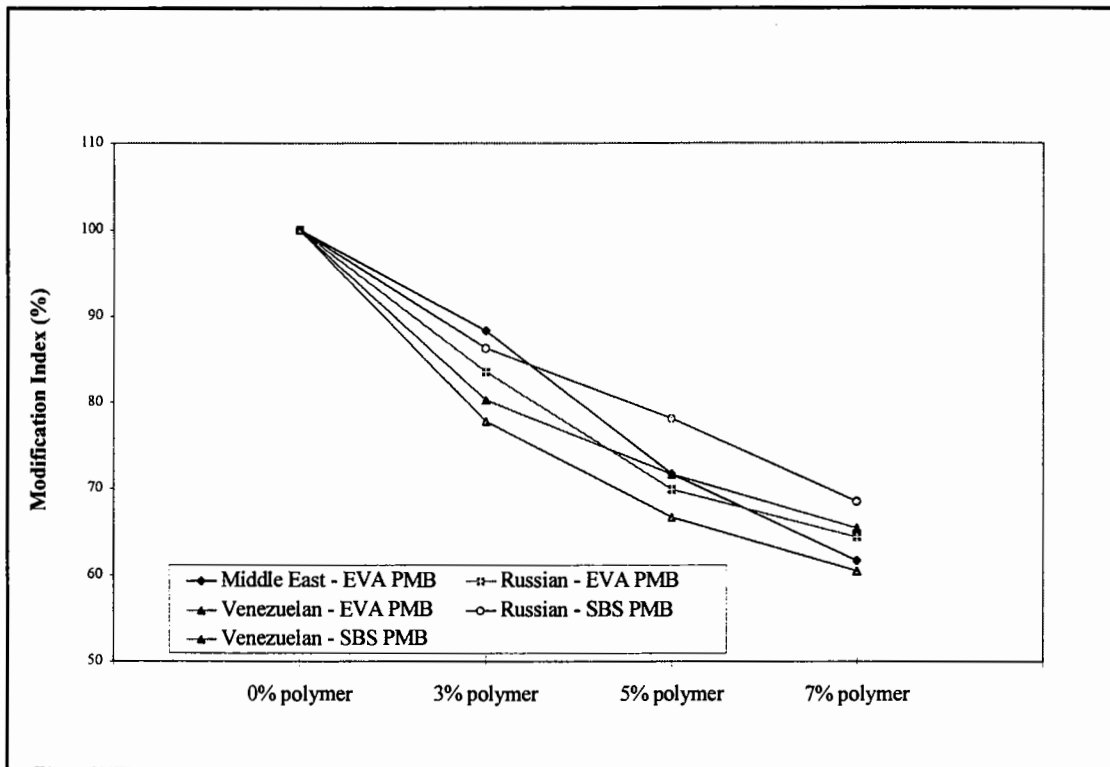


**Figure 4.3: Modification indices for Penetrations of PMB's**

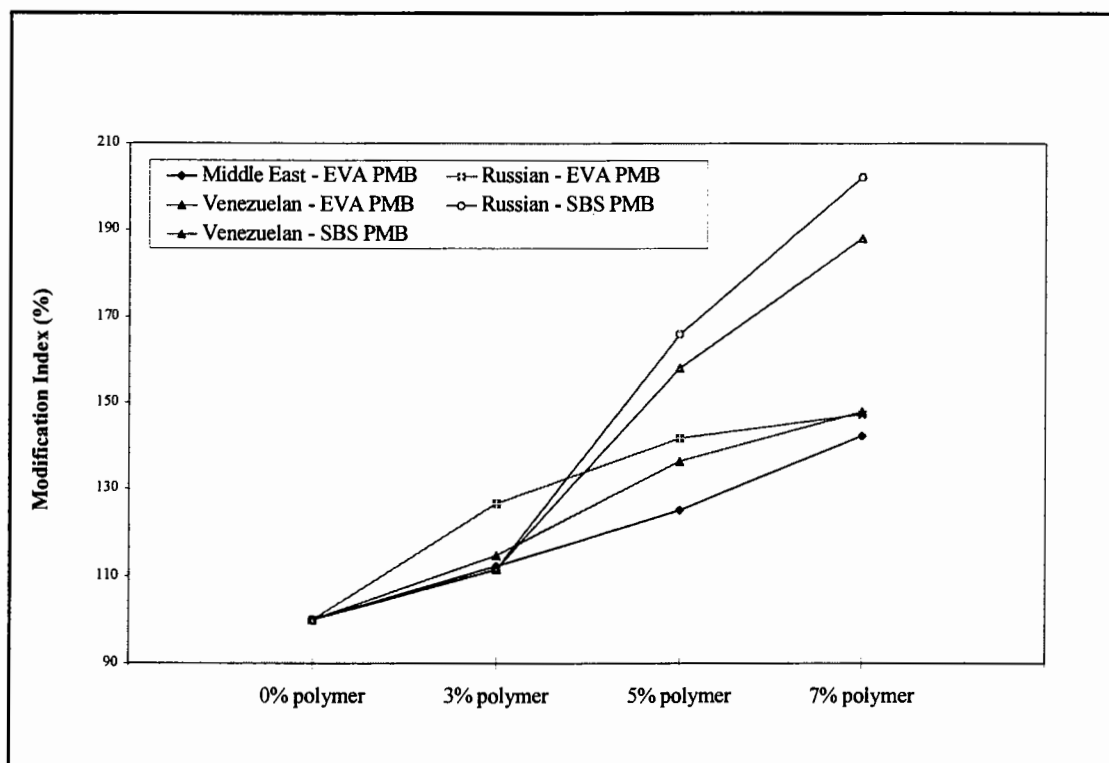


**Figure 4.4: Modification indices for Softening Points of PMB's**

bitumen.

The modification indices for the Softening Points differ from those seen for the Penetrations in that there are, firstly, two distinctly different trends for the EVA and SBS PMB's, and, secondly, slightly different trends amongst the EVA PMB's.

Considering the two different trends for the EVA and SBS PMB's, the EVA PMB's show a relatively consistent increase in Softening Point as the polymer content increases from 3% to 7%. However, for the SBS PMB's, the increase is relatively minor, approximately 10 percent, at the 3% polymer level, but shows a sharp increase at the 5% level, being approximately 160 percent, followed by a slight reduction in the slope of the increase to be approximately 200 percent at the 7% polymer level. These "S" shaped curves, for the two SBS PMB's in Figure 4.4, indicate that below a certain SBS content, there is no polymer network in the binder and the polymer only acts as a filler. Above another SBS content, the polymer forms a complete network and the bitumen acts as an extender [120]. Between these two limits, there is a sharp variation in the binder characteristics.

The different trends seen amongst the three EVA PMB's is not as clearly defined as those discussed above between the EVA and SBS PMB's, but does allow some explanation of the rheological characteristics of the PMB's. It was highlighted in the literature review that EVA copolymers are compatible with most bitumens, but that in order to see the advantages of polymer modification, a degree of incompatibility was desirable. Too high a degree of compatibility results in the EVA copolymer performing simply as a filler in the modified bitumen without attaining a rheologically polymer dominant system. It was mentioned in the literature review that this could be overcome by increasing the polymer content, but that this solution would probably not be cost effective.

Assuming that higher modification indices, with regard to softening point, are indicative of a greater degree of polymer modification, rather than simple filler-like modification, the three EVA PMB's show three distinctive trends. Firstly, the Middle East - EVA blend shows a consistent increase in modification index versus polymer content, but these

modifications levels, compared to those of the other two EVA PMB groups, are relatively low. Secondly, the Venezuelan - EVA blend starts with a low modification level, but then shows a sharp increase in modification at the 5% polymer level and a similar "S" shaped curve as seen for the SBS PMB's. Finally, the Russian - EVA blend shows a high degree of polymer modification from the low 3% polymer content level through to the 7% level.

#### 4.4.2 DSC Enthalpy Correlation

The DSC thermal behaviour of the EVA PMB's, has indicated that there is a relationship between enthalpy and compatibility of the EVA blends and, therefore, a possible relationship between enthalpy and degree of polymer modification. The DSC results in section 4.3.1 have shown that the Middle East - EVA blends are the most compatible, while the Russian - EVA blends are the least compatible. When the modification indices for softening point are plotted against DSC enthalpy, in Figure 4.5, there is a clear trend of an increase in modification with an increase in enthalpy, depicting an increase in modification with a decrease in compatibility between bitumen and EVA polymer.

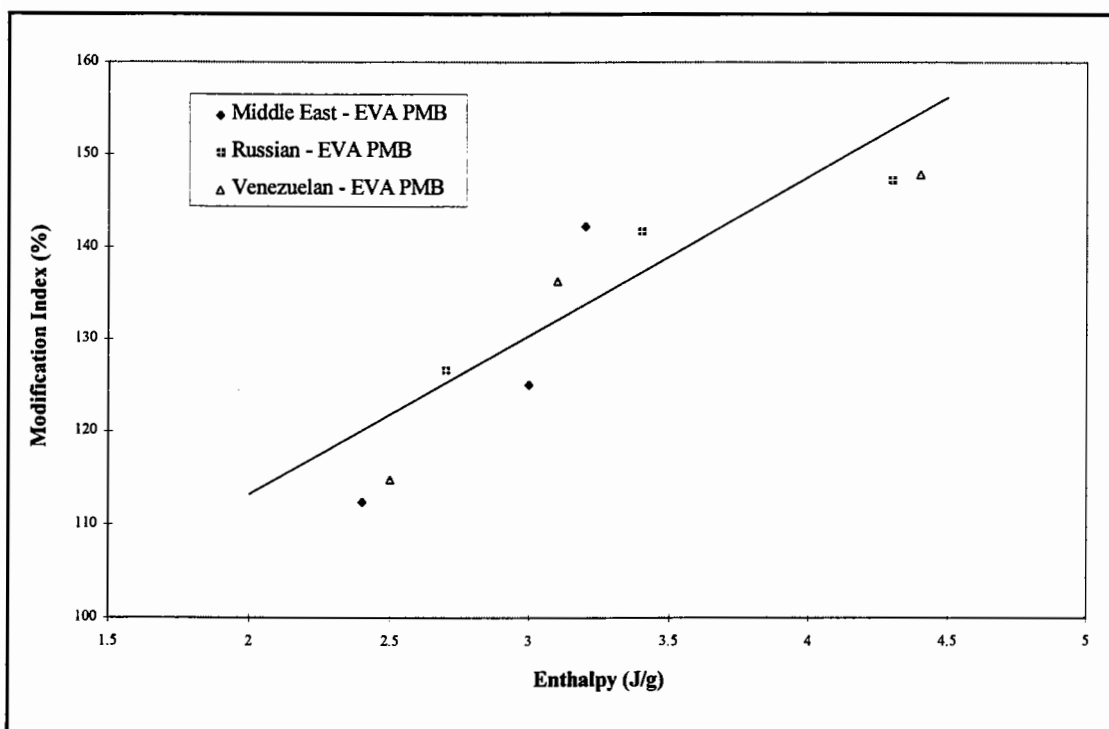


Figure 4.5: Relationship between Softening Point modification indices and DSC enthalpy

#### 4.4.3 Temperature Susceptibility

The temperature susceptibility, as indicated by PI, has been calculated for the EVA and SBS PMB's and presented in Table 4.5.

**Table 4.5: Temperature susceptibility of PMB's as measured by PI**

Bitumen	Modification	Penetration Index
Middle East 80/100	0% EVA	-1.08
	3% EVA	0.08
	5% EVA	0.86
	7% EVA	1.99
Russian 80	0% EVA	-1.08
	3% EVA	1.45
	5% EVA	2.31
	7% EVA	2.54
Venezuelan 80/100	0% EVA	-0.86
	3% EVA	0.35
	5% EVA	2.15
	7% EVA	2.86
Russian 80	0% SBS	-1.08
	3% SBS	-0.05
	5% SBS	4.41
	7% SBS	6.13
Venezuelan 70/100	0% SBS	-0.86
	3% SBS	-0.09
	5% SBS	3.67
	7% SBS	5.29

The PI's in Table 4.5 indicate an improvement in temperature susceptibility with modification. This finding is not surprising as the traditional use of polymers is to improve the temperature susceptibility of bitumens. However, the extent of the increase in temperature susceptibility differs amongst the five PMB groups.

The two SBS PMB groups obtain the highest PI values after modification compared to

the EVA groups, although the PI values for the 3% SBS PMB's are the lowest of all 15 PMB's. The increase in PI's for the EVA and SBS PMB's shows an identical trend to that seen with the increase in modification index as measured by softening point. The PI's for the Middle East - EVA PMB's, therefore, increase relatively constantly versus polymer content, but are lower than that of the other two EVA PMB groups. The Venezuelan - EVA PMB's show a sharp increase in PI at the 5% polymer content level, while the Russian groups shows a sharp increase from the 3% level.

In summary, the conventional tests, Penetration, Softening Point and finally PI, give two different explanations of the modification mechanisms associated with EVA and SBS polymer modification. The Penetration test indicates a relatively uniform behaviour for the PMB's and is probably due to the test temperature of 25°C being too low to allow a reasonable evaluation of the benefits of polymer modification, traditionally seen at higher service temperatures (> 40°C). The Penetration test, therefore, can only indicate the effect of polymer modification as a filler-type modification. The Softening Point test is able to differentiate between filler type modification and genuine polymer type modification when describing the rheological characteristics of polymer modification but overestimates the possible advantages of modification. The same modification mechanism is seen with PI analysis and can probably be linked directly to the use of Softening Point in the calculation of PI.

## **4.5 Viscosity Testing**

### **4.5.1 High Temperature Viscosity Analysis**

The rotational viscosities for the Russian PMB's are presented in Figure 4.6. As with the Penetration and Softening Point tests there is a clear indication of the hardening effect caused by the addition of either a EVA or SBS copolymer to bitumen. Similar results have been obtained for Middle East and Venezuelan base bitumen PMB's.

Figure 4.6 illustrates that there is a consistent increase in high temperature viscosity

coupled with the increase in the polymer content of the EVA and SBS PMB's. This increase is greater for the SBS PMB's, but other than requiring higher mixing and compaction temperatures for a similar polymer content SBS PMB compared to an EVA PMB, the rheological characteristics of the two polymer type PMB's are identical.

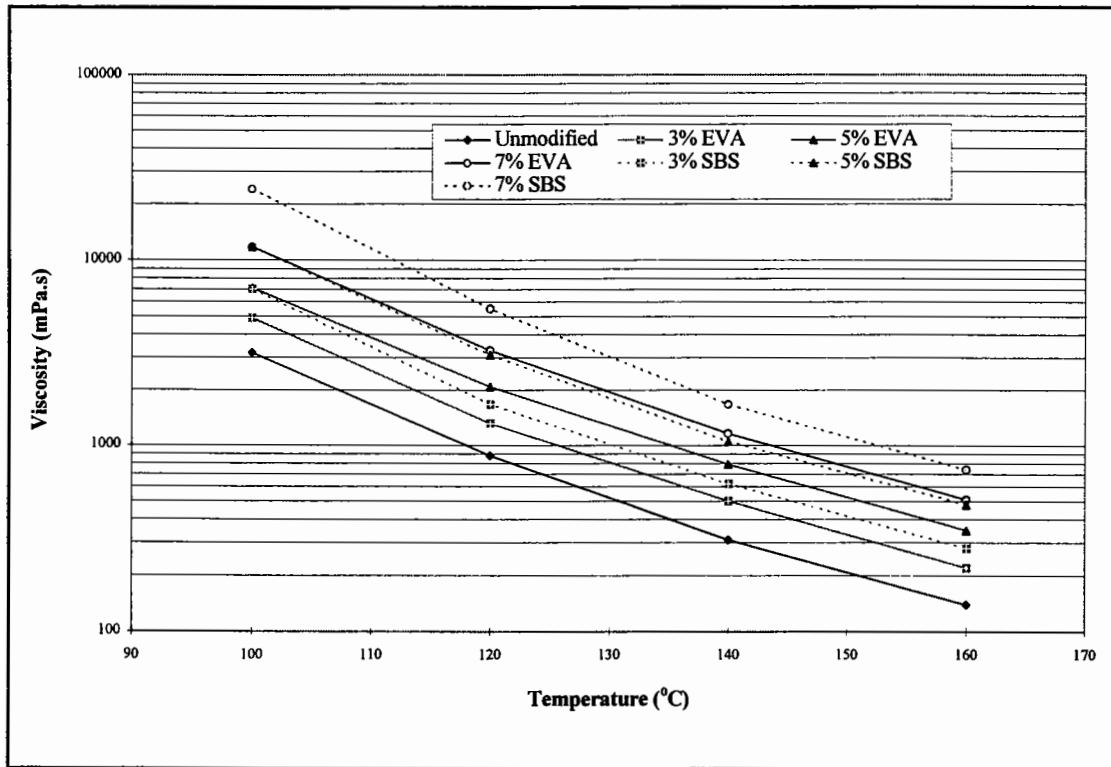


**Figure 4.6: High temperature viscosity for Russian PMB's**

The effect of modification on the high temperature viscosities of the PMB's are more indicative of a filler type modification than a rheologically polymer type modification. This is because the SBS copolymer melts at the glass transition temperature of the polystyrene of approximately 100°C, while the EVA copolymer melts at a lower temperature of approximately 65°C to 80°C. Both copolymers are, therefore, already in their melted state at temperatures of 100°C and higher. Generally, therefore, the high temperature viscosity, as with Penetration, only indicates the effect of polymer modification as a simple form of filler-like modification or hardening of the bitumen.



#### 4.5.2 Bitumen Test Data Chart

Heukelom's BTDC enables Penetration, Softening Point and rotational viscosities to be plotted on one chart as a function of temperature [75,76]. In addition to the conventional data presented in the BTDC, zero shear viscosities (steady state viscosities) obtained from the DMA have also been included. Two construction methods can be used to estimate the zero shear viscosity from the dynamic data obtained with the DSR. The first method consists of plotting complex viscosity,  $\eta^*$ , versus  $(1-\delta/90^\circ)^{1.5}$  and extrapolating to the intercept where  $(1-\delta/90^\circ)^{1.5}$  equal  $0^\circ$  [65]. When constructing this plot, the data should only include phase angles greater than approximately  $70^\circ$ . The second approach is to estimate the zero shear viscosity,  $\eta_0$ , by plotting the dynamic viscosity,  $\eta'$ , against shear rate for each loading frequency and extrapolating the calculated dynamic viscosity to a zero strain rate [72,122].

The SHRP [65] and Puzinauskas [72,122] plots for the Middle East base bitumen are shown in Figures 4.7 and 4.8. The zero shear viscosities extrapolating from these two construction methods are presented in Table 4.6 and show that both methods are suitable for calculating the  $\eta_0$  for unmodified bitumens.

**Table 4.6: Zero shear viscosities,  $\eta_0$ , for Middle East 80/100 pen bitumen**

Temperature ( $^\circ\text{C}$ )	SHRP - viscosity (Pa.s)	Puzinauskas - viscosity (Pa.s)
25	244,064	219,167
35	23,380	23,725
45	3,596	3,578
55	653	647
65	161	159
75	47	47

The SHRP method relies on the bitumen having typical viscoelastic behaviour, with the phase angle approaching  $90^\circ$  at high temperatures and/or low loading frequencies. The method therefore relies on the bitumen fulfilling the time-temperature superposition principle (TTSP) and, therefore, is not applicable for PMB's. The SHRP plots for the 7%

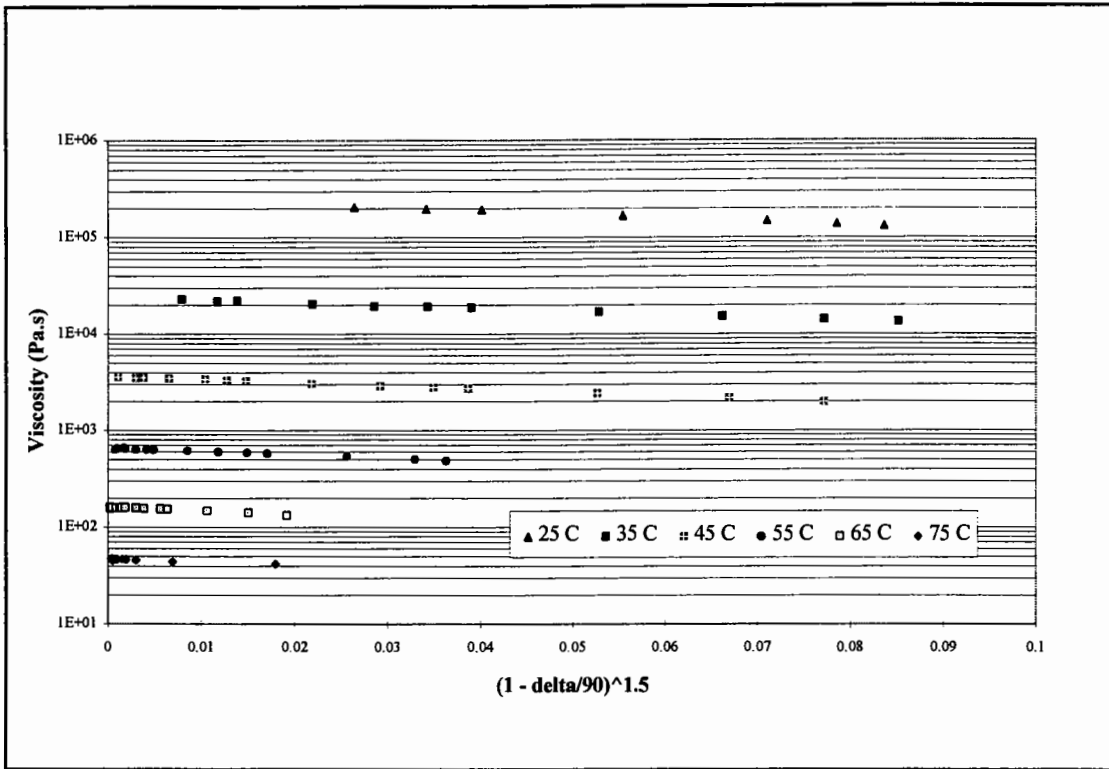


Figure 4.7: Zero shear viscosity - SHRP method for Middle East 80/100 pen

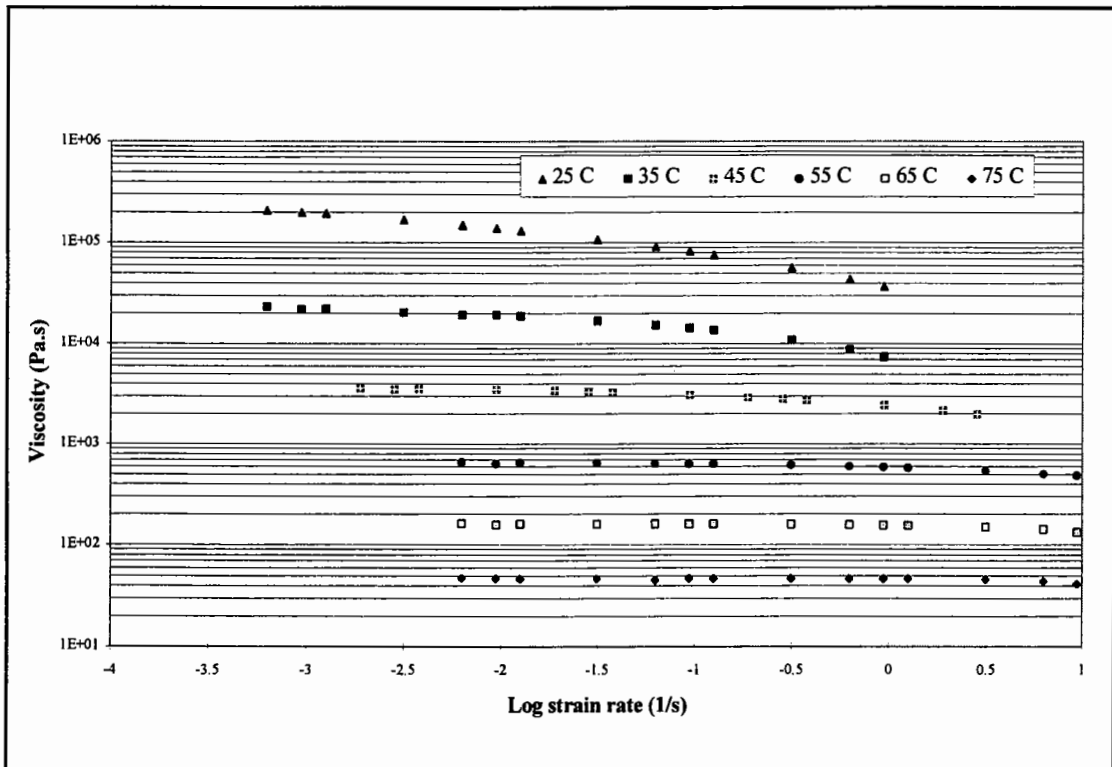


Figure 4.8: Zero shear viscosity - Puzinauskas method for Middle East 80/100 pen

EVA - Russian and 7% SBS - Russian PMB's are shown in Figures 4.9 and 4.10 which illustrate that the SHRP method, is unable to provide an estimate of the zero shear viscosity for PMB's. The limitation of the SHRP method can be attributed to its inability to account for the different crystalline structures found at different temperatures in the EVA PMB and the increased elasticity of the SBS copolymer. The Puzinauskas method was, therefore, used to determine  $\eta_0$  for the PMB's

Although, the BTDC was not designed to include the plotting of viscosity data at low and intermediate temperatures ( $< 60^\circ\text{C}$ ), the zero shear viscosities allow data to be plotted, together with the empirical data (Penetration, Softening Point), in the typical service temperature range of the bitumen. The BTDC charts for the 7% EVA and 7% SBS - Russian PMB's are shown in Figures 4.11 and 4.12. The charts are not meant to provide a fundamental analysis of the various PMB's, but do allow various observations to be made with regard to the suitability of conventional tests at describing the rheological characteristics of PMB's.

The charts show that a straight line can be fitted through the Penetration, Softening Point and high temperature viscosities, together with the zero shear viscosities, for the unmodified bitumen but not for the PMB's. The data plotted in Figure 4.11 for the Russian - EVA PMB highlights two aspects concerning the rheological characteristics of PMB's and the suitability of the various testing methods. Firstly, the zero shear viscosities, between  $35^\circ\text{C}$  and  $65^\circ\text{C}$ , are greater than what would have been estimated if a straight line had been drawn through the penetration and high temperature viscosity results. This increase in viscosity indicates the presence of a polymer dominant type of modification and confirms the finding by Dony and Turmel [123] that, although straight lines can be fitted through the data obtained for the unmodified bitumens (Class S bitumens), they cannot be produced for PMB's. Dony and Turmel [123], therefore, concluded that viscoelasticity measurements are more appropriate at evaluating the temperature susceptibility of modified bitumens than PI, as the viscosity data plotted on the BTDC shows that PMB's have different temperature susceptibilities within different temperature ranges.

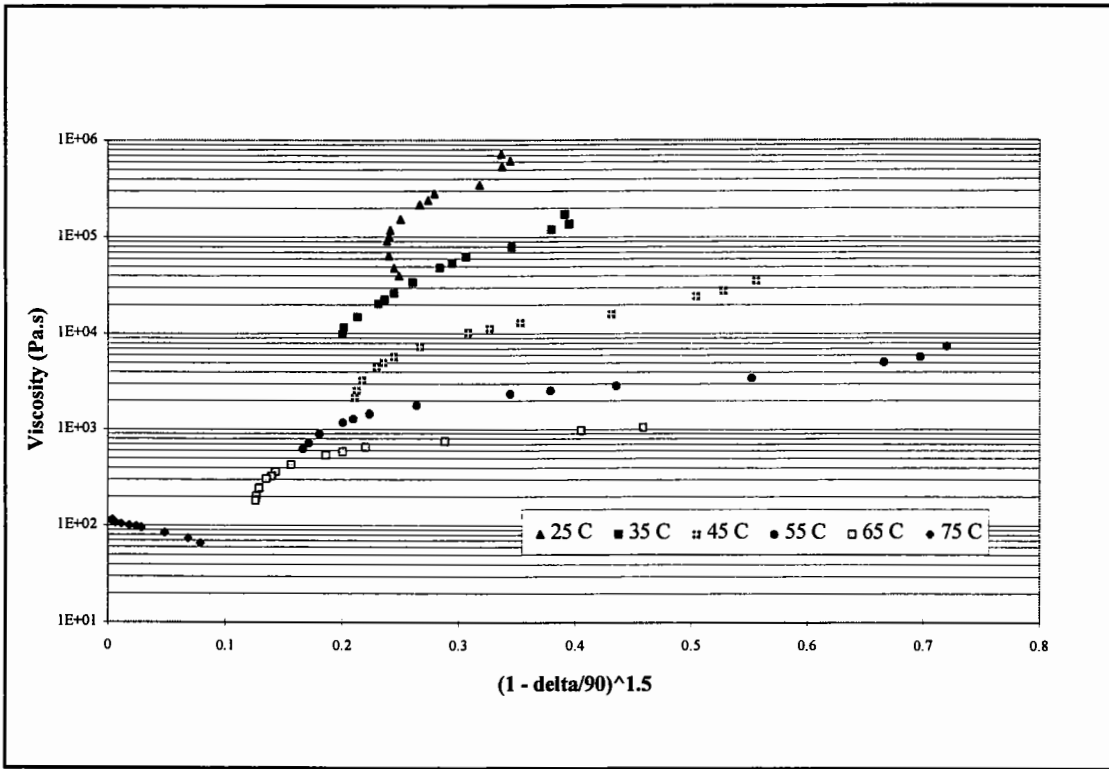


Figure 4.9: Zero shear viscosity - SHRP method for 7% EVA- Russian 80 pen

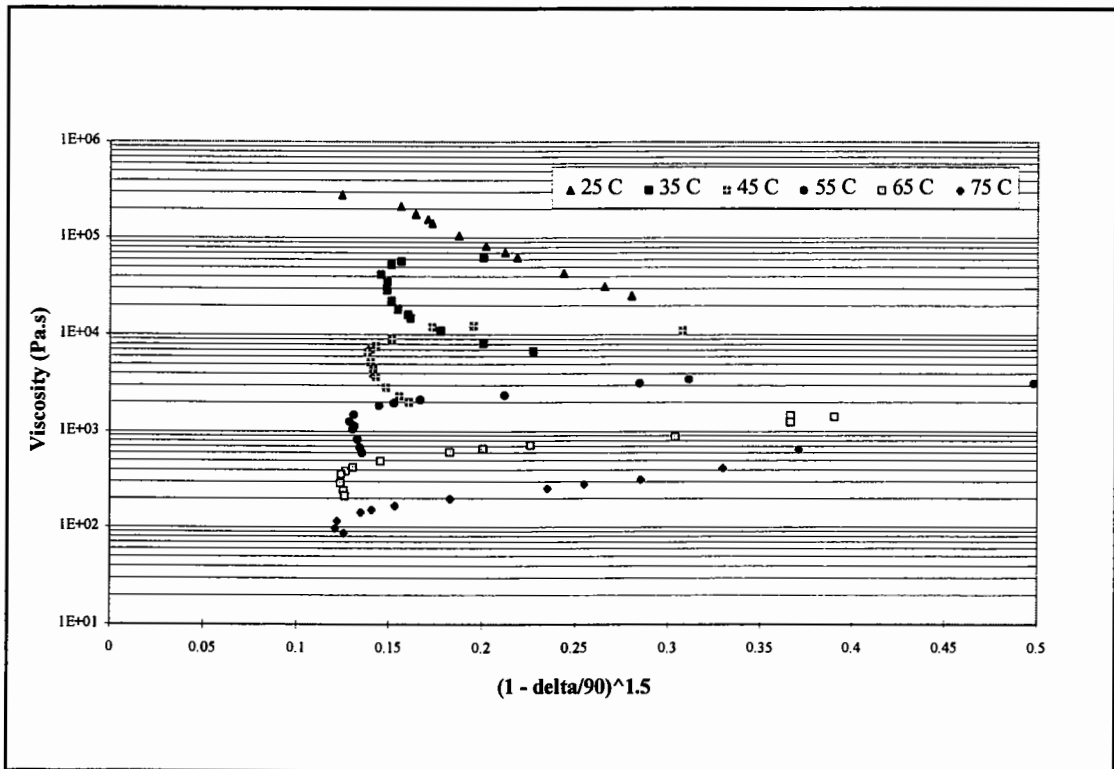


Figure 4.10: Zero shear viscosity - SHRP method for 7% SBS - Russian 80 pen

The second aspect that can be seen in Figure 4.11, it that the Softening Point for more polymeric type PMB's slightly overestimates the benefits of polymer modification. The same phenomenon can be seen in the BTDC for the Russian - SBS PMB in Figure 4.12, which illustrates that the Softening Points for the 7% PMB considerably overestimates the benefits of polymer modification. King et al [124] have found that the correlation between Softening Point and rutting resistance for PMB's is extremely poor for styrene butadiene (SB) block copolymer modified PMB's. The correlation is not bad for unmodified bitumens and low polymer content PMB's, but the correlation falls apart for highly modified PMB's. King et al [124], therefore, concluded that polymers can help resist rutting, but not as much as their elevated softening points imply, particular for soft, highly modified bitumens.

Figure 4.12 also illustrates that the increase in viscosity of the highly polymer modified 7% SBS PMB extends over a wider temperature range up to 75°C due to the higher melting temperature of the SBS copolymer compared to the EVA copolymer.

#### **4.5.3 Zero Shear Viscosity Analysis**

The zero shear viscosities, obtained from the DSR and the rotational viscometer, are plotted against temperature for the Middle East, Russian and Venezuelan base bitumen PMB's in Figures 4.13 to 4.15. The wider temperature range of these viscosity-temperature plots allow a better rheological characterisation of the different PMB's than that available with the Penetration, Softening Point and high temperature viscosity tests.

The viscosity-temperature relationship for the Middle East - EVA PMB's, Figure 4.13, shows a consistent increase in viscosity over the entire temperature range from 35°C to 140°C. The DSC analysis has indicated that the EVA copolymer melts within the temperature of approximately 40°C to 85°C, but there are no indications of this melting region in Figure 4.13. The modification index versus DSC enthalpy plot in Figure 4.5, has indicated that the Middle East - EVA blends may be too compatible, resulting in a masking of the polymeric properties of the PMB's.

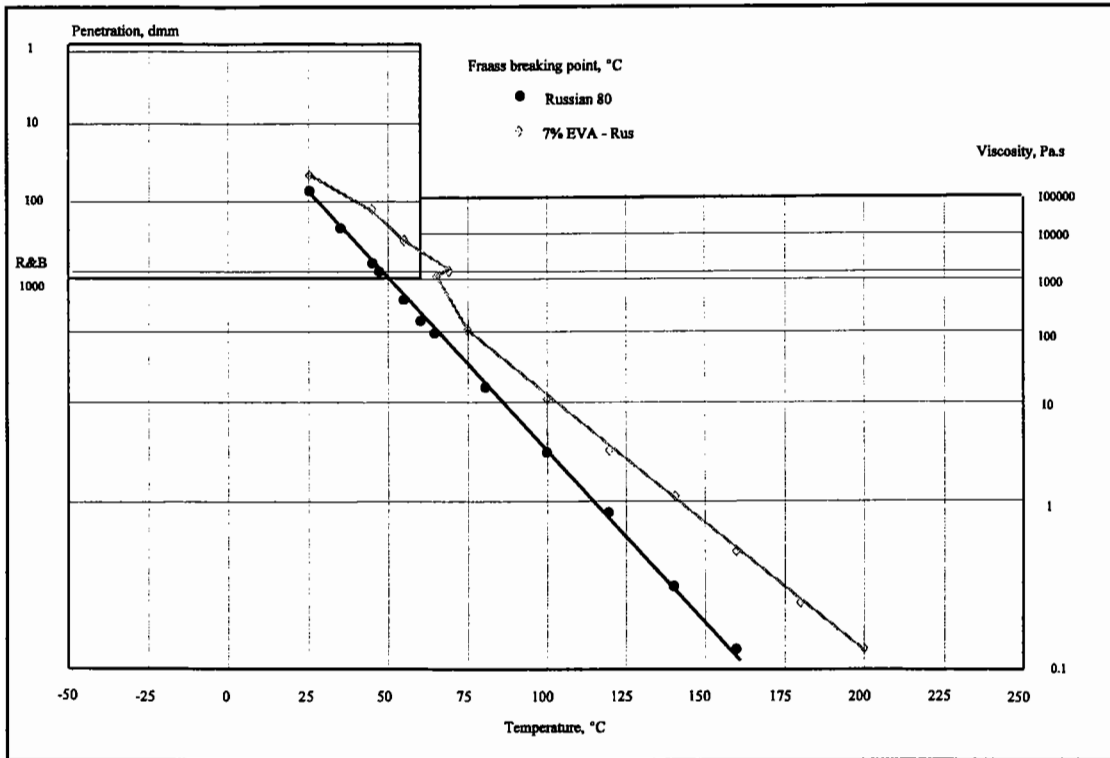


Figure 4.11: BTDC for Russian - EVA PMB

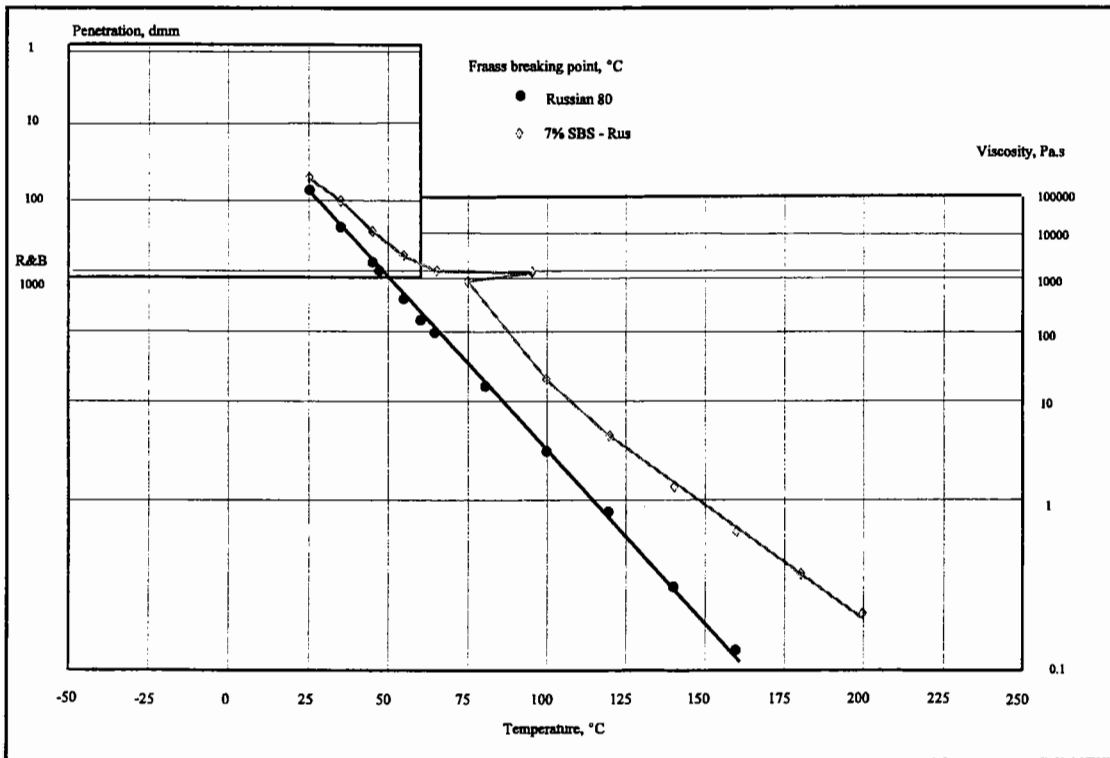


Figure 4.12: BTDC for Russian - SBS PMB

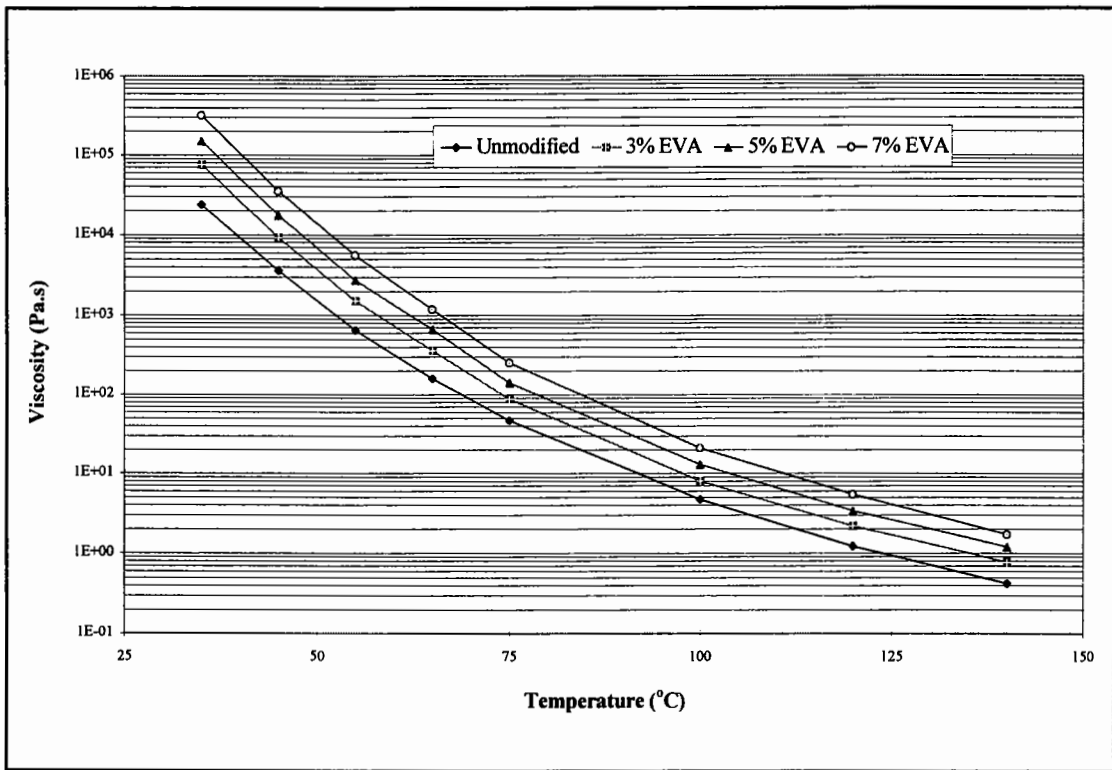


Figure 4.13: Viscosity-temperature plot for Middle East - EVA PMB's

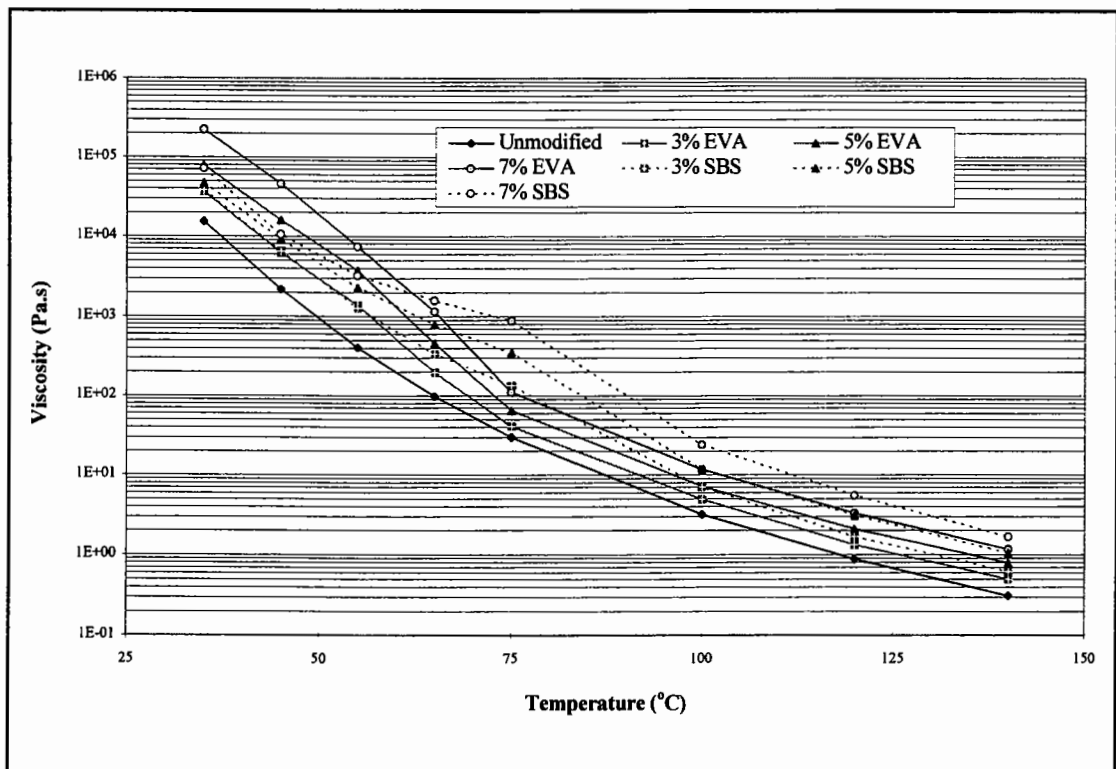
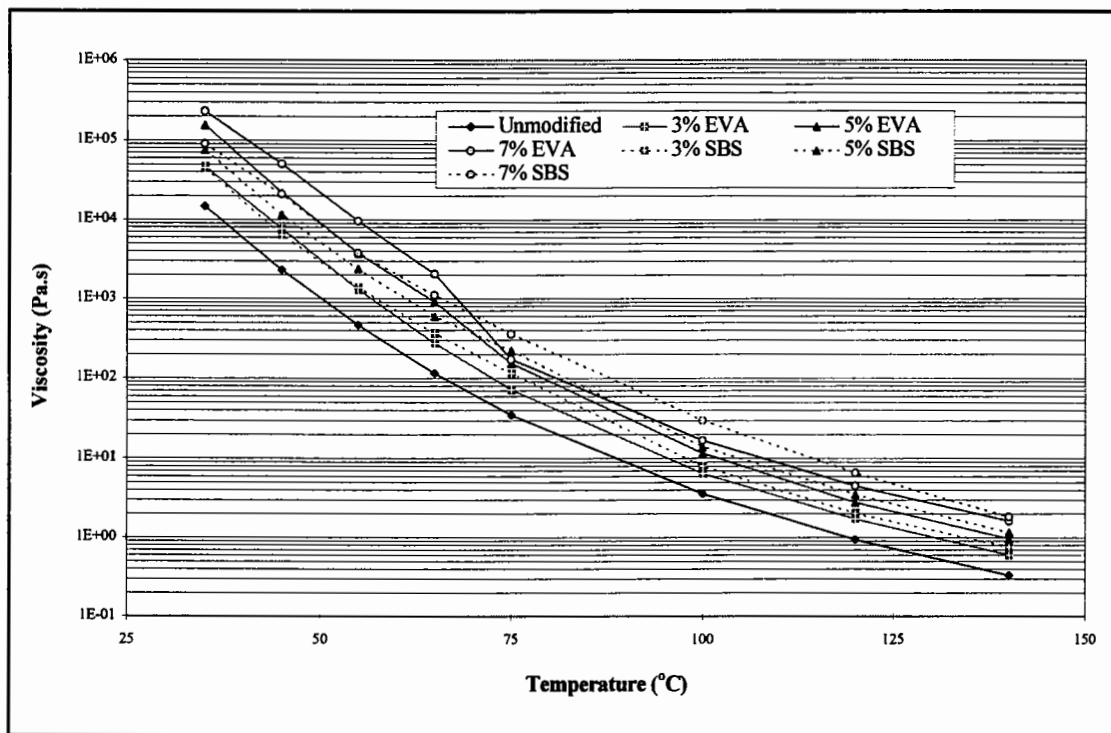


Figure 4.14: Viscosity-temperature plot for Russian PMB's

Figure 4.14 shows the viscosity-temperature relationships for the Russian - EVA and SBS PMB's within the temperature range of 35°C to 140°C. The viscosity curves for the three EVA - PMB's clearly indicate the melting (fusion) region of the EVA copolymer between 55°C and 75°C for the 3% EVA PMB and between 65°C and 75°C for the other two PMB's. These temperature ranges are smaller than the melting range of approximately 45°C to 80°C and 45°C to 85°C indicated by the DSC analysis, but the peak fusion temperature still occurs at the midpoint of the temperature range.

The curves for the SBS PMB's differ from that of the EVA PMB's. Compared to the EVA PMB's, the melting of the SBS copolymer occurs at a higher temperature of between 75°C and 100°C and probably just below 100°C [34]. The presence of the SBS polymer network allows an almost plateau-like viscosity behaviour to be seen within the temperature range of 55°C to 75°C.



**Figure 4.15: Viscosity-temperature plot for Venezuelan PMB's**

The different rheological characteristics of the EVA and SBS PMB's results in differences in the relative performance of the different PMB's as depicted in the viscosity-temperature plots. Within the temperature range 35°C to 55°C, the EVA PMB's



have a greater increase in viscosity after modification than the SBS PMB's. However, the relative performance of the EVA and SBS PMB's changes within the temperature range of 55°C to 100°C, principally due to the different melting zones of the two copolymers. The result is that the SBS PMB's show a higher viscosity within this temperature range, particularly at 75°C. The relative high temperature viscosity performance of the two polymers has been discussed in section 4.5.1.

The viscosity-temperature relationships for the Venezuelan - EVA and SBS PMB's are shown in Figure 4.15. The 3% and 5% EVA PMB's show a similar relationship to that seen for the Middle East - EVA PMB's, while the rheological behaviour of the 7% EVA PMB is similar to that of the Russian - EVA PMB's. The DSC analysis of the three EVA PMB groups showed that the Venezuelan group had a compatibility between that of the Middle East and Russian groups. This has resulted in the polymeric characteristics of the lower polymer content PMB's being masked by the bitumen, but being more evident for the high polymer content PMB.

The viscosity curves for the Venezuelan - SBS PMB's differ from those seen for the Russian - SBS PMB's. The differences in the behaviour of the two SBS PMB groups can be attributed to the different compatibilities experienced between the SBS copolymer and the paraffinic and naphthenic bitumens.

### **Modification Indices**

The modification indices related to the viscosities are illustrated in Figures 4.16 to 4.18. The modification indices allow the relative modification characteristics of the different PMB groups to be quantified.

The Middle East - EVA PMB's are presented in Figure 4.16, where the modification indices are at a maximum at 35°C and decrease continuously through the melting zone of the copolymer and remain at a constant level, dependant on the polymer content, through the high temperature viscosity region. The results clearly indicate the failure of the semi-crystalline polymer - bitumen blend to establish the mechanical characteristics

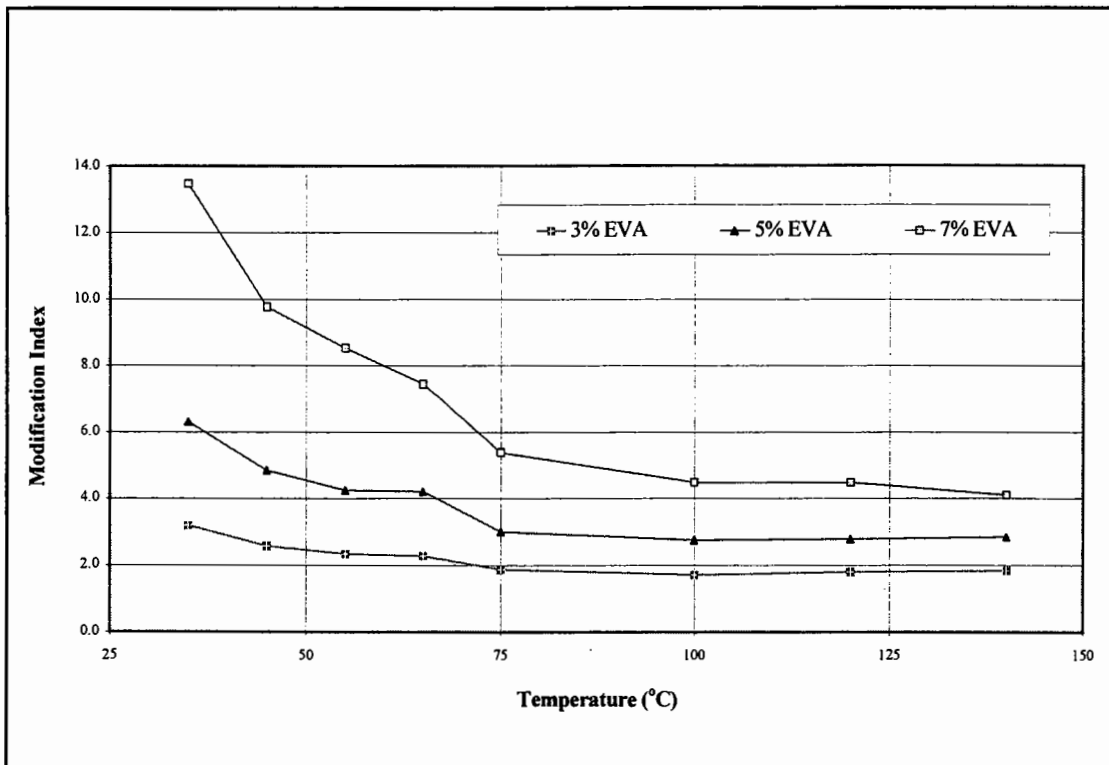


Figure 4.16: Modification indices for viscosity for Middle East PMB's

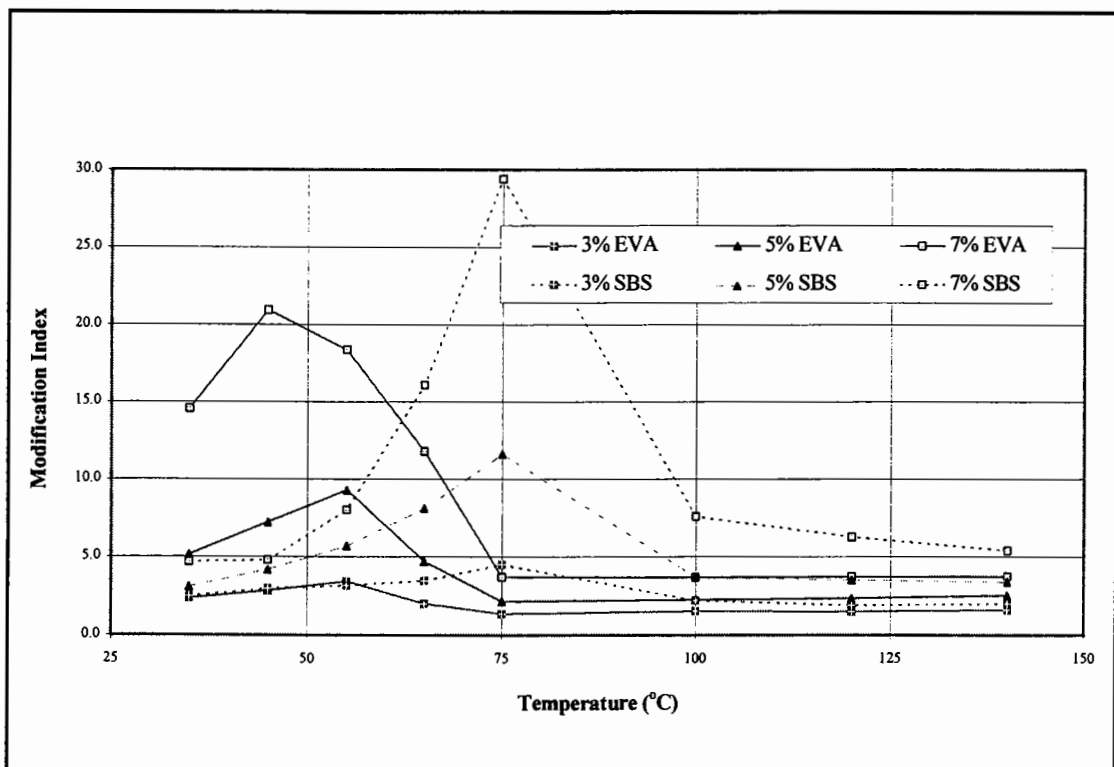
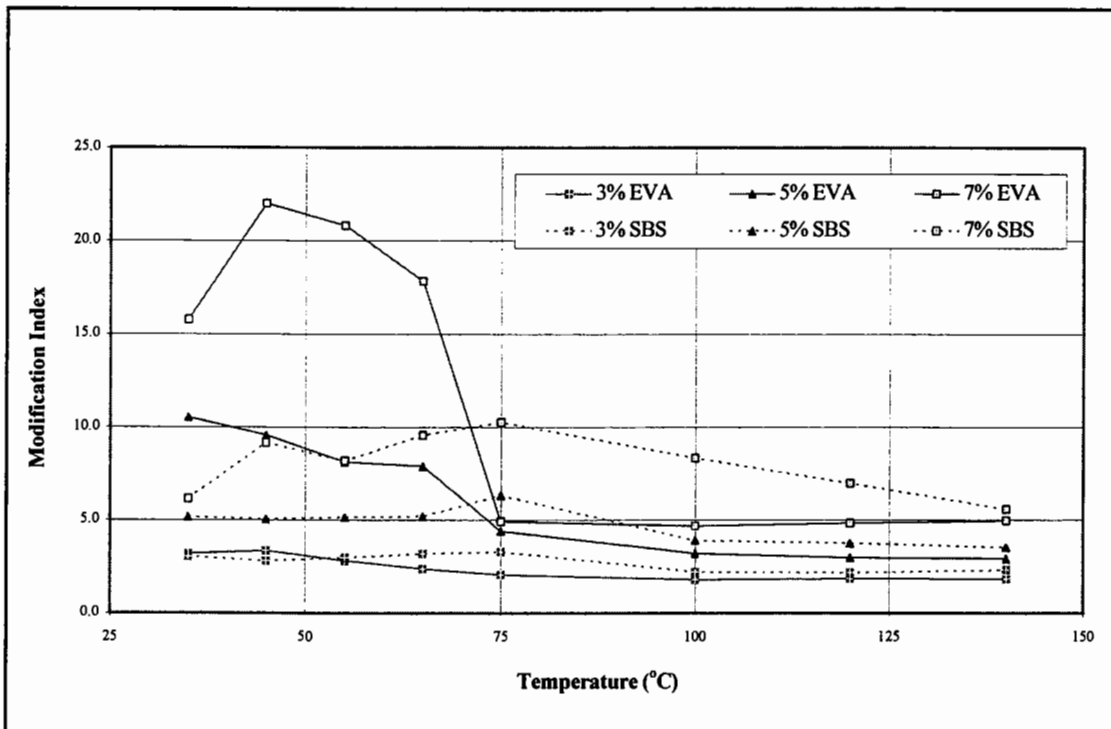


Figure 4.17: Modification indices for viscosity for Russian PMB's

of the ethylene copolymer. The high degree of compatibility of the three Middle East - EVA blends has dissolved the tough, rigid three dimensional network, that would have enhanced the modification of the blends within the temperature range of approximately 45°C to 75°C.

The modification indices for the Russian PMB's are shown in Figure 4.17. The three EVA PMB's show similar modification indices at 35°C, as seen for the Middle East - EVA PMB's, but rather than decreasing, they increase to a modification peak at 45°C or 55°C, before decreasing through the EVA melting zone and finally remaining constant at high temperatures. The increase in modification prior to the melting zone can be attributed to the tough, rigid three dimensional EVA network of the PMB's. The SBS PMB's show a peak in their modification indices at a higher temperature of 75°C, which is also greater in magnitude compared to the corresponding polymer content EVA PMB's.



**Figure 4.18: Modification indices for viscosity for Venezuelan PMB's**

The modification indices for the Venezuelan - EVA PMB's are shown in Figure 4.18 and show relationships similar to that seen for the Middle East PMB's, for the 3% and 5%

EVA PMB's, and similar to that seen for the Russian - EVA PMB's for the 7% EVA PMB. The modification indices for the Venezuelan - SBS PMB's are lower than for the Russian - SBS PMB's within the polymer dominant temperature range of 55°C to 75°C. However, above and below this temperature range, the modification indices are higher for the Venezuelan compared to the Russian PMB's.

## **4.6 Dynamic Mechanical Analysis**

### **4.6.1 Van der Poel's Nomograph**

Van der Poel's nomograph provides a link between empirical tests, Penetration and Softening Point, and the stiffness modulus of bitumen, which can be determined by means of DMA. The measured stiffness moduli, obtained from the DSR, have been plotted against the predicted stiffness moduli, from Van der Poel's nomograph, for the unmodified and EVA modified Middle East PMB's in Figure 4.19. The results indicate that for penetration grade bitumen and the low polymer content EVA PMB, the predicted stiffness values coincide with the DSR measured stiffness values. However, the predicted stiffness are greater than those of the measured stiffness, at temperatures greater than approximately 25°C, for the 5% and 7% EVA PMB's. The reason for the higher predicted values can be attributed to the use of excessively high Softening Points, as described for the BTDC's in section 4.5.2, in Van der Poel's nomograph.

The plots for the Russian - EVA PMB's are shown in Figure 4.20. The data lies almost exclusively below the equivalency line and clearly indicates the inability of the nomograph to predict the stiffness of a PMB from the Penetration and Softening Point of the binder. The figures show that, although Van der Poel's nomograph can reproduce the stiffness values for certain unmodified and even slightly polymer modified bitumens, the nomograph is dependent on the bitumen satisfying time-temperature equivalency (TTSP), and is, therefore, not suitable for rheologically polymer dominant PMB's.

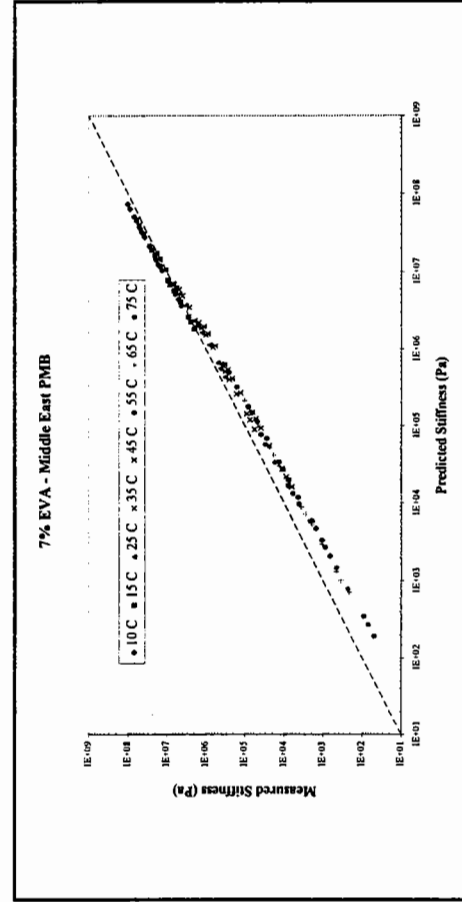
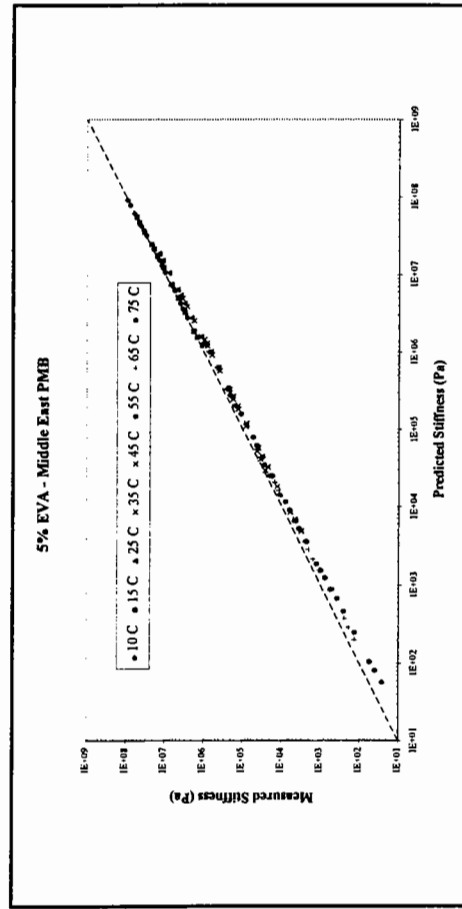
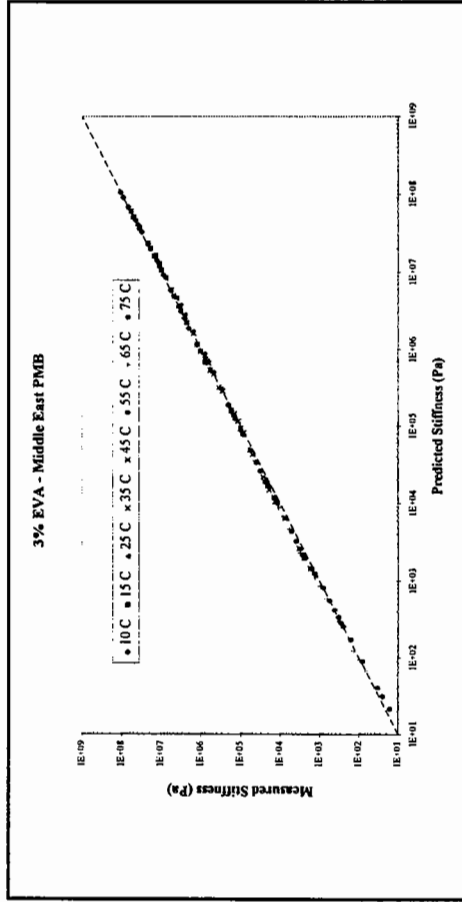
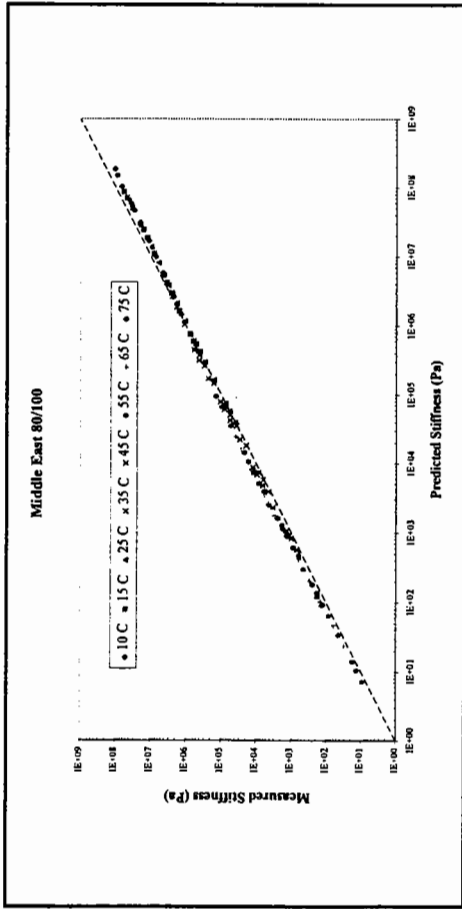


Figure 4.19:  $G^*$  versus van der Poel's stiffness for Middle East - EVA PMB's

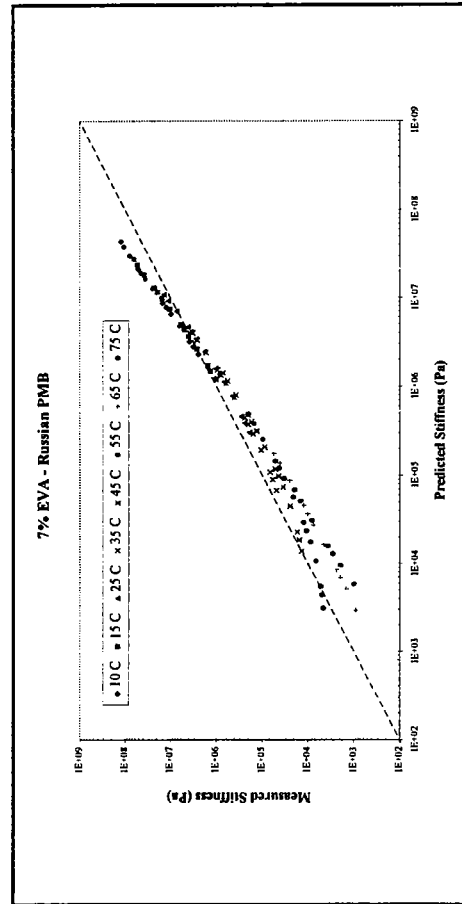
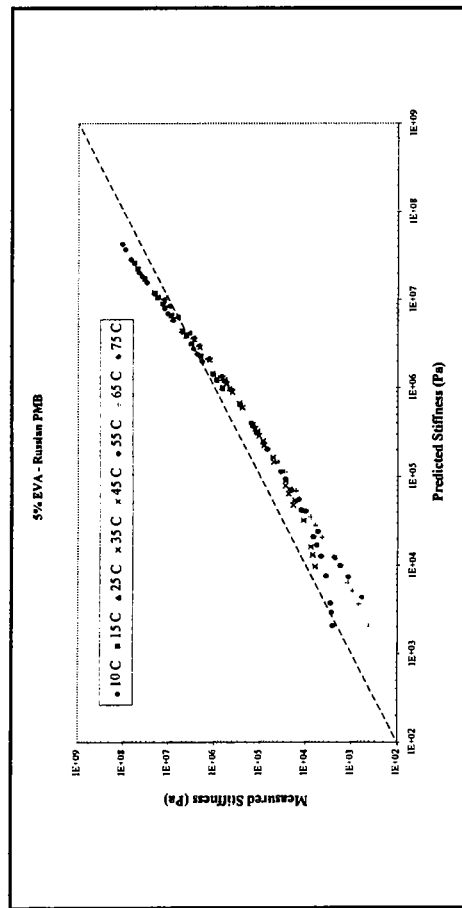
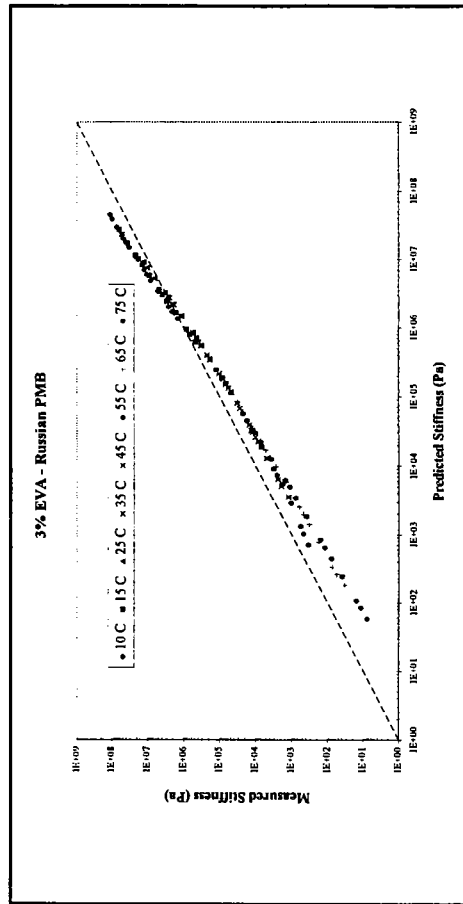
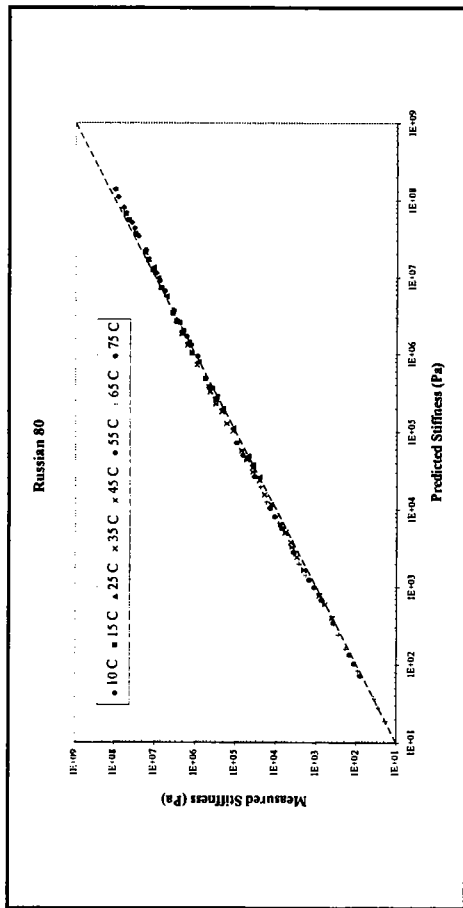


Figure 4.20:  $G^*$  versus van der Poel's stiffness for Russian - EVA PMB's

#### 4.6.2 Complex Modulus Isochronal Plots

The isochronal plots of complex modulus,  $G^*$ , versus temperature, at 0.02 Hz and 1 Hz, for the Russian PMB's are shown in Figures 4.21 and 4.22. The isochronal plots for the EVA PMB's, in Figure 4.21, show an increase in  $G^*$  and an improvement in temperature susceptibility with increasing polymer content up to a temperature of 55°C. The reduced temperature susceptibility of the PMB's is shown as a decrease in the slope of the complex modulus isochrones. At 55°C, the onset of the crystalline melting of the EVA polymers, results in a sharp increase in the slope of the PMB complex modulus isochrones and, therefore, a reduced increase in  $G^*$  after EVA modification and an increase in temperature susceptibility within the temperature range of 55°C to 75°C.

The isochronal plots for the SBS PMB's (Figure 4.21) also show an increase in  $G^*$  with increasing polymer content, but within the temperature range of 10°C to 55°C, this increase is less than that shown for the same polymer content EVA PMB's. However, within the temperature range of 55°C to 75°C, the elastomeric PMB's exhibit an continued decrease in the slope of the complex modulus isochrones and consequently a reduction in temperature susceptibility, while the plastomeric PMB's, as mentioned above, show a sharp increase in slope and, therefore, a rapid reduction in complex modulus with increasing temperature. The different rheological behaviour of two PMB groups results in the increase in  $G^*$  now being greater for the SBS PMB's compared to the EVA PMB's within the temperature range of 55°C to 75°C.

The finding discussed above are more noticeable at the lower frequency of 0.02 Hz (Figure 4.21) than at the higher frequency of 1 Hz (Figure 4.22), since the influence of the polymer is more evident and dominant in the polymer-bitumen blend at low frequencies and high temperatures. However, the isochronal plots at 1 Hz do allow the low temperature benefits of a reduction in stiffness for the 7% SBS PMB to be seen. The reduction of binder stiffness at low temperatures and increase at high temperatures provides the 7% SBS PMB with improved temperature susceptibility and the potential to improve the resistance of both cracking and rutting in a modified asphalt mixture.

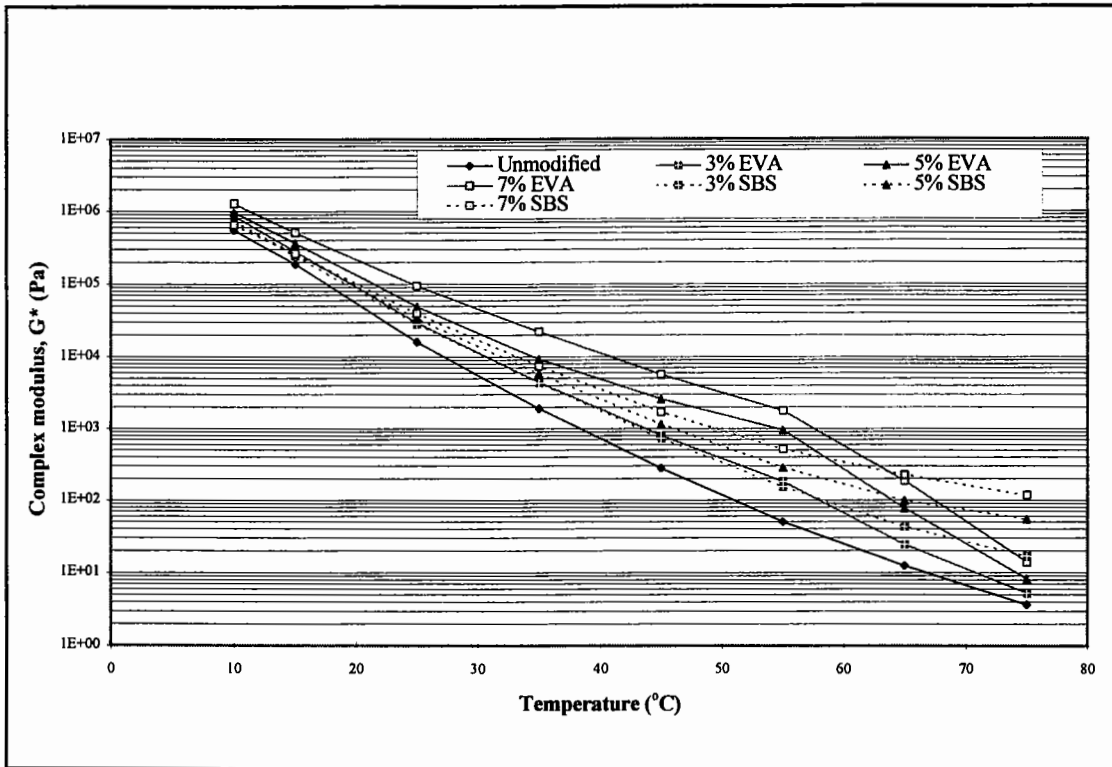


Figure 4.21: Complex modulus isochronal plot at 0.02 Hz for Russian PMB's

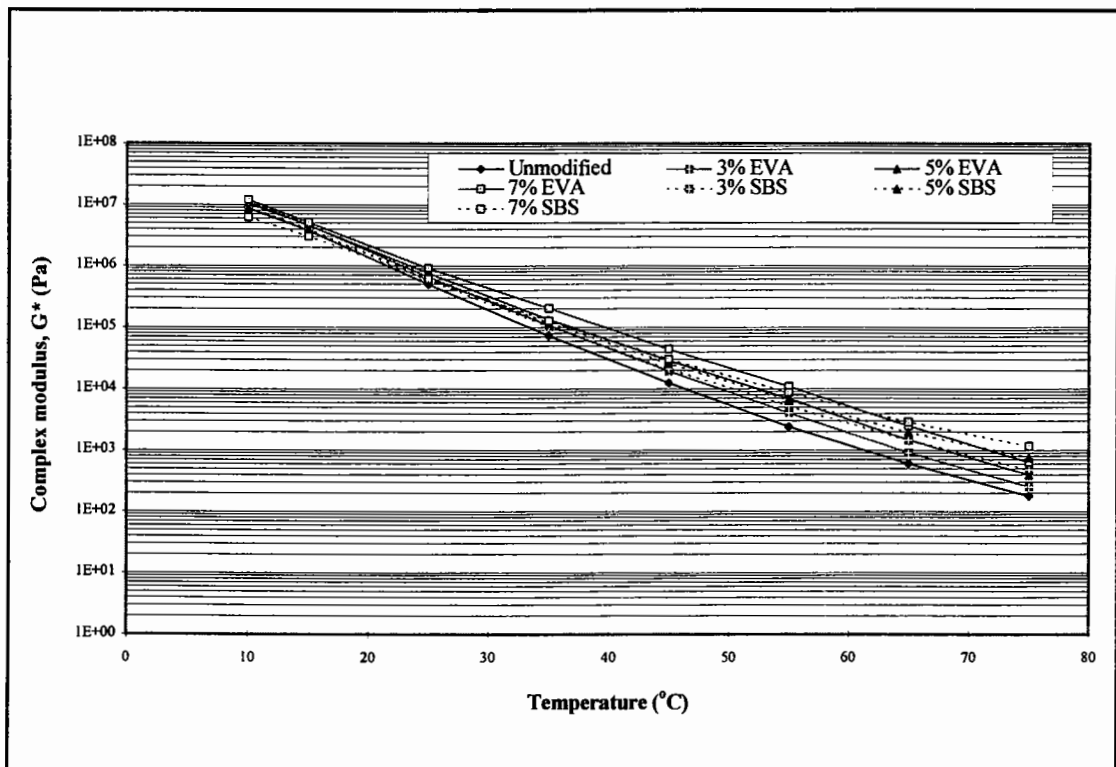


Figure 4.22: Complex modulus isochronal plot at 1 Hz for Russian PMB's



These findings agree with those of Lenoble et al [125], that at low temperatures ( $< 10^{\circ}\text{C}$ ) the complex modulus for a pure bitumen and various PMB's (EVA, EMA and SBS copolymers) are very similar and that most binders tend towards the same complex modulus at these low temperatures irrespective of the polymer and the bitumen grade. The exception to this rule was only found for elastomeric PMB's that contain high polymer contents ( $> 7\%$ ) which permit the lowering of the complex modulus at low temperatures. At temperatures above  $10^{\circ}\text{C}$ , the influence of the polymer begins to appear and the PMB's showed superior thermal susceptibility compare to the pure bitumen. These findings are, however, dependent on the PMB having the correct type of compatibility to allow the rheological characteristics of the polymer to become dominant.

### **Modification Indices**

The modification indices of  $G^*$  at 0.02 Hz and 1 Hz for the Russian PMB's are presented in Figures 4.23 and 4.24. The figures show similar trends to that seen for the modification indices of viscosity, with the EVA PMB's showing a peak modification at  $55^{\circ}\text{C}$  and the SBS PMB's showing a continued increase in modification up to a maximum value at  $75^{\circ}\text{C}$ .

The modification indices at the two frequencies allows the influence of loading time or frequency, as well as temperature, to be evaluated, compared to only temperature for the viscosity results. The modification indices at 1 Hz are considerably lower than those at 0.02 Hz, with the SBS PMB's being less affected than the plastomeric EVA PMB's. This means that the relative performance of the SBS compared to the EVA PMB's improves at higher frequencies, implying that the suitability of a particular PMB may differ depending not only on temperature, but also on loading time.

### **Pure Polymer**

The mechanism of polymer modification can be explained through the isochronal plot of complex modulus versus temperature for the pure EVA polymer and the Russian base bitumen in Figure 4.25. The isochronal plot, at a frequency of 0.1 Hz, shows that the temperature susceptibility of the Russian bitumen is relatively high compared to that of

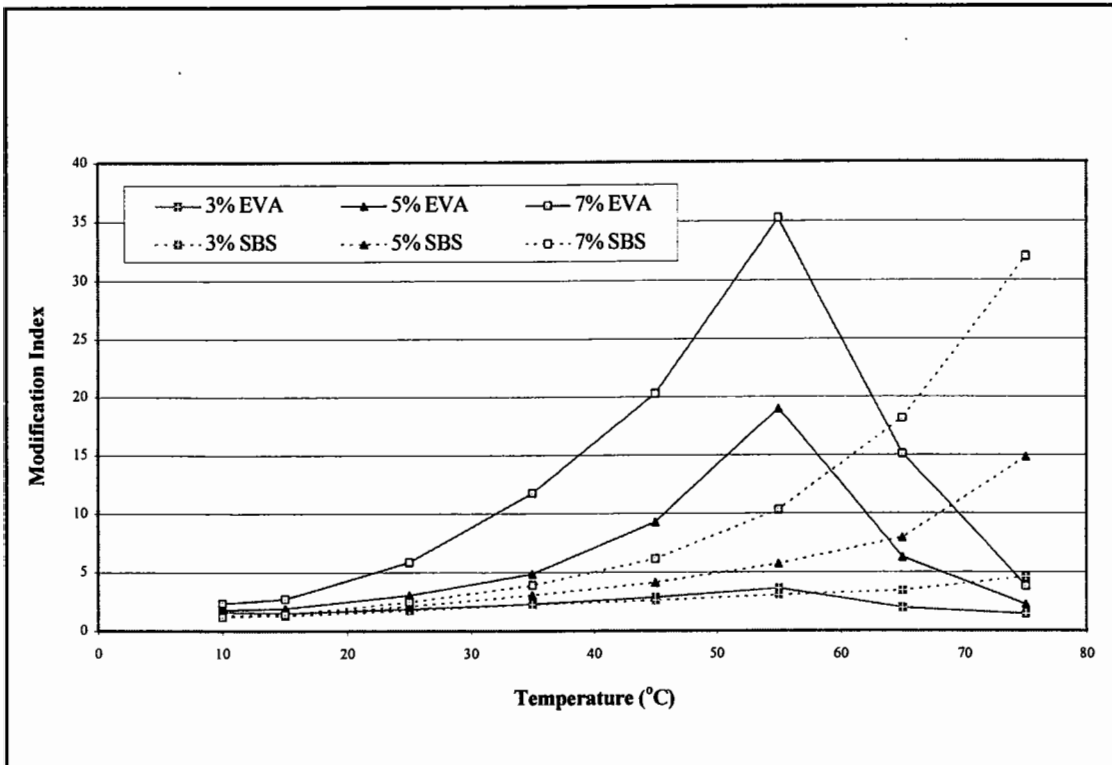


Figure 4.23: Modification indices for complex modulus at 0.02 Hz for Russian PMB's

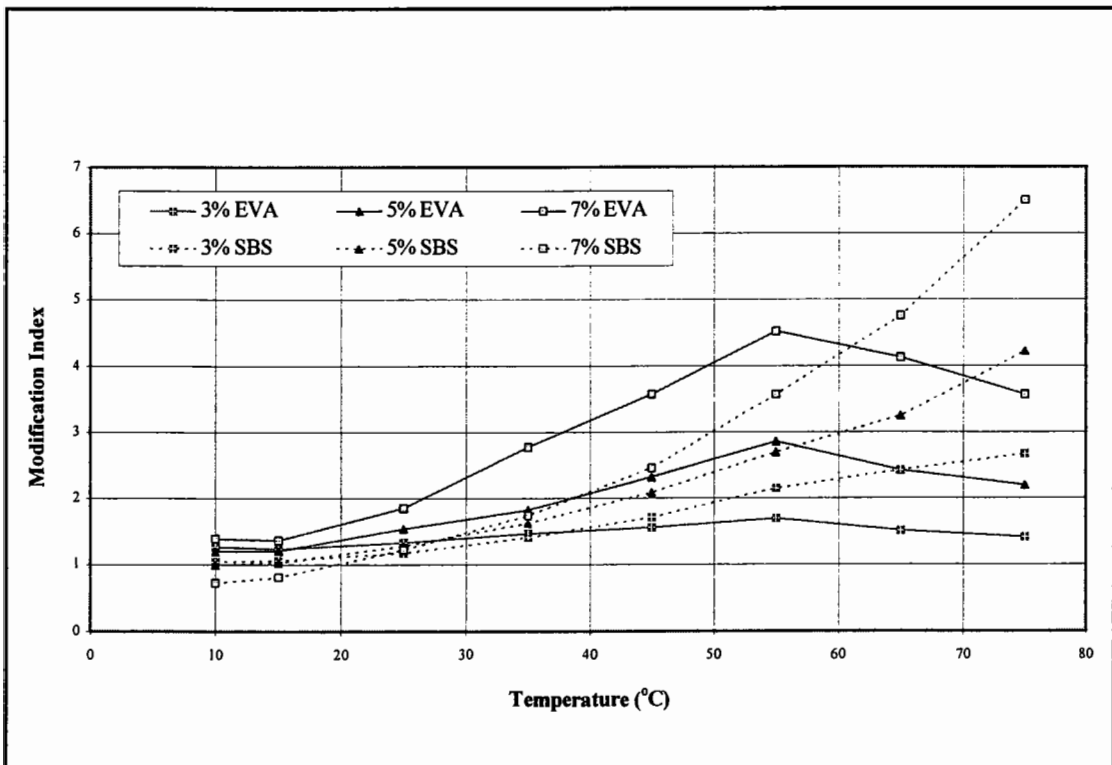
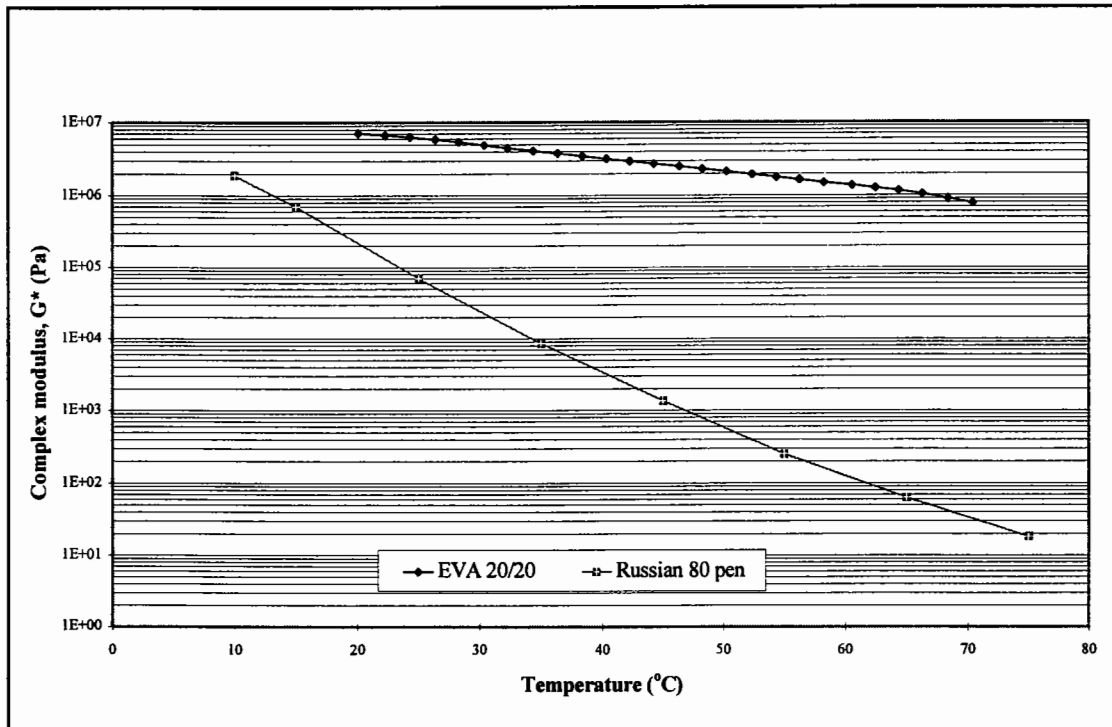


Figure 4.24: Modification indices for complex modulus at 1 Hz for Russian PMB's

the EVA polymer. A blend consisting of the base bitumen and the polymer, where the compatibility of the system allows the mechanical properties of the polymer to be evident, should have improved temperature susceptibility and increased  $G^*$  at high temperatures. The complex modulus of the two components, at low temperatures, should be relatively similar and may even be slightly lower for the polymer, resulting in either no change or a slight reduction in  $G^*$  for the PMB at low temperatures.



**Figure 4.25: Complex modulus at 0.1 Hz for EVA copolymer and Russian 80 pen**

### 4.6.3 Phase Angle Isochronal Plots

The phase angle isochrones at 0.02 Hz and 1 Hz for the Russian PMB's are presented in Figures 4.26 and 4.27. The phase angle,  $\delta$ , is generally considered to be more sensitive to the chemical structure and therefore the modification of bitumen than complex modulus,  $G^*$  [122].

The isochronal plots for the Russian - EVA PMB's illustrate that there is a reduction in  $\delta$  with increasing polymer content and that the phase angle reaches a minimum value at 55°C, after which there is a sharp increase towards a more viscous behaviour as the

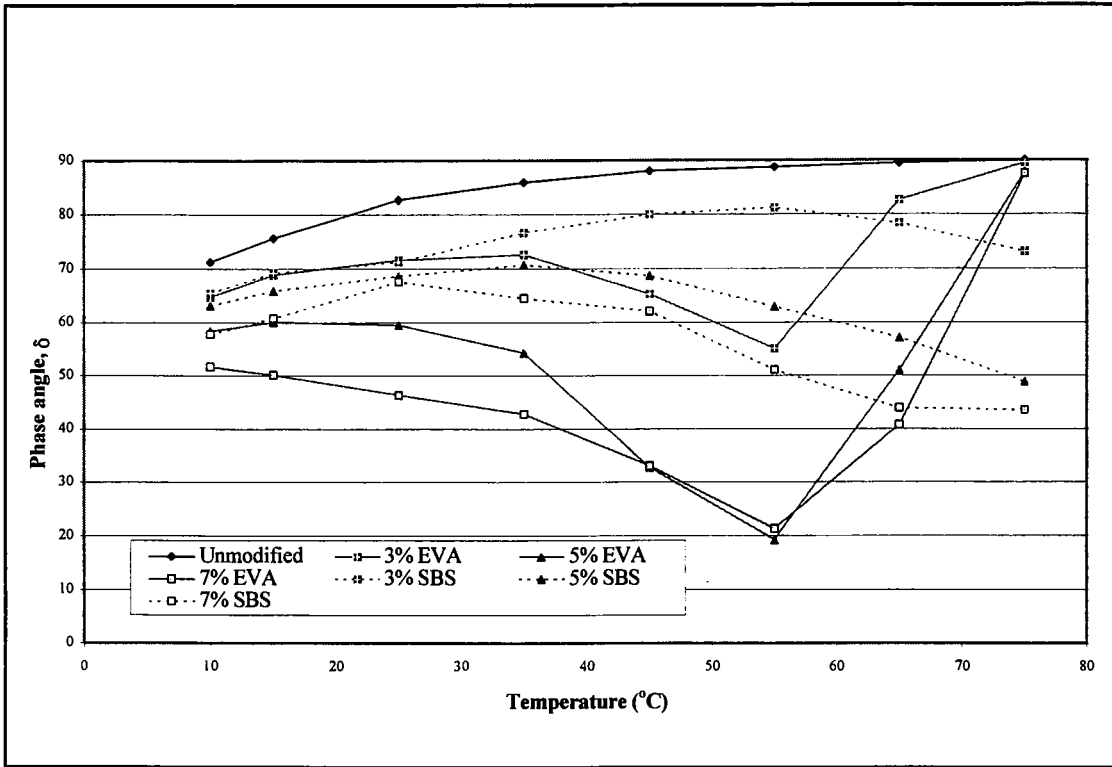


Figure 4.26: Phase angle isochronal plot at 0.02 Hz for Russian PMB's

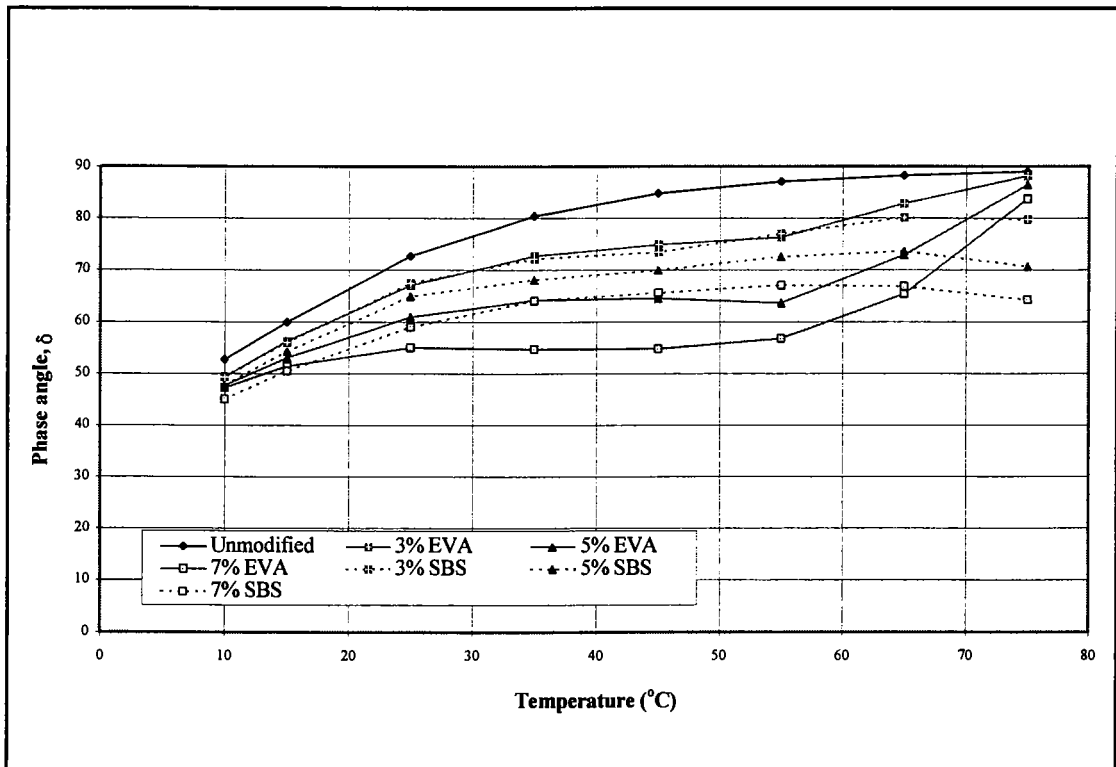
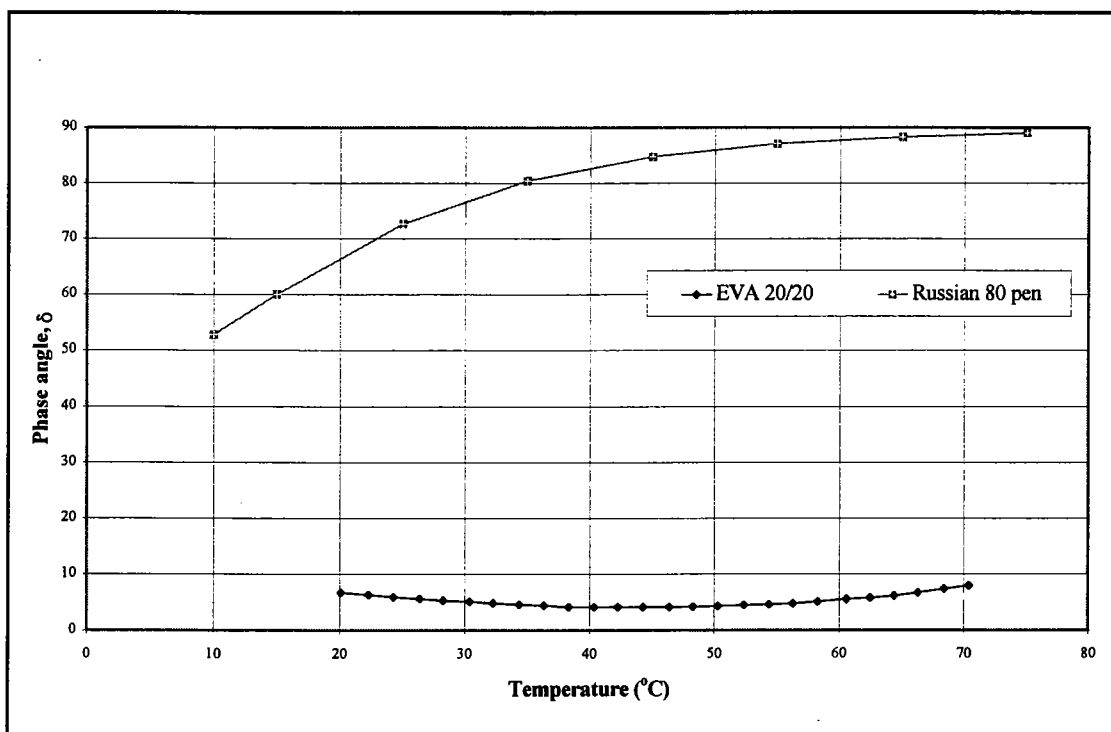


Figure 4.27: Phase angle isochronal plot at 1 Hz for Russian PMB's

polymer melts. There is a similar decrease in  $\delta$  towards a more elastic behaviour for the SBS PMB's, but this decrease is maintained throughout the temperature range of 10°C to 75°C. The effect of increasing the loading frequency is to reduce the magnitude of the decrease in phase angle, for both the EVA and SBS PMB's, and decrease  $\delta$  for the unmodified bitumen, resulting in a closer relationship between the unmodified and modified bitumens.

The isochronal plots in Figures 4.26 and 4.27 are similar to those seen by other researchers [125], who found that at low temperatures (< 10°C) there is no significant difference in the phase angles of pure bitumen and PMB's (EVA, EMA and SBS copolymers), and therefore proposed that the rheological properties of PMB's are dominated by the bitumen and not the polymer at low temperatures and high loading frequencies. Above 10°C, the properties of PMB's tend to be more influenced by the polymer [20].



**Figure 4.28: Phase angles at 0.1 Hz for EVA copolymer and Russian 80 pen**

### Pure Polymer

The effect of modification, with regard to phase angle, can be explained by looking at the

isochronal plot of phase angle at 0.1 Hz for the pure EVA polymer and the Russian bitumen in Figure 4.28. The figure shows that the phase angle for the pure polymer remains relatively constant at approximately  $5^\circ$ , while the phase angle of the bitumen increases from approximately  $50^\circ$  to  $90^\circ$ . A blend of the polymer and bitumen should therefore result in a reduction of the phase angle as seen in Figures 4.26 and 4.27. As with the complex modulus isochrones, in Figure 4.25, the decrease in phase angle and the increased elastic behaviour is more evident when the base bitumen approaches its highly viscous behaviour at high temperatures and low loading frequencies.

#### 4.6.4 Complex Modulus Master Curves

The master curves for the three EVA PMB groups are shown in Figures 4.29 to 4.31. All three groups show a similar shifting of the complex modulus master curves towards higher values as the polymer content increases, particularly at low reduced frequencies. This can be attributed to the stiffening effect of polymer modification and the improved temperature susceptibility of the PMB's.

The main difference between the master curves is the occurrence of 'branching' at low frequencies for the Russian - EVA PMB's and for the 5% and 7% Venezuelan - EVA PMB's. These 'branches' indicate the occurrence of polymeric-type modification of the PMB's rather than filler-type modification as seen for the Middle East PMB's and the 3% Venezuelan - EVA PMB.

The formation of the 'branches' can be seen in the production of the complex modulus master curve for the 7% EVA - Russian PMB in Figure 4.32. The 'branches' are formed due the occurrence of different EVA crystalline structures in the PMB at different temperatures, ranging from  $35^\circ\text{C}$  to  $65^\circ\text{C}$ . Once the semi-crystalline EVA polymer has melted at  $75^\circ\text{C}$ , the isotherm and the low frequency portion of the master curve, reverts back to a unit slope associated with the viscous asymptote found for unmodified bitumens or bitumens simply having a filler-type rather than a polymeric-type modification.

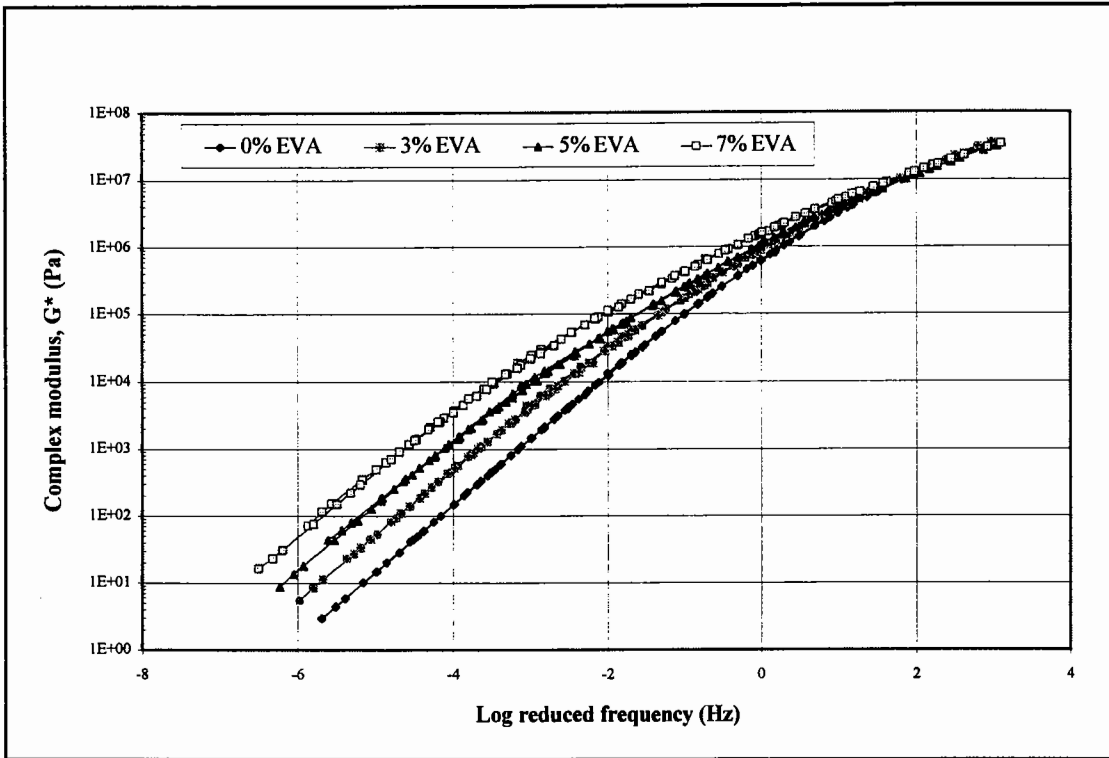


Figure 4.29: Complex modulus master curve for Middle East - EVA PMB's

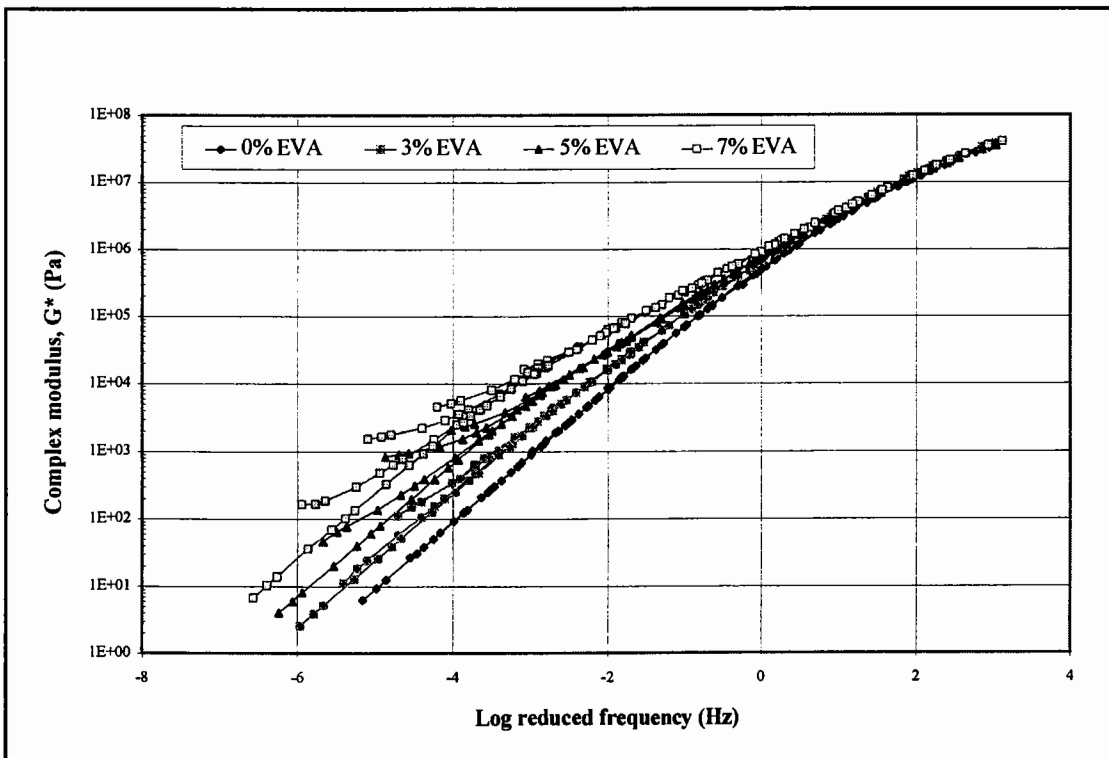


Figure 4.30: Complex modulus master curve for Russian - EVA PMB's

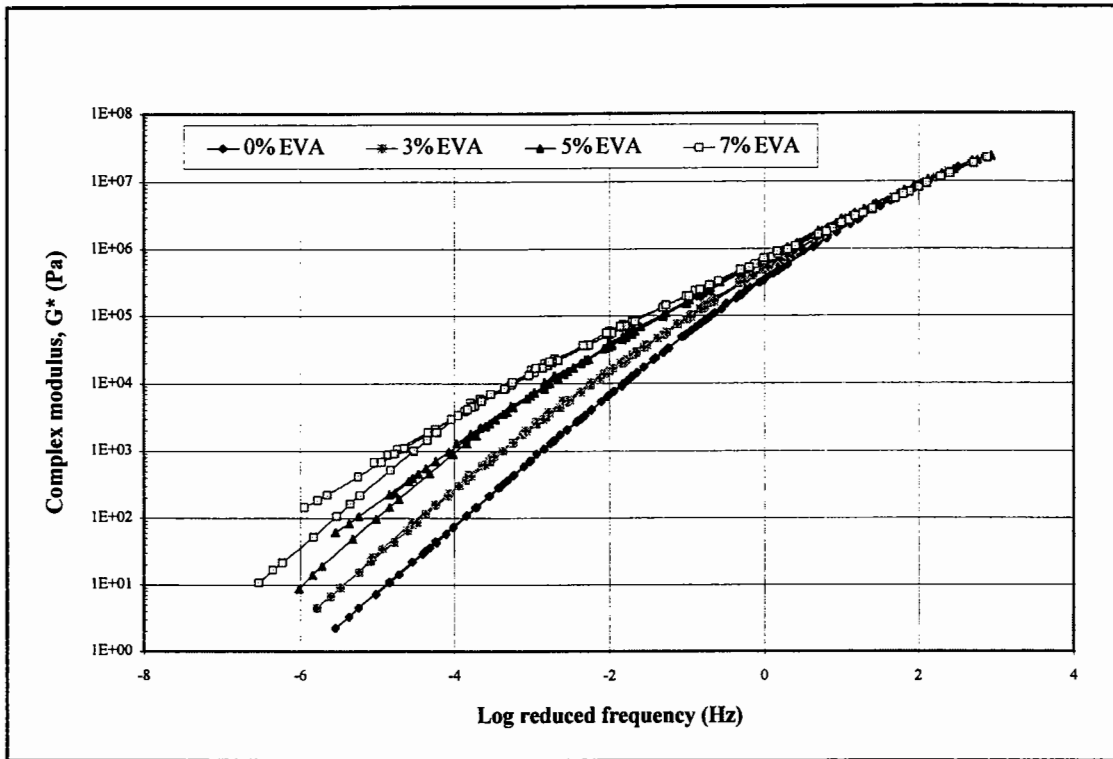


Figure 4.31: Complex modulus master curve for Venezuelan - EVA PMB's

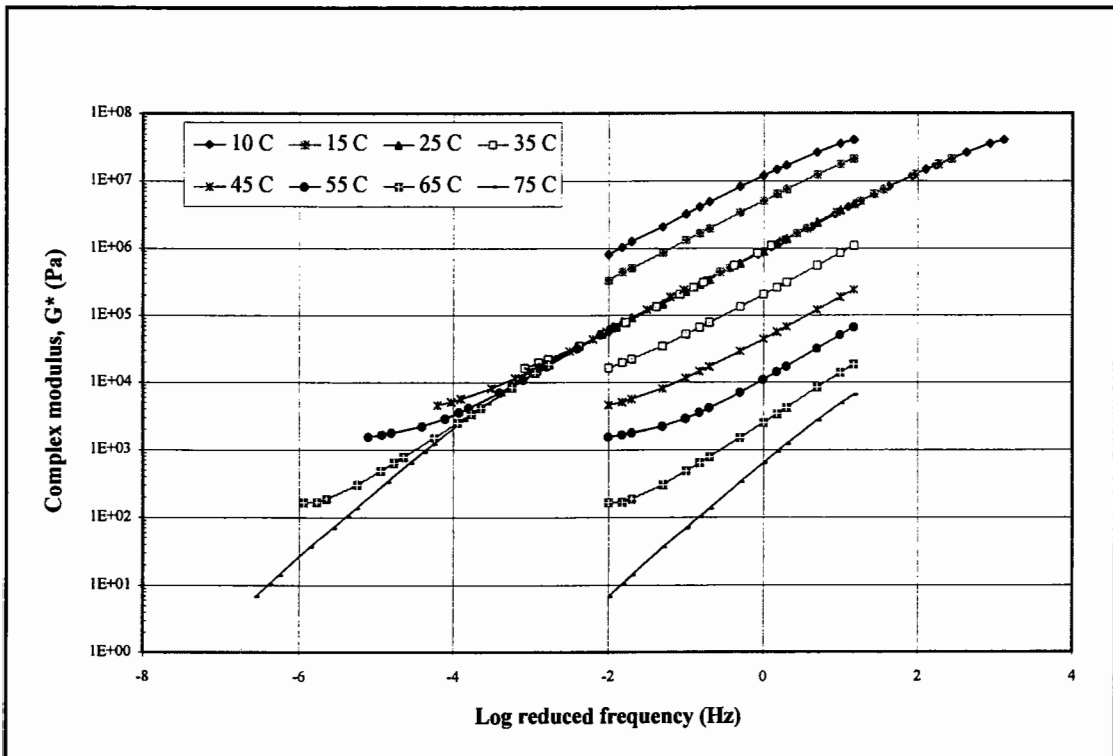


Figure 4.32: Complex modulus master curve for 7% EVA - Russian PMB



The complex modulus master curves for the SBS PMB groups are shown in Figures 4.33 and 4.34. The figures for the SBS PMB's differ from those seen for the EVA PMB's, in that the shift towards a higher complex modulus is lower and in the case of the 7% SBS - Russian PMB there is a decrease in complex modulus at the high frequency end of the master curve. The master curves for the SBS PMB's also do not show any 'branching' at low frequencies as seen for the rheologically polymer dominant EVA PMB's.

The reason for the different shape of the SBS PMB master curves can be explained by looking at the production of the master curve for the 7% SBS - Russian PMB in Figure 4.35. The figure illustrates that as the SBS PMB is an amorphous polymer-bitumen blend and not a semi-crystalline polymer-bitumen blend, the complex modulus isotherms can be shifted to form a smooth master curve. The increase dominance of the elastomeric SBS copolymer at high temperatures and low frequencies means that the slope of the master curve continues to decrease at low frequencies. Once the SBS copolymer has melted, at a temperature of approximately 100°C, the slope of the master curve will revert back to the unit slope found for unmodified bitumens.

#### **4.6.5 Phase Angle Master Curves**

The phase angle master curves for the three EVA PMB groups, in Figures 4.36 to 4.38, have been produced by using the shift factors derived from the complex modulus master curves. However, unlike the complex modulus master curves, the phase angle master curves differ in appearance for the three groups. This is not surprising as, firstly, the phase angle is more sensitive to the modification of the different PMB's than  $G^*$  and, secondly, the data presented in this chapter has indicated that the EVA PMB's differ considerably with regard to their rheological characteristics as a function of the compatibility of the different bitumen-polymer blends.

The phase angle master curves for the Middle East PMB's (Figure 4.36) show a reduction in phase angle and the presence of a slight phase angle plateau with increasing modification, but still have a relatively smooth curve. The only variation from the smooth

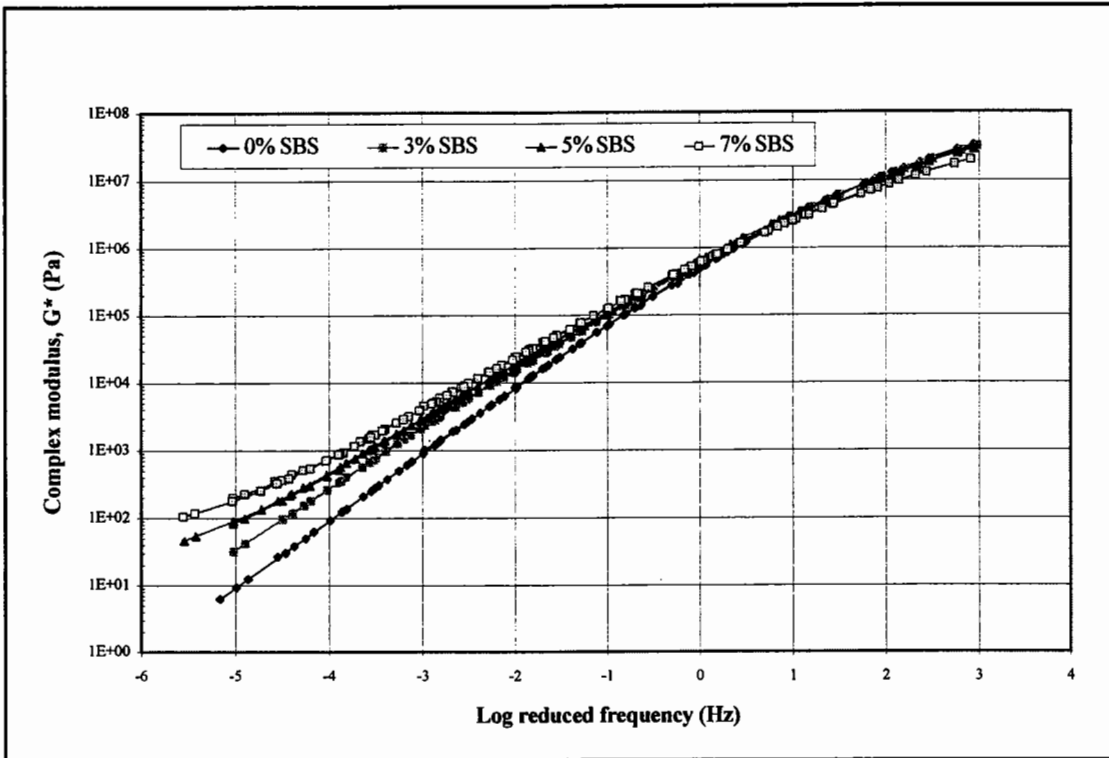


Figure 4.33: Complex modulus master curve for Russian - SBS PMB's

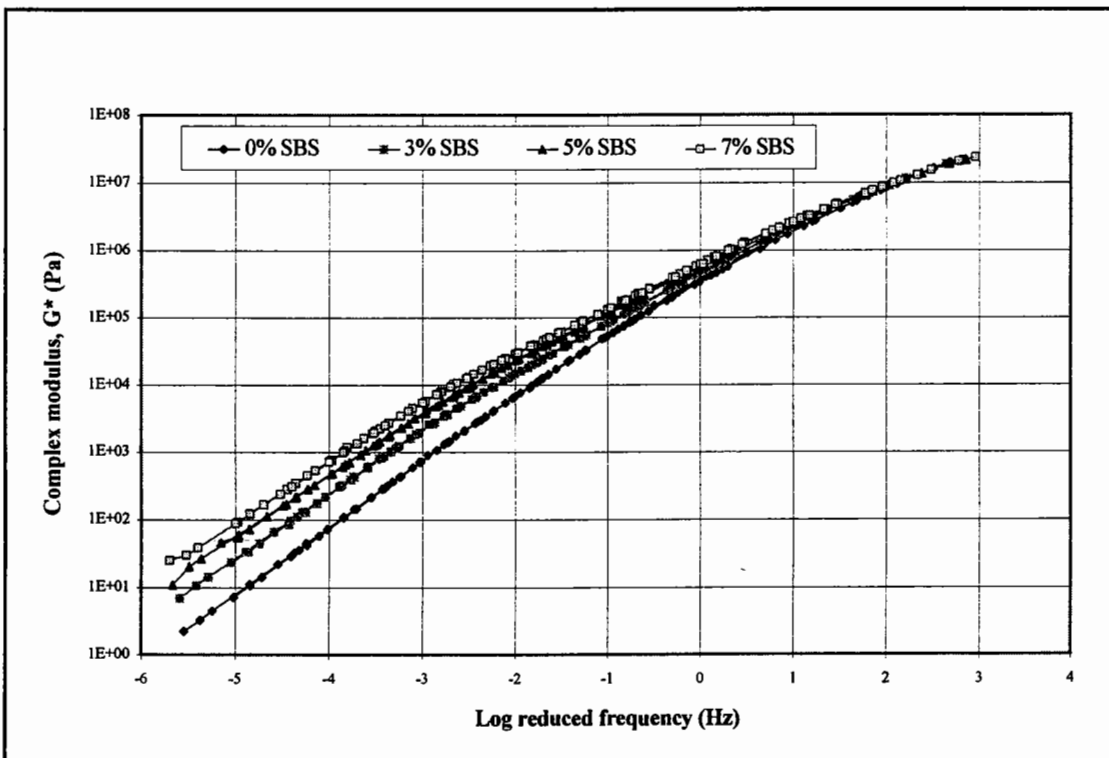


Figure 4.34: Complex modulus master curve for Venezuelan - SBS PMB's

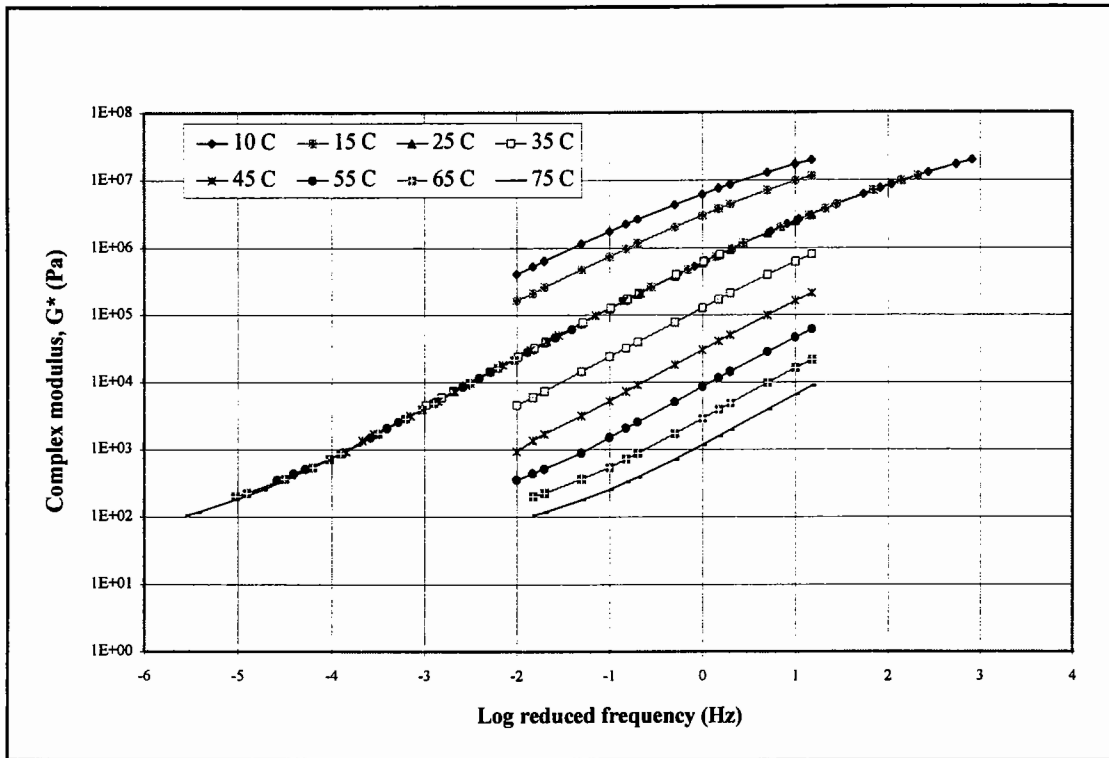


Figure 4.35: Complex modulus master curve for 7% SBS - Russian PMB

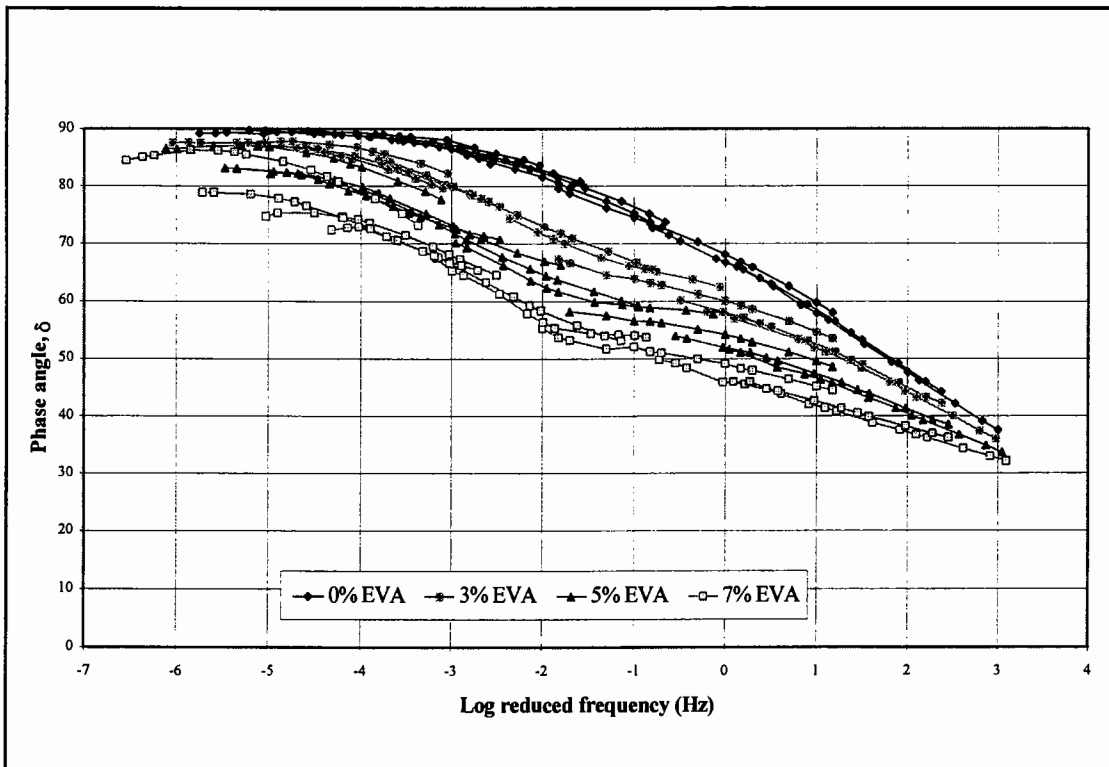
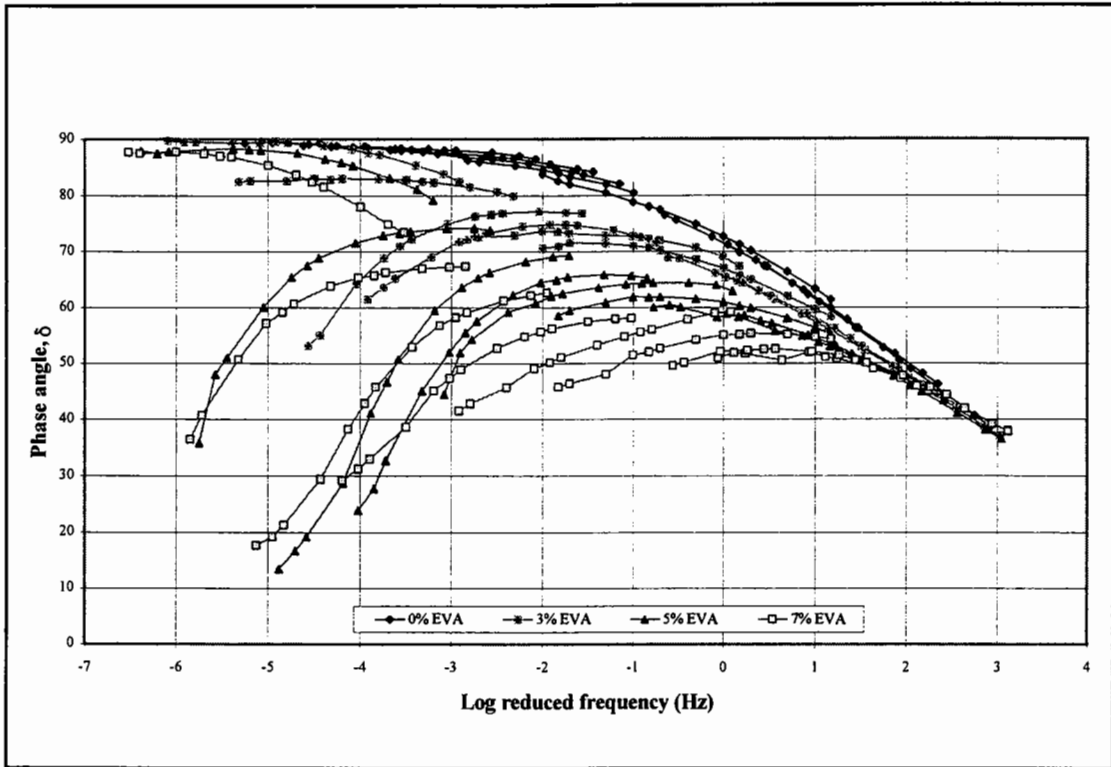
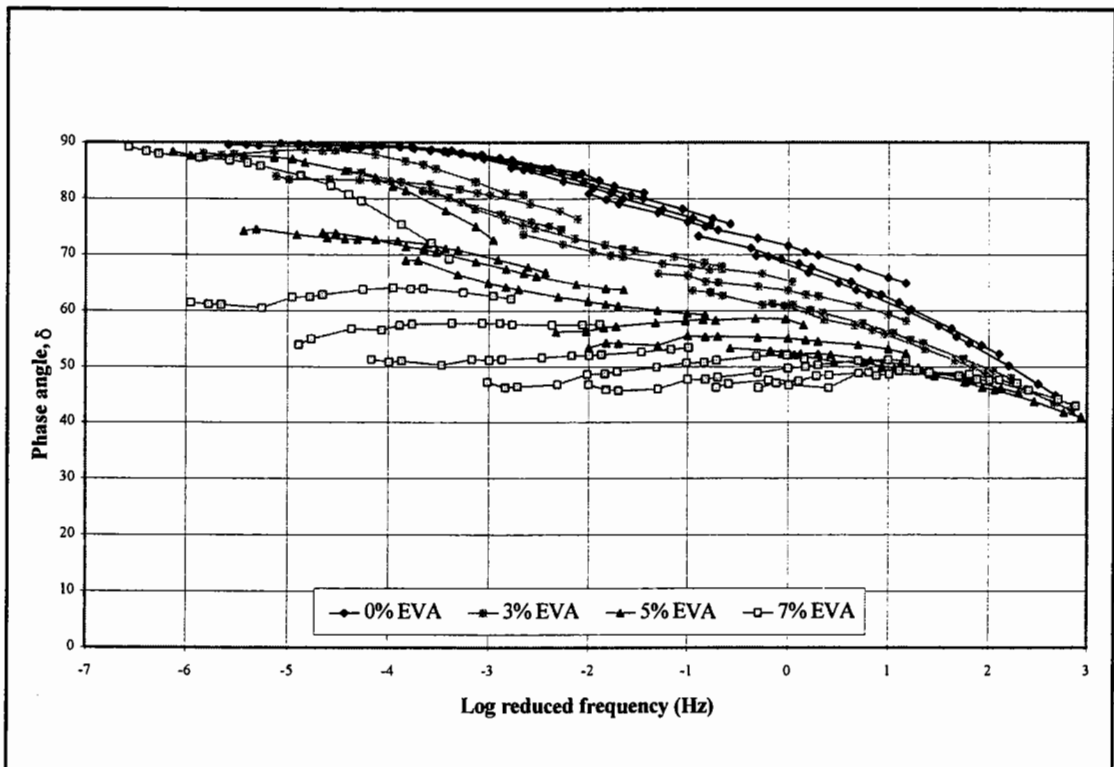


Figure 4.36: Phase angle master curve for Middle East - EVA PMB's



**Figure 4.37: Phase angle master curve for Russian - EVA PMB's**



**Figure 4.38: Phase angle master curve for Venezuelan - EVA PMB's**

curve occurs at the low frequency end, where there is a shifting and discontinuity of the curve, due to the completed melting of the semi-crystalline EVA polymer at a temperature of 75°C.

The phase angle master curves for the Russian - EVA PMB's, in Figure 4.37, show a considerable alteration to the smooth shape of the unmodified bitumen. The master curve consists of discontinuous 'waves' indicating the presence of different crystalline structures at different temperatures within the EVA PMB's. The only similarities between the Russian and Middle East - EVA PMB's is at the high frequency end, where the bitumen-rich phase of the PMB is dominant, and at the low frequency end, which is equivalent to high temperatures, where the semi-crystalline polymer has melted. The extend of the discontinuity and severity of the 'waves' increases with increasing polymer content.

The master curves for the Venezuelan - EVA PMB's (Figure 4.38) again show a unique behaviour. The curves for the 3% and slightly for the 5% EVA PMB's are similar to those seen for the Middle East - EVA PMB's. However, the master curve for the 7% EVA PMB shows considerable discontinuity and the presence of 'waves' as seen for the Russian - EVA PMB's. The shape of the 'waves' differ between the Venezuelan and Russian PMB's and can be considered to be indicative of the different modified chemical structures of the PMB's.

The phase angle master curves for the SBS PMB groups are shown in Figures 4.39 and 4.40 and have been constructed using the shift factors from the  $G^*$  master curves. These curves differ from those seen for the EVA PMB's in that, although they have a different shape compared to an unmodified bitumen, they still form a smooth continuous curve, unlike the disjointed curves found for the semi-crystalline PMB's.

Both the Russian and Venezuelan - SBS PMB's have a shift of the phase angle master curve towards lower phase angles and the formation of a distinctive phase angle plateau region with increasing polymer contents. However, the shape of the curves differ, with

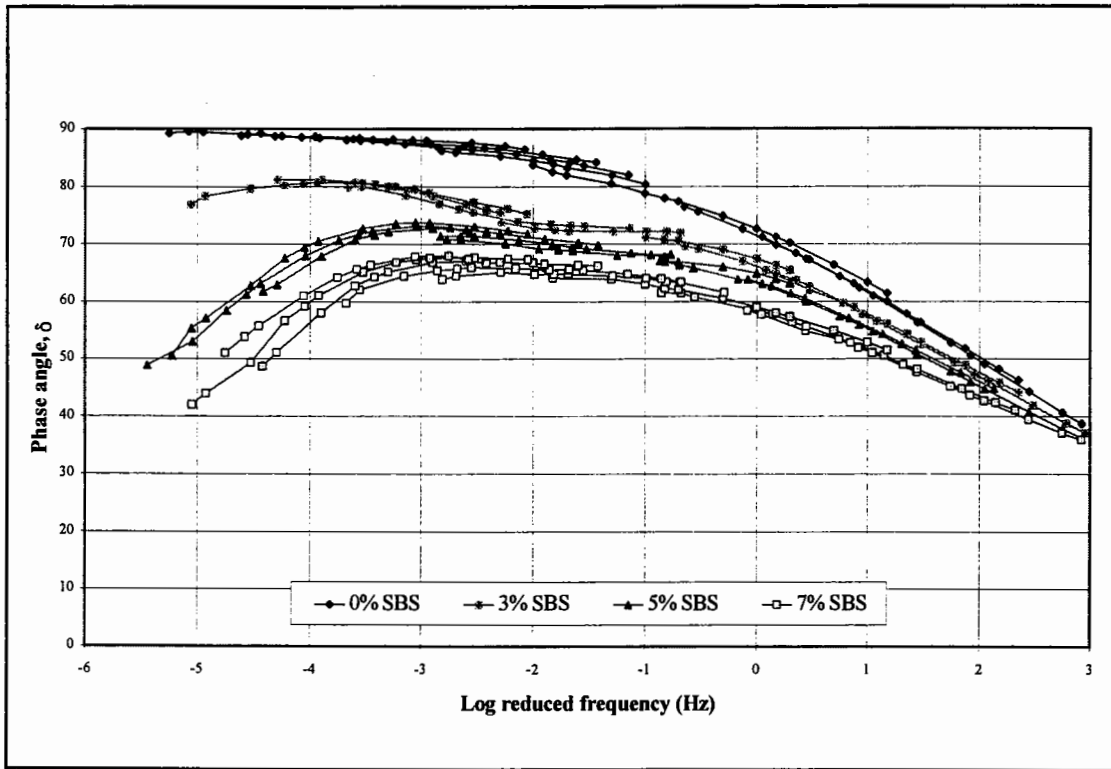


**Figure 4.39: Phase angle master curve for Russian - SBS PMB's**

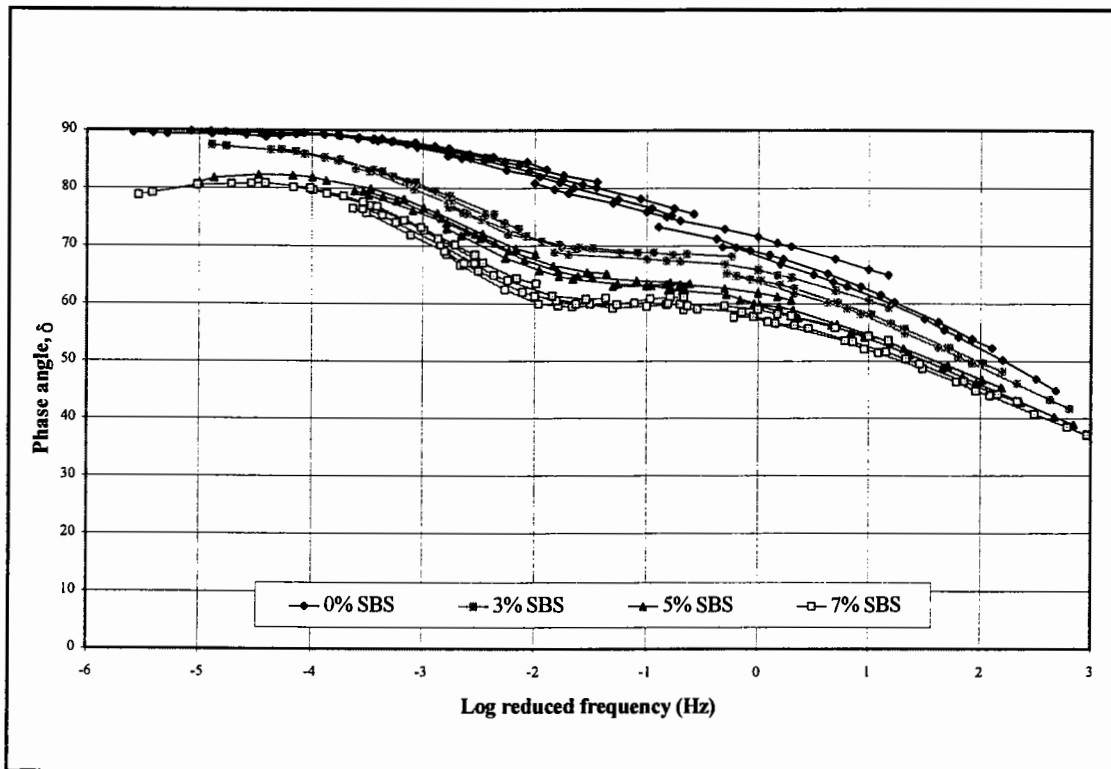


**Figure 4.40: Phase angle master curve for Venezuelan - SBS PMB's**

the Russian - SBS PMB's having a continued decrease in phase angle, while the Venezuelan - SBS PMB's have an increase in phase angle and a move towards a more viscous behaviour at the low frequency end.

#### 4.6.6 Black Diagrams

The Black diagrams allow all the experimental data to be presented on a single plot without requiring the shifting of data. The Black diagrams for the EVA PMB groups are shown in Figures 4.41 to 4.43. As with the phase angle master curves, the Black diagrams for the three EVA PMB groups are very distinctive. The Middle East - EVA PMB's show a shift of the relatively smooth Black diagram curves towards lower phase angles with increasing modification, as well as the discontinuity associated with the melting of the EVA copolymer.

The curves for the Russian - EVA PMB's also show a shift towards lower phase angles with increasing polymer content, but consist almost entirely of discontinuous 'waves' associated with the different crystalline structures found in the PMB's. The curves for the Venezuelan - EVA PMB's, in Figure 4.43, show a mixture of the trends seen for the Middle East and Russian - EVA PMB's. The lower 3% EVA PMB has a curve similar to that of the Middle East PMB's, while the 7% EVA PMB consists of a discontinuous curve with a number of 'waves'.

The Black diagrams for the SBS PMB's are presented in Figures 4.44 and 4.45. As with the phase angle master curves for these PMB's, the curves are relatively smooth but differ from those seen for unmodified bitumens. Both PMB groups have a plateau region of constant phase angle which migrates towards lower phase angles with increasing modification. The extent of modification is greater for the Russian PMB's showing a continued increase in elasticity as the complex modulus decreases.

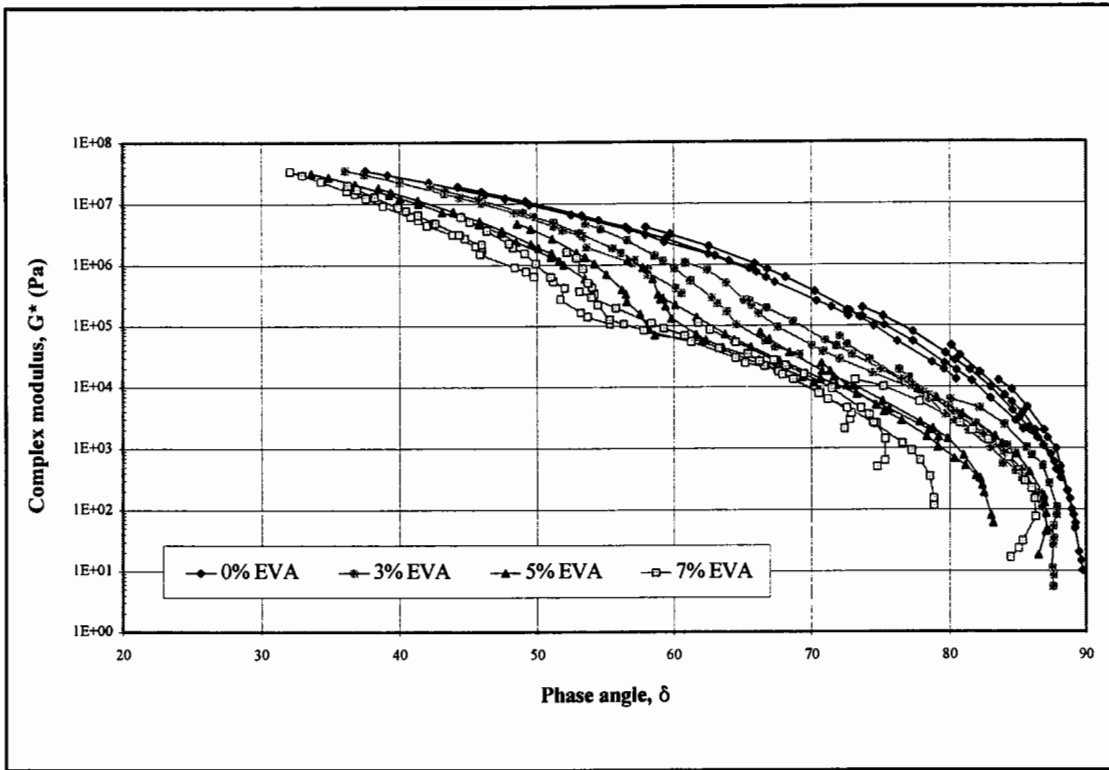


Figure 4.41: Black diagram for Middle East - EVA PMB's

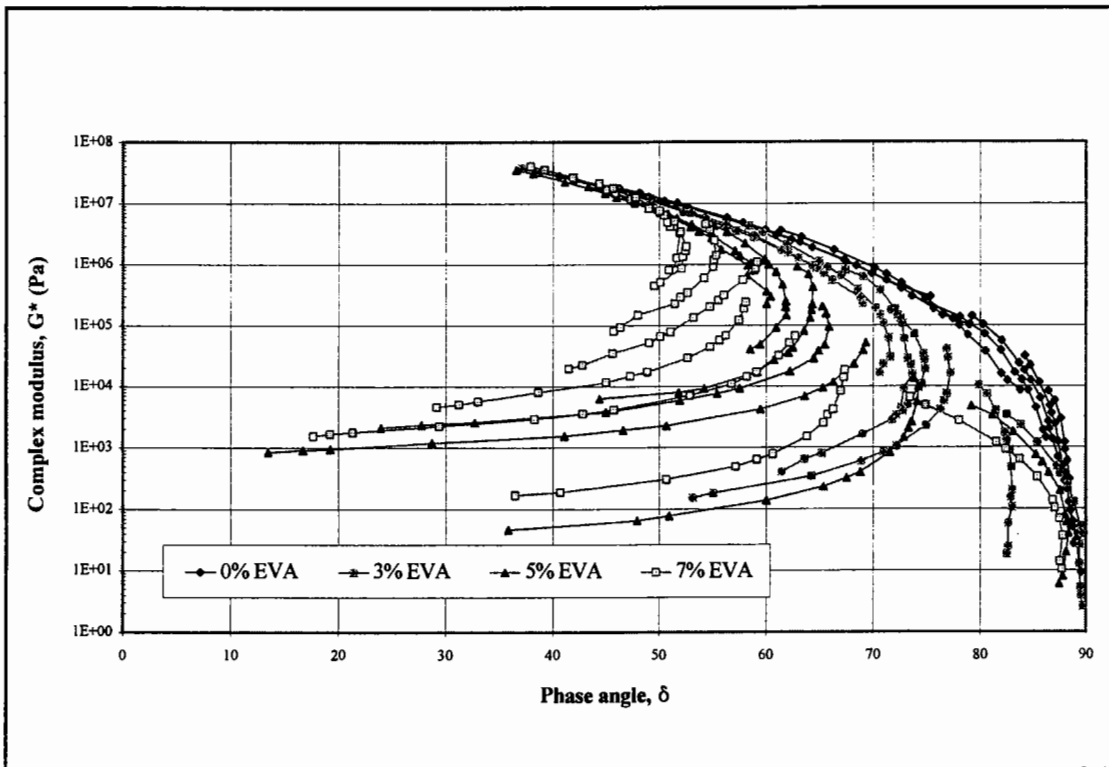


Figure 4.42: Black diagram for Russian - EVA PMB's



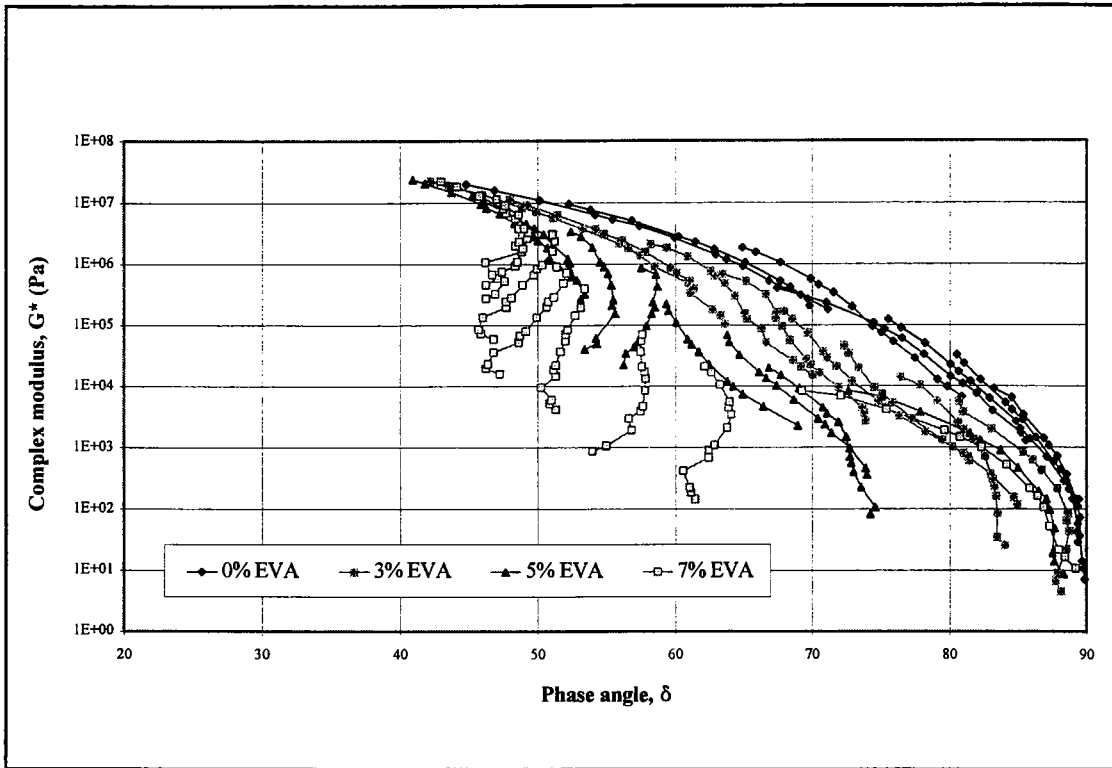


Figure 4.43: Black diagram for Venezuelan - EVA PMB's

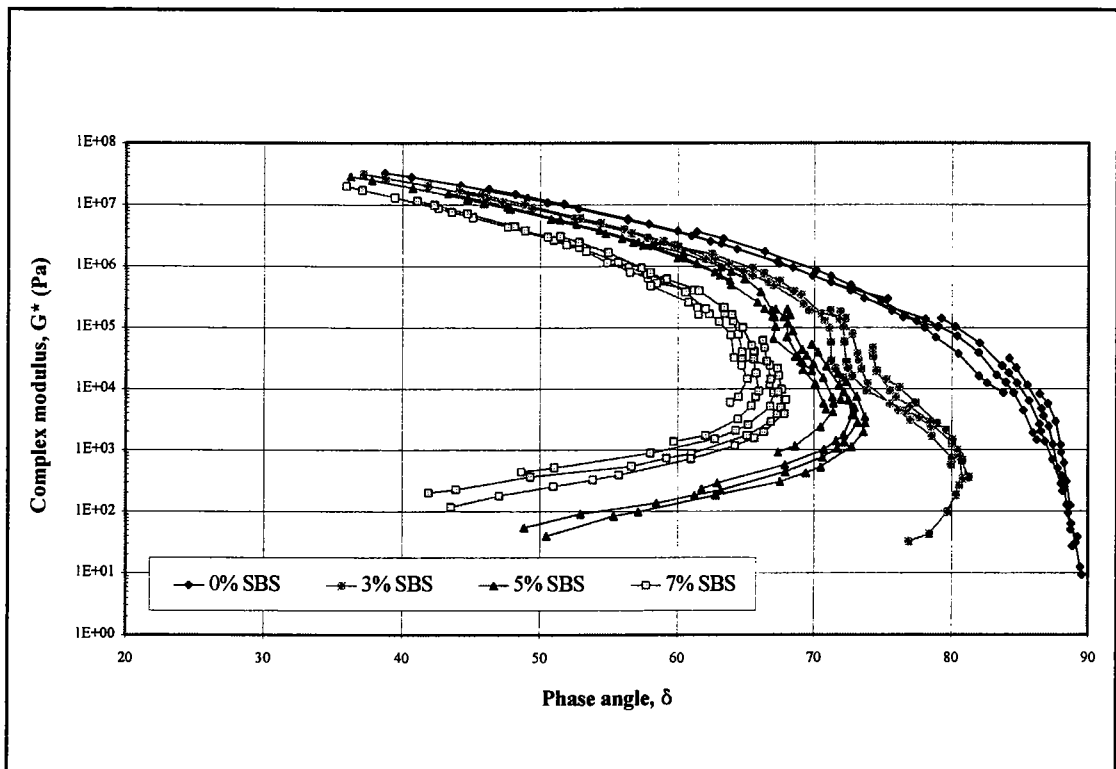


Figure 4.44: Black diagram for Russian - SBS PMB's

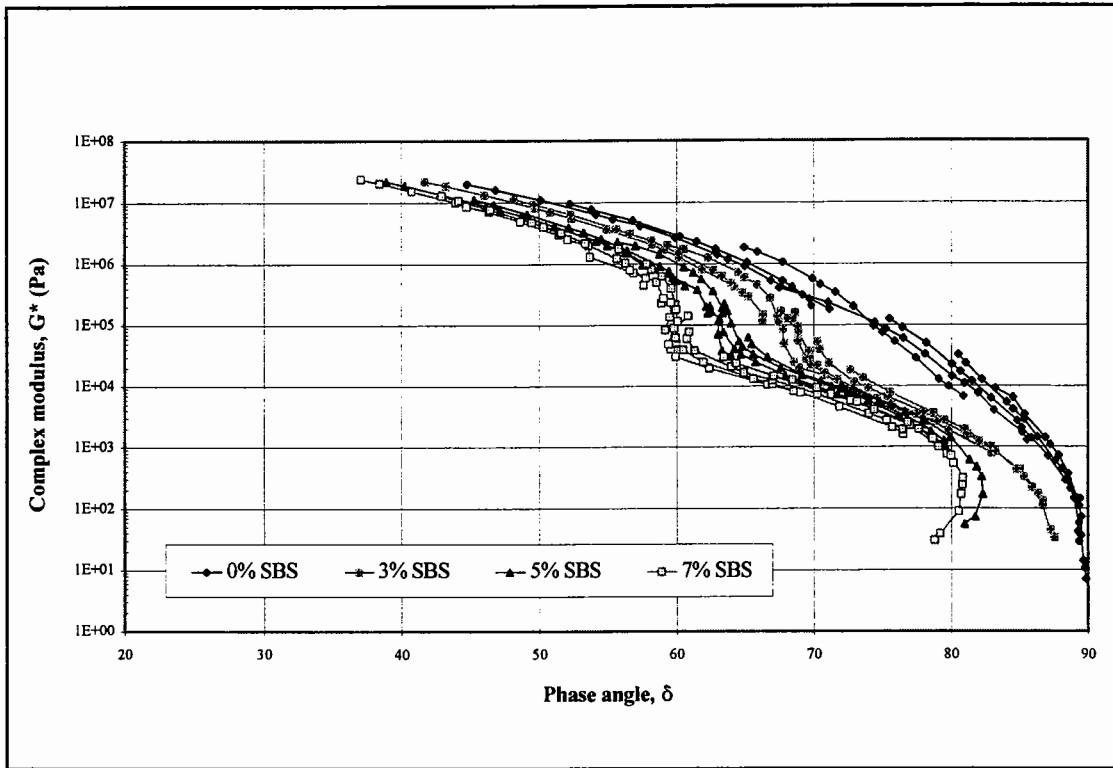


Figure 4.45: Black diagram for Venezuelan - SBS PMB's

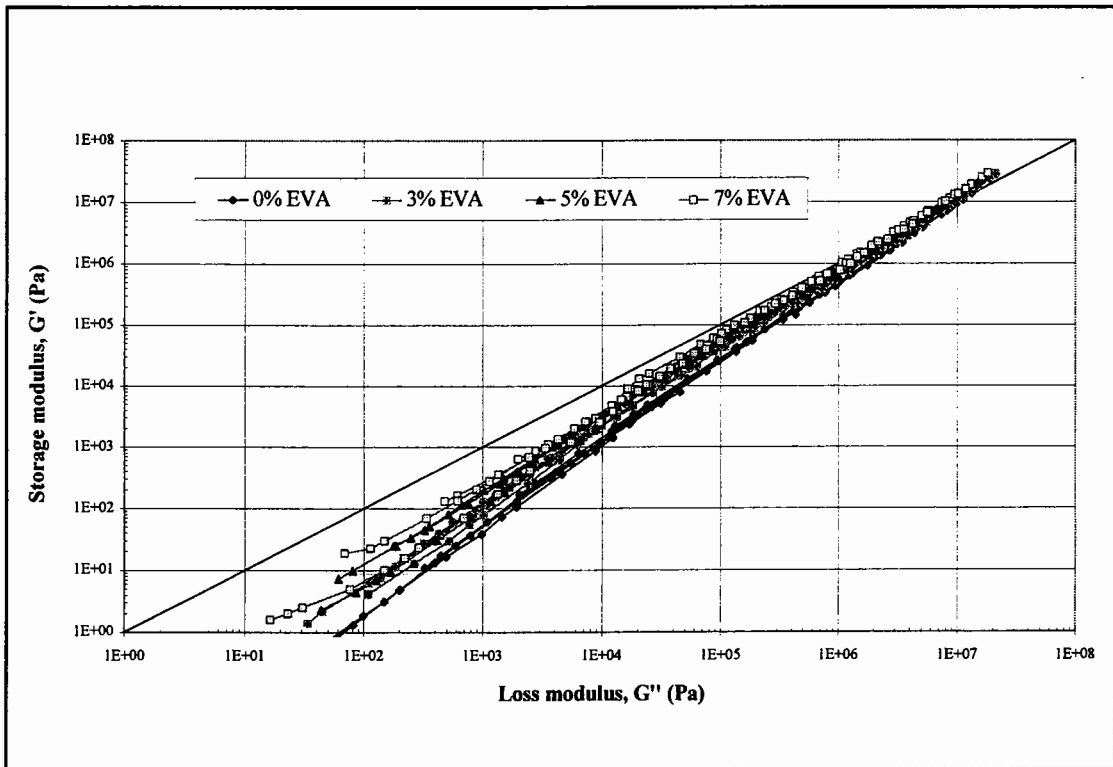


Figure 4.46: Cole-Cole diagram for Middle East - EVA PMB's

#### **4.6.7 Cole-Cole Diagrams**

The Cole-Cole diagrams for the EVA PMB's, in Figures 4.46 to 4.48, provide similar rheological information to that obtained from the complex modulus master curves. The plots show a constant shift towards a more elastic behaviour, as depicted by a shift towards the more elastic upper left-hand corner of the plot, and the presence of crystalline 'branching' for the more polymeric-type modified PMB's.

Likewise, the diagrams for the SBS PMB's, in Figures 4.49 and 4.50, are similar to those seen for the complex modulus master curves, with a continued increase in elasticity with modification, being more evident at low stiffness values.

### **4.7 Discussion**

The conventional tests and the more fundamental DMA have indicated that the rheological characteristics of plastomeric EVA and elastomeric SBS PMB's differ considerably. The semi-crystalline EVA copolymer provides the modification of bitumen through the crystallisation of rigid three dimensional networks within the bitumen. Different crystalline structures are formed at different temperatures, as shown by the occurrence of 'branching', in the complex modulus master curves and Cole-Cole diagrams, and 'waves', in the phase angle master curves and Black diagrams. The polymeric modification is confined by an upper temperature limit, related to the melting temperature of the EVA copolymer, whereafter the process is limited to a filler-type modification. The melting of the EVA copolymer can be seen in the viscosity-temperature plots, isochronal plots, master curves, Black diagrams and Cole-Cole diagrams and can be characterised by means of differential scanning calorimetry (DSC).

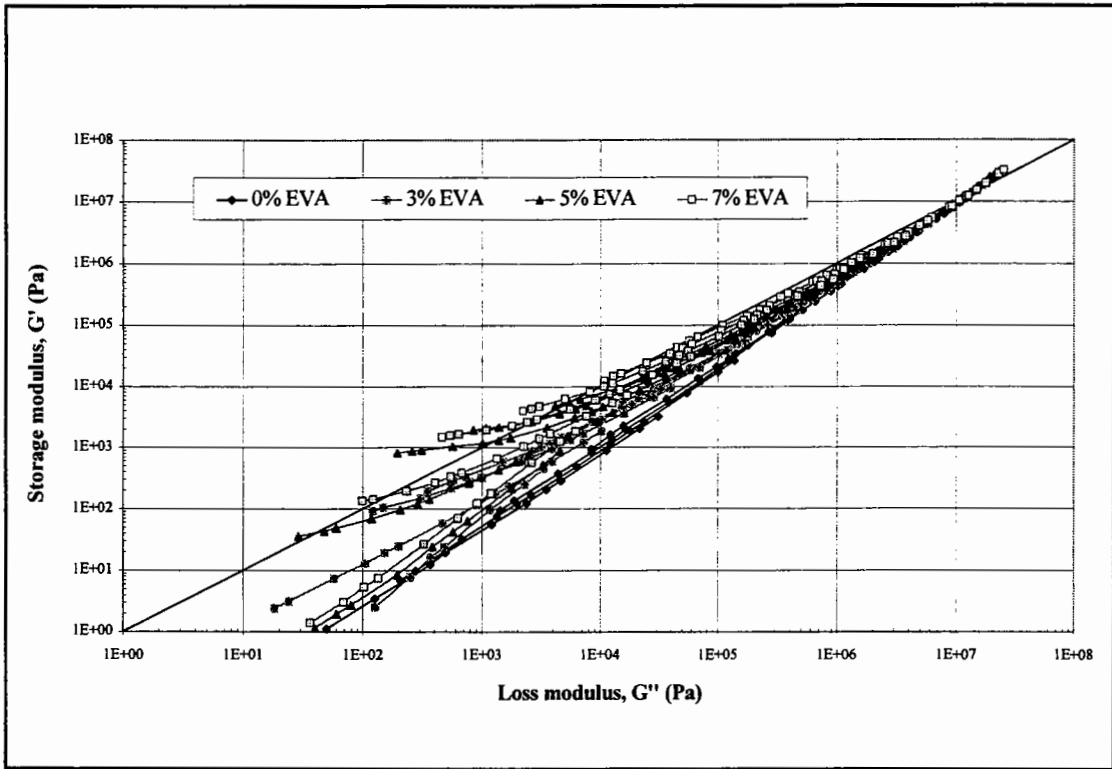


Figure 4.47: Cole-Cole diagram for Russian - EVA PMB's

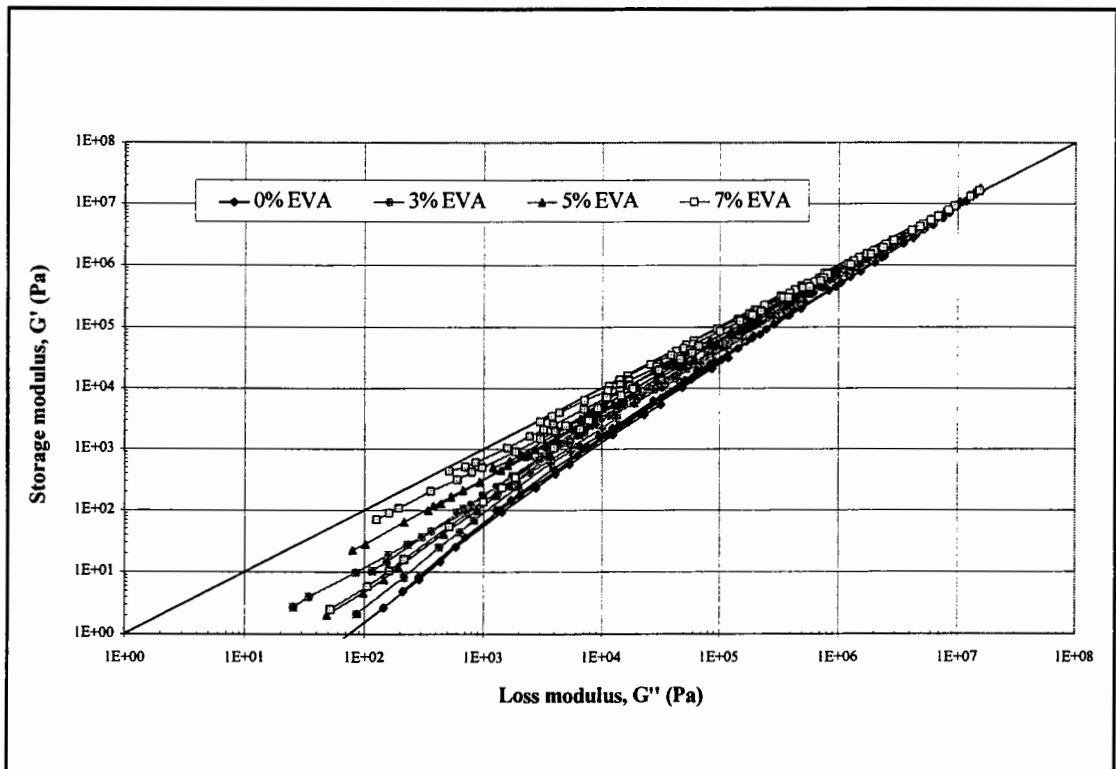


Figure 4.48: Cole-Cole diagram for Venezuelan - EVA PMB's

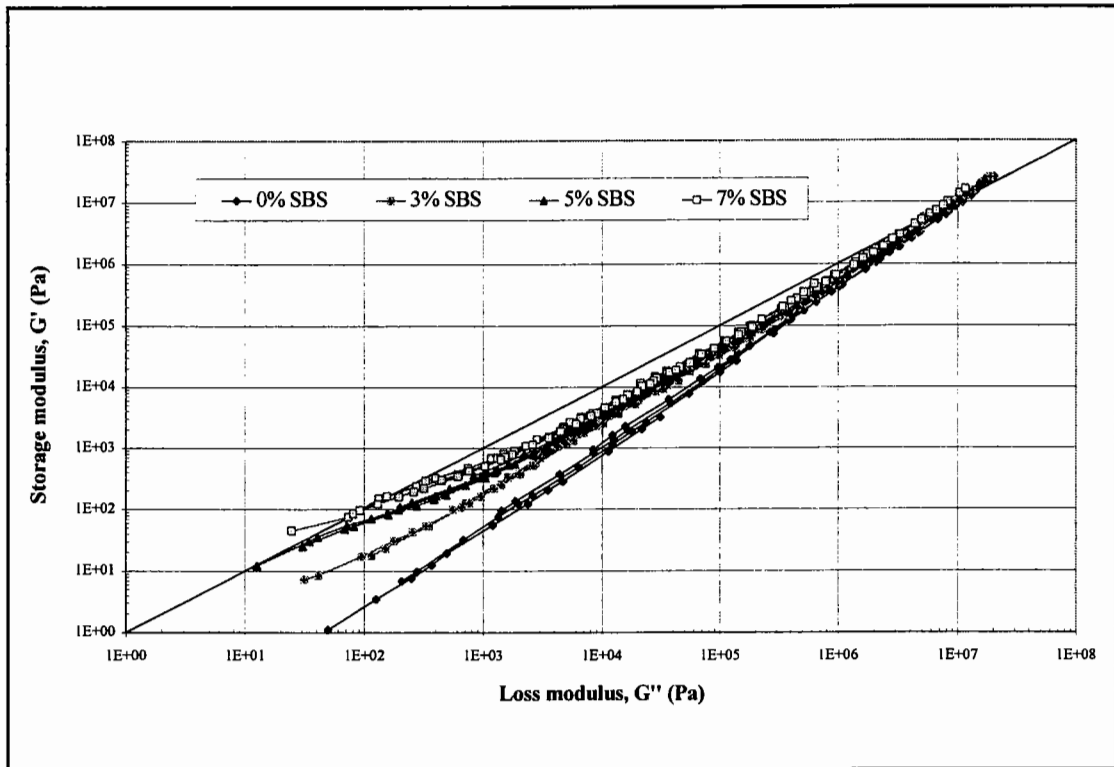


Figure 4.49: Cole-Cole diagram for Russian - SBS PMB's

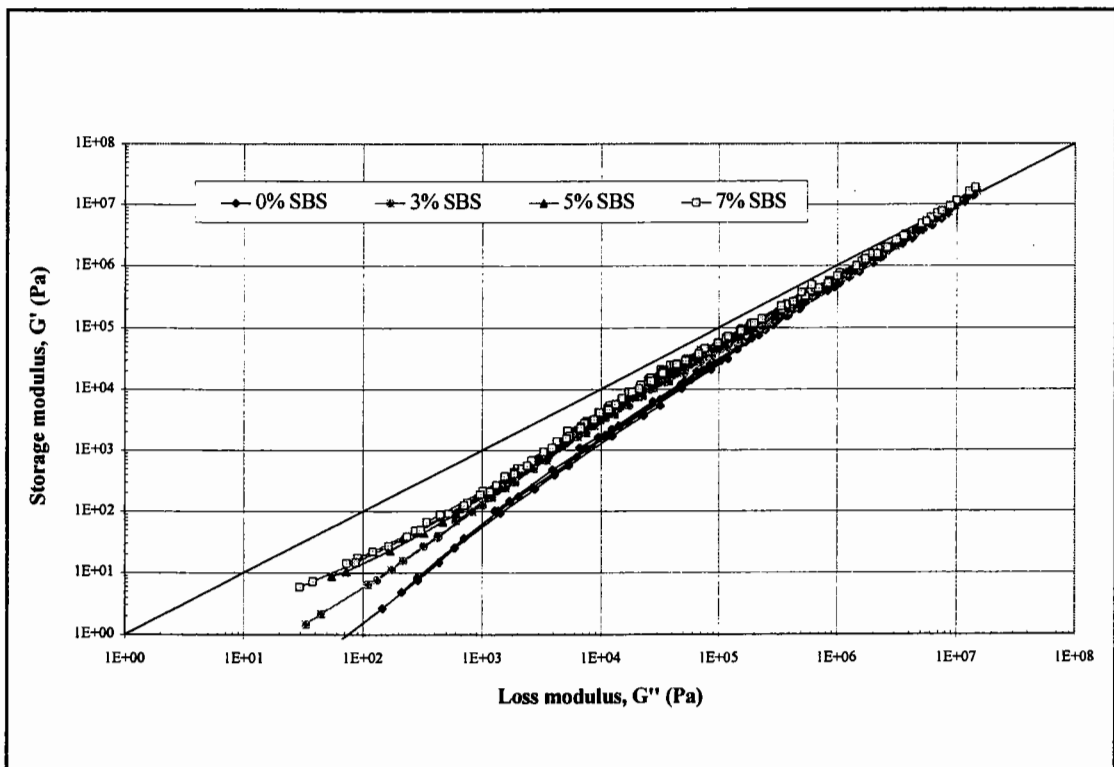


Figure 4.50: Cole-Cole diagram for Venezuelan - SBS PMB's

The rheological behaviour of the EVA PMB's can, therefore, be divided into three regions, namely:

- A region corresponding to a temperature range of approximately 10°C to 55°C, where there are large increases in viscosity, complex modulus and increased elasticity (decrease in phase angle) with increasing polymer content, which can be attributed to the EVA forming a three dimensional structure within the PMB. The extent of the modification depends on the compatibility of the bitumen-polymer blend and, therefore, the occurrence of polymeric-type or filler-type modification.
- A region corresponding to a temperature range of approximately 55°C to 75°C, where the melting (fusion) of the EVA crystalline structures results in a rapid reduction in the magnitude of the increase of viscosity and complex modulus and an alteration of the viscoelastic balance of the PMB towards a more viscous behaviour (increase in phase angle).
- A region corresponding to a temperature range greater than 75°C, where there are relatively small increases in viscosity and complex modulus with increasing polymer content, because the semi-crystalline EVA copolymer has melted and, therefore, only provides a filler-type modification.

The modification mechanism associated with the thermoplastic rubber SBS copolymer consists of the establishment of a highly elastic network within the bitumen. The amorphous polymer-bitumen blend increases the elasticity of the PMB at high temperatures as seen by the plateau-like behaviour of the binder in the viscosity-temperature plots, isochronal plots, master curves, Black diagrams and Cole-Cole diagrams. The higher melting temperature of the polystyrene blocks allows the rheological character of the SBS PMB's to be extended to temperatures of approximately 100°C. The higher temperature sustainability of the SBS PMB's means that the maximum modification generally occurs at a higher temperature than that found for the EVA

PMB's.

The rheological behaviour of the SBS PMB's can be divided into four regions:

- A region corresponding to a temperature range of approximately 10°C to 55°C, where there are increases in viscosity, complex modulus and elastic behaviour (decrease in phase angle).
- A region corresponding to a temperature range of approximately 55°C to 75°C, where there are large increases in viscosity, complex modulus and elasticity as the extended temperature range of the SBS polymer network allows the PMB to become increasingly polymer dominant, showing an almost completely polymeric-like behaviour.
- A region corresponding to a temperature range of approximately 75°C to 100°C, where there is a reduction in the magnitude of the increase of viscosity and complex modulus due to the melting of the SBS copolymer.
- A region corresponding to a temperature range greater than 100°C, where the SBS PMB's demonstrate a filler-type modification through the presence of the melted elastomeric polymer.

The establishment of both the semi-crystalline and elastomeric rheological characteristics within a PMB are, however, dependent on a suitable compatibility been found between the base bitumen and the polymer. Failure to provide a suitable compatibility results in the process resembling a filler-type modification.

Conventional tests and presentation methods, such as Penetration, Softening Point, PI, high temperature viscosity, BTDC and Van der Poel's nomograph do not provide a suitable means of measuring the rheological characteristics of PMB's. The Penetration and high temperature viscosity tests can only indicate the effect of polymer modification

as a filler-type mechanism, while the Softening Point test overestimates the possible advantages of modification. However, DMA does provide a suitable means of measuring the rheological characteristics of PMB's and will be used in the subsequent chapters of this thesis to investigate the rheological characteristics of aged PMB's.

The practical implications of the rheological characteristics of the laboratory blended EVA and SBS PMB's to asphalt mixture performance can be divided into three areas:

- Workability,
- Permanent deformation resistance, and
- Fatigue resistance of the modified asphalt mixture.

EVA PMB's have been known to improve the workability of asphalt mixtures [104]. The melting (fusion) of the EVA copolymer, within the temperature range of approximately 55°C to 75°C, results in a reduction of the stiffness (viscosity) and a more viscous behaviour of the PMB and, therefore, facilitates the compaction of the asphalt mixture at low compaction temperatures (< 100°C). However, the consequences of allowing the compaction temperature to fall within the crystallising temperature range of the EVA copolymer will be more detrimental for EVA modified asphalt mixtures than compacting at these low temperatures for SBS modified mixtures. This is because the stiffness (viscosity) and elasticity of the SBS PMB's, although greater at temperatures higher than approximately 65°C when compared to those of EVA PMB's, are generally lower at temperatures where the EVA copolymer has crystallised.

Both the increased stiffness and elasticity of the EVA and SBS PMB's at high pavement service temperatures (> 40°C) should significantly improve the permanent deformation resistance of the modified asphalt mixture. This improved permanent deformation resistance can be seen in the increased performance grade (PG) temperature of the SHRP rutting parameter for the 7% EVA and SBS - Russian PMB's in Table 4.7.



**Table 4.7: Superpave upper temperature PG grading**

Bitumen	G*/sinδ, minimum 1.00 kPa test temperature @ 10 rad/sec (°C)
Russian 80 pen	65
7% EVA - Russian	75
7% SBS - Russian	78

With regard to fatigue resistance, the strain versus number of loading cycles plot in Figure 4.51, illustrates the "distance" which separates conventional rheological analysis and the fatigue behaviour of a material. Rheological analysis in the linear and reversible range, while giving an indication of rutting resistance, cannot be expected to correlate with performance levels where materials have a non-linear and irreversible character. The practical implications of polymer modification for fatigue, therefore, needs to be investigated by means of asphalt mixture fatigue testing methods rather than linear viscoelastic analysis of the PMB.

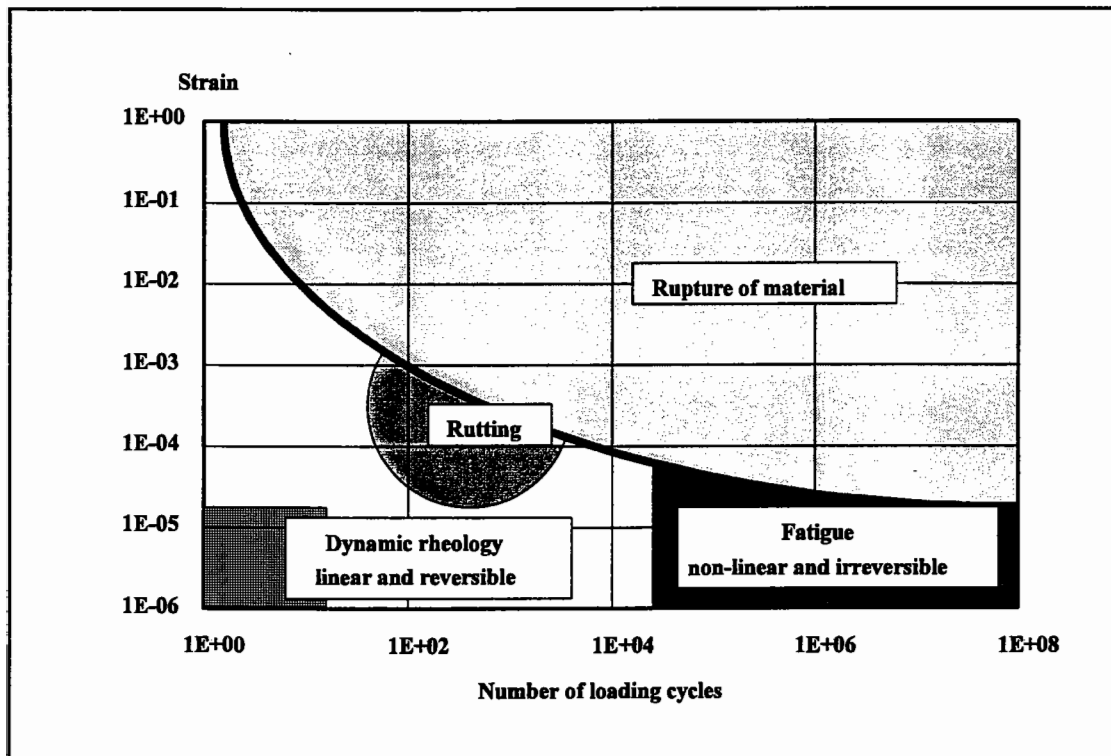


**Figure 4.51: Deformation versus for number of loading cycles for rheological analysis and fundamental testing [126]**

## 4.8 Conclusions

The rheological investigation of the EVA and SBS PMB's, by means of empirical methods and dynamic shear rheometry, has shown that there is a considerably difference in behaviour between, not only the plastomeric and elastomeric PMB's, but also between the different base bitumen-polymer blends.

The results have shown that semi-crystalline EVA copolymer provides the polymeric modification of the PMB through the crystallisation of three dimensional networks within the bitumen. These crystalline structures reduce the temperature susceptibility and increase the viscosity, stiffness and elastic component of the PMB up to the temperatures associated with the melting of these structures. The thermoplastic rubber SBS copolymer provides polymeric modification by means of a highly elastic network within the bitumen. This elastic network has a similar effect on the stiffness and viscoelastic balance of the PMB, but due to the higher melting temperature of the polystyrene blocks, is maintained to higher temperatures, well within the compaction temperature range of asphalt mixtures modified with the PMB.

The results have shown that empirical tests and presentation methods, such as Penetration, Softening Point, PI, high temperature viscosity, BTDC and Van der Poel's nomograph do not provide suitable means of measuring the rheological characteristics of PMB's. In order to accurately evaluate these rheological characteristics, dynamic shear rheometry using a Dynamic Shear Rheometer (DSR) together with rheological data presentation methods, such as isochronal plots, master curves and Black diagrams are recommended.

# **5 Rheological Characteristics of Aged Unmodified and Polymer Modified Bitumens**

## **5.1 Introduction**

Ageing of bitumen is an important cause of reduced durability of asphalt pavements. This is particularly true for asphalt mixtures with relatively high air void contents, such as porous asphalt, where polymer modified binders are recommended to increase the durability of the material. In the case of porous asphalt, the polymer is used to eliminate binder drainage and maximise the binder content. However, it is questionable whether the durability of particular asphalt mixtures, such as porous asphalt, are improved by PMB's due to the increased binder content and, therefore, thicker binder films or whether there are favourable mechanisms associated with the ageing of the PMB's.

The rheological and chemical changes associated with laboratory short term and long term ageing are well known and understood for unmodified, penetration grade, bitumens. However, the changes associated with ageing are not fully understood for polymer modified bitumens (PMB's). There is, therefore, a need to determine the suitability of various testing methods for describing the changes in the rheological performance of PMB's, after short term and long term ageing, and to characterise these changes by providing an explanation of the ageing process.

This chapter investigates the rheological changes associated with short term and long term laboratory ageing of various unmodified, penetration grade, bitumens and PMB's using conventional binder tests, chemical property tests and a Dynamic Shear Rheometer (DSR). Analysis of the rheological and chemical data indicates that the mechanism of age-hardening differs for unmodified bitumen, elastomeric and plastomeric PMB's.

## 5.2 Experimental Programme

### 5.2.1 Materials

Three bitumens, from different crude sources with different chemical compositions but with similar consistencies, were selected as the base bitumens for the production of various polymer modified bitumens (PMB's). The three bitumens were:

- Middle East, 80/100 penetration (Paraffinic),
- Russian, 80 penetration (Paraffinic), and
- Venezuelan, 70/100 penetration (Naphthenic).

The three base bitumens were blended with a plastomeric and an elastomeric polymer:

- EVA 20/20 (thermoplastic polymer), and
- SBS Cariflex linear (thermoplastic rubber).

at three polymer contents:

- 3 percent,
- 5 percent, and
- 7 percent by mass.

to produce 15 physically blended PMB's. No Middle East - SBS PMB's were produced.

### 5.2.2 Testing Programme

All 18 binders were subjected to laboratory short term and long term ageing in the RTFOT [96] and PAV [78]. The ageing parameters used with the RTFOT tests were:

- Ageing temperature: 163°C,
- Ageing time: 75 minutes.

The ageing parameters used with the PAV were:

- Ageing temperature: 100°C,
- Ageing time: 20 hours,
- Air pressure: 2.10 MPa.

A number of mechanical and chemical tests were then performed on the unaged, RTFOT and PAV aged bitumens in order to characterise their physical and chemical properties and investigate the effect of ageing on these properties. The tests ranged from conventional specification and empirical tests to more fundamental rheological and mechanical tests. The following tests were performed on the binders:

- Iatroscan (SARA chemical composition) (only for three base bitumens) (performed by Ooms Avenhorn b.v.),
- Penetration @ 25°C,
- Ring and Ball Softening Point,
- Rotational viscosity @ 60°C and 135°C,
- Dynamic mechanical analysis (DMA),
- DSC thermal analysis (only for the EVA PMB's) (performed by Jean Lefevre),
- HP-GPC (only for the three base bitumens and SBS PMB's) (performed by Jean Lefebvre), and
- FTIR (only for the three base bitumens and SBS PMB's) (performed by the Danish Road Institute).

The HP-GPC was used to measure the molecular size distribution of the unaged and aged bitumens. The chromatograms obtained from the HP-GPC analysis were converted into six numerical parameters consisting of the midpoint retention times and percentage areas of the three broad molecular size bands, shown in Figure 5.1, and listed as:

- Aggregates (large molecular size, short HP-GPC retention time),
- Micelles (medium molecular size, medium HP-GPC retention time), and
- Oils (small molecular size, long HP-GPC retention time).

The FTIR was used to measure oxygen uptake of the different bitumens during ageing. The oxygen uptake was measured by the growth in the carbonyl fraction at wavenumber  $1693\text{ cm}^{-1}$  and sulfoxide fraction at wavenumber  $1018\text{ cm}^{-1}$ . The growth in the amount of sulfoxide and carbonyl was determined by measuring their peak heights.

The DMA was performed using a Bohlin Model DSR50 Dynamic Shear Rheometer with the following test conditions:

- Mode of loading: Controlled-strain,
- Temperatures: 10, 15, 25, 35, 45, 55, 65, 75 and  $85^{\circ}\text{C}$ ,
- Frequencies: 0.01, 0.015, 0.02, 0.05, 0.1, 0.15, 0.2, 0.5, 1, 1.5, 2, 5, 10 and 15 Hz,
- Strain amplitude: 0.5 to 10% depending on temperature.

The dynamic mechanical data obtained from the DSR was presented in the form of master curves of complex modulus,  $G^*$ , and phase angle,  $\delta$ , at a reference temperature of  $25^{\circ}\text{C}$ , isochronal plots of  $G^*$  and  $\delta$  at two frequencies of 0.02 Hz and 1 Hz, Cole-Cole diagrams of storage modulus,  $G'$ , versus loss modulus,  $G''$ , and in the form of Black diagrams of  $G^*$  versus  $\delta$ .

The complex modulus and phase angle presented in an isochronal plot cannot be expected to convey the entire picture of the rheological behaviour of a bitumen as the data is

usually only presented for selected loading frequencies. This is particularly true for polymer modified bitumens where the applicability of the time-temperature superposition principle (TTSP) [66], used to shift data between different temperatures and loading frequencies, is questionable in cases of highly structured bitumens and PMB's. This implies that the data presented in an isochronal plot of limited frequencies can only provide a limited view of the particular rheological performance of the PMB.

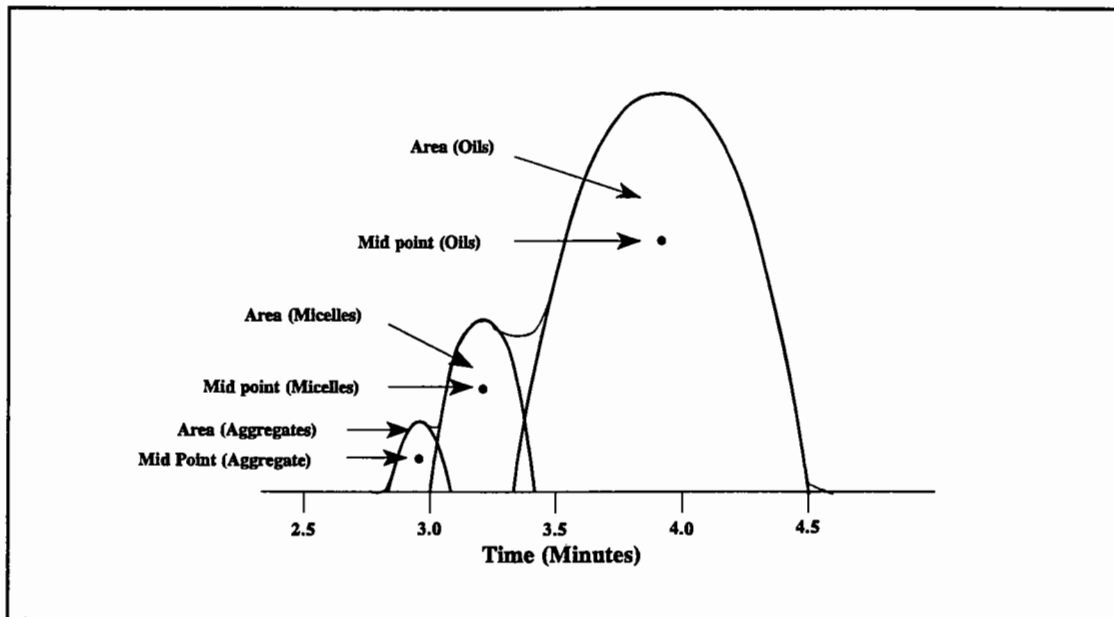


**Figure 5.1: HP-GPC molecular size parameters**

Black diagrams, on the other hand, allow all experimental data to be presented on a single plot without requiring the shifting of data using the TTSP. Black diagrams, therefore, allow the entire rheological performance of the bitumen to be analysed in one data plot. The use of master curves of  $G^*$  and  $\delta$ , isochronal plots, Cole-Cole diagrams and Black diagrams should allow a complete picture of the rheological behaviour to be evaluated.

## 5.3 Penetration Grade Bitumen

### 5.3.1 Chemical Characterisation of the Effect of Ageing

The most important changes that cause hardening of the binder in pavements are the changes in the composition of the bitumen molecules from reaction with oxygen,

molecular growth (forming of asphaltenes) and molecular structuring that produces different rheological behaviour [26,40].

### **Iatroscan Thin Layer Chromatography**

Bitumen is a colloidal system containing a wide spectrum of molecular types. The interaction of the various components of bitumen with each other form a balanced or compatible system [26]. The binding properties, originating from such a balanced system, change during ageing and can lead to pavement damage, such as cracking and ravelling.

One method that is used to study the changes associated with ageing of paving grade bitumen is to determine the generic composition of the aged bitumen. The changes in the percentages of the Saturates, Aromatics, Resins and Asphaltenes (SARA), obtained from Iatroscan thin layer chromatography, of the three paving grade bitumens after RTFOT and PAV ageing are shown in Table 5.1.

**Table 5.1: Changes in chemical composition due to ageing**

Bitumen	Condition	Saturates (%)	Aromatics (%)	Resins (%)	Asphaltenes (%)
Middle East 80/100	Unaged	5	69	15	11
	RTFOT	6	61	20	13
	PAV	6	52	24	18
Russian 80	Unaged	4	68	19	9
	RTFOT	4	64	21	11
	PAV	5	52	28	15
Venezuelan 70/100	Unaged	11	58	17	14
	RTFOT	13	54	17	16
	PAV	12	47	21	20

The SARA data, for all three bitumens, shows a similar decrease in aromatics with an increase in asphaltenes and resins with the percentage mass of saturates remaining fairly constant after ageing. The three paving grade bitumens, therefore, showed the expected changes in their chemical composition due to the ageing process (oxidative hardening) caused by RTFOT and PAV ageing.



This ageing process has been described in Chapter 2 and consists of an oxidative process resulting in:

- The formation of the highly polar, high molecular weight asphaltenes from the lower molecular weight, polar resins, and
- The formation of polar resins from the non-polar, low molecular weight naphthenic aromatic compounds.

The SARA data also indicates that the magnitude of the increase in asphaltenes and resins and decrease in aromatics is greater after PAV ageing compared to that after RTFOT ageing. This is understandable due to the severe oxidative ageing that occurs during PAV ageing.

#### **Fourier Transform Infrared Spectroscopy**

Another method that can be used to observe the change of bitumen during ageing is by measuring the increased amounts of oxygenated products, carbonyl and sulphoxide, formed during the oxidative ageing process. This oxidation increases the amount of polar molecules which increases the structuring and stiffening of the binder [40]. The increases in the amounts of carbonyl and sulphoxide after RTFOT and PAV ageing are presented in Table 5.2.

**Table 5.2: Increase in oxidative products during ageing**

Bitumen	Condition	Carbonyl	Sulphoxide	Carbonyl + Sulphoxide
Middle East 80/100	RTFOT - Unaged	0.071	0.068	0.139
	PAV - Unaged	0.279	0.295	0.574
Russian 80	RTFOT - Unaged	0.065	0.071	0.136
	PAV - Unaged	0.302	0.327	0.629
Venezuelan 70/100	RTFOT - Unaged	0.078	0.031	0.109
	PAV - Unaged	0.327	0.244	0.571

The FTIR data, in Table 5.2, shows, as with the Iatroscan SARA data, that all three

bitumens have a similar increase in oxidative products after ageing. The exact proportions of the carbonyl and sulphoxide products are dependent on the chemical composition of the two Paraffinic and one Naphthenic bitumens, with the ratio being relatively even for the Middle East and Russian bitumens and higher for carbonyl than sulphoxide for the Venezuelan bitumen.

Once again the amount of oxidative products are considerably greater after PAV ageing than after the short-term RTFOT ageing.

### High Pressure Gel Permeation Chromatography

The third method of observing the change of the bitumen as related to ageing is by means of HP-GPC. The midpoint and percentage area parameters for the aggregates, micelles and oils are presented in Table 5.3.

**Table 5.3: Changes in HP-GPC molecular size parameters due to ageing**

Bitumen	Condition	Aggregates		Micelles		Oils	
		Mid. Pt (min)	Area (%)	Mid. Pt (min)	Area (%)	Mid. Pt (min)	Area (%)
Middle East 80/100	Unaged	2.93	0.75	3.35	9.31	4.14	89.94
	RTFOT	2.99	2.21	3.53	15.88	4.19	82.21
	PAV	2.99	2.69	3.60	20.17	4.16	77.14
Russian 80	Unaged	2.85	1.01	3.04	2.56	4.09	96.42
	RTFOT	3.00	1.20	3.60	14.64	4.18	84.16
	PAV	2.95	1.90	2.95	14.80	4.16	83.40
Venezuelan 70/100	Unaged	3.00	0.84	3.26	7.22	4.16	91.93
	RTFOT	2.97	2.91	3.58	18.42	4.31	78.67
	PAV	2.97	3.39	3.51	17.49	4.30	79.12

The HP-GPC percentage area parameters show that there is an increase in the higher molecular sized aggregates and micelles and a reduction in the low molecular sized oils after ageing. This confirms the Iatroscan SARA analysis which also showed an increase in the higher molecular weight asphaltenes and resins and a reduction in the low

molecular weight aromatic oils after ageing.

### 5.3.2 Conventional Empirical Tests

The changes in Penetration, Softening Point, viscosity and Fraass breaking point after ageing are presented in Table 5.4.

**Table 5.4: Changes in conventional test data due to ageing**

Bitumen	Property	Unaged	RTFOT	PAV	Ageing Index	
					RTFOT/ unaged	PAV/ unaged
Middle East 80/100	Pen.(dmm)	60	45	24	0.75	0.40
	Soft. Pt (°C)	48.8	52.6	59.3	1.08	1.22
	Vis <sub>60°C</sub> (Pa.s)	262	505	2038	1.93	7.78
	Vis <sub>135°C</sub> (mPa.s)	510	660	1030	1.29	2.02
	Fraass (°C)	-18	-14	-12	-	-
Russian 80	Pen.(dmm)	73	51	24	0.70	0.33
	Soft. Pt (°C)	47	50.8	57.3	1.08	1.22
	Vis <sub>60°C</sub> (Pa.s)	165	343	1028	2.08	6.23
	Vis <sub>135°C</sub> (mPa.s)	370	470	760	1.27	2.05
	Fraass (°C)	-12	-11	-11	-	-
Venezuelan 70/100	Pen.(dmm)	81	53	28	0.75	0.40
	Soft. Pt (°C)	46.8	51.2	59.2	1.09	1.26
	Vis <sub>60°C</sub> (Pa.s)	213	455	1950	2.14	9.15
	Vis <sub>135°C</sub> (mPa.s)	380	520	870	1.37	2.29
	Fraass (°C)	-28	-21	-15	-	-

The conventional tests showed a decrease in Penetration and an increase in Softening Point, viscosity and Fraass for the three base bitumens after ageing. This indicates a hardening of the bitumen and corresponds to the oxidative processes identified by the SARA, FTIR and HP-GPC analysis.

The ageing indices for the RTFOT and PAV aged bitumens indicate that the changes in the traditional, empirical tests are greater after PAV ageing compared to those after RTFOT ageing. The relative magnitude of the ageing indices after RTFOT and PAV ageing differ for the different conventional test due to the different temperature and loading conditions used with the tests. This is particularly evident when comparing the ageing indices for viscosity at 60°C and 135°C. The different ageing indices can be attributed to the combined influence of temperature and rate of loading on the viscoelastic property at 60°C, whereas the viscosity at 135°C can be considered to be a measurement of purely Newtonian flow and therefore independent of strain rate.

### **5.3.3 Dynamic Mechanical Analysis**

The master curves, isochronal plots, Cole-Cole diagrams and Black diagrams for the three base bitumens are all similar and, therefore, the results will only be presented for one bitumen with the understanding that the commentary applies to all three base bitumens.

The master curves of complex modulus and phase angle for the Russian 80 pen bitumen are shown in Figures 5.2 and 5.3. The  $G^*$  master curves show a consistent increase in stiffness after ageing, corresponding to the increased hardness of the RTFOT and PAV aged bitumen. The phase angle master curve, in Figure 5.3, shows a decrease in  $\delta$  after ageing, corresponding to an increase elastic behaviour after ageing.

The smooth shifting of the  $G^*$  and  $\delta$  data to form the master curves in Figures 5.2 and 5.3 indicates that the TTSP is applicable for the three base bitumens and that there is an equivalency between time and temperature. Accordingly, a limited combination of temperatures and loading times (frequencies) should allow a general overview of the changes in rheological characteristics to be investigated. Therefore, the  $G^*$  and  $\delta$  values at one temperature of 25°C and two loading frequencies of 0.02 Hz and 1 Hz for the three paving grade bitumens are presented in Table 5.5.

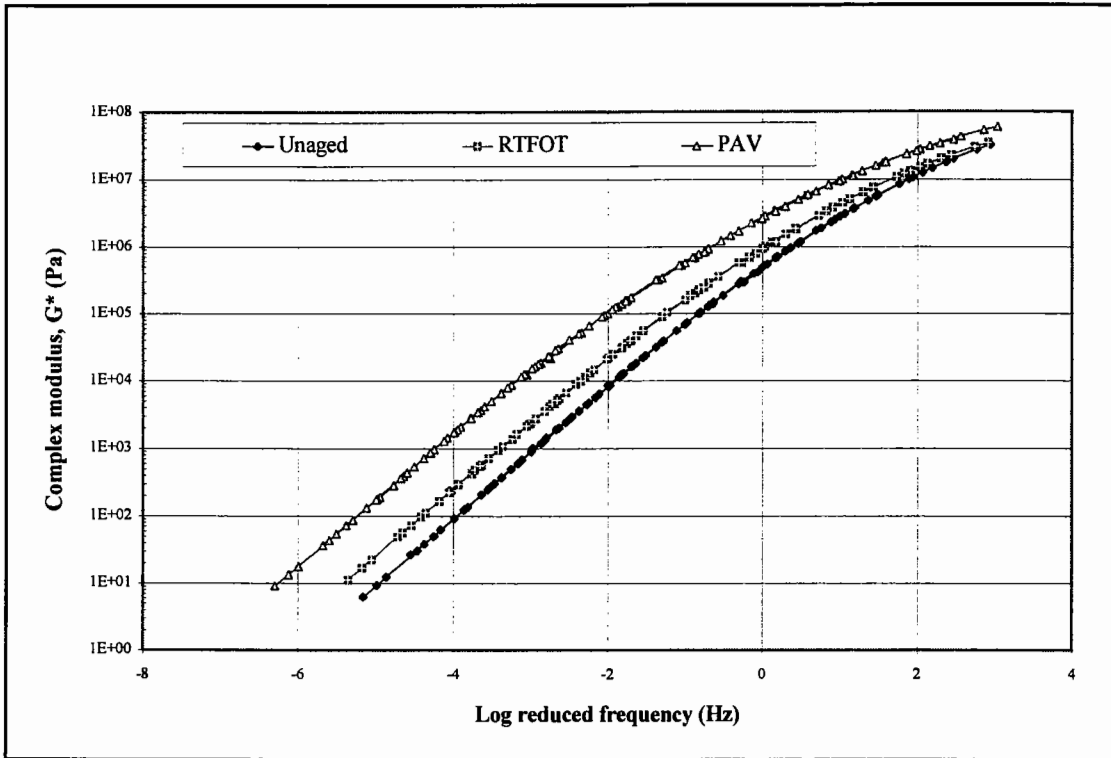


Figure 5.2: Complex modulus master curve for Russian 80 pen bitumen

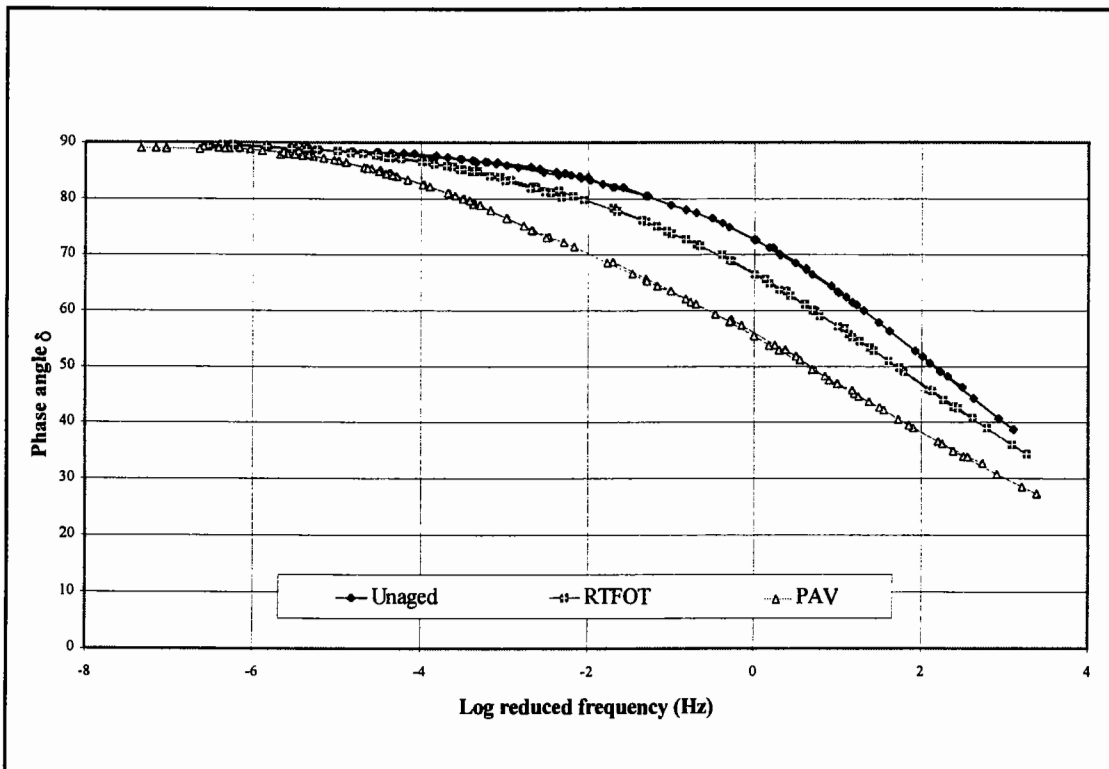


Figure 5.3: Phase angle master curve for Russian 80 pen bitumen

**Table 5.5: Changes in complex modulus and phase angle due to ageing**

Bitumen	Property	Unaged	RTFOT	PAV	Ageing Index	
					RTFOT/ unaged	PAV/ unaged
Middle East 80/100	$G^*_{25^\circ\text{C},0.02\text{ Hz}}$ (Pa)	24,800	56,150	230,500	2.26	9.29
	$G^*_{25^\circ\text{C},1\text{ Hz}}$ (Pa)	617,500	1,100,000	3,050,000	1.78	4.94
	$\delta_{25^\circ\text{C},0.02\text{ Hz}}$ (°)	79	75	65	-	-
	$\delta_{25^\circ\text{C},1\text{ Hz}}$ (°)	68	63	53	-	-
Russian 80	$G^*_{25^\circ\text{C},0.02\text{ Hz}}$ (Pa)	16,050	39,600	174,500	2.47	10.87
	$G^*_{25^\circ\text{C},1\text{ Hz}}$ (Pa)	492,500	938,000	2,650,000	1.90	5.38
	$\delta_{25^\circ\text{C},0.02\text{ Hz}}$ (°)	83	79	69	-	-
	$\delta_{25^\circ\text{C},1\text{ Hz}}$ (°)	73	66	55	-	-
Venezuelan 70/100	$G^*_{25^\circ\text{C},0.02\text{ Hz}}$ (Pa)	12,600	29,500	113,500	2.34	9.01
	$G^*_{25^\circ\text{C},1\text{ Hz}}$ (Pa)	343,000	582,000	1,535,000	1.70	4.48
	$\delta_{25^\circ\text{C},0.02\text{ Hz}}$ (°)	80	74	64	-	-
	$\delta_{25^\circ\text{C},1\text{ Hz}}$ (°)	72	66	55	-	-

The  $G^*$  and  $\delta$  data in Table 5.5, provides the same findings, as seen in Figures 5.2 and 5.3, of an increase in stiffness and elastic behaviour. The ageing indices for  $G^*$  indicate, as seen for the chemical characterisation and conventional tests, that the effect of oxidative ageing is more severe after PAV than RTFOT ageing.

The isochronal plots and the Black diagram for the Venezuelan 70/100 penetration bitumen are shown in Figures 5.4 to 5.6. The isochronal plots show a constant increase in complex modulus,  $G^*$ , over the temperature domain after ageing. The increase in  $G^*$  after PAV ageing is understandably greater than after RTFOT ageing due to the prolonged ageing process in the PAV. There is also a regular decrease of the phase angle,  $\delta$ , over the temperature domain after ageing. The result of ageing, for the penetration grade bitumen, is therefore an increase in  $G^*$  and a decrease in  $\delta$ .

The Black diagram, in Figure 5.6, shows a continuous shift of the curves towards lower phase angles after ageing. The shift in the Black diagram curves is caused by the dual

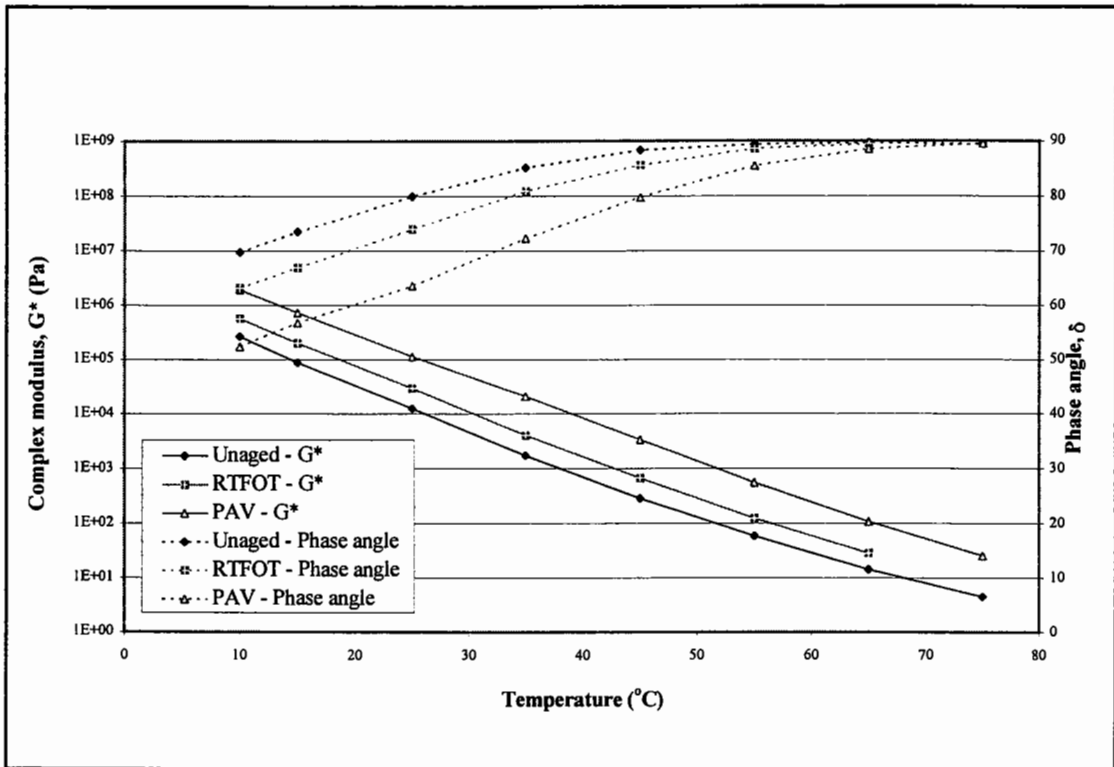


Figure 5.4: Isochronal plot at 0.02 Hz for Venezuelan 70/100 pen bitumen

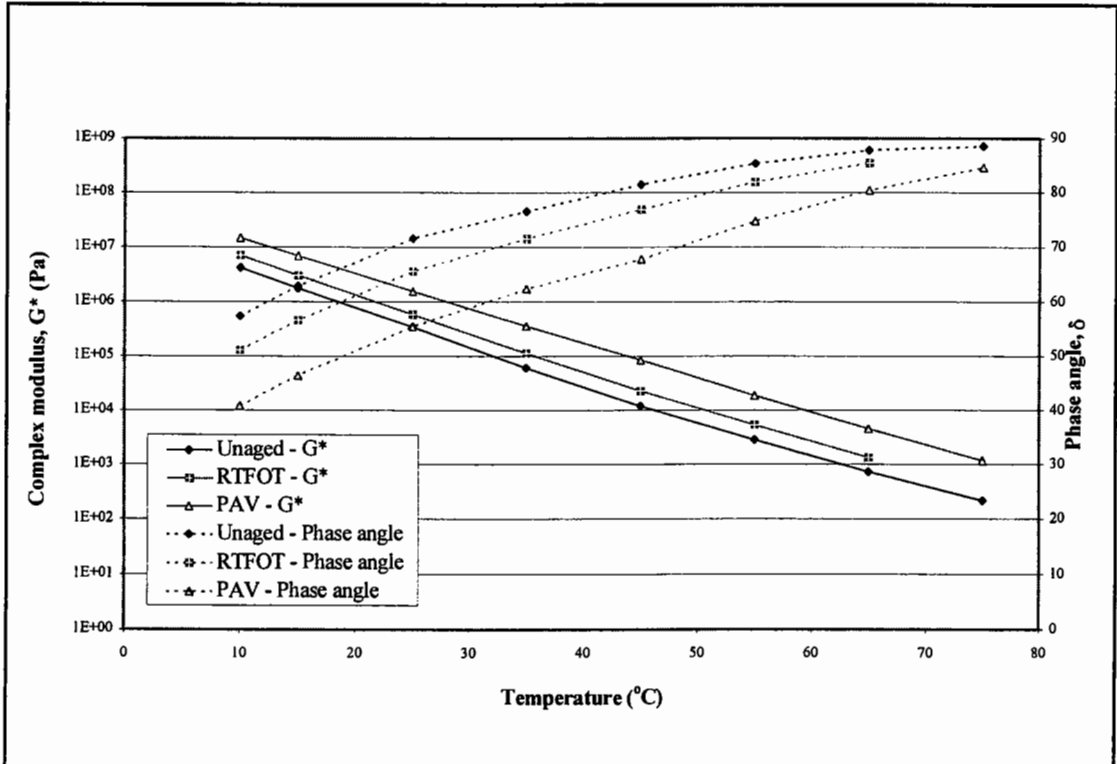


Figure 5.5: Isochronal plot at 1 Hz for Venezuelan 70/100 pen bitumen

actions of an increase in complex modulus, indicating the hardening of the bitumen, and a decrease in phase angle, indicating an increase in the elastic behaviour of the bitumen. The different magnitudes of these two actions results in the shifting of the Black diagrams curves towards lower phase angle values with more 'solid-like' properties and a greater percentage of elastic (brittle) behaviour.

The Cole-Cole diagram for the unaged and aged Russian base bitumen is shown in Figure 5.7. The diagram gives an indication of the viscoelastic balance of the bitumen without requiring temperature and/or loading frequency as one of the axes. Although, at a particular temperature and loading frequency, the viscoelastic balance of the bitumen after ageing becomes more elastic and less viscous, with the bitumen having a larger increase in storage modulus than loss modulus, the time-temperature equivalency of the bitumen means that the unaged and aged Cole-Cole diagrams overlap. This is seen in Figure 5.7, where the Cole-Cole plots for the aged Russian bitumen have simply shifted along the same line towards the upper right-hand corner of the diagram and towards a more elastic, stiffer rheological behaviour.

#### **5.3.4 Discussion**

The observations from the master curves, isochronal plots, Cole-Cole diagram and Black diagram confirm the results obtained using the conventional tests (Penetration, Softening Point and viscosity) that ageing (short term and long term) has hardened the bitumen. The analysis of the chemical composition of the unaged, RTFOT and PAV aged bitumens reinforced these conclusions with the base bitumens showing an increase in the proportions of resins and asphaltenes resulting in an increase in molecular weight (see Tables 5.1 and 5.3). It can, therefore, be assumed that any variation from this ageing behaviour for the PMB's can be attributed to the presence of the polymers and the possibly different ageing mechanisms associated with the various PMB's.

The empirically based rheological tests, such as Penetration and Softening Point, as well as the more fundamental viscosity test, seem to be able to adequately describe the



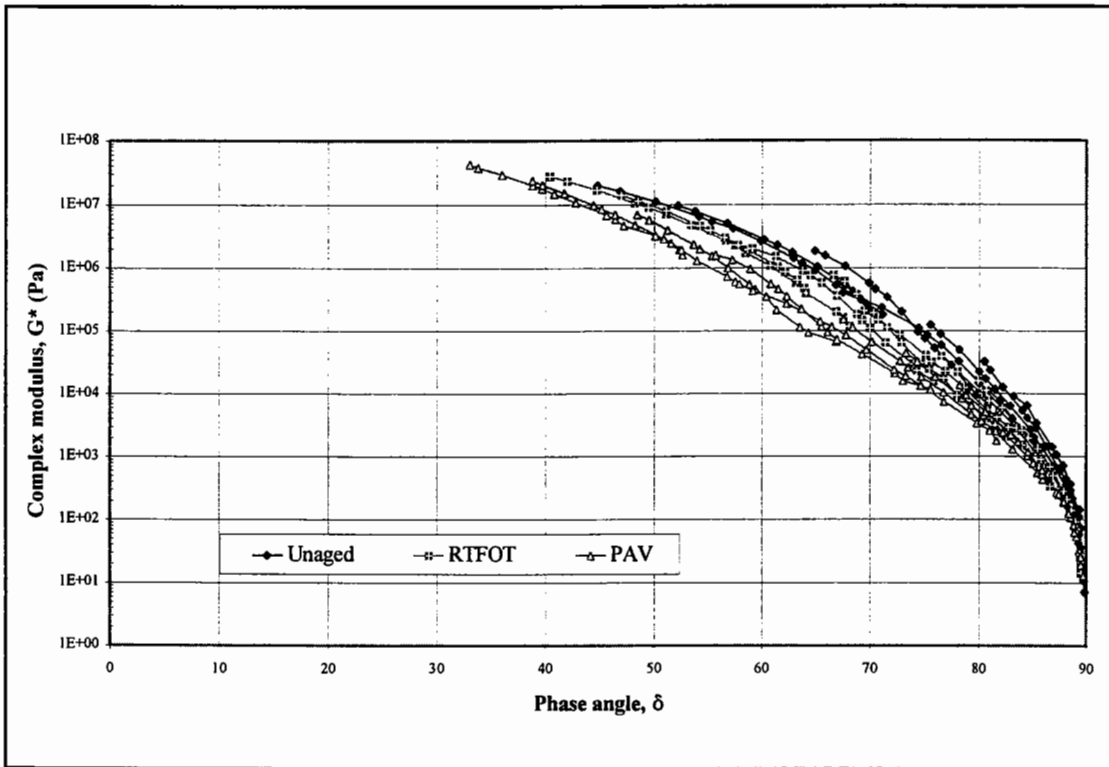


Figure 5.6: Black diagram for Venezuelan 70/100 pen bitumen

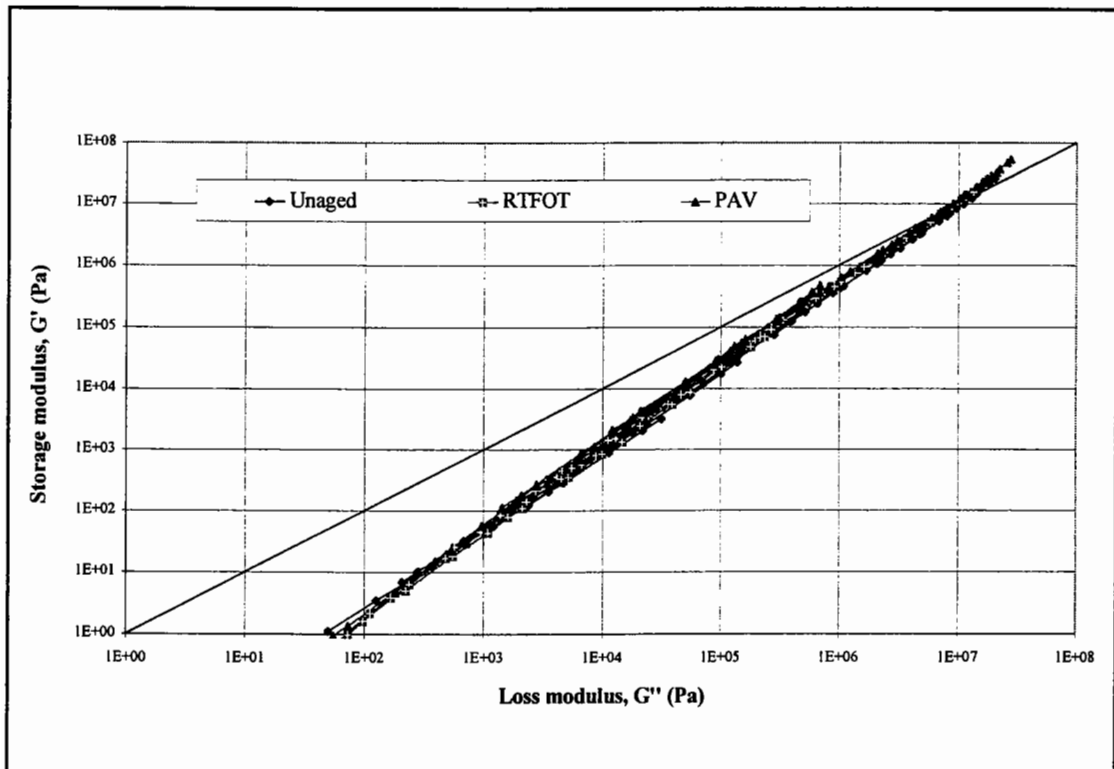


Figure 5.7: Cole-Cole diagram for Russian 80 pen bitumen

changes in the rheological performance of unmodified penetration grade bitumens after ageing. However, a shortcoming of the conventional (traditional) bitumen tests is that they only provide information at specific temperatures and/or loading frequencies and are, therefore, unable to give a complete picture of the rheological performance of the bitumen. Although this does not appear to be a problem when dealing with penetration grade bitumens, it may be a limiting factor when dealing with the more rheologically complicated PMB's.

## 5.4 Semi-crystalline Polymer Modified Bitumen

### 5.4.1 Differential Scanning Calorimetry Analysis of the Effect of Ageing

In an attempt to quantify the ageing mechanism associated with RTFOT and PAV ageing of the EVA PMB's, DSC thermal analysis was performed on the nine EVA PMB's. The results of the analysis are presented in Table 5.6.

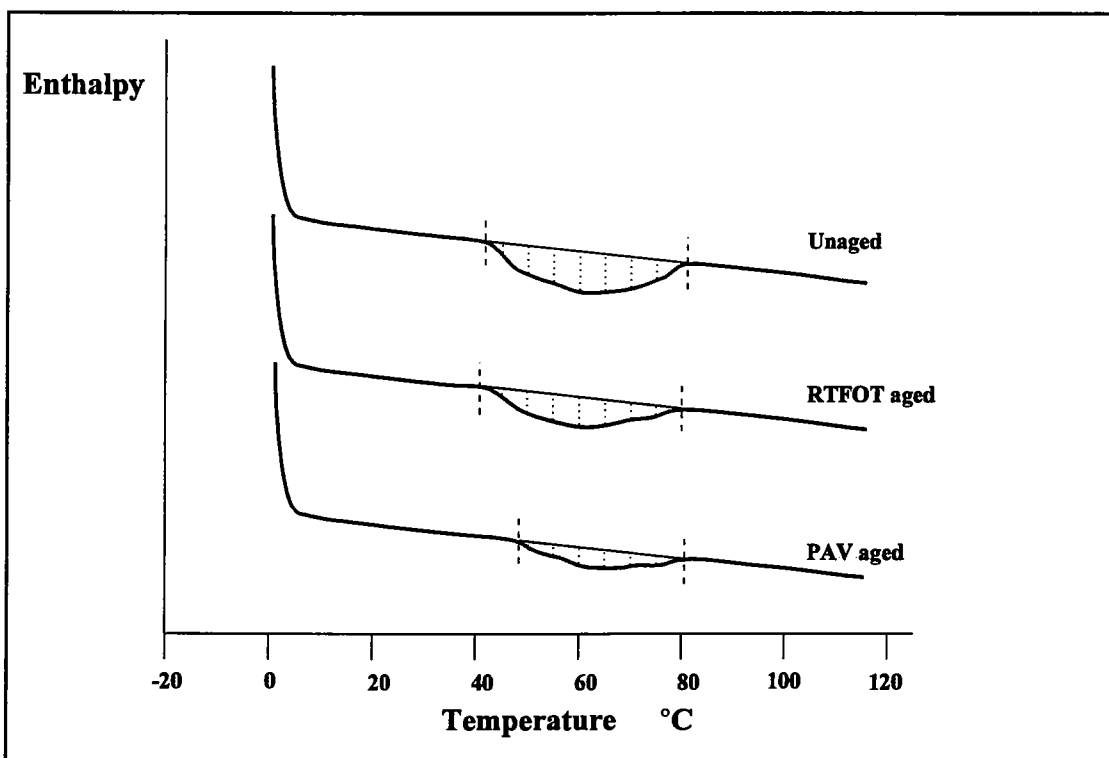


Figure 5.8: DSC plots for 5% EVA with 95% Venezuelan 70/100 pen bitumen

**Table 5.6: Variations in DSC parameters due to ageing for EVA PMB's**

Bitumen	Condition	Enthalpy (J/g)	Temperature Fusion Range		
			Peak Temp (°C)	Low Temp (°C)	High Temp (°C)
3% EVA - Rus	Unaged	2.7	66.7	44	80
	RTFOT	1.6	70.0	48	82
	PAV	-	-	-	-
5% EVA - Rus	Unaged	3.4	69.6	44	83
	RTFOT	3.3	67.4	42	80
	PAV	2.1	72.5	52	86
7% EVA - Rus	Unaged	4.3	69.9	43	85
	RTFOT	3.9	72.2	44	83
	PAV	3.6	72.8	44	86
3% EVA - Ven	Unaged	2.5	61.9	43	77
	RTFOT	1.4	64.2	42	78
	PAV	-	-	-	-
5% EVA - Ven	Unaged	3.1	61.5	42	81
	RTFOT	2.5	65.8	41	80
	PAV	2.0	66.0	48	81
7% EVA - Ven	Unaged	4.4	65.4	42	82
	RTFOT	3.8	66.6	41	78
	PAV	3.3	63.6	40	82
3% EVA - ME	Unaged	2.4	69.7	41	81
	RTFOT	1.4	69.0	53	82
	PAV	1.2	69.6	53	82
5% EVA - ME	Unaged	3.0	69.9	46	82
	RTFOT	2.9	70.5	46	87
	PAV	2.1	71.5	47	83
7% EVA - ME	Unaged	3.2	69.9	47	86
	RTFOT	3.1	71.9	47	85
	PAV	3.0	70.5	46	87

The DSC unaged, RTFOT and PAV aged plots for the 5% EVA with 95% Venezuelan 70/100 pen PMB are also shown in Figure 5.8.

The data in Table 5.6 and Figure 5.8 indicate that the temperatures associated with the fusion of the EVA copolymers remain relatively constant for the unaged and aged PMB's. However, there is a reduction in the magnitude of the enthalpy, measured for the endothermic reaction associated with the melting of the EVA copolymers, after RTFOT and PAV ageing.

#### 5.4.2 Conventional Tests

The ageing indices for the Penetration, Softening Point and viscosity tests for the nine EVA PMB's are presented in Table 5.7 together with those for the three base bitumens. One ageing index that differs from the pattern shown for penetration grade bitumens is highlighted in bold typeface.

**Table 5.7: Changes in conventional test data due to ageing for EVA PMB's**

Bitumen	Penetration Ageing Index		Softening point Ageing Index		Viscosity @ 135°C Ageing Index	
	RTFOT/ Unaged	PAV/ Unaged	RTFOT/ Unaged	PAV/ Unaged	RTFOT/ Unaged	PAV/ Unaged
Middle East 80/100	0.75	0.40	1.08	1.22	1.29	2.02
3% EVA - ME	0.74	0.34	1.05	1.22	1.33	-
5% EVA - ME	0.79	0.44	1.06	1.16	1.36	2.39
7% EVA - ME	0.84	0.49	1.03	1.10	1.41	2.32
Russian 80	0.70	0.33	1.08	1.22	1.27	2.05
3% EVA - Rus	0.69	-	<b>0.96</b>	-	1.32	-
5% EVA - Rus	0.73	0.37	1.02	1.05	1.36	2.38
7% EVA - Rus	0.77	0.26	1.04	1.08	1.49	2.42
Venezuelan 70/100	0.75	0.40	1.09	1.26	1.37	2.29
3% EVA - Ven	0.68	-	1.12	-	1.48	-
5% EVA - Ven	0.72	0.40	1.06	1.18	1.53	2.82
7% EVA - Ven	0.83	0.28	1.04	1.18	1.47	3.24

The ageing indices show the same trends as seen for the unmodified base bitumens, thereby indicating that the effect of ageing on the rheological characteristics of both the

base bitumens and the EVA PMB's are the same. The one exception is the Softening Point ageing index for the 3% EVA - Russian PMB that showed a decrease in Softening Point after ageing, indicating that the effect of ageing on the rheological performance of PMB's may well differ from that found for unmodified penetration grade bitumens.

#### 5.4.3 Dynamic Mechanical Analysis

In order to understand the changes that occur due to ageing of a PMB, Cotte and Such [107] conducted DMA on the bitumen-rich phase and the polymer-rich phase of two PMB's before and after RTFOT ageing. The first PMB consisted of a base bitumen that was modified with a plastomeric copolymer. The following findings were obtained from the study:

- The bitumen-rich phase undergoes hardening shown by an increase in  $G^*$  over the temperature domain of an isochronal plot.
- The polymer-rich phase showed no significant change in  $G^*$  except that there was a slight reduction in  $G^*$  at low temperatures and slight increase in  $G^*$  at high temperatures.
- The bitumen-rich phase showed a regular decrease in phase angle over the temperature domain of the isochronal plot.
- There were indications that the melting and recrystallising of the EVA polymer during ageing results in a change in the chemical state of the polymer.

Based on these findings, it can be concluded that the bitumen phase is aged in the same manner in a PMB as in an unmodified bitumen. Conversely, the polymer-rich phase tends to only undergo minor changes, although these slight changes probably involve some form of chemical changes of the EVA copolymer. These conclusions were taken into account when evaluating the effects of ageing on the rheological performance of the EVA modified PMB's.

The ageing indices for  $G^*$  at two temperatures of 25°C and 65°C and two loading

frequencies of 0.02 Hz and 1 Hz are presented in Table 5.8, together with the ageing indices for the three base bitumens.

**Table 5.8: Complex modulus ageing indices for EVA PMB's**

Bitumen	G* <sub>25°C, 0.02 Hz</sub>		G* <sub>25°C, 1 Hz</sub>		G* <sub>65°C, 0.02 Hz</sub>		G* <sub>65°C, 1 Hz</sub>	
	RTFOT/ Unaged	PAV/ Unaged	RTFOT/ Unaged	PAV/ Unaged	RTFOT/ Unaged	PAV/ Unaged	RTFOT/ Unaged	PAV/ Unaged
Middle East	2.26	9.29	1.78	4.94	1.75	5.90	1.69	5.29
3% EVA - ME	2.12	6.49	1.72	3.70	1.84	7.71	1.83	6.41
5% EVA - ME	2.53	8.08	2.09	5.02	1.94	7.77	1.99	6.46
7% EVA - ME	1.52	5.66	1.29	3.60	2.15	8.69	1.93	6.42
Russian	2.47	10.87	1.90	5.38	1.83	6.08	1.81	5.68
3% EVA - Rus	2.50	-	1.89	-	2.29	-	2.15	-
5% EVA - Rus	2.55	9.11	1.77	4.90	1.68	4.77	2.29	7.90
7% EVA - Rus	2.16	7.60	1.60	4.94	2.15	4.40	2.45	6.94
Venezuelan	2.34	9.01	1.70	4.48	2.00	7.64	1.84	6.26
3% EVA - Ven	2.68	-	1.87	-	2.91	-	2.39	-
5% EVA - Ven	2.32	7.85	1.72	4.61	2.05	9.95	1.76	6.79
7% EVA - Ven	1.74	7.81	1.47	5.45	2.04	8.79	1.71	7.54

The ageing indices for the EVA PMB's, in Table 5.8, show the same trend as that seen for the paving grade bitumens. This trends differs only slightly, with the ageing indices at 25°C being on average slightly lower and at 65°C slightly higher than those seen for the base bitumens. The effect of these differences is that the increase in stiffness, at high stiffness values, is less and, at low stiffness values, greater than that seen for paving grade bitumens resulting in the possibility of superior performance with regard to high temperature permanent deformation resistance and low temperature cracking resistance of the aged PMB pavement material.

#### **Russian 80 penetration grade bitumen - EVA PMB's**

The G\* and  $\delta$  master curves for the 7% EVA with 93% Russian 80 penetration PMB are illustrated in Figures 5.9 to 5.10. The G\* master curve, in Figure 5.9, shows an increase

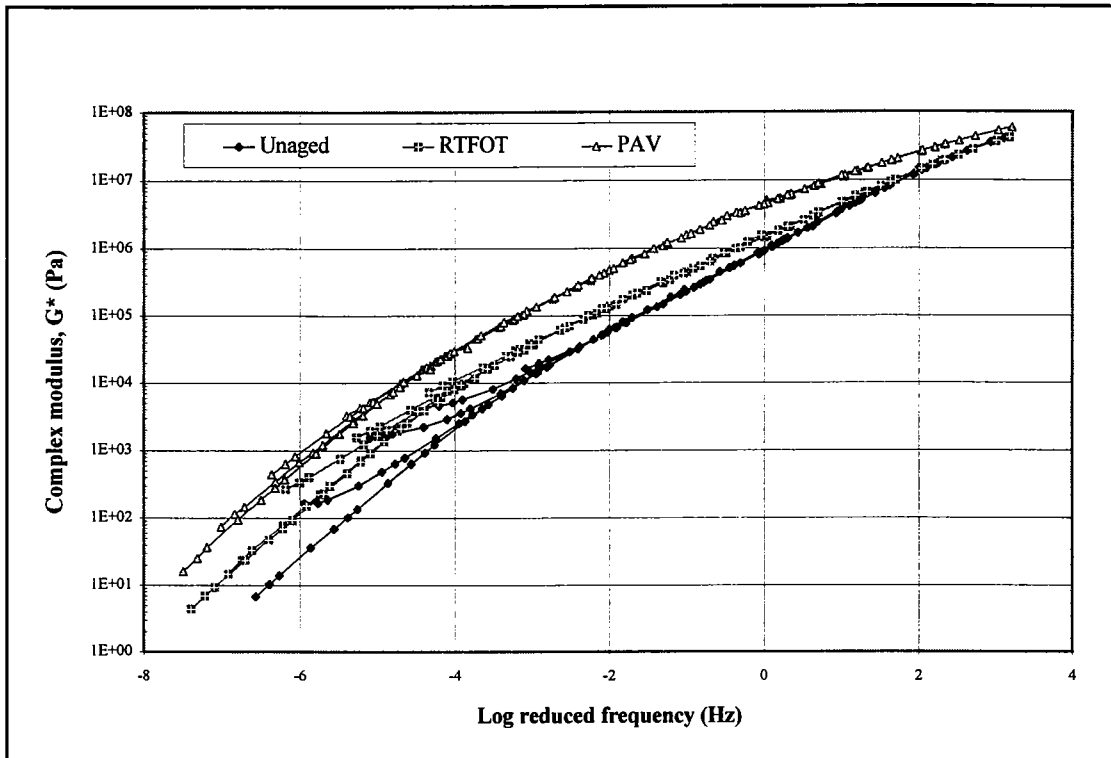


Figure 5.9: Complex modulus master curve for 7% EVA - Russian 80 pen

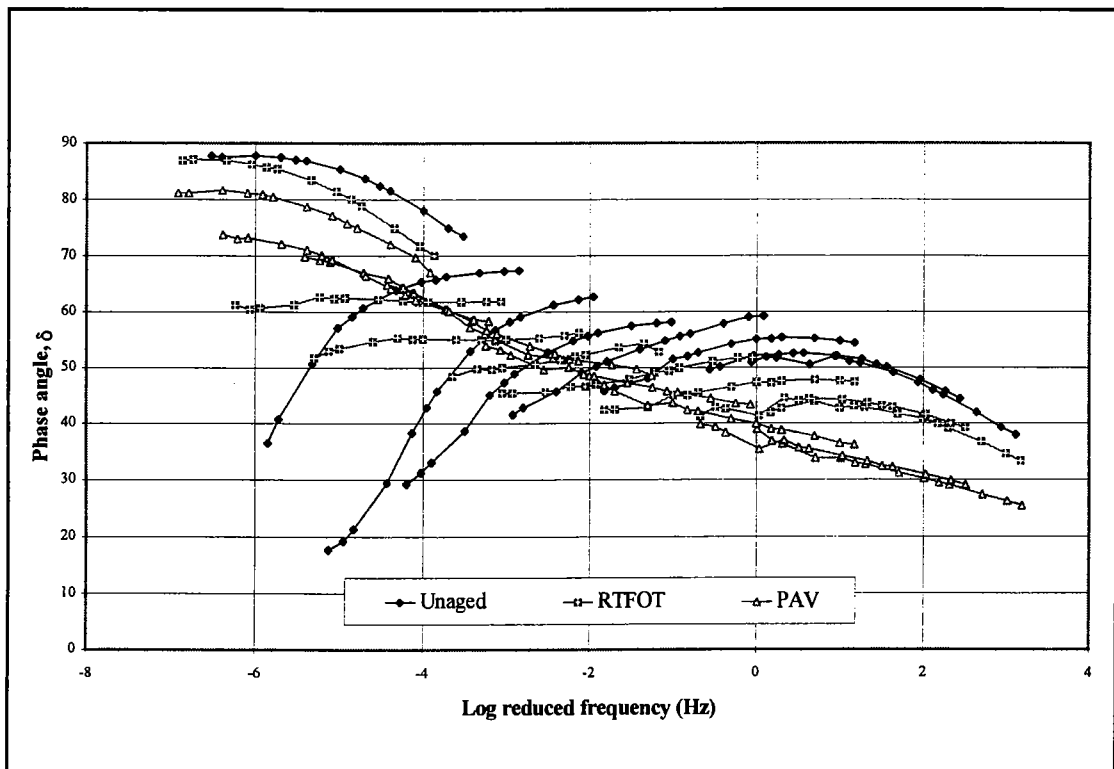


Figure 5.10: Phase angle master curve for 7% EVA - Russian 80 pen

in  $G^*$  after ageing, particularly at low loading frequencies and/or high temperatures. The master curves also show the occurrence of 'branching' at low frequencies attributed to the different EVA crystalline structures found in the PMB at different temperatures. The effect of ageing is to reduce this 'branching' with the 'branching' being almost entirely destroyed after PAV ageing.

The phase angle master curves, in Figure 5.10, have been produced by using the shift factors derived from the  $G^*$  master curves. The phase angle is generally considered to be more sensitive to the chemical structure and, therefore, the modification of bitumen than  $G^*$  and clearly shows the presence of the EVA crystalline structures as discontinuous 'waves' for the unaged PMB. The discontinuous shape of the phase angle master curve confirms that the TTSP does not hold for highly polymer modified bitumens.

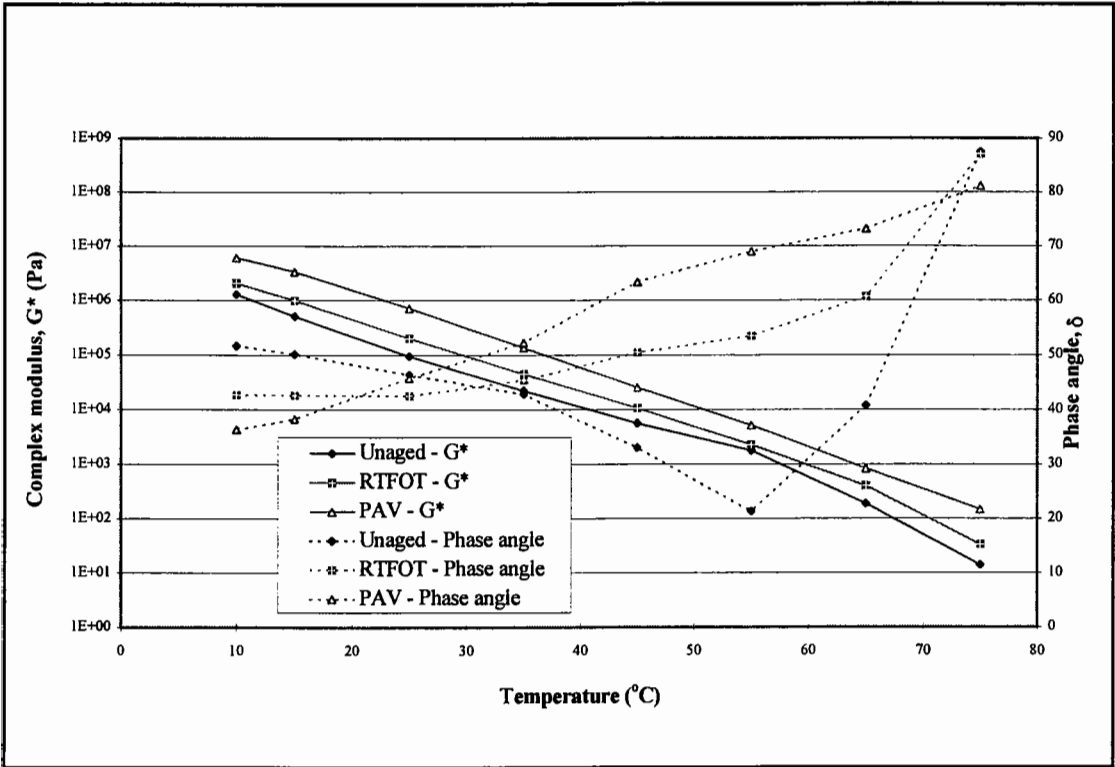


Figure 5.11: Isochronal plot at 0.02 Hz for 7% EVA - Russian 80 pen



As with the  $G^*$  master curves, the  $\delta$  master curves show that the effect of ageing is to reduce the extent of the discontinuous 'waves', with the PAV aged bitumen having a smooth, almost continuous curve similar to that found for unmodified bitumens. The phase angles at four combinations of temperature and loading frequency are presented in Table 5.9.

**Table 5.9: Phase angles for unaged, RTFOT and PAV aged Russian - EVA PMB's**

Bitumen	Property	Unaged	RTFOT	PAV
3% EVA - Russian	$\delta_{25^\circ\text{C},0.02\text{ Hz}} (^\circ)$	72	66	-
	$\delta_{25^\circ\text{C},1\text{ Hz}} (^\circ)$	67	61	-
	$\delta_{65^\circ\text{C},0.02\text{ Hz}} (^\circ)$	83	83	-
	$\delta_{65^\circ\text{C},1\text{ Hz}} (^\circ)$	83	80	-
5% EVA - Russian	$\delta_{25^\circ\text{C},0.02\text{ Hz}} (^\circ)$	59	55	53
	$\delta_{25^\circ\text{C},1\text{ Hz}} (^\circ)$	61	53	45
	$\delta_{65^\circ\text{C},0.02\text{ Hz}} (^\circ)$	51	71	81
	$\delta_{65^\circ\text{C},1\text{ Hz}} (^\circ)$	73	73	73
7% EVA - Russian	$\delta_{25^\circ\text{C},0.02\text{ Hz}} (^\circ)$	46	42	46
	$\delta_{25^\circ\text{C},1\text{ Hz}} (^\circ)$	55	47	40
	$\delta_{65^\circ\text{C},0.02\text{ Hz}} (^\circ)$	41	61	73
	$\delta_{65^\circ\text{C},1\text{ Hz}} (^\circ)$	65	62	64

Although the trend of a decrease in  $\delta$  after ageing can be seen at the lower temperature and/or higher frequency conditions, there is a trend towards a more viscous, higher  $\delta$  behaviour after ageing for the higher temperature and/or lower frequency conditions. As the data in Table 5.9 is limited, the data is also shown in the isochronal plots and Black diagram of Figures 5.11 to 5.13.

In Figure 5.11, it can be seen that there is a similar shift in  $G^*$  after ageing as shown for the unmodified bitumens, except at  $55^\circ\text{C}$ . The difference in the shape of the isochrone at  $55^\circ\text{C}$  can be attributed to the EVA polymer increasing the complex modulus more in the unaged than in the aged PMB's. Figure 5.12 illustrates that there is a slight reduction in the magnitude of the increase in  $G^*$  at the lower end of the temperature domain. These results agree with the hypothesis that the increase in  $G^*$  is attributed almost solely to the

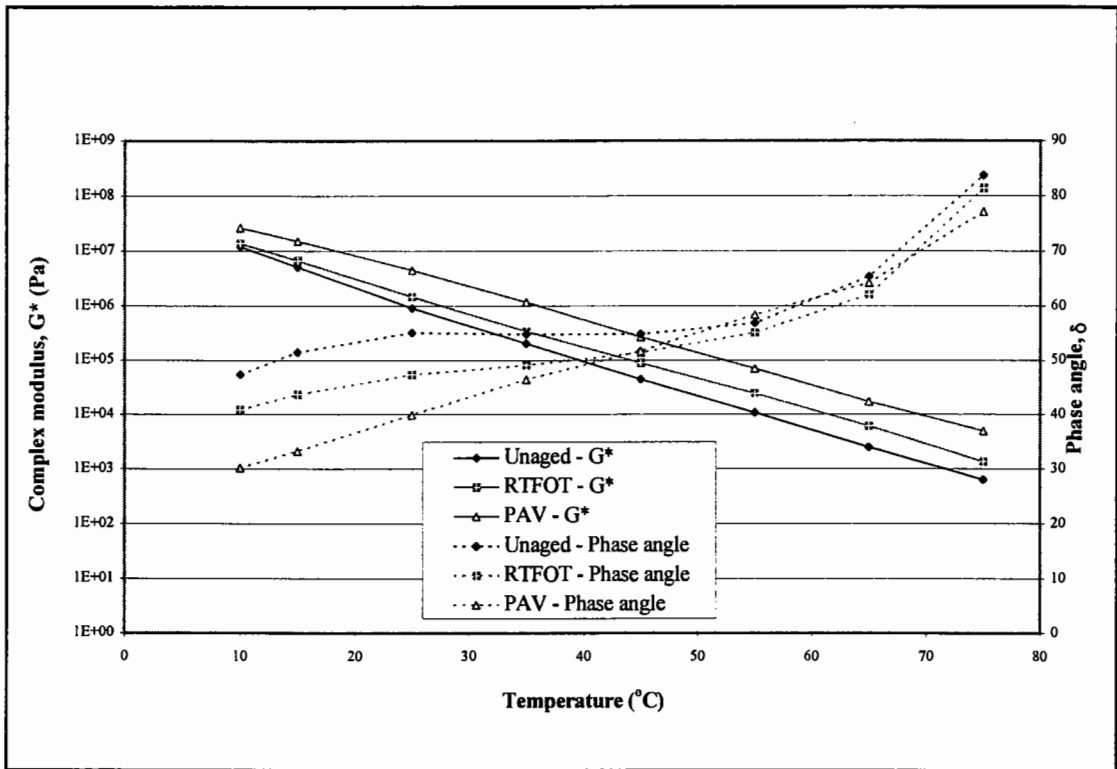


Figure 5.12: Isochronal plot at 1 Hz for 7% EVA - Russian 80 pen

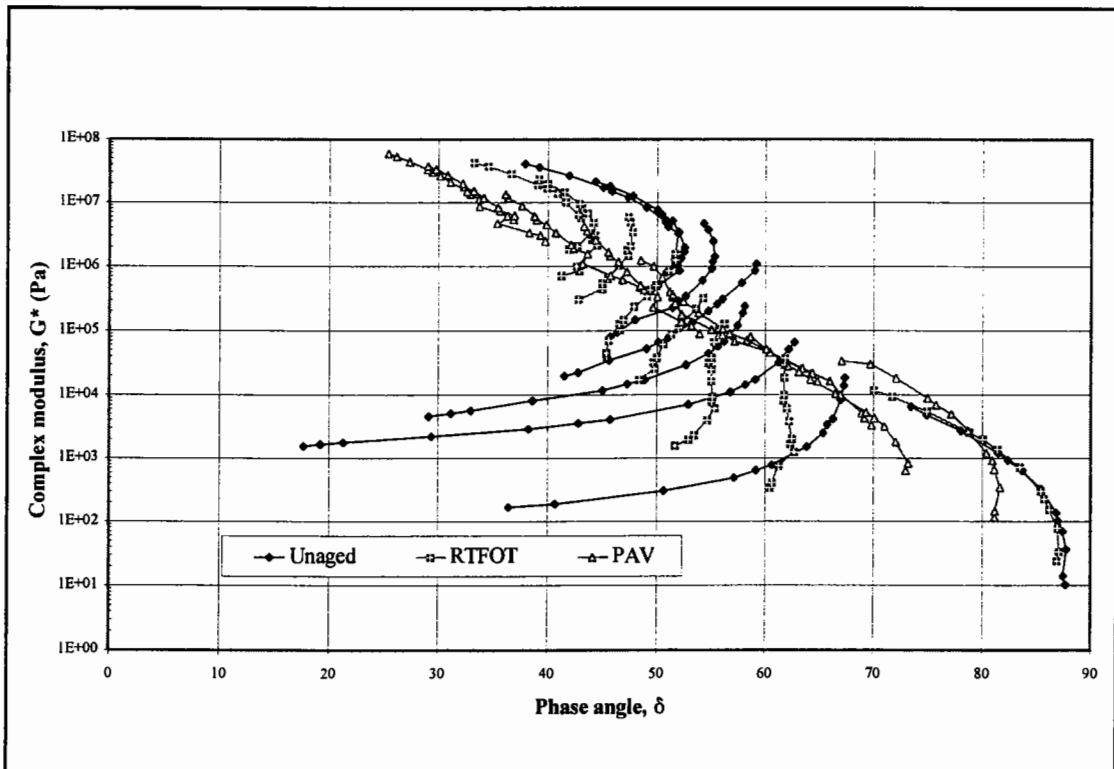


Figure 5.13: Black diagram for 7% EVA - Russian 80 pen

oxidative ageing of the base bitumen. The slight reduction in the magnitude of the increase in  $G^*$  at  $10^\circ\text{C}$  can be attributed to the combination of a slight decrease in  $G^*$  for the polymer phase together with the accepted increase in  $G^*$  for the bitumen phase after ageing.

The changes shown for  $\delta$  after ageing differ considerably from those shown for the penetration grade bitumens. The expected behaviour of a decrease in phase angle after ageing is observed at the low and high ends of the temperature domain ( $10^\circ\text{C}$  and  $75^\circ\text{C}$ ). However, within the temperature range of  $25^\circ\text{C}$  to  $65^\circ\text{C}$ , in Figure 5.11, and  $45^\circ\text{C}$  to  $65^\circ\text{C}$ , in Figure 5.12, the behaviour of the phase angle differs from that shown for penetration grade bitumens in that the magnitude of the decrease in phase angle after ageing is severely reduced and, in certain instances, there is even an increase in phase angle after ageing. This is particularly noticeable at the lower loading frequency of  $0.02\text{ Hz}$  in Figure 5.11, where there are considerable increases in phase angle after RTFOT and PAV ageing within the temperature domain of  $45^\circ\text{C}$  to  $65^\circ\text{C}$ . It is at these lower loading frequencies that the dominance of the polymer phase is extremely evident.

In addition to the differences seen in the isochronal plots for the PMB and the penetration grade bitumens, the Black diagram, in Figure 5.13, also differs considerably from that for the penetration grade bitumens (Figure 5.6). The shift of the curves towards lower phase angles is observed in Figure 5.13 for complex modulus,  $G^*$ , values greater than  $10^7\text{ Pa}$  and also within the phase angle domain between  $70^\circ$  and  $90^\circ$ . However, for the  $G^*$  values below  $10^7\text{ Pa}$  and  $\delta$  values less than  $70^\circ$ , the behaviour of the Black diagram curves differ considerably from those seen for unmodified bitumens. In this region the waves of  $G^*$  versus  $\delta$  have different aspects depending on their aged condition. This substantiates the hypothesis that the plastomeric EVA polymer undergoes some form of chemical change during the ageing process.

The conventional behaviour of a decrease in phase angle with ageing, within the temperature regions of  $10^\circ\text{C}$  to  $25^\circ\text{C}$  and greater than  $75^\circ\text{C}$  (Figure 5.12), and the shifting of the Black diagram curves at the high  $G^*$  ( $> 10^7\text{ Pa}$ ) and high  $\delta$  ( $> 70^\circ$ ) ends

(Figure 5.13), can be attributed to two factors. Firstly, the similar behaviour to a penetration grade bitumen at high temperatures ( $> 75^{\circ}\text{C}$ ) and high viscous phase angles is due to the fusion of the EVA polymer at these elevated temperatures and the PMB reverting to a more unmodified bitumen type of behaviour. Secondly, the behaviour within the lower temperature range ( $10^{\circ}\text{C}$  to  $25^{\circ}\text{C}$ ) and high complex modulus ( $> 10^7$  Pa) is due to the base bitumen being rheologically dominant within this temperature domain.

The variations in the ageing behaviour of the PMB's, as seen in the isochronal plots of  $\delta$  between  $25^{\circ}\text{C}$  to  $65^{\circ}\text{C}$  (Figure 5.11) and  $45^{\circ}\text{C}$  to  $65^{\circ}\text{C}$  (Figure 5.12) and in the Black diagram for  $G^*$  values less than  $10^7$  Pa and  $\delta$  values less than  $70^{\circ}$ , can be directly attributed to the presence of the EVA copolymer in the PMB blend.

#### **Venezuelan 70/100 penetration grade bitumen - EVA PMB's**

A similar behaviour as seen for the Russian - EVA PMB can be seen for the  $G^*$  and  $\delta$  master curves of the unaged and aged 7% EVA with 93% Venezuelan 70/100 pen PMB's in Figures 5.14 and 5.15. Although, the shape of the 'branches' in Figure 5.14 and the 'waves' in Figure 5.15 differ from those seen in Figures 5.9 and 5.10, the ageing process still results in a reduction of the 'branching' and 'waves'.

The phase angles for the Venezuelan - EVA PMB's at the four temperature and frequency combinations are presented in Table 5.10. However, the trend of an increase in  $\delta$  after ageing, as seen for the Russian - EVA PMB's, is only evident for the 7% EVA PMB at the high temperature and low frequency combination. The majority of the results show the same trend as seen for the paving grade bitumens of an increase in elastic behaviour after ageing.

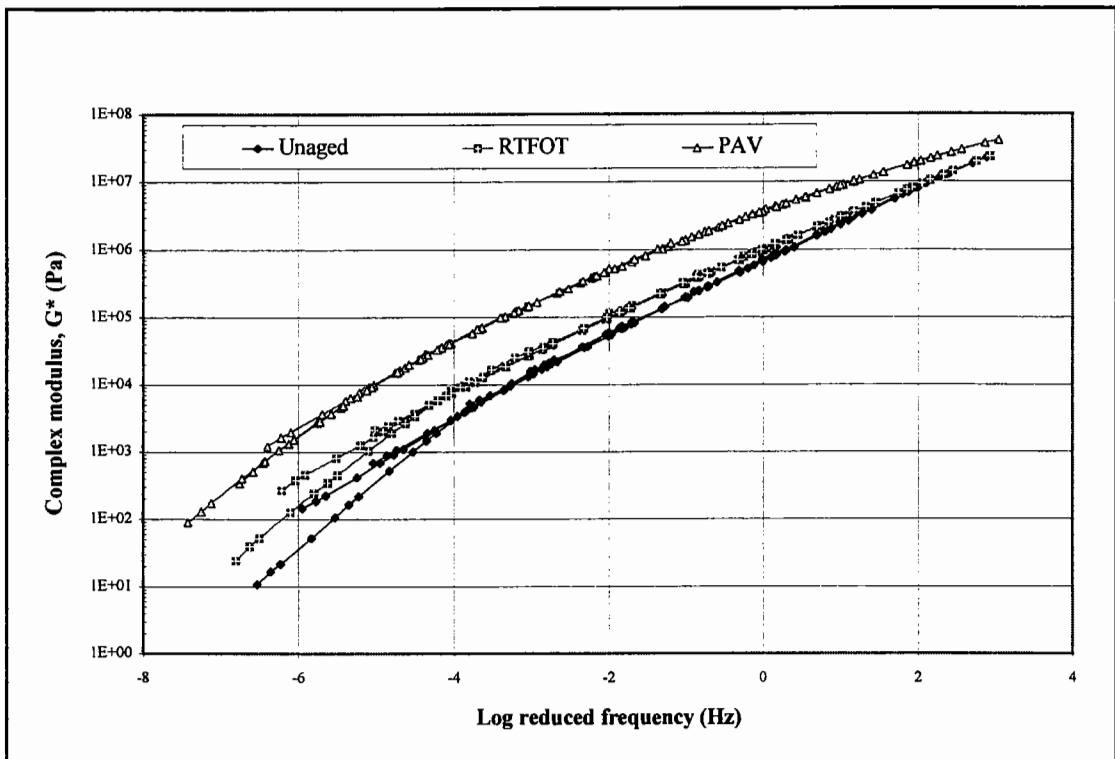


Figure 5.14: Complex modulus master curve for 7% EVA - Venezuelan 70/100 pen

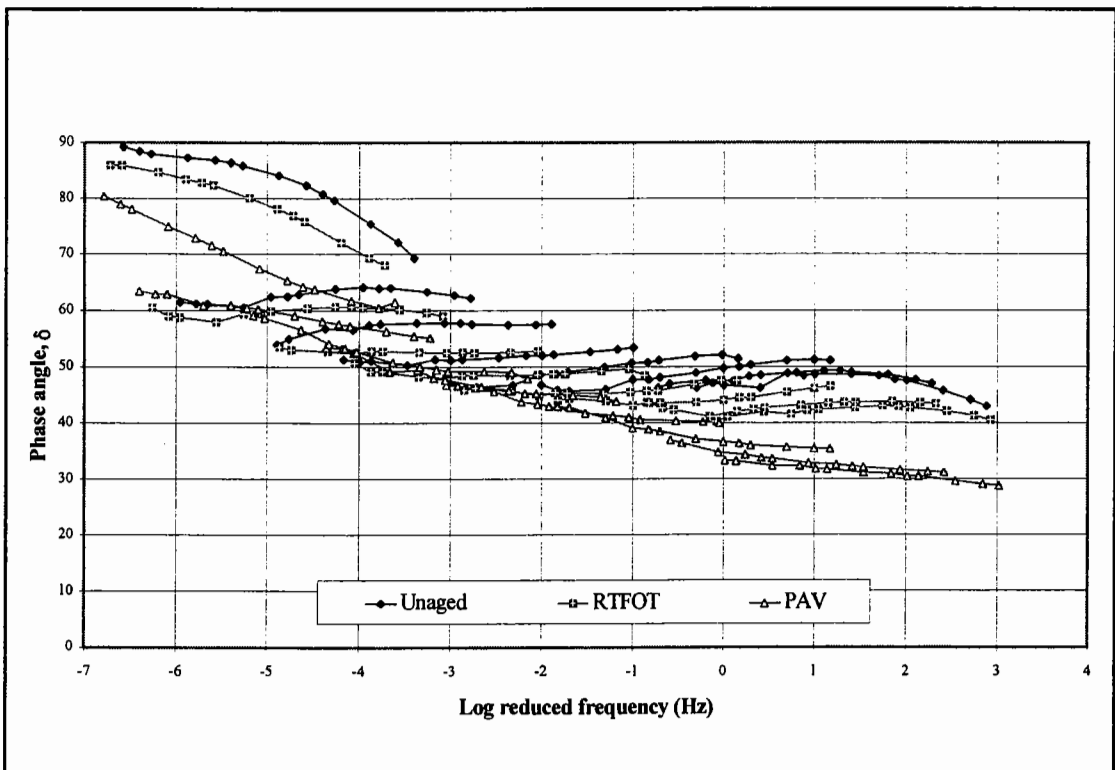


Figure 5.15: Phase angle master curve for 7% EVA - Venezuelan 70/100 pen

**Table 5.10: Phase angles for unaged, RTFOT and PAV aged Venezuelan - EVA PMB's**

Bitumen	Property	Unaged	RTFOT	PAV
3% EVA - Venezuelan	$\delta_{25^{\circ}\text{C},0.02 \text{ Hz}} (^{\circ})$	69	60	-
	$\delta_{25^{\circ}\text{C},1 \text{ Hz}} (^{\circ})$	64	56	-
	$\delta_{65^{\circ}\text{C},0.02 \text{ Hz}} (^{\circ})$	83	81	-
	$\delta_{65^{\circ}\text{C},1 \text{ Hz}} (^{\circ})$	82	77	-
5% EVA - Venezuelan	$\delta_{25^{\circ}\text{C},0.02 \text{ Hz}} (^{\circ})$	54	51	47
	$\delta_{25^{\circ}\text{C},1 \text{ Hz}} (^{\circ})$	55	49	41
	$\delta_{65^{\circ}\text{C},0.02 \text{ Hz}} (^{\circ})$	75	72	70
	$\delta_{65^{\circ}\text{C},1 \text{ Hz}} (^{\circ})$	72	68	62
7% EVA - Venezuelan	$\delta_{25^{\circ}\text{C},0.02 \text{ Hz}} (^{\circ})$	46	44	43
	$\delta_{25^{\circ}\text{C},1 \text{ Hz}} (^{\circ})$	50	44	37
	$\delta_{65^{\circ}\text{C},0.02 \text{ Hz}} (^{\circ})$	61	59	63
	$\delta_{65^{\circ}\text{C},1 \text{ Hz}} (^{\circ})$	64	61	58

The isochronal plots and Black diagram for the PMB are shown in Figures 5.16 to 5.18. The observations that can be made from the three figures are similar to those made for the Russian - EVA PMB. Once again, there is an increase in  $G^*$  over the temperature domain after ageing, with a slight reduction in the magnitude of the increase at the low temperature end in Figure 5.17. There is a decrease in  $\delta$  over the temperature domain after ageing for tests at 1 Hz (Figure 5.17), but at 0.02 Hz (Figure 5.16) the effect of ageing on  $\delta$  is inconsistent within the temperature range of 25°C to 65°C.

The Black diagram, in Figure 5.18, also has the same pattern as the Black diagram in Figure 5.13. There is a shift of the curves towards lower phase angles after RTFOT and PAV ageing for  $G^*$  values greater than  $10^7$  Pa and also within the phase angle domain between 70° and 90°. For the  $G^*$  values below  $10^7$  Pa and  $\delta$  values less than 70°, the waves of  $G^*$  versus  $\delta$  have different aspects depending on their aged condition.

Although the behaviour after ageing for the Venezuelan - EVA PMB and the Russian - EVA PMB are similar, the severity of the variations in the ageing behaviour of the Venezuelan - EVA PMB is reduced. Although the isochronal plot and Black diagram in

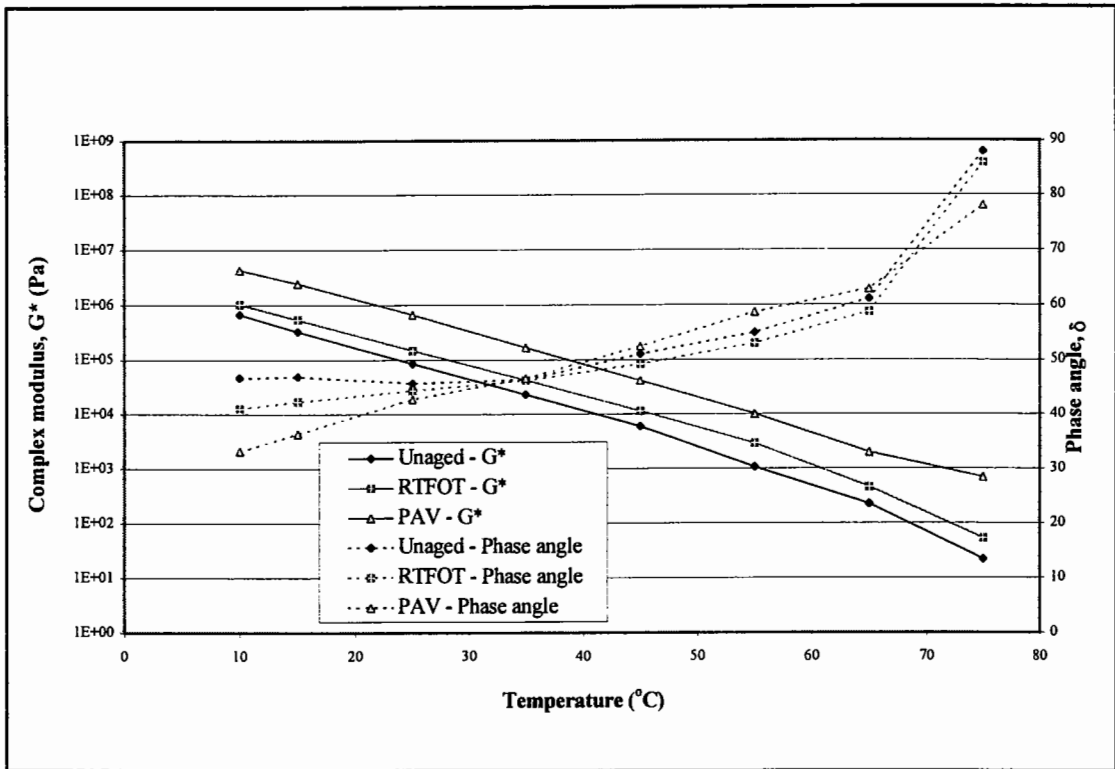


Figure 5.16: Isochronal plot at 0.02 Hz for 7% EVA - Venezuelan 70/100 pen

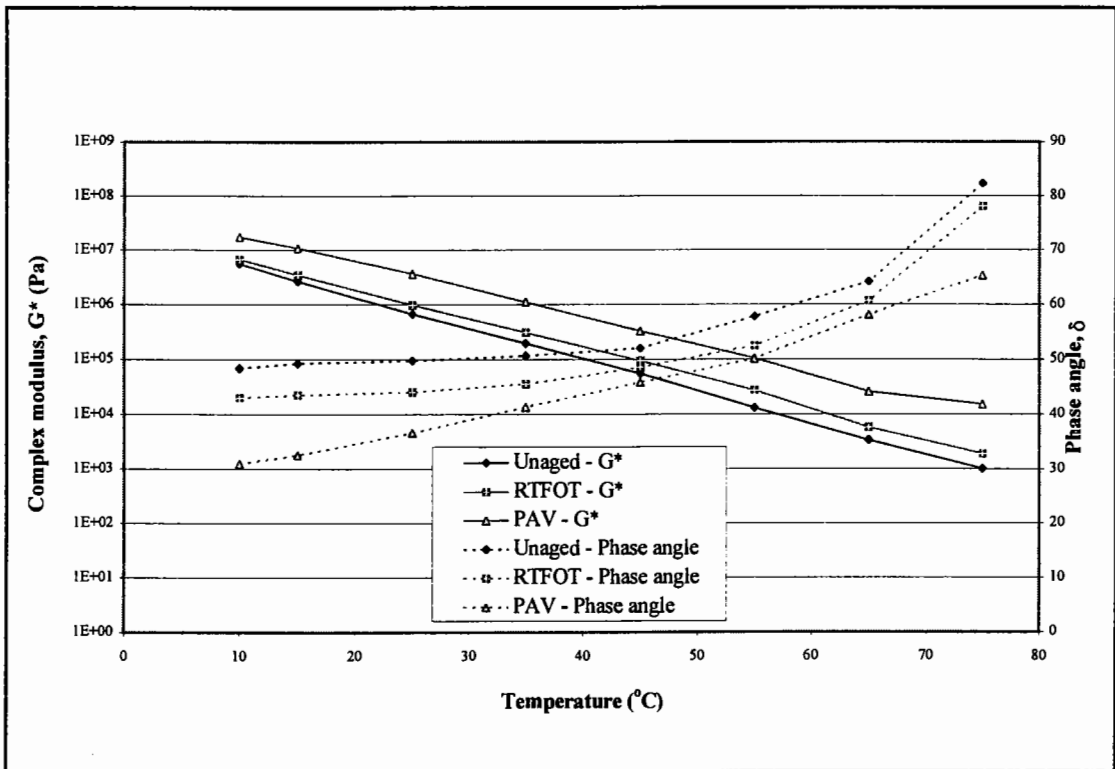
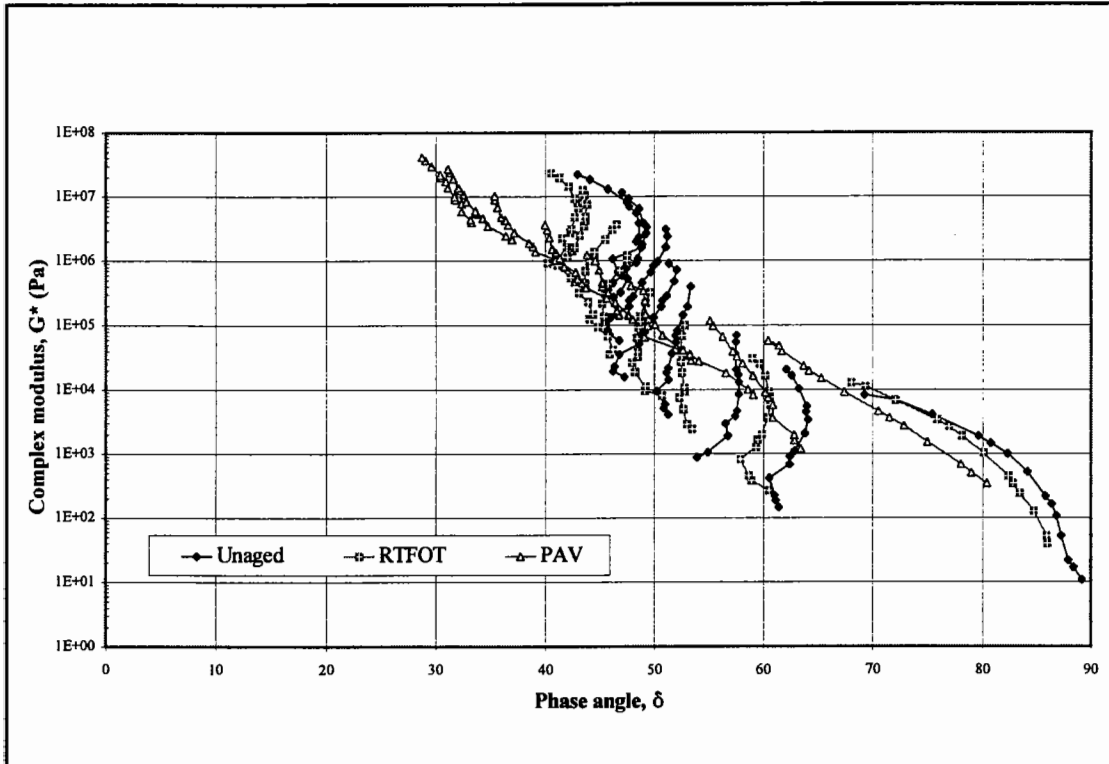


Figure 5.17: Isochronal plot at 1 Hz for 7% EVA - Venezuelan 70/100 pen

Figures 5.16 to 5.18 still differ from those seen for the penetration grade bitumen in Figures 5.4 to 5.6, the difference is not as marked as that seen for the Russian - EVA PMB in Figures 5.11 to 5.13.



**Figure 5.18: Black diagram for 7% EVA - Venezuelan 70/100 pen**

### **Middle East 80/100 penetration grade bitumen - EVA PMB's**

The  $G^*$  and  $\delta$  master curves for the unaged and aged 7% EVA - Middle East PMB's, in Figures 5.19 and 5.20, resemble more those seen for the base bitumens (Figures 5.2 and 5.3) than those seen for the other two EVA PMB groups (Figures 5.9, 5.10, 5.14 and 5.15). The only indications of EVA modification are the slight 'branching' in Figure 5.19 and the discontinuity of the phase angle curve where the semi-crystalline EVA polymer has melted at 75°C in Figure 5.20. However, the effect of ageing on the rheological characteristics of the EVA PMB are similar to that seen for the previous two EVA PMB groups.



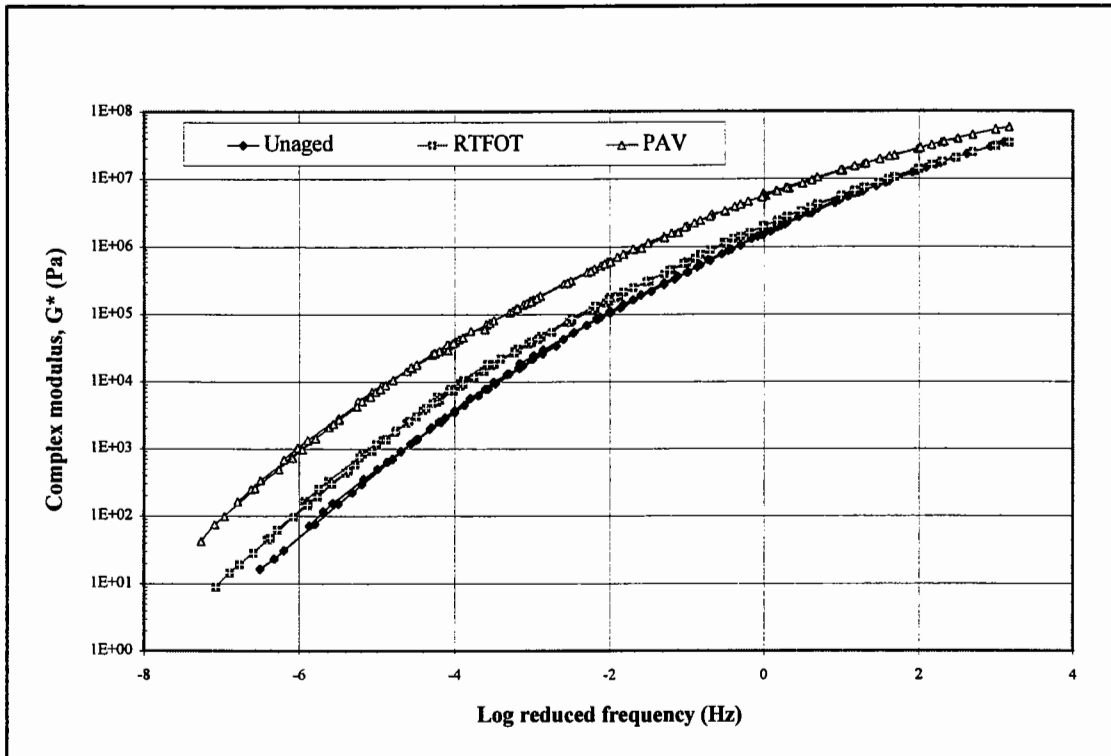


Figure 5.19: Complex modulus master curve for 7% EVA - Middle East 80/100 pen

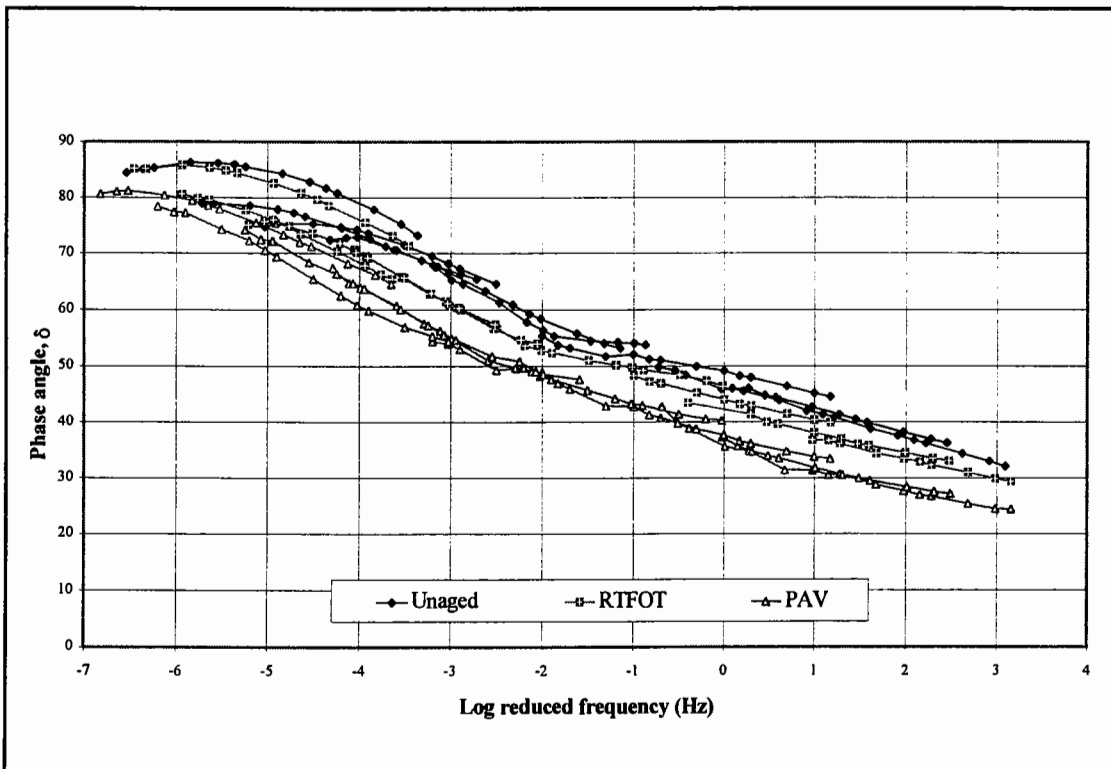


Figure 5.20: Phase angle master curve for 7% EVA - Middle East 80/100 pen

The phase angles for the unaged and aged Middle East - EVA PMB are presented in Table 5.11. The effect of ageing is shown as a decrease in  $\delta$  with an increase in elastic behaviour, similar to that seen for the unmodified bitumens.

**Table 5.11: Phase angles for unaged, RTFOT and PAV aged Middle East - EVA PMB's**

Bitumen	Property	Unaged	RTFOT	PAV
3% EVA - Middle East	$\delta_{25^{\circ}\text{C},0.02\text{ Hz}} (^{\circ})$	67	63	55
	$\delta_{25^{\circ}\text{C},1\text{ Hz}} (^{\circ})$	60	55	46
	$\delta_{65^{\circ}\text{C},0.02\text{ Hz}} (^{\circ})$	87	89	87
	$\delta_{65^{\circ}\text{C},1\text{ Hz}} (^{\circ})$	81	80	74
5% EVA - Middle East	$\delta_{25^{\circ}\text{C},0.02\text{ Hz}} (^{\circ})$	58	55	51
	$\delta_{25^{\circ}\text{C},1\text{ Hz}} (^{\circ})$	54	50	42
	$\delta_{65^{\circ}\text{C},0.02\text{ Hz}} (^{\circ})$	83	86	84
	$\delta_{65^{\circ}\text{C},1\text{ Hz}} (^{\circ})$	77	75	70
7% EVA - Middle East	$\delta_{25^{\circ}\text{C},0.02\text{ Hz}} (^{\circ})$	53	51	46
	$\delta_{25^{\circ}\text{C},1\text{ Hz}} (^{\circ})$	49	44	38
	$\delta_{65^{\circ}\text{C},0.02\text{ Hz}} (^{\circ})$	79	80	77
	$\delta_{65^{\circ}\text{C},1\text{ Hz}} (^{\circ})$	73	68	62

The isochronal plots and Black diagram for the PMB are shown in Figures 5.21 to 5.23. Once again, there is an increase in  $G^*$  over the temperature domain after ageing, with a slight reduction in the magnitude of the increase at the low temperature end in Figure 5.22. However, the decrease in  $\delta$  over the temperature domain after ageing resembles the pattern shown for the penetration grade bitumens rather than that shown for the other EVA modified bitumens. The only variation from this pattern is seen within the temperature range 55°C to 65°C in Figure 5.21 where there is a slight increase in  $\delta$  after RTFOT ageing.

The Black diagram, in Figure 5.23, also has a closer resemblance to the Black diagram for the penetration grade bitumen in Figure 5.6 than to the Black diagrams for the other two EVA modified bitumens. However, the three areas identified in Figures 5.13 and 5.18 can still be seen in Figure 5.23. Firstly, the area where the EVA polymer has fused

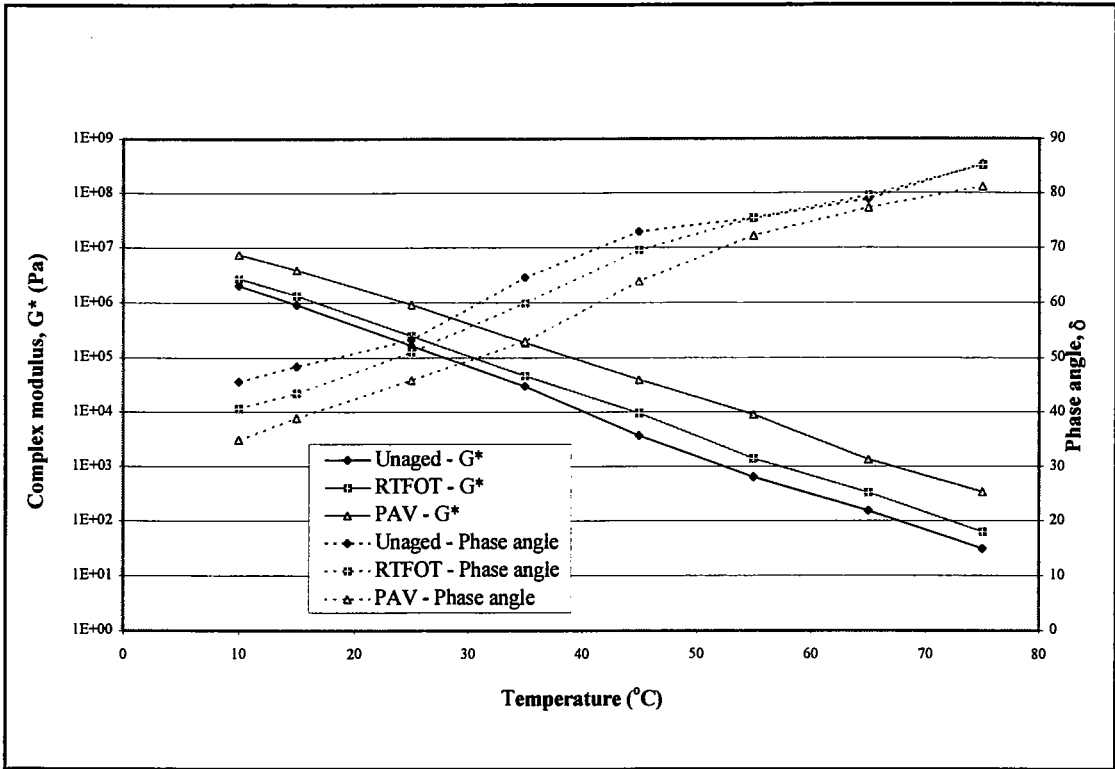


Figure 5.21: Isochronal plot at 0.02 Hz for 7% EVA - Middle East 80/100 pen

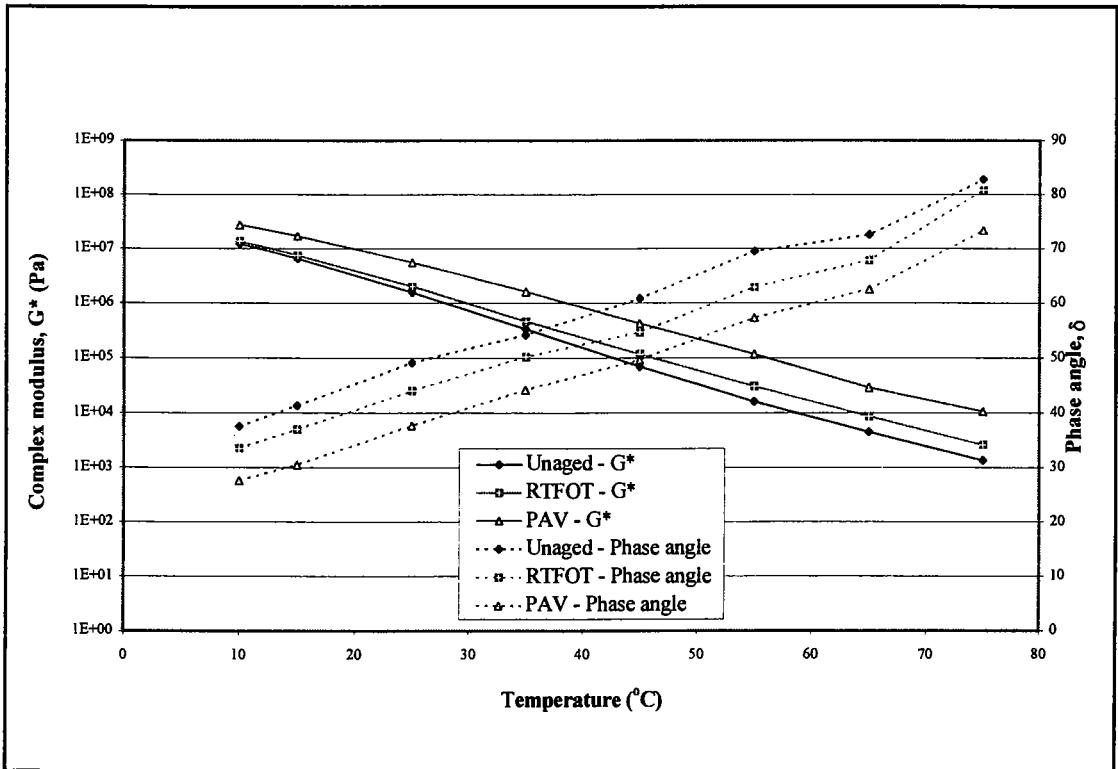


Figure 5.22: Isochronal plot at 1 Hz for 7% EVA - Middle East 80/100 pen

at high temperatures and high  $\delta$  values can be seen for  $\delta$  values greater than  $80^\circ$ . Secondly, the area where the base bitumen is rheologically predominant can be seen at high complex modulus values ( $> 10^7$  Pa), and finally there is an area in the centre of the Black diagram where the waves of  $G^*$  versus  $\delta$  have different aspects depending on their aged condition.

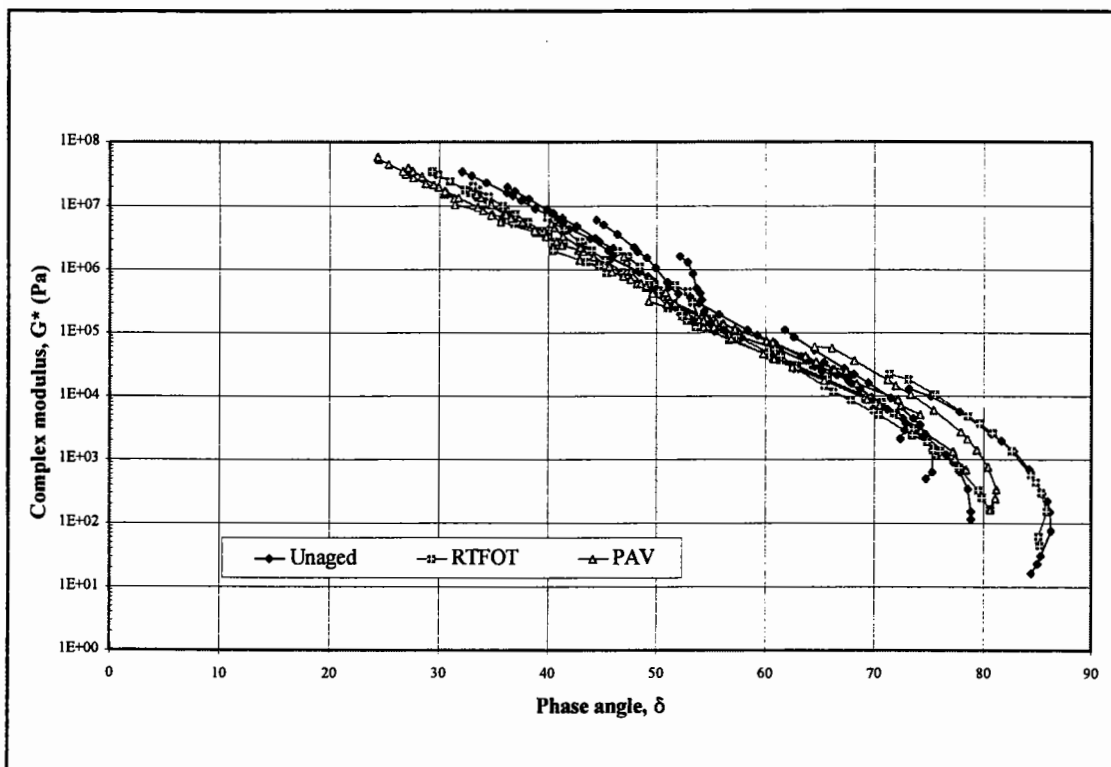


Figure 5.23: Black diagram for 7% EVA - Middle East 80/100 pen

#### 5.4.4 Discussion

It is assumed that the polymer behaviour or reaction to ageing will be the same for all three EVA modified PMB groups, but that the compatibility of the base bitumen and the polymer will result in variations in this rheological behaviour. It can be concluded from the observations that the effect of ageing on the rheological performance of the Middle

East - EVA PMB is primarily dominated by the rheological behaviour of the base bitumen over almost the entire temperature domain. At the other extreme, it can be concluded that the effect of ageing on the rheological performance of the Russian - EVA PMB is primarily dominated by the rheological behaviour of the polymer over a temperature range of approximately 35°C to 65°C.

The DSC results, in Table 5.6 and Figure 5.8, confirm the hypothesis that there is a form of chemical change of the EVA copolymer. This chemical change leads to a degradation of the polymer and, therefore, a transition of the rheological behaviour for the PMB towards that of an unmodified bitumen after RTFOT and PAV ageing. The extent of these rheological changes are a function of the type and chemical composition of the semi-crystalline copolymer, the source and chemical composition of the base bitumen and the polymer content of the PMB blend.

The use of the conventional, empirical tests (Penetration, Softening and viscosity) and the limited DMA data, such as the  $G^*$  and  $\delta$  values at specific temperatures and loading frequencies in Tables 5.8 to 5.11, do not provide a complete and accurate characterisation of the rheological changes associated with ageing. Highly polymer modified PMB's are known not to satisfy the TTSP or time-temperature equivalency and, therefore, require a more extensive set of measurements for their full characterisation [21]. DMA data representation in the form of master curves, isochronal plots and particularly Black diagrams are, therefore, required to explain the rheological changes associated with RTFOT and PAV ageing.

## 5.5 Elastomeric Polymer Modified Bitumen

### 5.5.1 Chemical Characterisation of the Effect of Ageing

#### Fourier Transform Infrared Spectroscopy

The increase in the amounts of the oxygenated products, carbonyl and sulphoxide, after ageing for the SBS PMB's and their base bitumens are presented in Table 5.12 and in Figure 5.24.

**Table 5.12: Increase in oxidative products during ageing for SBS PMB's**

Bitumen	Condition	Carbonyl	Sulphoxide	Carbonyl + Sulphoxide
Russian 80	RTFOT - Unaged	0.065	0.071	0.136
3% SBS - Russian	RTFOT - Unaged	0.066	0.052	0.118
5% SBS - Russian		0.051	0.054	0.105
7% SBS - Russian		0.048	0.023	0.071
Russian 80	PAV - Unaged	0.302	0.327	0.629
3% SBS - Russian	PAV - Unaged	0.268	0.220	0.488
5% SBS - Russian		0.262	0.276	0.538
7% SBS - Russian		0.277	0.233	0.510
Venezuelan 70/100	RTFOT - Unaged	0.078	0.031	0.109
3% SBS - Venezuelan	RTFOT - Unaged	0.109	0.039	0.148
5% SBS - Venezuelan		0.073	0.036	0.109
7% SBS - Venezuelan		0.080	0.032	0.112
Venezuelan 70/100	PAV - Unaged	0.327	0.244	0.571
3% SBS - Venezuelan	PAV - Unaged	0.236	0.205	0.441
5% SBS - Venezuelan		0.241	0.184	0.425
7% SBS - Venezuelan		0.237	0.185	0.422

The FTIR data in Table 5.12 and in Figure 5.24 show that the SBS PMB's have smaller changes in their carbonyl and sulphoxide peaks and, therefore, fewer ageing products compared to the two base bitumens. This implies that the PMB's are more resistant to

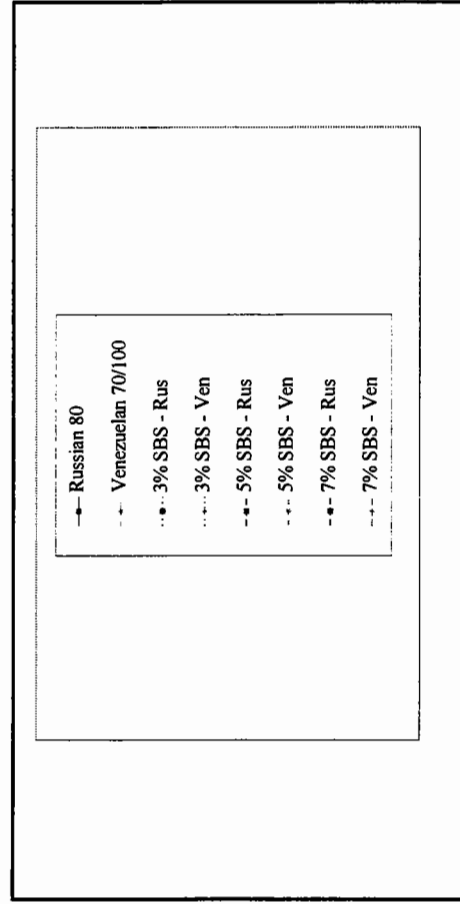
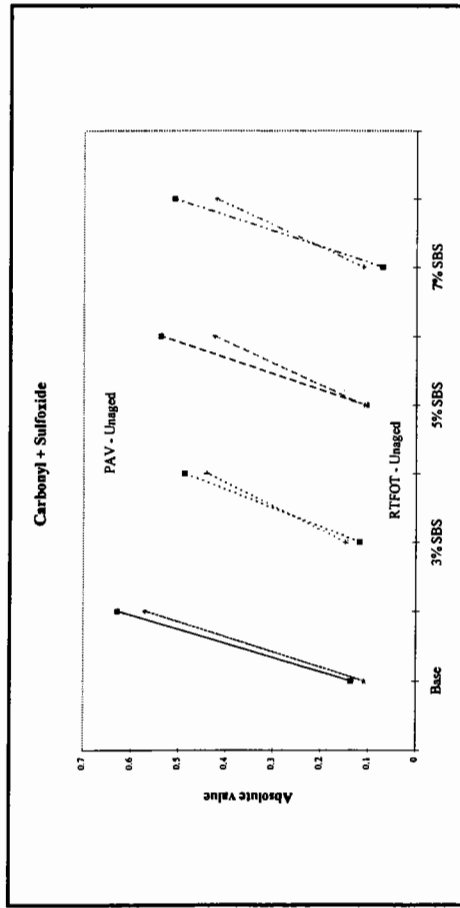
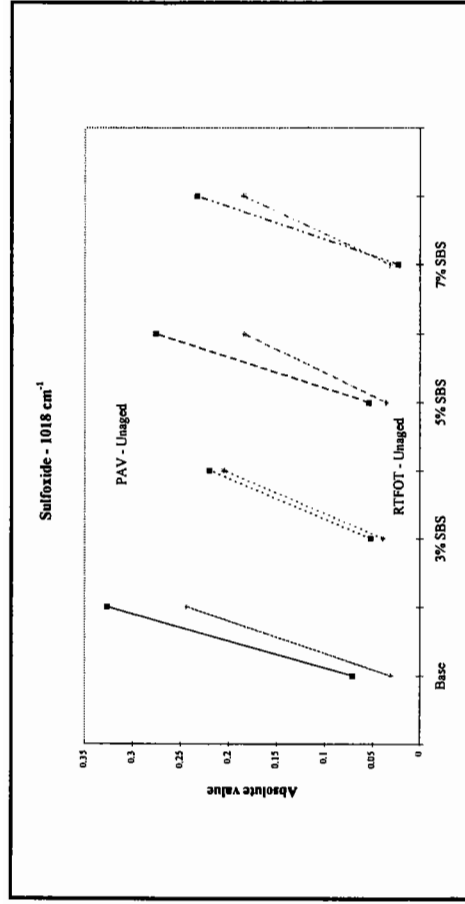
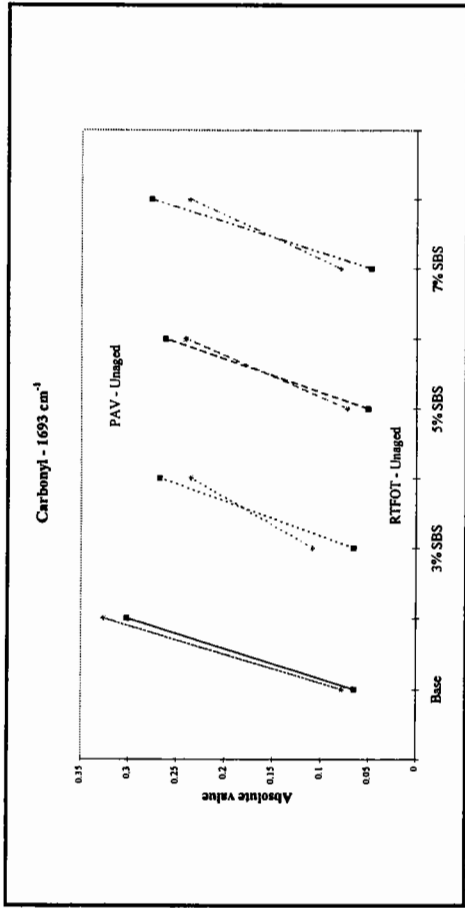


**Figure 5.24: FTIR analysis of aged SBS PMB's**

oxidative ageing, as determined by their oxygen uptake measured by the growth in the carbonyl and sulphoxide fractions, than unmodified paving grade bitumens.

### High Pressure Gel Permeation Chromatography

HP-GPC was performed on the six SBS PMB's in their unaged, RTFOT and PAV aged conditions in order to clarify the ageing mechanism associated with SBS copolymer modified bitumens. An example of the HP-GPC chromatograms obtained for the SBS PMB's is shown in Figure 5.25.

The HP-GPC analysis of the 7% SBS with 93% Venezuelan 70/100 pen PMB shows changes in the molecular size of both the polymer and the bitumen phase. The SBS copolymer has degraded to a lower molecular size after RTFOT, with a further degradation after PAV ageing. The opposite is true for the bitumen phase, which shows an increase in the larger molecular size fractions (asphaltenes) after RTFOT and PAV ageing.

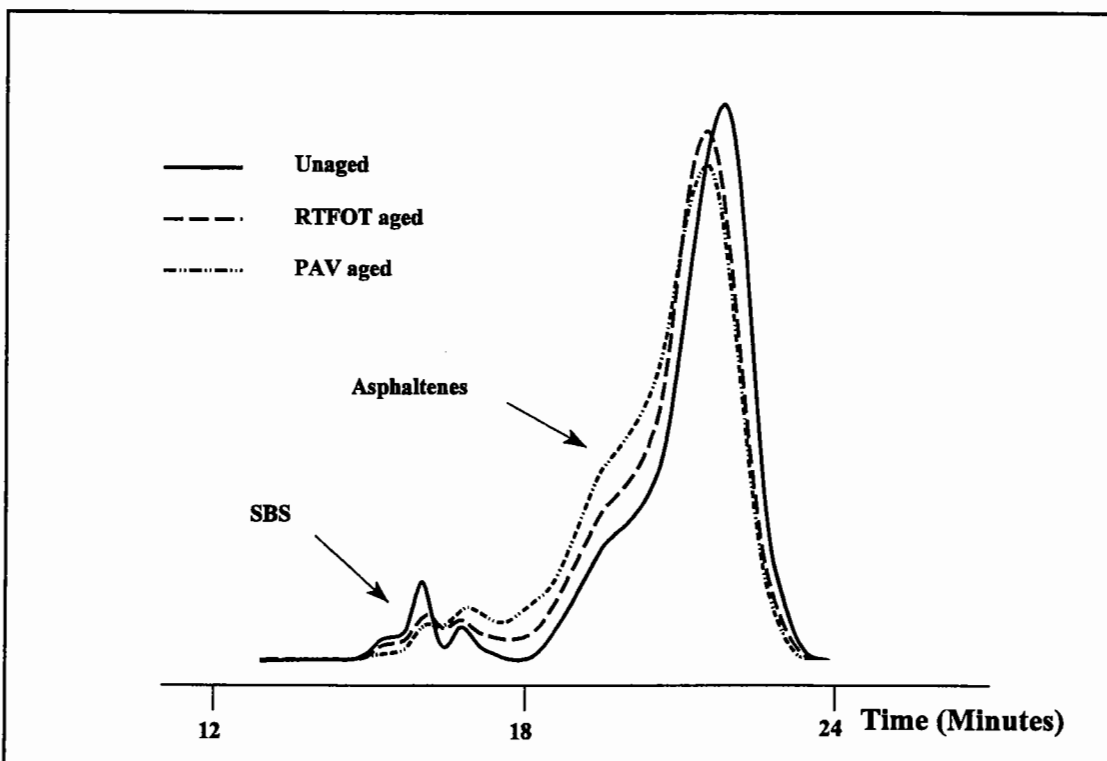


Figure 5.25: HP-GPC plots for 7% SBS with 93% Venezuelan 70/100 pen bitumen



### 5.5.2 Conventional Tests

The ageing indices for the Penetration, Softening Point and viscosity tests for the six SBS PMB's and their base bitumens are presented in Table 5.13. Those ageing indices that differ from the pattern shown for penetration grade bitumens have been highlighted in bold typeface.

**Table 5.13: Changes in conventional test data due to ageing for SBS PMB's**

Bitumen	Penetration Ageing Index		Softening point Ageing Index		Viscosity @ 135°C Ageing Index	
	RTFOT/ Unaged	PAV/ Unaged	RTFOT/ Unaged	PAV/ Unaged	RTFOT/ Unaged	PAV/ Unaged
Russian 80	0.70	0.33	1.08	1.22	1.27	2.05
Rus - 3% SBS	0.70	0.35	1.07	1.22	1.27	2.08
Rus - 5% SBS	0.74	0.42	<b>0.82</b>	<b>0.88</b>	1.26	1.85
Rus - 7% SBS	0.80	0.50	<b>0.95</b>	<b>0.85</b>	1.18	1.79
Venezuelan 70/100	0.75	0.40	1.09	1.26	1.37	2.29
Ven - 3% SBS	0.70	0.37	1.11	1.25	1.22	1.81
Ven - 5% SBS	0.76	0.44	<b>0.87</b>	<b>0.94</b>	1.22	1.90
Ven - 7% SBS	0.78	0.51	<b>0.88</b>	<b>0.84</b>	1.21	1.70

The ageing indices for the Penetration and viscosity tests show the same trends as seen for the unmodified base bitumens indicating that the effect of ageing on the rheological performance of both the base bitumens and the SBS PMB's are the same. However, the Softening Point ageing indices indicate a decrease in Softening Point after ageing, so the effect of ageing on the rheological performance of SBS PMB's may well differ from that found for unmodified penetration grade bitumens.

### 5.5.3 Dynamic Mechanical Analysis

The second PMB that was studied by Cotte and Such [107] consisted of a base bitumen that was modified with an elastomeric copolymer. The following findings were obtained

for this PMB:

- The bitumen-rich phase undergoes the same shifting of curves, as seen for the plastomeric PMB, over the temperature domain of the isochronal plot.
- There were indications that there was a transformation of the polymer substructure with the polymer part of the PMB being broken by the effect of heat and oxygen and rearranged in smaller fragments. This has resulted in the PMB showing a more fluid behaviour after ageing.

Based on these findings it can be concluded, as for the EVA - PMB's, that the bitumen phase is aged in the same manner in a PMB as in an unmodified bitumen. Alternatively, the polymer-rich phase undergoes a reduction in molecular weight indicated by more viscous behaviour at high temperatures where the polymer is dominant. These conclusions were taken into account when evaluating the effects of ageing on the rheological performance of the SBS modified PMB's.

The ageing indices for  $G^*$  for the SBS PMB's and their two base bitumens are presented in Table 5.14.

**Table 5.14: Complex modulus ageing indices for SBS PMB's**

Bitumen	$G^*_{25^\circ\text{C}, 0.02 \text{ Hz}}$		$G^*_{25^\circ\text{C}, 1 \text{ Hz}}$		$G^*_{65^\circ\text{C}, 0.02 \text{ Hz}}$		$G^*_{65^\circ\text{C}, 1 \text{ Hz}}$	
	RTFOT/ Unaged	PAV/ Unaged	RTFOT/ Unaged	PAV/ Unaged	RTFOT/ Unaged	PAV/ Unaged	RTFOT/ Unaged	PAV/ Unaged
Russian	2.47	10.87	1.90	5.38	1.83	6.08	1.81	5.68
3% SBS - Rus	2.21	8.02	2.02	4.58	1.40	3.98	1.53	4.07
5% SBS - Rus	2.16	6.17	1.84	3.78	0.96	2.90	1.71	4.45
7% SBS - Rus	1.69	9.30	1.56	5.70	0.66	2.06	1.49	4.30
Venezuelan	2.34	9.01	1.70	4.48	2.00	7.64	1.84	6.26
3% SBS - Ven	2.26	7.06	1.77	4.24	1.82	7.68	1.60	4.64
5% SBS - Ven	1.89	4.95	1.52	3.36	2.30	8.84	1.92	4.96
7% SBS - Ven	1.83	4.92	1.54	3.47	1.94	6.37	1.57	3.51

The ageing indices for the SBS PMB's are similar to those seen for the paving grade bitumens, although there is a tendency for them to be slightly lower, particularly after PAV ageing, indicating a superior resistance to age-hardening.

### **Russian 80 penetration grade bitumen - SBS PMB's**

The  $G^*$  and  $\delta$  master curves for the 7% SBS - Russian PMB are shown in Figures 5.26 and 5.27. The complex modulus master curves show an increase in  $G^*$  after ageing but this increase is not as marked at long loading frequencies and/or high temperatures after RTFOT ageing as seen for the paving grade bitumens and EVA PMB's. In addition to the smaller increases in  $G^*$  after RTFOT, there is even a decrease in  $G^*$  at reduced frequencies below  $10^{-5}$  Hz.

The decreased slope of the unaged SBS PMB master curve at low frequencies, which is attributed to the elastomeric SBS copolymer network, is not evident in the RTFOT and PAV aged master curves. This would indicate that the effect of ageing is to reduce the dominance of the SBS copolymer with regard to the rheological behaviour of the PMB.

The phase angle master curves have been produced by using the shift factors derived from the  $G^*$  master curves. Figure 5.27 illustrates that the effect of ageing differs in the two regions where the polymer-rich is dominant at low loading frequencies, and where the bitumen phase is dominant at high loading frequencies. In the bitumen dominant region, the rheological changes associated with ageing are similar to that seen for paving grade bitumens, with a decrease in  $\delta$  after ageing. In the polymer dominant region, there is an increase in  $\delta$  and, therefore, a more viscous fluid-like behaviour after ageing.

The Cole-Cole diagram for the unaged and aged Russian - SBS PMB, in Figure 5.28, also illustrates that the effect of ageing differs in two region dominated by the bitumen phase and the polymer phase. The rheological behaviour at  $G''$  values greater than  $10^4$  Pa is similar to that seen for the unmodified bitumens. In this region the effect of ageing is simply to shift the Cole-Cole plot towards the upper right-hand corner of the diagram and, therefore, towards a more elastic, stiffer rheological behaviour. The rheological

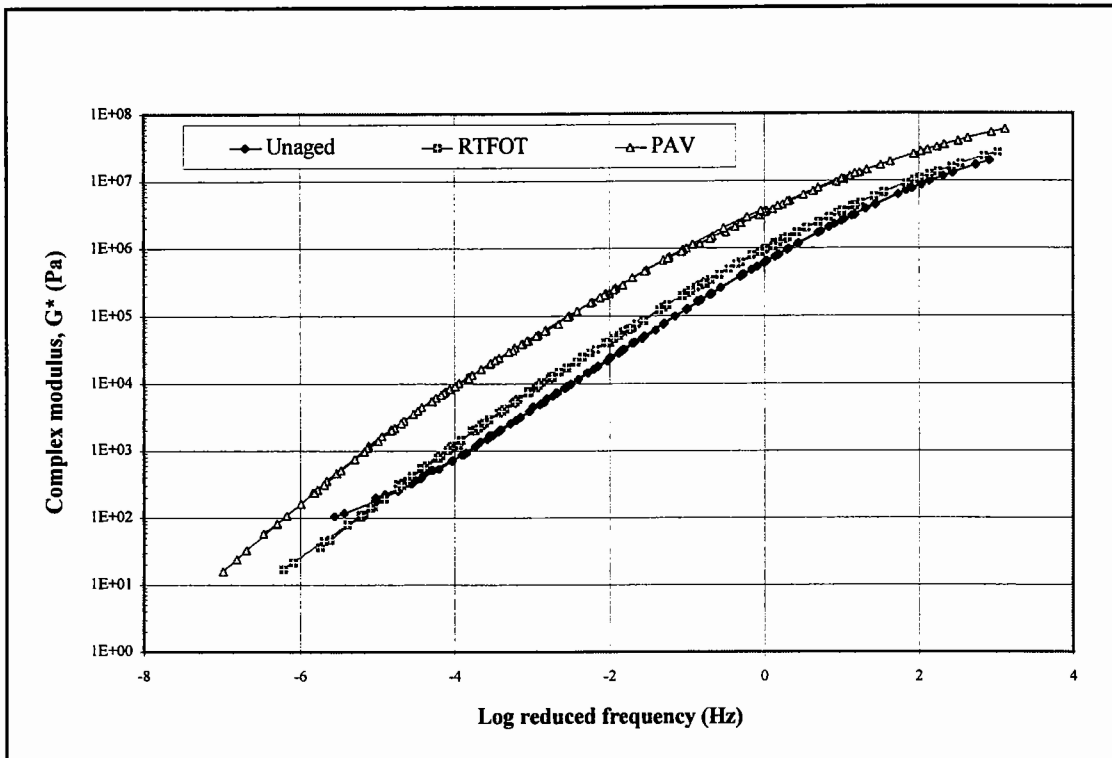


Figure 5.26: Complex modulus master curve for 7% SBS - Russian 80 pen

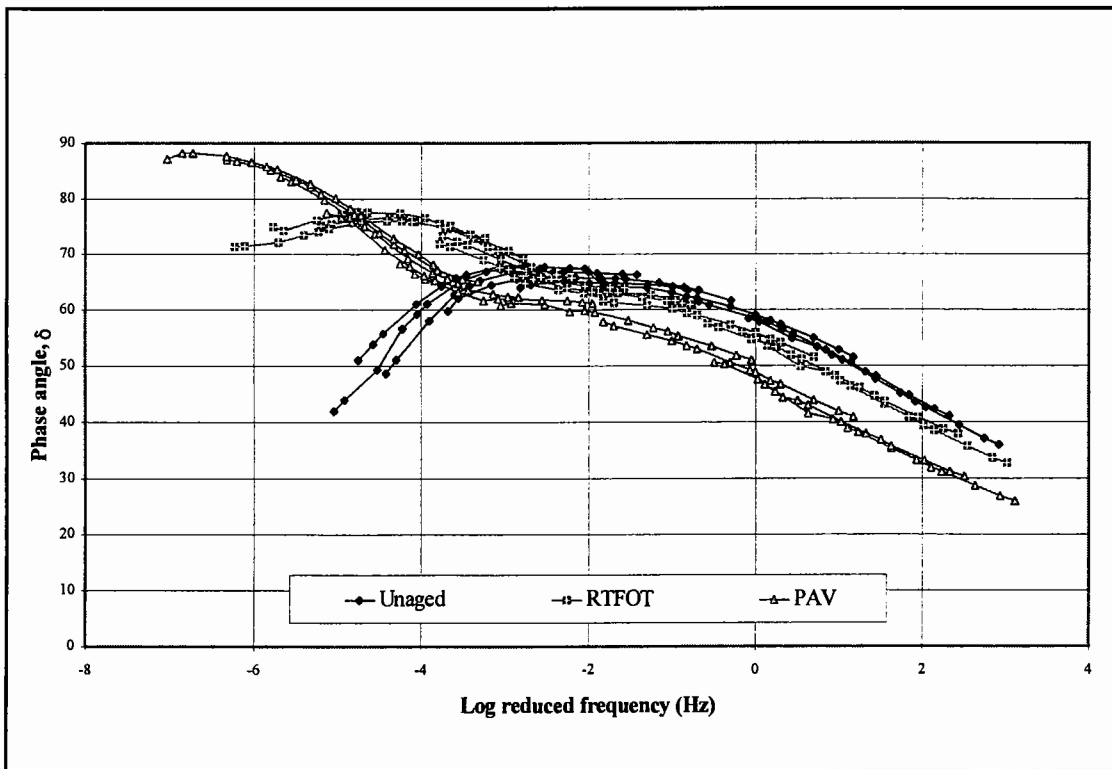


Figure 5.27: Phase angle master curve for 7% SBS - Russian 80 pen

behaviour at  $G''$  values below  $10^4$  Pa shows a shifting of the plot towards a more viscous fluid-like behaviour after ageing. The plateau-like behaviour, attributed to the polymer network, is also broken down after PAV and RTFOT ageing.

The phase angles at four temperature and loading frequency combinations for the SBS PMB's are presented in Table 5.15.

**Table 5.15: Phase angles for unaged, RTFOT and PAV aged Russian - SBS PMB's**

Bitumen	Property	Unaged	RTFOT	PAV
3% SBS - Russian	$\delta_{25^\circ\text{C},0.02 \text{ Hz}} (^\circ)$	71	69	61
	$\delta_{25^\circ\text{C},1 \text{ Hz}} (^\circ)$	67	62	51
	$\delta_{65^\circ\text{C},0.02 \text{ Hz}} (^\circ)$	78	84	86
	$\delta_{65^\circ\text{C},1 \text{ Hz}} (^\circ)$	80	80	75
5% SBS - Russian	$\delta_{25^\circ\text{C},0.02 \text{ Hz}} (^\circ)$	69	66	61
	$\delta_{25^\circ\text{C},1 \text{ Hz}} (^\circ)$	65	60	51
	$\delta_{65^\circ\text{C},0.02 \text{ Hz}} (^\circ)$	57	84	84
	$\delta_{65^\circ\text{C},1 \text{ Hz}} (^\circ)$	74	76	71
7% SBS - Russian	$\delta_{25^\circ\text{C},0.02 \text{ Hz}} (^\circ)$	68	61	57
	$\delta_{25^\circ\text{C},1 \text{ Hz}} (^\circ)$	59	56	49
	$\delta_{65^\circ\text{C},0.02 \text{ Hz}} (^\circ)$	44	75	83
	$\delta_{65^\circ\text{C},1 \text{ Hz}} (^\circ)$	67	73	67

The phenomena seen in Figure 5.27 can, to a limited degree, also be seen in Table 5.15. The phase angles at the high temperature and low loading frequency combination show an increase after RTFOT and PAV ageing, while there is a traditional paving grade bitumen type behaviour of a decrease in  $\delta$  after ageing at the low temperature and high frequency DSR testing condition.

The isochronal plots and Black diagram for the Russian - SBS PMB are shown in Figures 5.29 to 5.31. There is a constant increase in  $G^*$  across the temperature domain after ageing for tests at 1 Hz in Figure 5.30. This phenomenon is identical to that seen for the penetration grade bitumens and confirms the hypothesis that the increase in  $G^*$  is attributed solely to the oxidative ageing of the base bitumen in the PMB and that the

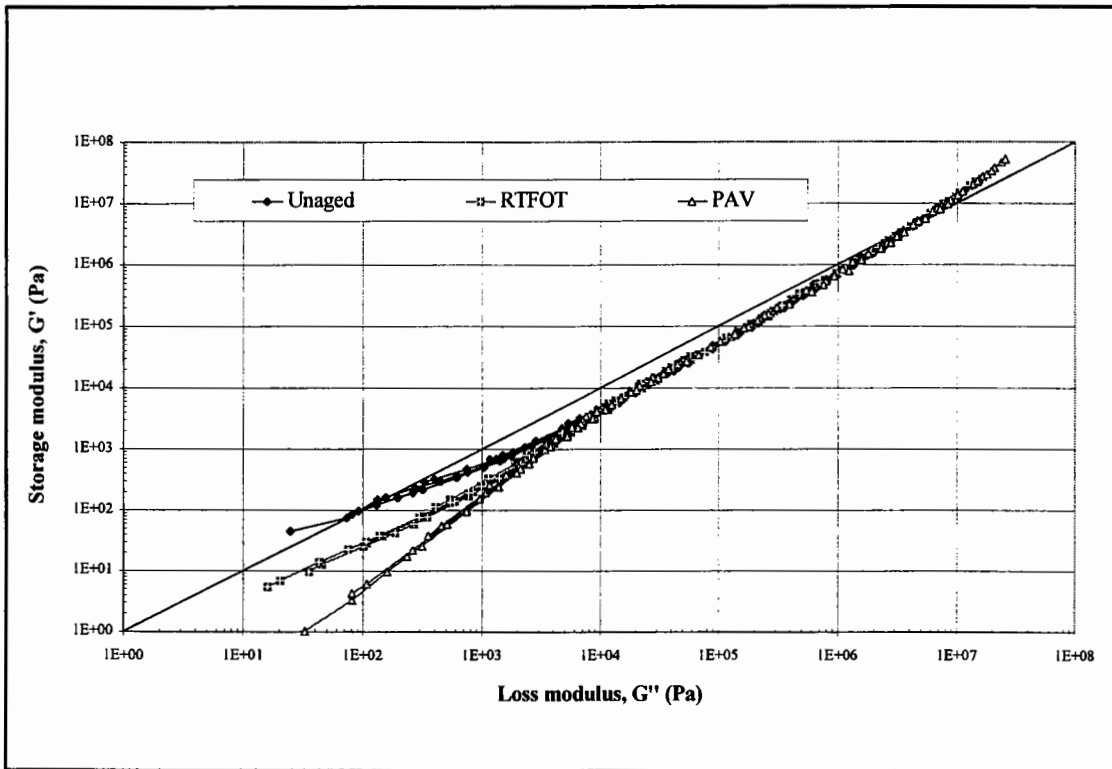


Figure 5.28: Cole-Cole plot for 7% SBS - Russian 80 pen

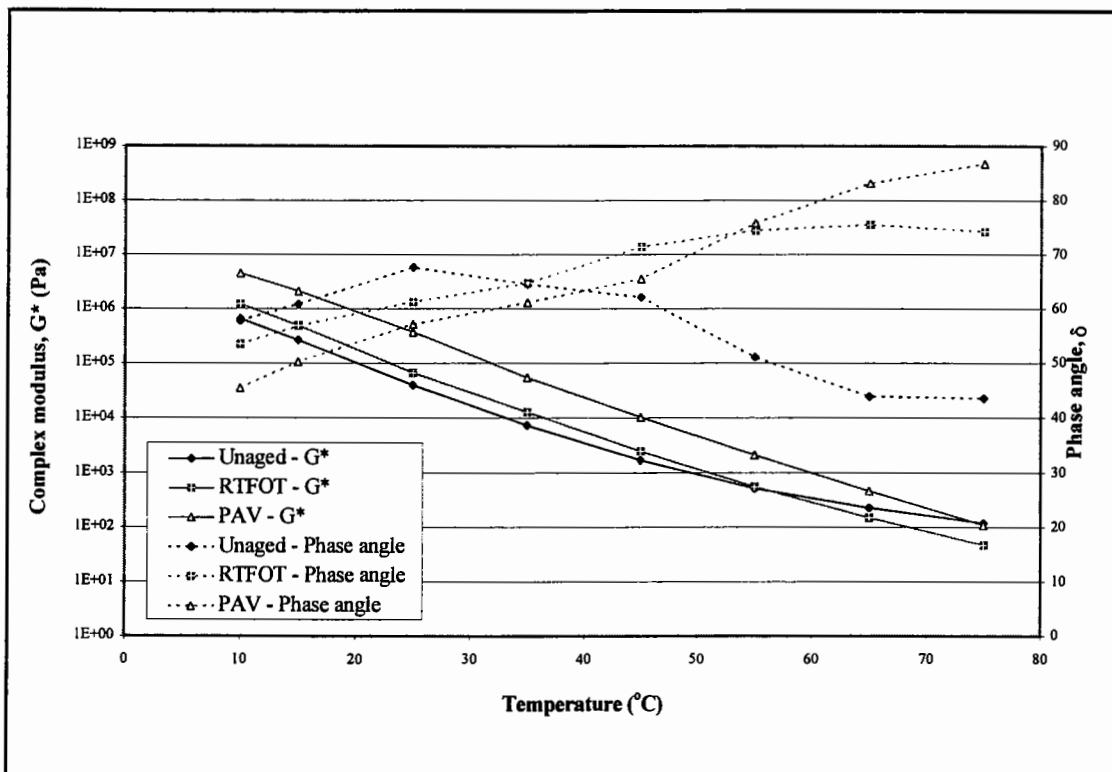


Figure 5.29: Isochronal plot at 0.02 Hz for 7% SBS - Russian 80 pen

bitumen phase in the PMB is aged in a similar manner to that of an unmodified bitumen. However, there is a decrease in  $G^*$  after ageing within the temperature range of 55°C to 75°C for the 0.02 Hz isochronal plot in Figure 5.29. This tends to confirm the hypothesis that there is a rearrangement of the SBS copolymer into lower molecular weight fragments after ageing leading to a "softening" of the PMB. This phenomenon is more noticeable at the lower loading frequency of 0.02 Hz where the influence of the polymer will be more evident compared to that of the bitumen phase of the PMB.

The changes in  $\delta$  after ageing are the same as those shown for an unmodified bitumen in the temperature domain of 10°C to approximately 35°C. This region corresponds to conditions in which the base bitumen component is dominant and, therefore, this correlation with the behaviour shown for unmodified bitumens is expected. In the temperature domain greater than 40°C, where the SBS polymer is rheologically dominant, the changes after ageing are different from those experienced for the unmodified bitumens.

In Figure 5.30, at a temperature of 45°C, the magnitude of the decrease in phase angle after ageing has decreased compared to that at the lower temperatures. At a temperature of 55°C, the phase angle after RTFOT ageing is identical to the phase angle before ageing. This implies that the ageing process has not increased the elastic behaviour of the PMB as would be experienced for a unmodified bitumen. At temperatures greater than 55°C there is an increase in phase angle after RTFOT ageing indicating a more viscous behaviour for the PMB than that found before ageing. At a temperature of 65°C, the phase angle after the PAV ageing is identical to that of the unaged PMB and at temperatures greater than 65°C there is an increase in the phase angle after PAV ageing.

In Figure 5.29, the effects discussed above have shifted to lower temperatures due to the lower loading frequency and greater dominance of the polymer phase. The increase in  $\delta$  after RTFOT ageing now occurs at temperatures greater than 35°C and there is an increase in  $\delta$  after PAV ageing compared to RTFOT ageing at temperatures greater than 55°C .

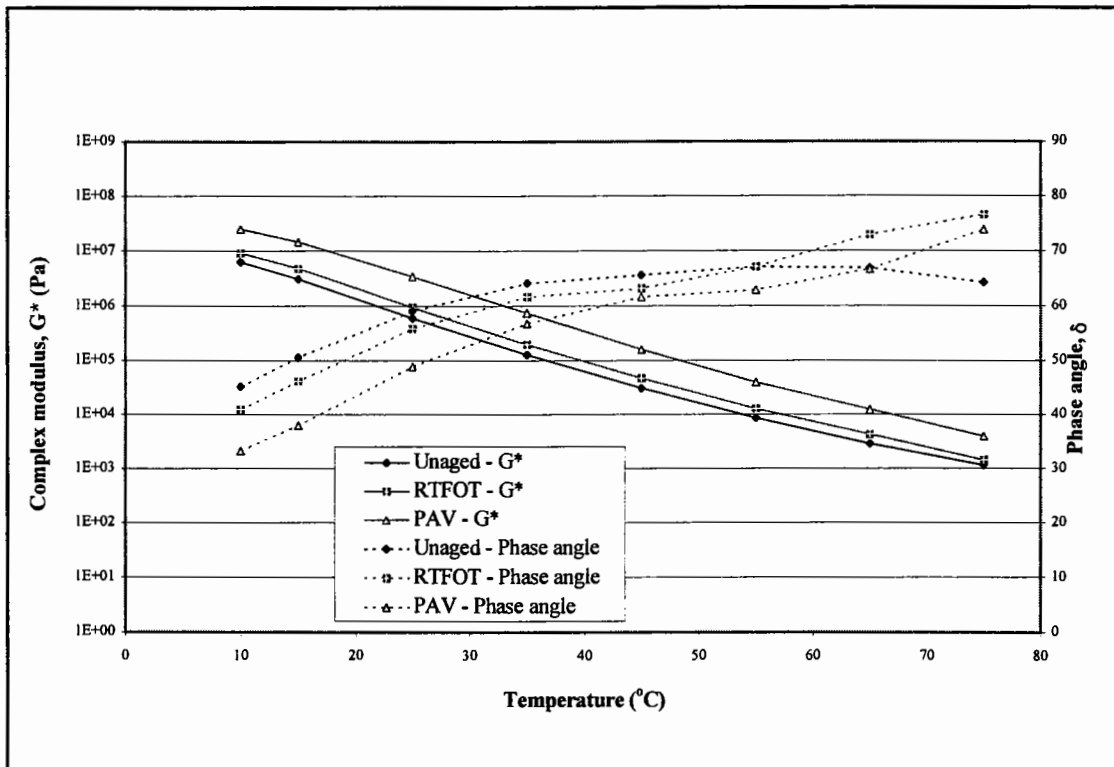


Figure 5.30: Isochronal plot at 1 Hz for 7% SBS - Russian 80 pen

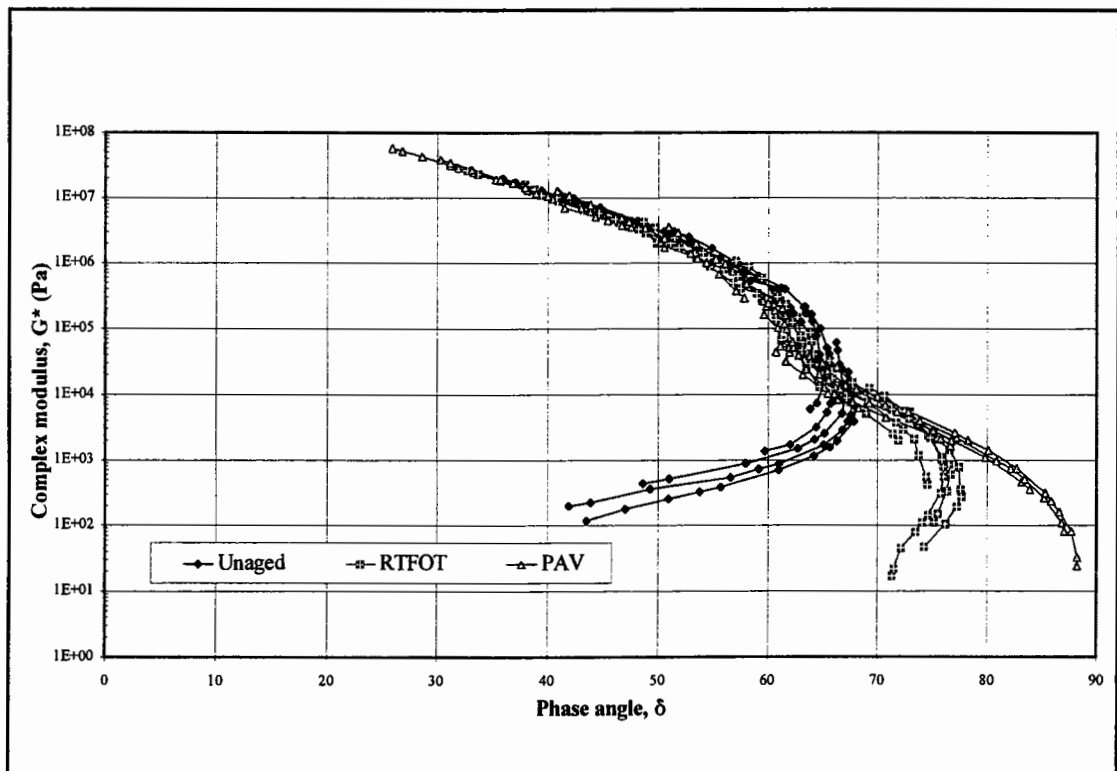


Figure 5.31: Black diagram for 7% SBS - Russian 80 pen



The Black diagram, in Figure 5.31, differs completely from that seen for the unmodified penetration grade bitumens and for the EVA PMB's. It can be divided up into two sections. The first section occurs above a complex modulus value of  $10^4$  Pa and shows a shift of the curve towards lower phase angles indicating the hardening (ageing) of the PMB. The phenomenon is similar to the hardening effect seen for the penetration grade bitumens and for high complex modulus and high phase angle regions of the EVA modified PMB's.

The second section occurs below the complex modulus value of  $10^4$  Pa and shows an opposite shift of the curve towards higher phase angles rather than lower phase angles, thereby indicating a change towards a more viscous rather than more elastic behaviour after ageing. This change towards a more viscous behaviour after ageing, in the Black diagram, and the increase in  $\delta$  after ageing, in the temperature domain greater than approximately  $40^\circ\text{C}$  in Figures 5.29 and 5.30, agrees with the assumption that there is a breakdown of the polymer substructure during ageing into smaller copolymer structures.

#### **Venezuelan 70/100 penetration grade bitumen - SBS PMB's**

The master curves of  $G^*$  and  $\delta$  for the 7% SBS - Venezuelan PMB, in Figures 5.32 and 5.33, differ from those seen for the Russian - SBS PMB in Figures 5.26 and 5.27, principally due to the different degrees of compatibility between the SBS copolymer and the two base bitumens. The lower degree of dominance of the SBS network in the Venezuelan - SBS PMB means that the polymeric plateau region at low frequencies is not as marked as seen for the Russian - SBS PMB. This results in the changes in the rheological behaviour of the PMB being closer to that of a paving grade bitumen than that seen for the Russian - SBS PMB.

The phase angles for the Venezuelan - SBS PMB are presented in Table 5.16. The limited rheological data obtained from the table shows that the behaviour of the aged SBS PMB's is similar to that seen for the unmodified bitumens, with a decrease in  $\delta$  and a more elastic behaviour.

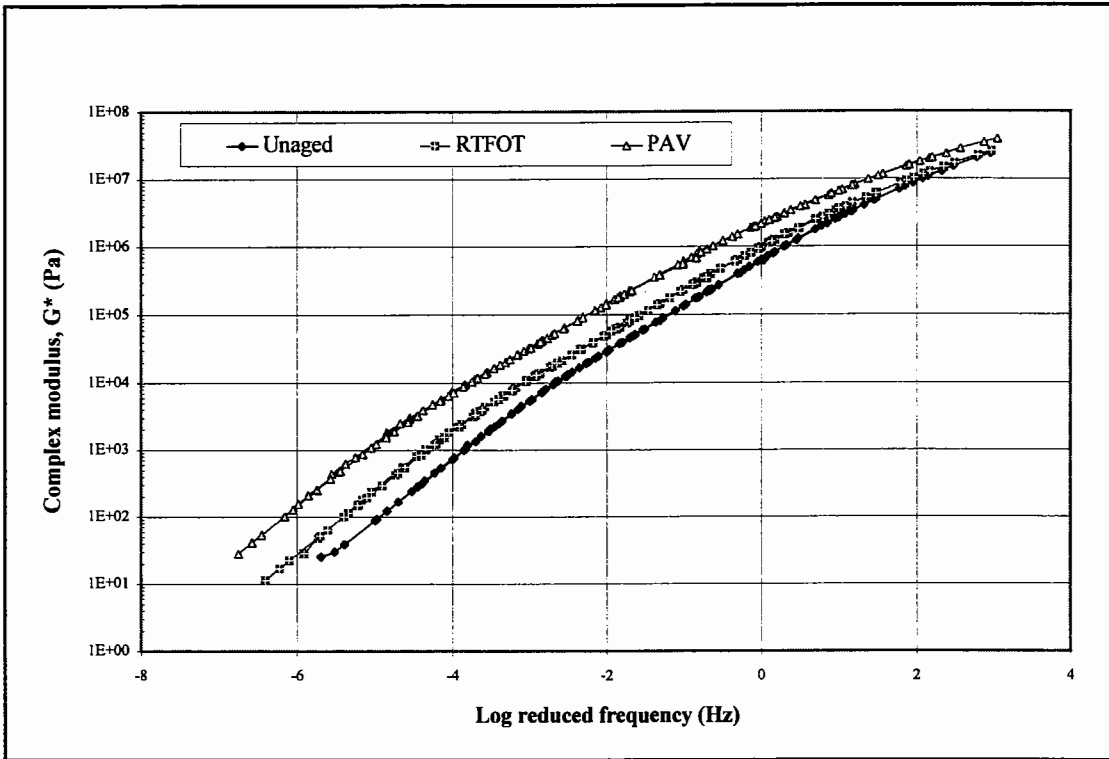


Figure 5.32: Complex modulus master curve for 7% SBS - Venezuelan 70/100 pen

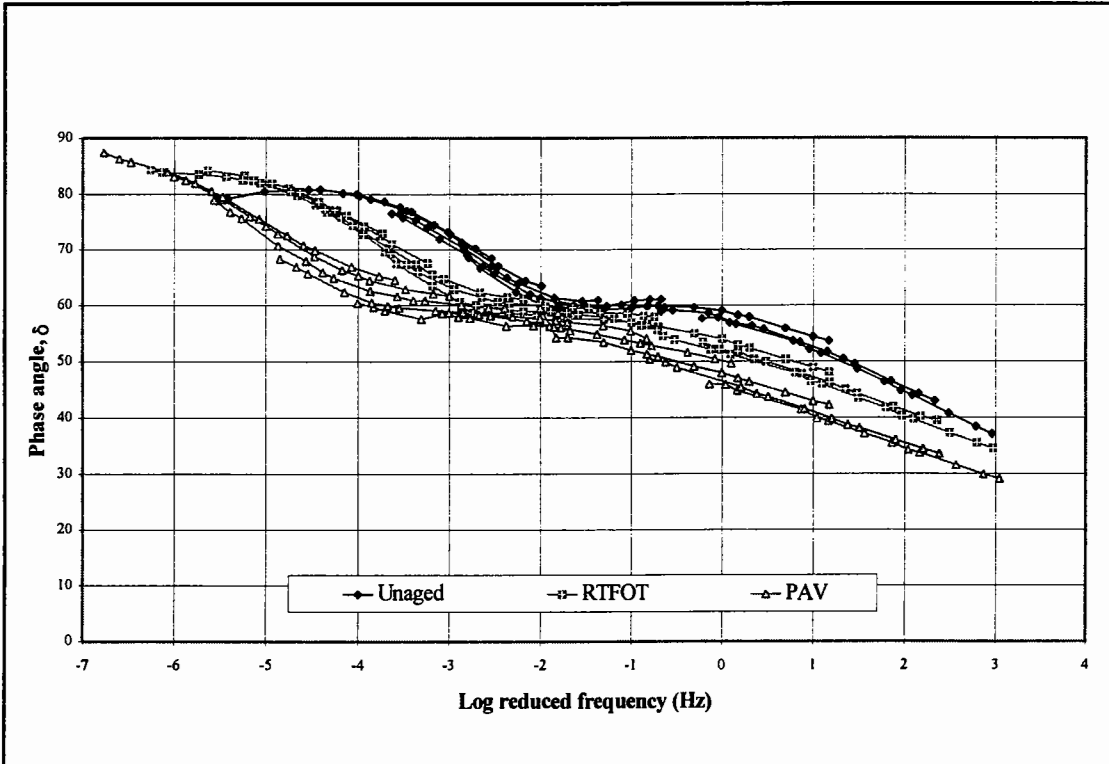


Figure 5.33: Phase angle master curve for 7% SBS - Venezuelan 70/100 pen

**Table 5.16: Phase angles for unaged, RTFOT and PAV aged Venezuelan - SBS PMB's**

Bitumen	Property	Unaged	RTFOT	PAV
3% SBS - Venezuelan	$\delta_{25^{\circ}\text{C},0.02\text{ Hz}} (^{\circ})$	69	66	59
	$\delta_{25^{\circ}\text{C},1\text{ Hz}} (^{\circ})$	66	61	51
	$\delta_{65^{\circ}\text{C},0.02\text{ Hz}} (^{\circ})$	87	87	82
	$\delta_{65^{\circ}\text{C},1\text{ Hz}} (^{\circ})$	81	77	70
5% SBS - Venezuelan	$\delta_{25^{\circ}\text{C},0.02\text{ Hz}} (^{\circ})$	63	62	56
	$\delta_{25^{\circ}\text{C},1\text{ Hz}} (^{\circ})$	62	57	49
	$\delta_{65^{\circ}\text{C},0.02\text{ Hz}} (^{\circ})$	82	83	77
	$\delta_{65^{\circ}\text{C},1\text{ Hz}} (^{\circ})$	78	71	65
7% SBS - Venezuelan	$\delta_{25^{\circ}\text{C},0.02\text{ Hz}} (^{\circ})$	57	58	54
	$\delta_{25^{\circ}\text{C},1\text{ Hz}} (^{\circ})$	59	54	48
	$\delta_{65^{\circ}\text{C},0.02\text{ Hz}} (^{\circ})$	80	82	76
	$\delta_{65^{\circ}\text{C},1\text{ Hz}} (^{\circ})$	74	67	62

The isochronal plots and Black diagram for the PMB are shown in Figures 5.34 to 5.36. The observations that can be made from the three figures are similar to those made for the Russian - SBS PMB. There is a constant increase in  $G^*$  across the temperature domain after ageing and a decrease in  $\delta$  in the temperature domain of  $10^{\circ}\text{C}$  to approximately  $35^{\circ}\text{C}$ .

The observations of  $\delta$  at a temperature of  $25^{\circ}\text{C}$  in Figure 5.34 and  $45^{\circ}\text{C}$  in Figure 5.35 are also similar to that seen for the Russian - SBS PMB with the magnitude of the decrease in  $\delta$  after ageing having decreased compared to that at lower temperatures. However, unlike the behaviour of the Russian - SBS PMB, there is no continuation of the decrease in magnitude or even an increase in  $\delta$  after ageing at the temperatures greater than  $25^{\circ}\text{C}$  in Figure 5.34. In fact the changes in  $\delta$ , associated with the ageing of the PMB within the temperature range of  $25^{\circ}\text{C}$  to  $55^{\circ}\text{C}$  in Figure 5.34 and  $55^{\circ}\text{C}$  to  $75^{\circ}\text{C}$  in Figure 5.35, are similar to that seen for unmodified penetration grade bitumens and only at temperatures greater than  $55^{\circ}\text{C}$ , in Figure 5.34, is the behaviour similar to that seen for the Russian - SBS PMB.

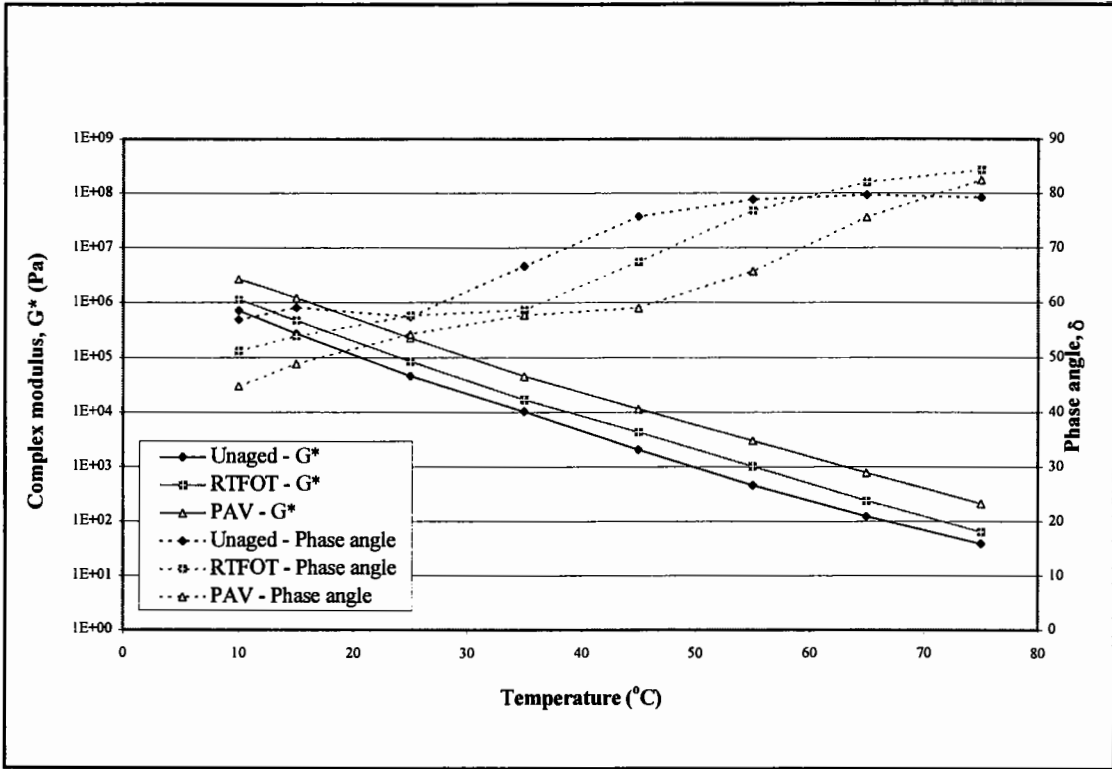


Figure 5.34: Isochronal plot at 0.02 Hz for 7% SBS - Venezuelan 70/100 pen

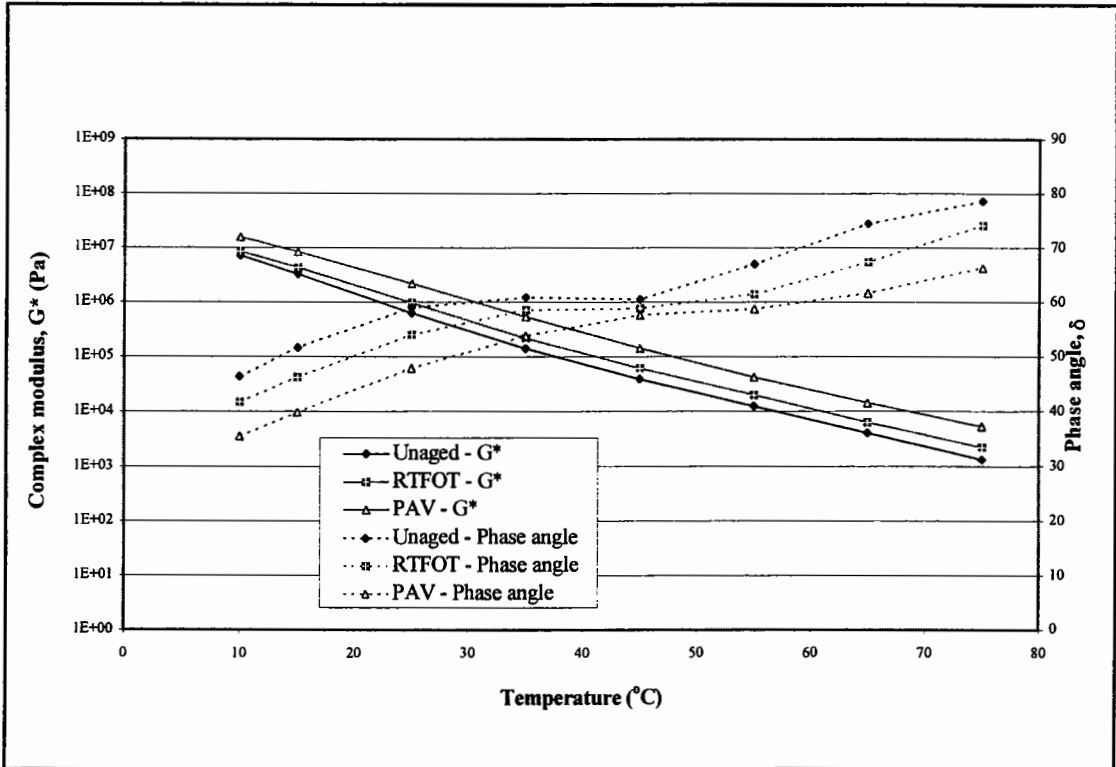


Figure 5.35: Isochronal plot at 1 Hz for 7% SBS - Venezuelan 70/100 pen

The Black diagram, in Figure 5.36, shows a continuous shift of the curves towards lower phase angles after ageing similar to that seen for penetration grade bitumens. However, there are two exceptions that occur at values of  $G^*$  between  $10^4$  Pa and  $10^5$  Pa and at values of  $G^*$  below  $10^3$  Pa, where there is a shift towards higher phase angles as seen for the Russian - SBS PMB at  $G^*$  values below  $10^4$  Pa.

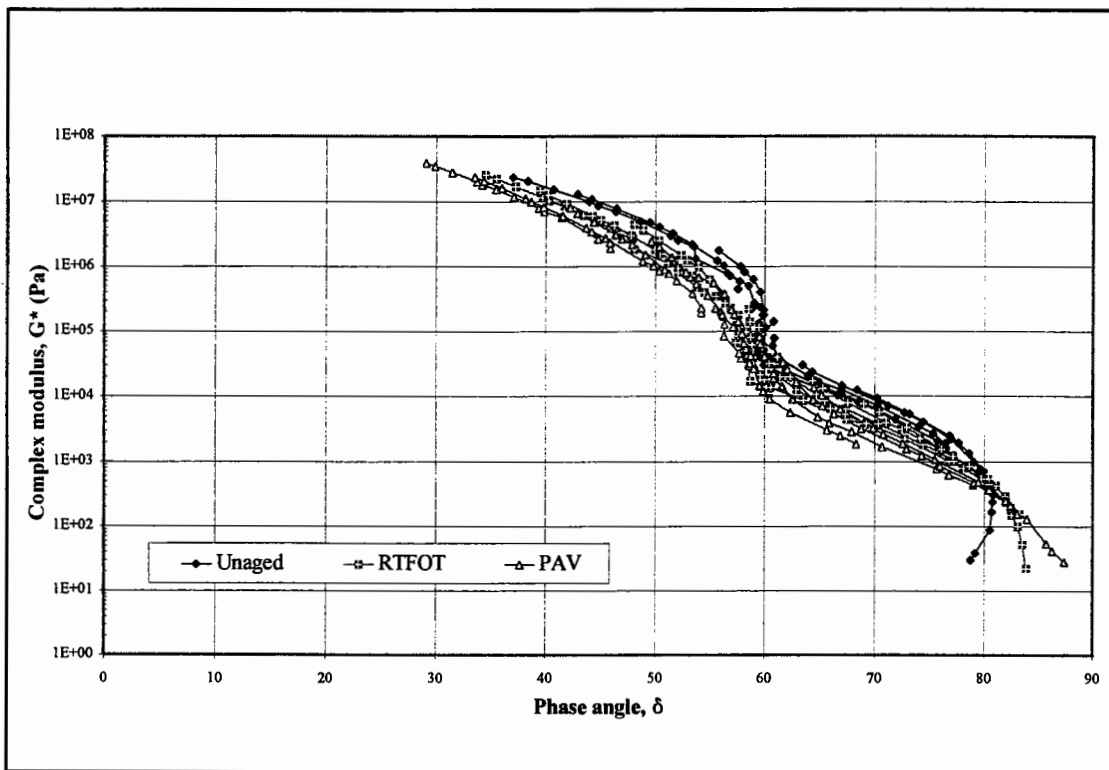


Figure 5.36: Black diagram for 7% SBS - Venezuelan 70/100 pen

#### 5.5.4 Discussion

The FTIR analysis of the oxygen uptake of the SBS-PMB's (Table 5.12 and Figure 5.24) indicates that lower amounts of the chemical functional groups, carbonyl and sulphoxide, are formed after RTFOT and PAV ageing compared to that formed for unmodified bitumens. The formation of these polar, strongly interacting, oxygen-containing chemical functional groups greatly increases the viscosity and alters the complex flow properties of bitumen leading to embrittlement and ultimately pavement failure. A reduction in the amounts of these chemical functional groups produced during ageing can, therefore, be considered to be beneficial to the durability of the binder.

However, the HP-GPC analysis, in Figure 5.25, also indicates that there is a degradation of the molecular size of the SBS polymer substructure. This phenomenon has been seen by other researchers [127,128] and confirms the hypothesis that there is a breakdown of the polymer substructure due to the effect of heat and oxygen. The effect of the breakdown of the SBS substructure into fragmented parts on the rheological characteristics of the aged PMB is a shifting towards more viscous, fluid-like behaviour rather than more elastic, brittle behaviour.

As with the EVA modified PMB's, the influence of the SBS copolymer on the rheological performance of the PMB seems to be greater for the Russian - SBS PMB compared to the Venezuelan - SBS PMB. This can be attributed to the different degrees of compatibility between the SBS copolymer and the two base bitumens.

As for the EVA PMB's, the use of the conventional, empirical tests (Penetration, Softening and viscosity) and the limited DMA data, such as the  $G^*$  and  $\delta$  values at specific temperatures and loading frequencies in Tables 5.14 to 5.16, do not provide a complete and accurate characterisation of the rheological changes associated with ageing. DMA data representation in the form of master curves, isochronal plots and particularly Black diagrams are, therefore, required to explain the rheological changes associated with RTFOT and PAV ageing of the SBS PMB's.

## **5.6 Conclusions**

The dynamic mechanical analysis of the effect of ageing on the rheological performance of the 18 binders has shown that there is a considerable difference in behaviour between penetration grade bitumens and certain PMB's. The empirical tests were, firstly, unable to identify the occurrence of these differences and, secondly, completely unable to quantify the different patterns of rheological behaviour. It can, therefore, be concluded that, although the conventional tests were able to adequately describe the effect of ageing on the rheological properties of unmodified penetration grade bitumens, they were limited in their ability to do so for PMB's.

Based on the dynamic mechanical analysis (DMA) of the EVA and SBS modified PMB's, it can be concluded that the bitumen component of the PMB's ages in a manner similar to that experienced for an unmodified penetration grade bitumen. The aged PMB, therefore, shows similar rheological changes after ageing to that of a penetration grade bitumen in the temperature and loading frequency regions where the bitumen is the dominant component (low temperatures, high loading frequencies) or where the copolymer has melted (high temperatures for EVA copolymers).

The rheological changes that occur after ageing for the PMB's differ from those experienced for penetration grade bitumen in the regions where the polymer is the dominant component. This occurs at temperatures greater than approximately 40°C for the SBS copolymer and between the temperatures of approximately 35°C to 65°C for the EVA copolymer.

The DMA indicates that the rheological changes that occur after ageing for EVA modified PMB's can be linked to a chemical change of the copolymer due to fusion of the crystallites. This chemical change was shown as a reduction in the magnitude of the enthalpy, measured for the endothermic reaction associated with the melting of the EVA copolymers, after RTFOT and PAV ageing.

The rheological changes associated with ageing for the SBS modified PMB's can be linked to a breakdown of the molecular structure of the SBS copolymer to form a lower molecular weight polymer substructure. This results in an increased viscous behaviour in the polymer dominated domain after ageing compared to the increased elastic behaviour found for unmodified penetration grade bitumens.

# 6 Discussion, Conclusions and Recommendations for Future Research

## 6.1 Discussion

The research in this thesis looked at three areas:

- The laboratory techniques associated with the testing geometry and procedure used with dynamic shear rheological testing of bitumens and PMB's,
- The applicability of conventional empirically-based tests and fundamental dynamic shear tests at describing the rheological characteristics of bitumens and PMB's, and
- The explanation of the ageing mechanisms associated with the changes in the rheological characteristics of aged bitumens and PMB's.

The research was therefore built up in three stages, starting with the selection of the appropriate testing methodology to be used with the Bohlin DSR50 Dynamic Shear Rheometer (DSR), followed by the rheological testing of various penetration grade bitumens and polymer modified bitumens (PMB's) and, finally, the novel research into the ageing mechanisms associated with the changes in the rheological characteristics of laboratory aged bitumens and PMB's. The laboratory ageing methods used in the thesis, namely the Rolling Thin Film Oven Test (RTFOT) and the pressure ageing vessel (PAV), have been found to respectively simulate the hardening that a bitumen undergoes during mixing [97,98] and to simulate the changes in the physical and chemical properties of the bitumen after long-term, in-service oxidative ageing [93]. However, the ability of these laboratory ageing methods at simulating the field ageing of PMB's is uncertain and, therefore, the ageing mechanisms identified for the SBS and EVA PMB's are, at present,



only valid for PMB's aged in the laboratory.

### **Bitumen Rheology Testing Procedure**

Although the Dynamic Mechanical Analysis (DMA) [19,20] procedure is now well known with various pieces of standard DSR equipment and testing methods, there is still limited guidance of how to evaluate and quantify the rheological data with regard to the unconditional acceptance of possibly unrealistic or misleading results. Accurate temperature control and correct sample geometry are fundamental for successful rheological testing of bituminous binders, with the transition from one testing geometry to another being controlled by defined complex modulus intervals [65,78]. However, with the large variation in the rheological characteristics of different binders, particularly PMB's, it is essential to undertake rheological testing over wide temperature and frequency ranges, thereby transgressing these standard complex modulus intervals while using a particular testing geometry.

Isochronal plots of complex modulus and phase angle, obtained using different testing geometries, provide a means of identifying the discrepancies between the different testing geometries. However, due to the limited amount of rheological data that can be presented in an isochronal plot, the selection of the correct test geometry and rheological data is dependent on the choice of loading frequency used in the plots. This problem is overcome with the use of Black diagrams, due to their ability to present all the rheological data, obtained for a particular bitumen, in one plot. Black diagrams, therefore, provide a means of identifying the inconsistencies in rheological data resulting from the different testing geometries over a wide range of DSR testing temperatures and frequencies.

The testing procedure recommended in the thesis is, therefore, to overlap the different testing configurations, such as the 8 mm diameter disk with a 2 mm gap with that of the 25 mm diameter disk with a 1 mm gap, at the complex modulus values normally associated with the transition from one configuration to the next. The rheological data can then be plotted in a Black diagram and the appropriate data selected for further analysis.

Although this increases the time required to completely characterise the binder, it minimises the risk of incorrectly determining the stiffness and viscoelastic balance of the binder by using the incorrect testing configuration.

### **Rheological Testing of Polymer Modified Bitumens**

DSR testing was performed on various polymer modified bitumens (PMB's) consisting of combinations of three base bitumens, one plastomeric polymer, namely ethylene vinyl acetate (EVA), one elastomeric polymer, namely styrene butadiene styrene (SBS) and three polymer contents. Although these combinations represent only a small proportion of the PMB's used in pavement engineering, the DSR results showed that the rheological characteristics of PMB's differ considerably between different generic polymer types, different polymer and bitumen proportions and different bitumen-polymer compatibilities. The implications of these findings are that, within the confines of polymer modification, PMB's show very different rheological characteristics which can only be quantified by extensive rheological testing at various loading frequencies and temperatures.

The breakdown of the time-temperature superposition principle (TTSP), when applied to high polymer modified PMB's, necessitates the measurement of increased amounts of rheological data compared to that required for "thermorheologically simple" penetration grade bitumens. These large amounts of rheological data tend to be difficult to analyse in isothermal and isochronal plots but provide a comprehensive explanation of the rheological characteristics of the PMB when plotted in Black diagrams.

Empirical tests, such as Penetration, Softening Point and high temperature viscosity cannot provide the extensive rheological data required for the complete analysis of the rheological characteristics of PMB's. The empirical nature of these tests, coupled with their restrictions to specific test temperatures and rates of loading, means that without DSR testing the occurrence of the different crystalline structures in EVA PMB's and the increased elastic behaviour at high temperatures of SBS PMB's cannot be identified.

### **Rheological Characteristics of Aged Polymer Modified Bitumens**

The rheological evaluation of the ageing mechanisms in EVA and SBS PMB's provides the novel area of the thesis. The various EVA and SBS PMB's were subjected to laboratory simulated short term and long term ageing in the Rolling Thin Film Oven Test (RTFOT) and the pressure ageing vessel (PAV). The ageing mechanisms for the PMB's, as measured by the changes in their rheological characteristics after ageing, were found to differ considerable from that found for penetration grade bitumens. In addition, the ageing mechanisms were found to differ between the EVA and SBS PMB's.

The rheological characteristics of the EVA PMB's were found to change after ageing, either towards a rheological characteristic normally associated with a lower polymer content PMB, or in the case of those PMB's that had initially shown a lower degree of modification, towards that normally associated with an unmodified bitumen. This chemical change can be explained as a change in the shape and orientation of the different crystalline structures of the EVA PMB's as seen in the Black diagrams of complex modulus versus phase angle and by a reduction in enthalpy as measured by differential scanning calorimetry (DSC).

The rheological characteristics of the SBS PMB's were found to change after ageing towards a more viscous, fluid-like behaviour as represented by an increase in phase angle, in the temperature and frequency regions where the polymer is dominant. This increased viscous behaviour after ageing corresponds to a degradation of the SBS copolymer resulting in a reduction of the molecular weight of the copolymer as measured by high performance gel permeation chromatography (HP-GPC).

### **Validation study**

Dynamic shear rheometry using the Bohlin Model DSR50 Dynamic Shear Rheometer has been used to determine the rheological characteristics of laboratory blended EVA and SBS PMB's. These PMB's are "physical" blends of base bitumen and polymer and not as complex as "chemically" blended proprietary PMB's, such as the SBS copolymer based Sealoflex PMB. In order to verify, firstly, the ability of DMA to characterise the

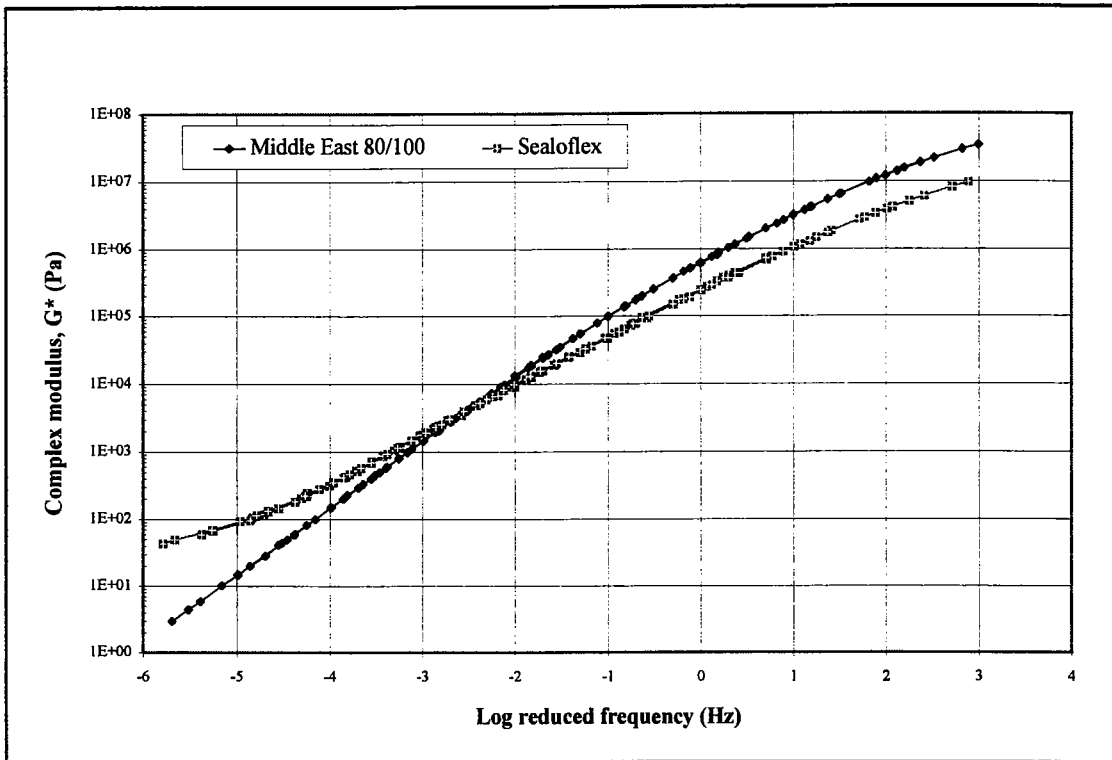


Figure 6.1: Complex modulus master curve for Sealoflex

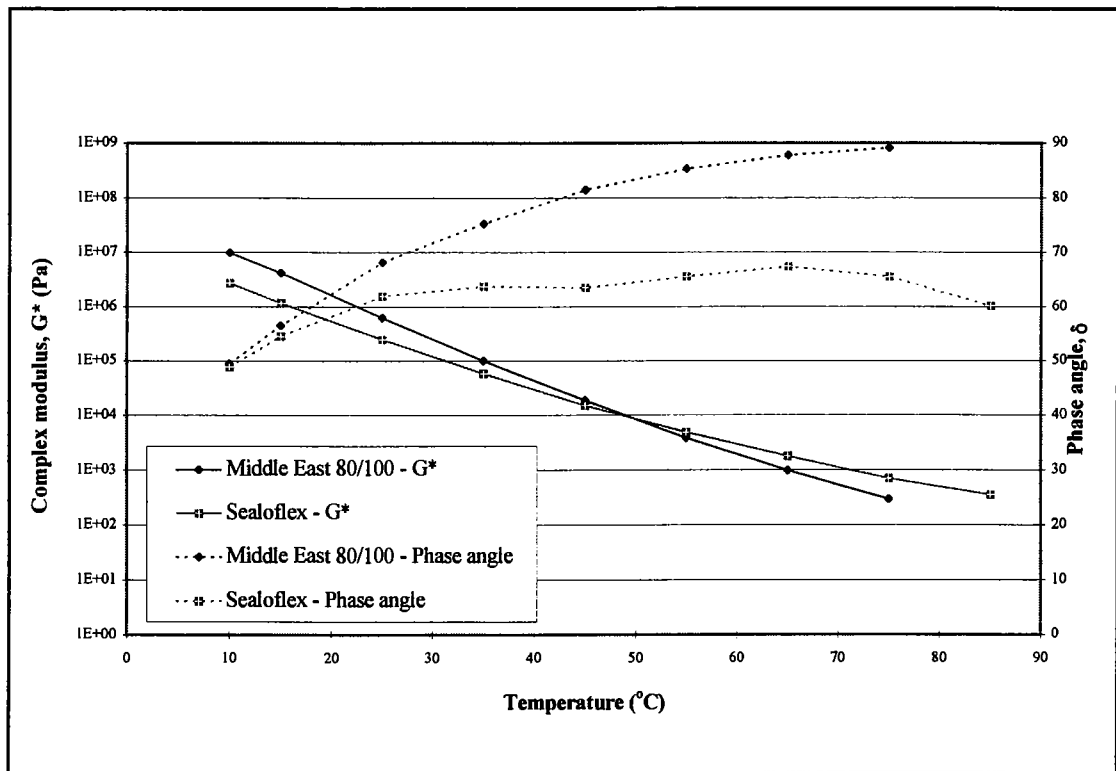


Figure 6.2: Isochronal plot at 1 Hz for Sealoflex

rheological behaviour of unaged and aged PMB's and, secondly, the ageing mechanism associated with SBS PMB's, DSR testing was performed on the Sealoflex PMB.

The complex modulus master curve and the isochronal plots of  $G^*$  and  $\delta$  at a frequency of 1 Hz are shown in Figures 6.1 and 6.2. The master curve and the isochronal plot show that the effect of modification on the rheological characteristics of the Sealoflex PMB are similar to those seen for the highly polymeric Russian - SBS PMB's. However, in addition to the increase in stiffness and elasticity at high temperatures and long loading times, the "chemically" blended Sealoflex PMB shows a reduction in stiffness at low temperatures and high loading frequencies when compared to rheological properties of the base bitumen. This results in the Sealoflex PMB, with its improved temperature susceptibility, being able to improve the low temperature thermal cracking resistance, as well as the rutting resistance at high temperatures, of a modified asphalt mixture.

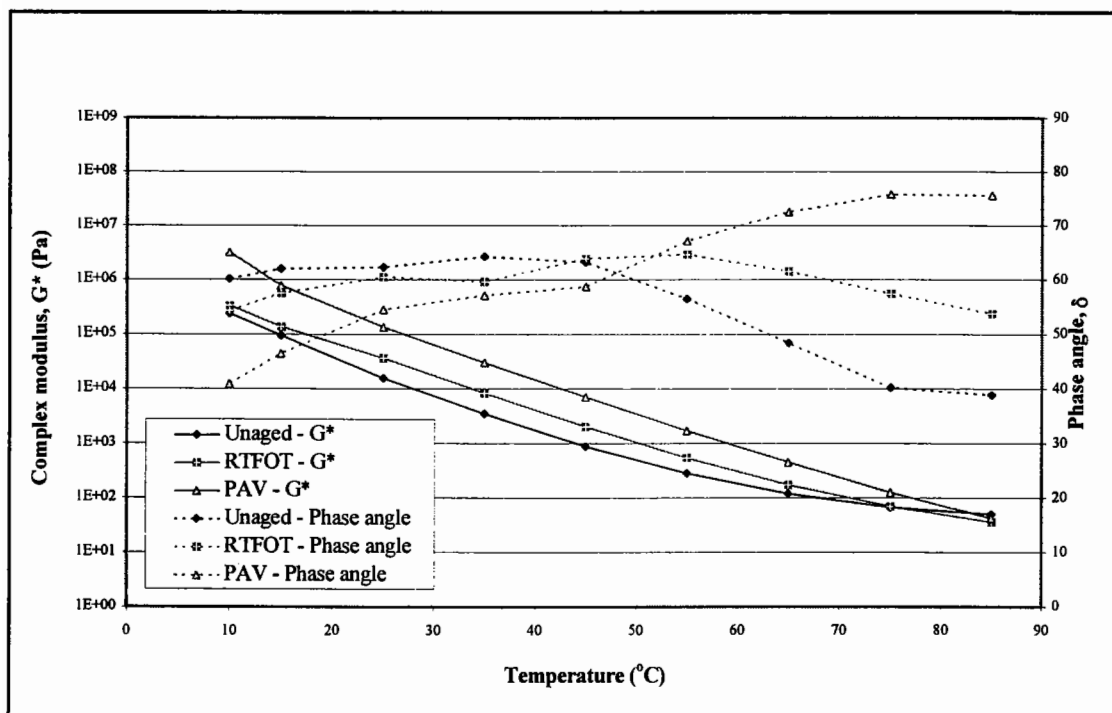


Figure 6.3: Isochronal plot at 0.02 Hz for unaged, RTFOT and PAV aged Sealoflex

The isochronal plots of  $G^*$  and  $\delta$  at 0.02 Hz and 1 Hz and the Black diagram for the unaged, RTFOT and PAV aged Sealoflex PMB are presented in Figures 6.3 to 6.5. The rheological changes associated with the ageing of the PMB are once again similar to

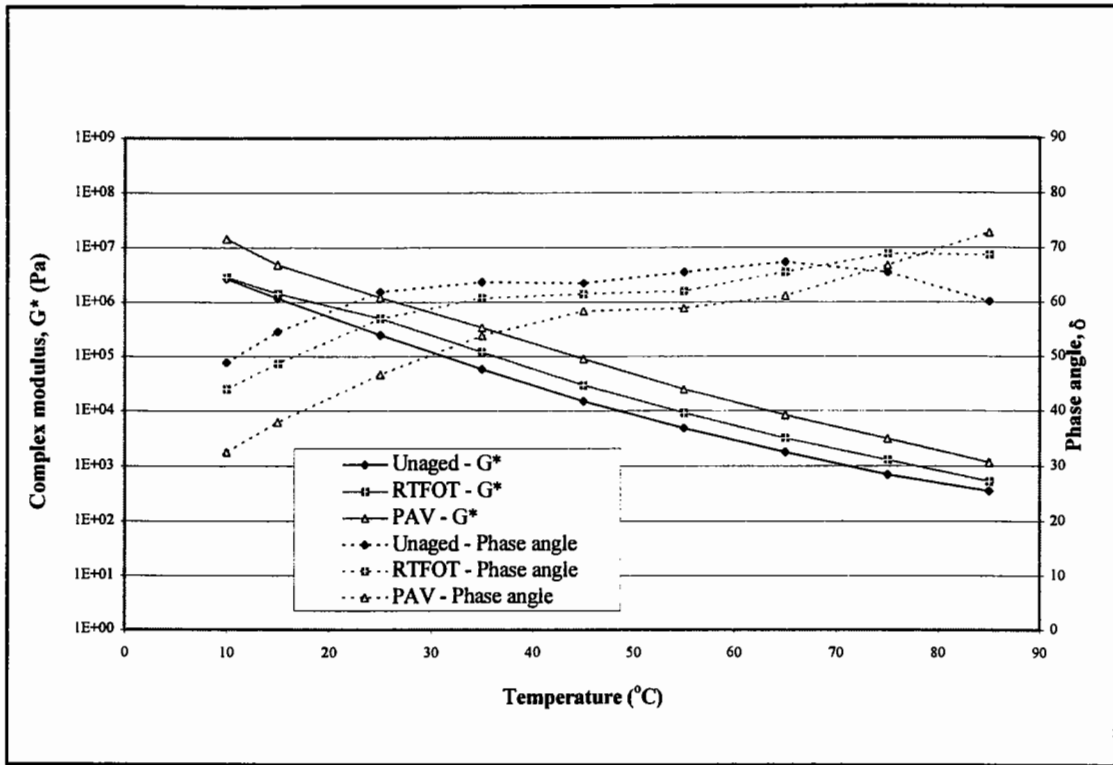


Figure 6.4: Isochronal plot at 1 Hz for unaged, RTFOT and PAV aged Sealoflex

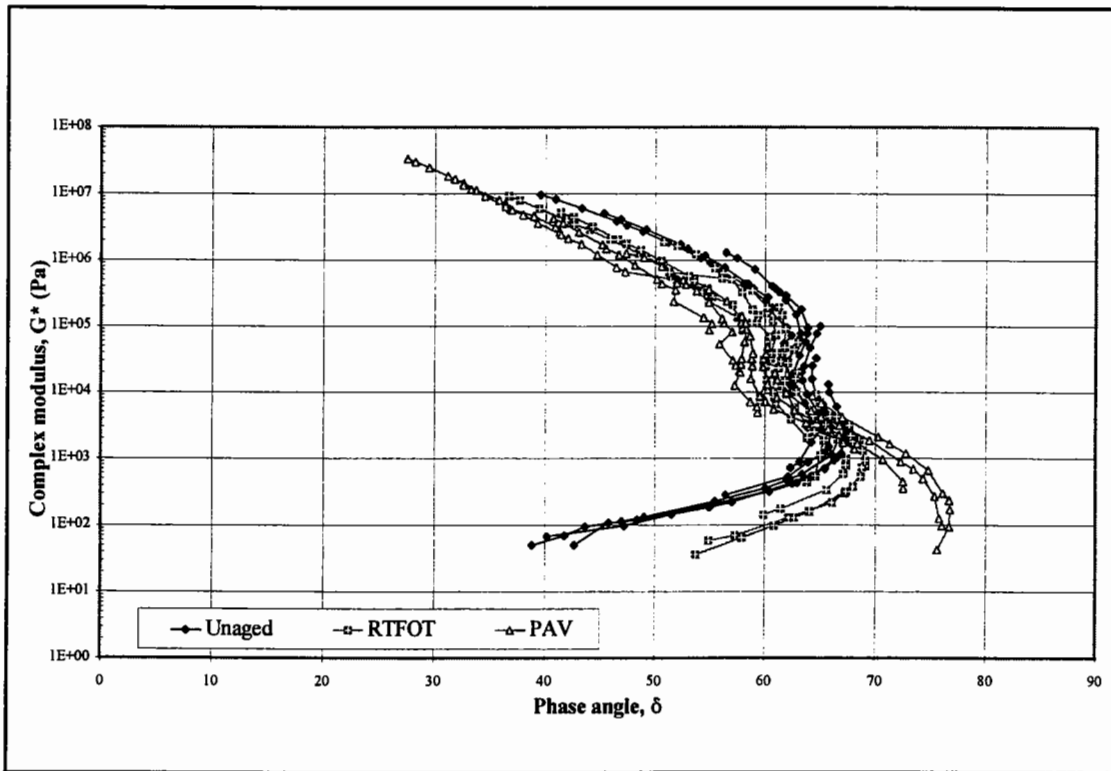


Figure 6.5: Black diagram for unaged, RTFOT and PAV aged Sealoflex

those seen for the laboratory blended SBS PMB's with a shift towards more viscous, fluid-like rheological behaviour after ageing. This confirms the ageing mechanism of a breakdown of the molecular structure of the SBS copolymer even in a "chemically" blended proprietary SBS product such as Sealoflex.

In addition to the use of laboratory "physically" blended PMB's, the ageing methods used in the thesis consisted of laboratory simulated ageing tests, namely the RTFOT and PAV. Further research is therefore needed to verify whether these laboratory methods accurately simulate the ageing mechanisms found in the field, particularly with regard to the ageing of PMB's.

## 6.2 Conclusions

The main conclusions that can be drawn from the rheological research undertaken in this thesis are:

1. Fundamental rheological testing of PMB's using a Dynamic Shear Rheometer (DSR) has enabled the different modification methods associated with EVA and SBS PMB's to be identified. The rheological characteristics of these two generic PMB groups depend not only on the nature of the EVA and SBS copolymers but also on the compatibility of the bitumen-polymer blend and polymer content and, therefore, differ considerably amongst the PMB's. The rheological characteristics of a PMB are therefore unique to that particular PMB and should not be considered to be representative of all bitumens subjected to polymer modification.
2. The ageing mechanisms for EVA and SBS PMB's were found to differ from the oxidative ageing and consequential hardening found for penetration grade bitumens. The ageing mechanism for EVA PMB's consists of a reduction in enthalpy that can be associated with the fusion and crystallisation of the semi-crystalline polymer and a shifting of the rheological characteristics of the aged

PMB towards that of an unmodified bitumen. The ageing mechanism for SBS PMB's consists of a degradation of the SBS copolymer with a shifting of the rheological characteristics of the aged PMB to a more viscous behaviour.

In addition to these main conclusions, the following conclusions have been drawn from the various chapters of the thesis.

### **Literature Review**

The following conclusions have been drawn from the literature review in Chapter 2:

- Various chemistry tests, such as high performance gel permeation chromatography (HP-GPC) and differential scanning calorimetry (DSC), were identified as suitable tests for evaluating the chemical properties of both penetration grade bitumens and polymer modified bitumens (PMB's). These tests were deemed suitable due to their ability to measure properties associated with polymer modification, such as the DSC measurement of enthalpy associated with melting (fusion) of EVA copolymers and the HP-GPC high molecular weight determination of SBS copolymers. Infrared spectroscopy (IR) was selected due to its ability to measure various functional groups produced during oxidative ageing of both penetration grade bitumens and PMB's.
- Dynamic shear rheological testing using a Dynamic Shear Rheometer (DSR) provides a practical and relatively simple method of obtaining the large quantities of rheological data, at various temperatures and loading frequencies, required for the complete characterisation of PMB's.
- Oxidative ageing of penetration grade bitumens results in a chemical transition of the light, non-polar components to heavier, polar components and a consequential hardening of the bitumen. The Rolling Thin Film Oven Test (RTFOT) and the Pressure Ageing Vessel (PAV) provide the laboratory means to simulate the short and long-term ageing of bituminous binders.



- The rheological characteristics of different PMB's depend on the nature of the polymer, the polymer content and the nature of the base bitumen. The compatibility of the different bitumen-polymer blends dictates whether the modification will be dominated by the polymer (polymeric-type modification) or simply a filler-type modification. With regard to EVA PMB's, a degree of incompatibility is required to obtain a polymeric-type modification and, therefore, polymeric-type or polymer-modified rheological behaviour. Highly compatible blends dissolve the EVA copolymer so that the polymeric nature of the copolymer is lost resulting in a filler-type modification and rheological behaviour. At the other extreme, EVA copolymers that cannot absorb sufficient quantities of "oil fraction" to dissolve the copolymer will also result in filler-type modification and rheological behaviour. With regard to SBS PMB's, a compatible balance between the solvency power of the aromatic oils and the high molecular weight of the SBS copolymer is essential for the creation of an effective polymeric-type modification and rheological behaviour.

### **Dynamic Shear Rheometry Testing**

The following conclusions can be drawn from Chapter 3 dealing with the selection of the appropriate testing geometry and test procedure for dynamic shear rheometry:

- Accurate temperature control during dynamic shear testing with the Bohlin DSR50 can be provided by means of a circulating fluid bath and an accurate means of controlling the test temperature during rheological tests within  $\pm 0.1^\circ\text{C}$ .
- Representative rheological results for penetration grade bitumens and PMB's can be produced by means of the Bohlin DSR50 using a combination of the 8 mm and 25 mm diameter disk configurations. The combination of the two configurations is governed by the stiffness and composition of the unmodified and polymer modified bitumens. Black diagrams provide a convenient means of presenting all the rheological data, generated by the different sample geometries, in one plot, thereby aiding the selection of the correct testing geometry and rheological data.

- The repeatability of the Bohlin DSR50 was found to be well within the repeatability and reproducibility findings of the RILEM interlaboratory study [111,112]. As with the RILEM study, the variability was found to be greater for complex modulus than phase angle.

### **Rheological Characteristics of Polymer Modified Bitumens**

The conclusions that can be drawn from the investigation of the rheological characteristics of PMB's are:

- The rheological observations of EVA PMB's are consistent with the semi-crystalline EVA copolymer providing the polymeric modification of PMB's through the crystallisation of three dimensional networks within the bitumen. These crystalline structures increase the viscosity, stiffness and elastic behaviour of the PMB up to the temperatures associated with the melting of these structures.
- The thermoplastic rubber SBS copolymer provides polymeric modification by means of a highly elastic network within the bitumen. This elastic network increases the viscosity, stiffness and elastic behaviour of the PMB, but due to the high melting temperature of the polystyrene blocks (approximately 100°C), this modification is maintained to high temperatures, well within the compaction temperature range of asphalt mixtures modified with the PMB.
- Empirical tests and presentation methods, such as Penetration, Softening Point, Penetration Index (PI), high temperature viscosity, Bitumen Test Data Chart (BTDC) and Van der Poel's nomograph do not provide suitable means of quantifying the rheological characteristics of PMB's.
- Dynamic shear rheometry using a Dynamic Shear Rheometer (DSR) together with rheological data presentation methods, such as isochronal plots, master curves and Black diagrams, when used in concert and properly interpreted, provide a means of representing the rheological characteristics of PMB's. Black

diagrams, unlike master curves, do not require the rheological data to be shifted and, therefore, can present rheological data over a wide range of temperatures and frequencies without relying on the bitumen fulfilling TTSP.

### **Rheological Characteristics of Aged Polymer Modified Bitumens**

The following conclusions can be drawn from the investigation into the ageing mechanisms associated with PMB's:

- Empirical tests, although able to adequately describe the effect of ageing on the rheological properties of unmodified penetration grade bitumens, are unable to quantify the changes in the rheological behaviour of aged PMB's. They can even give misleading results by indicating that there is an increase in hardness of the aged PMB when in reality there is an increase in viscous fluid-like behaviour at certain temperatures and loading frequencies.
- The bitumen component of the PMB's ages in a manner similar to that experienced for an unmodified penetration grade bitumen. The aged PMB, therefore, shows similar rheological changes after ageing to that of a penetration grade bitumen in the temperature and loading frequency regions where the bitumen is the dominant component (low temperatures, high loading frequencies) or where the copolymer has melted (high temperatures for EVA copolymers).
- The rheological changes that occur after ageing for the PMB's differ from those experienced for penetration grade bitumen in the regions where the polymer is the dominant component. This occurs at temperatures greater than approximately 40°C for the SBS copolymer and between the temperatures of approximately 35°C to 65°C for the EVA copolymer.
- The rheological changes that occur after ageing for EVA modified PMB's can be linked to a chemical change in the semi-crystalline copolymer that can be quantified as a reduction in the magnitude of the enthalpy, measured for the

endothermic reaction associated with the melting of the EVA copolymers. This results in a change in shape and orientation of the rheological "waves" and "branches" seen in the Black diagrams and master curves of the EVA PMB's and a shifting of the rheological characteristics of the aged PMB towards that of an unmodified bitumen.

- The rheological changes associated with ageing for the SBS modified PMB's can be linked to a breakdown of the molecular structure of the SBS copolymer to form a lower molecular weight polymer substructure. This results in an increased viscous behaviour in the polymer dominated domain after ageing compared to the increased elastic behaviour found for unmodified penetration grade bitumens.

### **6.3 Recommendations for Future Research**

With the advent of performance-based specifications, there is increasing interest in the use of fundamental rheological parameters to specify binders. The fundamental research undertaken in the thesis, with regard to the rheological characteristics of unaged and aged PMB's, has particular relevance to the selection of the parameters and testing conditions that will form part of a performance-based specification. The fact that PMB's do not obey time-temperature superposition means that the selection of specific loading times and temperatures may discriminate against those binders that require a wider range of temperatures and loading times to fully characterise their rheological behaviour.

The 8th edition of the Department's Specification for Highway Works is to include a new clause 943 designed to supersede the long-established empirically-based specifications for asphalt wearing courses. The new performance-based specifications are based on wheel tracking at one of two temperatures (45°C and 60°C) depending on traffic-induced stresses. A key benefit of the new clause is the increased use of new binders, such as PMB's, to produce asphalt mixtures that achieve the specification requirements at 60°C.

However, based on the research undertaken in this thesis, there are two potential problems with clause 943.

Firstly, the use of a high testing temperature of 60°C as a means of providing a harsh testing regime will only be appropriate if the bituminous material obeys time-temperature superposition, with the high temperature being equivalent to long loading times and high stresses. The high temperature will be an inappropriate testing condition for an asphalt mixture containing an EVA PMB due to the formation of different crystalline structures within the PMB at different temperatures and therefore the lack of equivalency between temperature and loading frequency. Care should therefore be taken when using the wheel tracking test as a means of evaluating the performance of EVA modified asphalt mixtures. A better solution may be the use of more fundamental testing methods, such as a form of triaxial testing, which has a greater potential to reproduce the different temperature and loading conditions experienced in the pavement and, therefore, provide a more fundamental evaluation of the performance of different asphalt mixtures .

Secondly, the assumption that the permanent deformation resistance of an asphalt mixture will improve with time, due to the age hardening of the binder, may not be applicable for SBS PMB's. Whereas penetration grade bitumens show an increase in complex modulus and a decrease in phase angle after ageing, laboratory aged SBS PMB's, although showing an increase in complex modulus, show an increase in phase angle and, therefore, a more viscous, fluid-like behaviour after ageing. The implication of this increased viscous behaviour with laboratory ageing is the possibility of permanent deformation failure of the aged asphalt mixture if the same laboratory ageing mechanisms are found in the field.

New performance-based specifications, therefore, need to be able to fully characterise the rheological behaviour of bituminous binders, particularly PMB's, over a wide range of loading times and temperatures. In addition the specifications need to address the long-term performance of the binders due to the different ageing mechanisms associated with penetration grade bitumens, EVA PMB's and SBS PMB's.

Dynamic Mechanical Analysis (DMA) of the EVA and SBS PMB's in this thesis have enabled their rheological characteristics to be quantified. The rheological measurements have shown that the EVA and SBS copolymers provide different polymeric modification methods and that the degree of modification is based on the compatibility of the different bitumen-polymer blends. However, further research is needed to investigate whether these different rheological characteristics are evident within asphalt mixtures incorporating these modified bitumens. It is, therefore, recommended that dynamic, oscillatory type testing of polymer modified asphalt mixtures, incorporating the PMB's used in this thesis, should be undertaken. Asphalt mixture specimens can be testing by means of axial tension-compression tests in a servo-hydraulic machine at various frequency and temperature conditions to produce a rheological characterisation of the modified mixtures.

Dynamic shear rheometry testing has also been used in this thesis to quantify the rheological changes associated with the laboratory ageing of EVA and SBS PMB's. These rheological changes also need to be identified and quantified for EVA and SBS polymer modified asphalt mixtures by means of dynamic tension-compression testing. In addition the laboratory ageing methods need to be validated with regard to their equivalency to field ageing. The laboratory ageing mechanisms found for the EVA and SBS PMB's need to be verified by conducting DMA on recovered field aged PMB's. The testing of the recovered PMB's will provide a means of evaluating the suitability of the Rolling Thin Film Oven (RTFO) and Pressure Ageing Vessel (PAV) tests at simulating the ageing of PMB's.

Although the EVA and SBS copolymers are two of the most widely used polymers in bitumen modification, further rheological testing of other PMB's, including SBR and EMA PMB's and various proprietary PMB's is required to verify the different rheological changes associated with ageing that were found for the plastomeric and elastomeric PMB's. The rheological changes found for the Sealoflex PMB have provided the first confirmation of the ageing mechanism found for SBS copolymer modified bitumens but further testing of other proprietary PMB's is recommended.

The research in this thesis has concentrated on moderate to high temperature testing of bitumen. In order to obtain a broader understanding of the rheological characteristics of bitumens, particularly PMB's, low temperature rheological testing using testing equipment such as the Bending Beam Rheometer (BBR) and the fracture Direct Tension Tester (DTT) are recommended. These rheological tests should not be limited to the laboratory blended PMB's used in this thesis but should include other PMB types as well as "chemically" blended proprietary PMB's.

# References

1. Whiteoak, C.D. "The Shell Bitumen Handbook". Shell Bitumen, Surrey, UK, 1990.
2. Abraham, H. "Asphalts and Allied Substances, Their Occurrence, Modes of Production, Uses in the Arts and Methods of Testing". Fifth Edition, Vol. 1, D van Nostrand Company, January 1945.
3. Petersen, J.C., Robertson, J.F., Branthaver, J.F., Harnsberger, P.M., Duvall, J.J. and Kim, S.S. "Binder Characterization and Evaluation, Volume 1", SHRP-A-367, Strategic Highways Research Program, National Research Council, Washington, D.C., 1994.
4. Morgan, P. and Mulder, A. "The Shell Bitumen Industrial Handbook." Surrey, UK, 1995.
5. "Statistical Year Book." British Aggregate Construction Materials Industries, London, 1994.
6. Pell, P.S. "Characterisation of Fatigue Behaviour." Structural Design of Asphalt Concrete Pavements to Prevent Fatigue Cracking, Special Report 140, Highway Research Board, Washington, pp. 49-64, 1973.
7. Brown, S.F. "Effect of Mix Properties on Structural Design: A Review." Proceedings of the Association of Asphalt Paving Technologists, Vol. 57, pp. 245-261, 1988.
8. Hofstra, A. and Klomp, A.J.G. "Permanent Deformation of Flexible Pavements under Simulated Traffic Conditions." Proceedings for the Third International



Conference on the Structural Design of Asphalt Pavements, Vol. 1, pp. 613-621, London, 1972.

9. Eisenmann, J. and Hilmer, A. "Influence of Wheel Load and Inflation Pressure on the Rutting Effect at Asphalt Pavements - Experiments and Theoretical Investigations." Proceedings of the Sixth International Conference on the Structural Design of Asphalt Pavements, Vol. 1, pp. 392-404, Ann Arbor, 1987.
10. Jung, D. and Vinson, T.S. "Low Temperature Cracking Resistance of Asphalt Concrete Mixtures." Journal of the Association of Asphalt Paving Technologists, Vol. 62, pp. 54-92, 1993.
11. Brown, S.F., Cooper, K.E., Gibb, J.M., Read, J.M. and Scholz, T.V. "Practical Tests for Mechanical Properties of Hot Mix Asphalt." Proceedings of the 6th Conference on Asphalt Pavements for Southern Africa, Vol. 2, pp. 29-45, Cape Town, South Africa, 1994.
12. "Focus on HMAT - Hot Mix Asphalt Technology." National Asphalt Pavement Association (NAPA), Summer edition, Vol. 1, No. 2, pp. 21-23, 1996.
13. "European Asphalt Magazine." Official Journal of the European Asphalt Pavement Association (EAPA), 2/96, pp. 10-27, 1996.
14. Harrigan, E.T., Leahy, R.B. and Youtcheff, J.S. "The SUPERPAVE Mix Design System Manual of Specifications, Test Methods and Practices." SHRP-A-379, Strategic Highways Research Program, National Research Council, Washington, D.C., 1994.
15. Carswell, J., Claxton, M.J. and Green, P.J. "Dynamic Shear Rheometers: Making Accurate Measurements on Bitumens." Proceedings of The Asphalt Yearbook 1997, The Institute of Asphalt Technology, pp. 79-84, 1997.

16. Gubler, R., Hugener, M., Partl, M.N. and Angst, Ch. "Comparison of Different Approaches in Standardisation and Characterisation of Bituminous Binders." Proceedings of the 5th International Rilem Symposium on Mechanical Tests for Bituminous Materials, Editors H. Di Benedetto and L. Francken, pp. 53-60, Lyon, France, 1997.
17. "WI105: Specification of Modified Bitumen." CEN TC19 SC1 WG4, 1995.
18. "Asphalt Technology News." A Publication of the National Center for Asphalt Technology, Auburn University, Vol. 9, No. 1, p. 7, 1997.
19. Goodrich, J.L. "Asphalt and Polymer Modified Asphalt Properties Related to the Performance of Asphaltic Concrete Mixes." Proceedings of the Association of Asphalt Paving Technologists, Vol. 57, pp. 116-175, 1988.
20. Goodrich, J.L. "Asphaltic Binder Rheology, Asphalt Concrete Rheology and Asphalt Concrete Mix Properties." Journal of the Association of Asphalt Pavings Technologists, Vol. 60, pp. 80-120, 1991.
21. Philipps, M.C. "Developments in Specifications for Bitumens and Polymer-Modified Binders, Mainly from a Rheological Point of View." Proceedings of the 2nd European Symposium on the Performance and Durability of Bituminous Materials, Editor J.G. Cabrera, pp. 3-18, Leeds, 1997.
22. Van der Poel, C. "A General System Describing the Visco-Elastic Properties of Bitumen and its Relation to Routine Test Data." Journal of Applied Chemistry, Vol. 4, pp. 221-236, 1954.
23. Traxler, R.N. "The Physical Chemistry of Asphaltic Bitumen". Chemical Review, Vol. 19, No. 2, 1936.

24. Romberg, J.W., Nesmitts, S.D. and Traxler, R.N. "Some Chemical Aspects of the Components of Asphalt". *Journal of Chemical and Engineering Data*, Vol. 4, No. 2, April 1959.
25. Traxler, R.N. and Coombs, C.E. "The Colloidal Nature of Asphalt as Shown by its Flow Properties". Thirteenth Colloid Symposium, St. Louis, Missouri, June 1936.
26. Petersen, J.C. "Chemical Composition of Asphalt as Related to Asphalt Durability: State of the Art". TRR 999, Transportation Research Board, pp. 13-30, Washington D.C., 1984.
27. Halstead, W.J. "Relation of Asphalt Chemistry to Physical Properties and Specifications". *Proceedings of the Association of Asphalt Paving Technologists*, Vol. 54, pp. 91-117, 1985.
28. Wada, Y and Hirose, H. "Glass Transition Phenomena and Rheological Properties of Petroleum Asphalt". *Journal of the Physical Society of Japan*, 15(10): pp. 1885-1894, 1960.
29. Schmidt, R.J. and Barrall, E.M. "Asphalt Transitions". *Journal of the Institute of Petroleum*, 51(497): pp. 162-168, 1965.
30. Rostler, F.S. and White, R.M. "Influence of the Chemical Composition of Asphalts on Performance, Particularly Durability". STP 277, American Society for Testing and Materials, pp. 68-84, 1959.
31. Corbett. L.C. "Relationship Between Composition and Physical Properties of Asphalts". *Proceedings of the Association of Asphalt Paving Technologists*, Vol. 39, pp. 481-491, 1970.

32. Corbett, L.C. "Composition of Asphalt Based on Generic Fractionation Using Solvent Deasphalting, Elution-Adsorption Chromatography and Densimetric Characterisation". *Analytical Chemistry*, Vol. 41, pp. 576-579, 1969.
33. Torres, J., Gonzalez, J.Ma, and Peralta, X. "Correlation between the Fractionation of Bitumen according to the Methods ASTM D4124 and Iatrosan." *Proceedings of the 5th Eurobitume Congress, Stockholm, Volume 1A, 1.38*, pp. 203-208, 1993.
34. Isacsson, U. and Lu, X. "Testing and Appraisal of Polymer Modified Road Bitumens - State of the Art." *Materials and Structures*, Vol. 28, pp. 139-159, 1995.
35. Tallafigo, M.F. "Evolution of Chemical Composition of Bitumen during Oxidation in Laboratory with the Thin Film Oven Test Method." *Proceedings of the 5th Eurobitume Congress, Stockholm, Volume 1A, 1.40*, pp. 214-219, 1993.
36. Tallafigo, M.F. "Comparison between Oxidation Changes obtained in Laboratory with the Methods - Thin Film Oven Test and Thermal Stressing in a Rotating Flask." *Proceedings of the 5th Eurobitume Congress, Stockholm, Volume 1A, 1.41*, pp. 220-223, 1993.
37. Gaestel, C., Smadja, R. and Lamminan, K.A. "Contribution a la connaissance des bitumes routiers." *Revue Generale des Routes et Aerodromes*, No. 466, France, 1971.
38. Ozdemir, G. and Partl, M. "Application of High-Pressure Gel Permeation Chromatography (HP-GPC) to determine Trinidad Naturasphalt Content in Bituminous Binders." *Proceedings of the 5th Eurobitume Congress, Stockholm, Volume 1A, 1.42*, pp. 224-228, 1993.

39. Stroup-Gardiner, M. "The Significance of Phase Angle Measurements for Asphalt Cements." *Journal of the Association of Asphalt Paving Technologists*, Vol. 65, pp. 321-356, 1996.
40. Branthaver, J.F., Petersen, J.C., Robertson, R.E., Duvall, J.J., Kim, S.S., Harnsberger, P.M., Mill, T., Ensley, E.K., Barbour, F.A. and Schabron, J.F. "Binder Characterization and Evaluation, Volume 2: Chemistry." SHRP-A-368, Strategic Highways Research Program, National Research Council, Washington, D.C., 1994.
41. Santagata, E. and Montepara, A. "An NMR Based Method for the Chemical Characterisation and Rheological Selection of Modified Bitumens." *Proceedings of the 5th Eurobitume Congress, Stockholm, Volume 1A, 1.24*, pp. 143-147, 1993.
42. Mascherpa, A. and Vecchi, C. "Application of Instrumental Techniques like NMR and GPC in the Field of Polymer Modified Bitumens." *Proceedings of the Eurasphalt & Eurobitume Congress, Session 5: Binders - Functional Properties and Performance Testing, E&E.5.132*, Strasbourg, May 1996.
43. Pieri, N., Planche, J-P., Martin, D., Germanaud, L. and Kister, J. "A New Approach to Predict Rheological Properties of Bitumens from their Chemical Composition determined by FTIR and Synchronous U.V. Fluorescence." *Proceedings of the Eurasphalt & Eurobitume Congress, Session 5: Binders - Functional Properties and Performance Testing, E&E.5.120*, Strasbourg, May 1996.
44. Choquet, F.S. and Ista, E.J. "The Determination of SBS, EVA and APP Polymers in Modified Bitumens." *Polymer Modified Asphalt Binders*, Editors K.R. Wardlaw and S. Shuler, ASTM, STP 1108, pp. 35-49, 1992.

45. Kister, J., Pieri, N. and Germanaud, L. "Chemical Characterisation of Bitumen Hardening using FTIR and UV Synchronous Fluorescence." Proceedings of the 5th Eurobitume Congress, Stockholm, Volume 1A, 1.05, pp. 46-50, 1993.
46. Claudy, P., Letoffe, J.M., King, G., Planche, J.P. and Germanaud, L. "Using Thermoanalytical Methods to Characterise Bitumen Structure." Proceedings of the 5th Eurobitume Congress, Stockholm, Volume 1A, 1.08, pp. 61-65, 1993.
47. Shutt, R., Turmel, C. and Touzard, B. "Differential Scanning Calorimetry Analysis and Rheological Properties of Bitumens Modified by Semi-Crystalline Polymers." Proceedings of the 5th Eurobitume Congress, Stockholm, Volume 1A, 1.11, pp. 76-80, 1993.
48. Gazeau, S., Maze, M., Brule, B. and Perret, P. "Application of Differential Scanning Calorimetry (DSC) to the Characterisation of Ethylene Copolymers Modified Bitumen." Proceedings of the Eurasphalt & Eurobitume Congress, Session 5: Binders - Functional Properties and Performance Testing, E&E.5.109, Strasbourg, May 1996.
49. Brule, B. and Gazeau, S. "Characterisation of Rheological and Thermal Behaviour of Asphalt Cements Modified by Ethylene Copolymers." ACS Symposium on Modified Asphalts, Orlando, Florida, August 25-30, 1996.
50. Nellensteyn, F.J. "The Constitution of Asphalt." Journal of the Institute of Petroleum Technologists, Vol 10, pp. 311-325, 1924.
51. Mack, C.J. "Colloid Chemistry of Asphalts." Journal of Physical Chemistry, Vol. 36, pp. 2901-2914, 1932.
52. Pfeiffer, J.P. and Saal, R.N.J. "Asphaltic Bitumen as Colloidal System." Physical Chemistry, Vol. 44, pp. 139-149, 1940.

53. Labout, J.W.A. "Constitution of Asphaltic Bitumen." *The Properties of Asphaltic Bitumen*, J.P. Pfeiffer, Ed. Elsevier, New York, pp. 13-48, 1950.
54. Saal, R.N.J. and Labout, J.W.A. "Rheological Properties of Asphalts." *Rheology: Theory and Applications*, Vol. II, F.R. Eirich, Ed., New York, Academic Press, Chapter 9, 1958.
55. Girdler, R.B. "Constitution of Asphaltenes and Related Studies." *Proceedings of the Association of Asphalt Paving Technologists*, Vol. 34, pp. 45, 1965.
56. "Glossary of Rheological Terms - A Practical Summary of the Most Common Concepts." *Rheology of Bituminous Binders*, Edited by Eurobitume, 1996.
57. Emery, S.J. and Zacharias, M.P. "Temperature Susceptibility of South African Bitumens." *Proceedings of the 6th Conference on Asphalt Pavements for Southern Africa*, Vol. 2, pp. V13-V30, Cape Town, October 1994.
58. British Standard 2000: Part 49: 1983: "Penetration of Bituminous Materials."
59. British Standard 2000: Part 58: 1983: "Softening Point of Bitumen (Ring and Ball)."
60. Zacharias, M.P. and Emery, S.J. "Application of the Brookfield Viscometer Test Method in South African Road Grade Bitumen Specifications." *Proceedings of the 6th Conference on Asphalt Pavements for Southern Africa*, Vol. 2, pp. V109-V123, Cape Town, October 1994.
61. Bell, C.A. "Introduction to Bituminous Binders." *Residential Course on Bituminous Pavements*, Lecture Notes, University of Nottingham, 1992.
62. Collins, J.H., Bouldin, M.G., Gelles, R. and Berker, A. "Improved Performance

- of Paving Asphalts by Polymer Modification." *Journal of the Association of Asphalt Paving Technologists*, Vol. 60, pp. 43-79, 1991.
63. Anderson, D.A., Christensen, D.W. and Bahia, H. "Physical Properties of Asphalt Cement and the Development of Performance-Related Specifications." *Journal of the Association of Asphalt Technologists*, Vol. 60, pp. 437-532, 1991.
  64. Dukatz, E.L. and Anderson, D.A. "The effect of various fillers on the mechanical behaviour of asphalt and asphalt concrete." *Proceedings of the Association of Asphalt Paving Technologists*, Vol. 49, pp. 530-549, 1980.
  65. Anderson, D.A., Christensen, D.W., Bahia, H.U., Dongre, R., Sharma, M.G., Antle, C.E. and Button, J. "Binder Characterization, Volume 3: Physical Characterization." SHRP-A-369, Strategic Highways Research Program, National Research Council, Washington, D.C., 1994.
  66. Ferry, J.D. "Viscoelastic Properties of Polymers." New York: John Wiley and Sons, 1971.
  67. Traxler, R.N., Schweyer, H.E. and Romberg, H.W. "Rheological Properties of Asphalt." *Industrial and Engineering Chemistry*, Vol. 36, No. 9, pp. 823-829, 1944.
  68. Anderson, D.A., Dukatz, E.L. and Rosenberger, J.L. "Properties of Asphalt Cement and Asphaltic Concrete." *Proceedings of the Association of Asphalt Paving Technologists*, Vol. 52, pp. 291-324, 1983.
  69. Griffen, R.L., Miles, T.K., Penther, C.J. and Simpson, W.C. "Sliding Plate Microviscometer for Rapid Measurements of Asphalt Viscosity in Absolute Units." *American Society for Testing and Materials, ASTM Special Technical Publication*, Vol. 212, p. 36, 1956.



70. Moavenzadeh, J. and Stander, R.R., Jr. "Effect of Aging on Flow Properties of Asphalts." Highway Research Board Record, Vol. 178, pp. 1-29, 1967.
71. Romberg, J.W. and Traxler, R.N. "Rheology of Asphalt." Journal of Colloid Science, Vol. 2, pp. 33-47, 1947.
72. Puzinauskas, V.P. "Properties of Asphalt Cements." Proceedings of the Association of Asphalt Paving Technologists, Vol. 48, pp. 646-710, 1979.
73. Pfeiffer, J.Ph. and Van Doormal, P.M. "The Rheological Properties of Asphaltic Bitumens." Journal of the Institute of Petroleum, Vol. 22, pp. 414-440, 1936.
74. McLeod, N.W. "A 4-year Survey of Low Temperature Transverse Pavement Cracking on Three Ontario Test Roads." Proceedings of the Association of Asphalt Paving Technologists, Vol. 41, pp. 424-493, 1972.
75. Heukelom, W. "A Bitumen Test Data Chart for Showing the Effect of Temperature on the Mechanical Behaviour of Asphaltic Bitumens." Journal of the Institute of Petroleum Technologists, Vol. 55, pp. 404-417, 1969.
76. Heukelom, W. "An Improved Method of Characterising Asphaltic Bitumens with the Aid of their Mechanical Properties." Proceedings of the Association of Asphalt Paving Technologists, Vol. 42, pp. 62-98, 1973.
77. Heukelom, W. "Observations on the Rheology and Fracture of Bitumens and Asphalt Mixes." Proceedings of the Association of Asphalt Paving Technologists, Vol. 36, pp. 359-397, 1966.
78. Petersen, J.C., Robertson, R.E., Branthaver, J.F., Harnsberger, P.M., Duvall, J.J., Kim, S.S., Anderson, D.A., Christensen, D.W., Bahia, H.U., Dongre, R., Sharma,

- M.G., Antle, C.E., Button, J.W. and Glover, C.J. "Binder Characterization and Evaluation, Volume 4: Test Methods." SHRP-A-370, Strategic Highways Research Program, National Research Council, Washington, D.C., 1994.
79. Pink, H.S., Merz, R.E. and Bosniack, D.S. "Asphalt Rheology: Experimental Determination of Dynamic Moduli at Low Temperatures." Proceedings of the Association of Asphalt Technologists, Vol. 49, p. 64, 1980.
  80. Dobson, G.R. "The Dynamic Mechanical Properties of Bitumen." Proceedings of the Association of Asphalt Paving Technologists, Vol. 38, p. 123, 1969.
  81. Anderson, D.A., Christensen, D.W., Roque, R. and Robyak, R.A. "Rheological Properties of Polymer-Modified Emulsion Residue." Polymer Modified Asphalt Binders, Editors K.R. Wardlaw and S.Shuler, ASTM, STP 1108, pp. 20-34, 1992.
  82. Williams, M.L., Landel, R.F. and Ferry, J.D. "The Temperature-Dependence of Relaxation Mechanisms in Amorphous Polymers and Other Glass-Forming Liquids." Journal of the American Chemical Society, Vol. 77, pp. 3701-3706, 1955.
  83. Brodnyan, J.G., Gaskins, F.H., Philippoff, W. and Thelen, E. "The Rheology of Asphalt. III. Dynamic Mechanical Properties of Asphalt." Transactions of the Society of Rheology, Vol. 4, pp.279-296, 1960.
  84. Jongepier, R. and Kuilman, B. "Characterization of the Rheology of Bitumens." Proceedings of the Association of Asphalt Paving Technologists, Vol. 38, pp. 98-122, 1969.
  85. Nielsen, E. "Complex Modulus for Original and Hardened Binder." Proceedings of the Rheology of Bituminous Binders European Workshop, Eurobitume, Paper No. 28, Brussels, 1995.

86. Marasteanu, M. and Anderson, D.A. "Time-Temperature Dependency of Asphalt Binders - An Improved Model." *Journal of the Association of Asphalt Paving Technologists*, Vol. 65, pp. 408-448, 1996.
87. Schmidt, R.J. and Santucci, L.E. "A Practical Method for Determining the Glass Transition Temperature of Asphalts and Calculation of Their Low Temperature Viscosities." *Proceedings of the Association of Asphalt Paving Technologists*, Vol. 35, pp. 61-90, 1966.
88. Brule, B., Planche, J.P., King, G.N., Claudy, P. and Letoffe, J.M. "Characterisation of Paving Asphalts by Differential Scanning Calorimetry." *Fuel Science and Technology International*, 9(1), pp. 71-91, 1991.
89. Lesueur, D., Gerard, J.F., Claudy, P., Letoffe, J.M., Planche, J.P. and Martin, D. "A Structure-Related Model to Describe Bitumen Linear Viscoelasticity." *Proceedings of the Eurasphalt & Eurobitume Congress, Session 5: Binders - Functional Properties and Performance Testing, E&E.5.114, Strasbourg, May 1996.*
90. Planche, J.P., Lesueur, D., Hines, M.L. and King, G.N. "Evaluation of Elastomer Modified Bitumens using SHRP Binder Specifications." *Proceedings of the Eurasphalt & Eurobitume Congress, Session 5: Binders - Functional Properties and Performance Testing, E&E.5.121, Strasbourg, May 1996.*
91. Dickinson, E.J. and Witt, H.P. "The Dynamic Shear Modulus of Paving Asphalts as a Function of Frequency." *Transaction of the Society of Rheology*, Vol. 18, No. 4, pp. 591-605, 1974.
92. Dobson, G.R. "On the Development of Rational Specifications for the Rheological Properties of Bitumens." *Journal of the Institute of Petroleum*, Vol.

58, No. 559, pp.14-24, 1972.

93. Christensen, D.W. and Anderson, D.A. "Interpretation of Dynamic Mechanical Test Data for Paving Grade Asphalt Cements." *Journal of the Association of Asphalt Paving Technologists*, Vol. 61, pp. 67-116, 1992.
94. Anderson, D.A. and Kennedy, T.W. "Development of SHRP Binder Specification." *Journal of the Association of Asphalt Paving Technologists*, Vol. 62, pp. 481-507, 1993.
95. Lewis, R.H. and Welborn, J.Y. "Report on the Properties of the Residues of 50-60 and 85-100 Penetration Asphalts from Oven Tests and Exposure." *Proceedings of the Association of Asphalt Paving Technologists*, Vol. 11, pp. 86-157, 1940.
96. "Annual Book of ASTM Standards." Vol. 04.03, ASTM, Philadelphia.
97. Hveem, F.N., Zube, E. and Skog, J. "Proposed New Tests and Specifications for Paving Grade Asphalts." *Proceedings of the Association of Asphalt Paving Technologists*, Vol. 32, pp. 247-327, 1963.
98. "The Rolling Thin Film Oven Test." *Shell Bitumen Review* 42, pp. 18-19, 1973.
99. Brown, S.F., Rowlett, R.D. and Boucher, J.L. "Asphalt Modification." *Proceedings of the Conference on US SHRP Highway Research Program: Sharing the Benefits*, ICE, pp. 181-203, 1990.
100. Terrel, R.L. and Epps, J.A. "Asphalt Modifiers." *A Users Manual for Additives and Modifiers in Hot Mix Asphalt*. National Asphalt Paving Association, 1988.
101. Cooper, K.E. and Brown, S.F. "Comparative Testing to Establish the Effect of 'Chemcrete' on Basecourse and Roadbase Materials used on a Full Scale Trial."

University of Nottingham, 1987.

102. Cooper, K.E. and Brown, S.F. "Early Life Tests on Rolled Asphalt Wearing Course: The Effect of 'Chemcrete'." University of Nottingham, 1987.
103. Denning, J.H. and Carswell, J. "Improvements in Rolled Asphalt Surfacing by the Addition of Sulphur." Transport and Road Research Laboratory, Report LR 963, 1981.
104. Goos, D. and Carre, D. "Rheological Modelling of Bituminous Binders a Global approach to Road Technologies." Proceedings of the Eurasphalt & Eurobitume Congress, Session 5: Binders - Functional Properties and Performance Testing, E&E.5.111, Strasbourg, May 1996.
105. Loeber, L., Durand, A., Muller, G., Morel, J., Sutton, O. and Bargiacchi, M. "New Investigations on the Mechanism of Polymer-Bitumen Interaction and Their Practical Application for Binder Formulation." Proceedings of the Eurasphalt & Eurobitume Congress, Session 5: Binders - Functional Properties and Performance Testing, E&E.5.115, Strasbourg, May 1996.
106. Cavaliere, M.G., Diani, E. and Vitalini Sacconi, L. "Polymer Modified Bitumens for Improved Road Application." Proceedings of the 5th Eurobitume Congress, Stockholm, Volume 1A, 1.23, pp. 138-142, 1993.
107. Cotte, C. and Such, C. "Influence of RTFOT Ageing on the Rheological Behaviour of Polymer Modified Bitumen and Their Associated Phases." Proceedings of the Eurasphalt & Eurobitume Congress, Session 5: Binders - Functional Properties and Performance Testing, E&E.5.105, Strasbourg, May 1996.
108. Bonemazzi, F., Braga, V., Corrieri, R., Giavarini, C. and Sartori, F.

- “Correlation between the Properties of Polymers and of Polymer-Modified Bitumens.” Proceedings of the Euraspalt & Eurobitume Congress, Session 5: Binders - Functional Properties and Performance Testing, E&E.5.128, Strasbourg, May 1996.
109. Bull, A.L. and Vonk, W.C. “Thermoplastic rubber/bitumen blends for roof and road.” Shell Chemical Technical Manual TR 8. 15, 1984.
110. American Association of State Highway and Transportation Officials. AASHTO TP5. “Standard Test Method for Determining the Rheological Properties of Asphalt Binder Using a Dynamic Shear Rheometer (DSR).” AASHTO, Washington, D.C., 1995.
111. Francken, L. “RILEM Interlaboratory Test Programme on Bituminous Binders.” Proceedings of the Rheology of Bituminous Binders European Workshop, Eurobitume, Paper No.12, Brussels, 1995.
112. Francken, L. “RILEM Interlaboratory Test on Binder Rheology.” Proceedings of the Fifth International RILEM Symposium, Mechanical Test for Bituminous Materials - Recent Improvements and Future Prospects, Editors H. Di Benedetto and L. Francken, Lyon, France, pp. 3-7, 1997.
113. Teugels, W. and Gustavsson, B. “Practical Experience in Working with a Controlled Stress Rheometer.” Proceedings of the Rheology of Bituminous Binders European Workshop, Eurobitume, Paper No.3, Brussels, 1995.
114. Green, P.J. and Claxton, M.J. “The Measurement of Bitumen Rheology Using the Carrimed Controlled Stress Rheometer.” Proceedings of the Rheology of Bituminous Binders European Workshop, Eurobitume, Paper No.5, Brussels, 1995.

115. Teugels, W. and Nilsson, A.M. "Comparison of Two Different Temperature Control Systems on a Controlled Stress Rheometer." Proceedings of the Rheology of Bituminous Binders European Workshop, Eurobitume, Paper No.3, Brussels, 1995.
116. Cointe, F. and Monnoye, R. "Correlation between Two Dynamic Rheometers: Rheometrics RDA II and Bohlin CS 50." Proceedings of the Rheology of Bituminous Binders European Workshop, Eurobitume, Paper No.4, Brussels, 1995.
117. Anderson, D.A. and Knechtel, K. "Factors Affecting the Precision of the Dynamic Shear and Bending Beam Rheometers." Proceedings of the Fifth International RILEM Symposium, Mechanical Test for Bituminous Materials - Recent Improvements and Future Prospects, Editors H. Di Benedetto and L. Francken, Lyon, France, pp. 79-86, 1997.
118. Dobson, G.R. "An Apparatus for Measuring the Dynamic Elastic Properties of Bitumens." Journal of Scientific Instrumentation, Vol. 44, p 375, 1967.
119. Dobson, G.R. "Viscoelastic Properties of Bitumens. What to Measure and What Can Go Wrong." Proceedings of the Rheology of Bituminous Binders European Workshop, Eurobitume, Paper No.23, Brussels, 1995.
120. Serfass, J.P., Joly, A. and Samanos, J. "SBS-modified Asphalts for Surface Dressing - A Comparison between Hot-applied and Emulsified Binders." Polymer Modified Asphalt Binders, Editors K.R. Wardlaw and S. Shuler, ASTM, STP 1108, pp. 281-308, 1992.
121. Bernard, B. Private Communication, 1997.
122. Puzinauskas, V.P. "Evaluation of Properties of Asphalt Cements with

Emphasis on Consistencies at Low Temperatures, Proceedings of the Association of Asphalt Paving Technologists, Vol. 36, pp. 489-512, 1967.

123. Dony, A. and Turmel, C. "Polymer Bitumen Blends; Let Us Fit Our Tests to Today's Techniques." Proceedings of the 5th Eurobitume Congress, Stockholm, Volume 1A, 1.09, pp. 66-70, Stockholm, 1993.
124. King, G.N., King, H.W., Chaverot, P., Planche, J.P. and Harders, O. "Using European Wheel-tracking and Restrained Tensile Tests to Validate SHRP Performance-graded Binder Specifications for Polymer Modified Asphalts." Proceedings of the 5th Eurobitume Congress, Stockholm, Volume 1A, 1.06, pp. 51-55, 1993.
125. Lenoble, C., Vercoe, T. and Soto, T. "Rheology as a Performance Indicator for Modified Bitumen." Proceedings of the 5th Eurobitume Congress, Stockholm, Volume 1A, 1.10, pp. 71-75, 1993.
126. Di Benedetto, H. and Des Croix, P. "Binder-Mix Rheology: Limits of Linear Domain, Non Linear Behaviour." Proceedings of the Eurasphalt & Eurobitume Congress, Session 5: Binders - Functional Properties and Performance Testing, E&E.5.107, Strasbourg, May 1996.
127. Linde, S. and Johansson, U. "Thermo-oxidative Degradation of Polymer Modified Bitumen." Polymer Modified Asphalt Binders, Editors K.R. Wardlaw and S. Shuler, ASTM, STP 1108, 1992.
128. Kuppens, E.A.M. "Ageing Resistance of Bitumen." Proceedings of the Rheology of Bituminous Binders European Workshop, Eurobitume, Paper No.49, Brussels, 1995.



**Appendix A**  
**DSR Testing Protocol**

## Testing Protocol for

# **Determining the Rheological Properties of Bitumen Using the Bohlin Model DSR50 Dynamic Shear Rheometer**

## **1 SCOPE**

This test method covers the determination of the complex shear modulus and phase angle of bitumen when tested in dynamic (oscillatory) shear using parallel plate test geometry. It is applicable to bitumens having complex modulus values between 100 Pa to 10 MPa, generally found between 10°C to 85°C. The test method is intended for determining the linear viscoelastic properties and not the full viscoelastic properties of bitumen.

## **2 DEFINITIONS**

- 2.1 Complex shear modulus,  $G^*$  - ratio of the absolute value of the peak-to-peak shear stress,  $\sigma$ , divided by the absolute value of the peak-to-peak shear strain,  $\gamma$ .
- 2.2 Phase angle,  $\delta$  - the angle in degrees between a sinusoidally applied strain and the resultant sinusoidal stress in a controlled strain testing mode, or between the applied stress and resultant strain in a controlled stress testing mode.
- 2.3 Storage shear modulus,  $G'$  - the complex shear modulus multiplied by the cosine of the phase angle expressed in degrees. It represents the in-phase component of the complex modulus that is a measure of the energy stored during a loading cycle.
- 2.4 Loss shear modulus,  $G''$  - the complex shear modulus multiplied by the sine of the phase angle expressed in degrees. It represents the component of the complex

modulus that is a measure of the energy lost (dissipated) during a loading cycle.

- 2.5 Parallel plate geometry - a testing geometry in which the test sample is sandwiched between two relatively rigid parallel plates and subjected to oscillatory shear.
- 2.6 Oscillatory shear - refers to a type of loading in which a shear stress or shear strain is applied to a test sample in an oscillatory manner such that the shear stress or strain varies in amplitude about zero in a sinusoidal manner.
- 2.7 Linear viscoelastic - refers to a region of behaviour in which the dynamic shear modulus is independent of shear stress or strain.

### **3 APPARATUS**

The Dynamic Shear Rheometer test system consists of parallel metal plates, an environmental water chamber, a loading device and a control and data acquisition system.

- 3.1 Test plates - metal test plates with smooth polished surfaces, one 8 mm in diameter and one 25 mm in diameter. Base plate consisting of a flat 2 mm raised plate with a 25 mm diameter, as shown in Figure A1.
- 3.2 Environmental water chamber - to control the test specimen temperature. A separate circulating bath temperature control unit (TCU) is required to pump the bath water through the test chamber. The environmental water chamber and the TCU can control the temperature of the specimen to an accuracy of  $\pm 0.1^\circ\text{C}$ . The chamber completely encloses the top and bottom plates to minimise thermal gradients.

- 3.3 Loading device - The loading device applies a sinusoidal oscillatory load to the specimen at various frequencies. When the load is strain controlled, the loading device applies a cyclic torque sufficient to cause an angular rotational strain accurate within 100  $\mu$ rad of the specified strain. If the load is stress controlled, the loading device applies a cyclic torque accurate to within 10 mN.m of the specified torque.
- 3.4 Control and Data Acquisition System - provides a record of the test temperature, frequency, deflection angle and torque. In addition, the system calculates and records the shear stress, shear strain, complex modulus,  $G^*$ , and phase angle,  $\delta$ .

#### **4 PREPARATION OF APPARATUS**

- 4.1 Mount lower test plate and either the 25 mm or 8 mm diameter, depending on testing temperature range, upper test plate on the DSR and tighten firmly.
- 4.2 Establish the zero gap level for the test plates, at a temperature corresponding to the middle of the expected testing temperature range, by manually spinning the moveable top plate. While the plate is spinning, close the gap until the movable plate touches the bottom fixed plate. The zero gap is reached when the plate stops spinning completely.
- 4.3 Move the plates apart and establish a gap setting of 1 mm plus 0.05 mm (for the 25 mm diameter test specimens) or 2 mm plus 0.05 mm (for the 8 mm diameter test specimens).

## **6 PREPARING SAMPLES AND TEST SPECIMENS**

- 6.1 Heat bitumen to be tested until it is sufficiently fluid to pour the required test specimen, stirring occasionally during the heating process to ensure homogeneity and to remove air bubbles.
- 6.2 Heat the plates in the environmental water chamber to a temperature of approximately 65°C for penetration grade bitumens and 85°C for polymer modified bitumens (PMB's).
- 6.3 Remove the cover of the environmental water chamber and raise the loading mechanism and upper plate to provide enough room to pour the bitumen specimen.
- 6.4 Dry the surfaces of both plates to ensure that the bitumen specimen adheres to both plates uniformly.
- 6.5 Pour a sufficient amount of bitumen onto the centre of the bottom fixed plate to ensure that the bitumen is uniformly squeezed out between the plates for trimming.
- 6.6 Lower the loading mechanism and the upper plate to the gap width plus 0.05 mm, squeezing out the excess bitumen from between the two plates.
- 6.7 Trim the excess bitumen from the specimen by moving a heated trimming tool around the upper and lower plate perimeters.
- 6.8 When the trimming is completed, decrease the gap by 0.05 mm to the desired testing gap. This will cause a slight bulging of the bitumen at the periphery of the test specimen.

- 6.9 Replace the cover of the environmental water chamber, ensuring that both the upper and lower plates and the bitumen specimen are immersed in the water.

## **7 TESTING PROCEDURE**

- 7.1 Bring the specimen to the required test temperature corresponding to the lowest temperature of the required testing temperature range.
- 7.2 Start the test after the temperature has remained at the desired temperature  $\pm 0.1^\circ\text{C}$  for at least 10 minutes.
- 7.3 When operating in strain controlled mode, vary the strain value from 0.5% at  $10^\circ\text{C}$  uniformly to 10% at  $85^\circ\text{C}$ . These strains are within the linear region defined at small strains where the complex modulus is relatively independent of shear strain. This region varies with the magnitude of complex modulus and is defined as the range of strains where the complex modulus is 95% or more of the zero-strain value. This linear region can be determined by strain sweeps, as shown in Figure A2, which need to be performed at a temperature of  $20^\circ\text{C}$ ,  $40^\circ\text{C}$  and  $60^\circ\text{C}$  before fundamental testing is undertaken.
- 7.4 Increase the testing temperature to the next temperature and repeat the testing procedure. The tests should be performed from the lowest to the highest temperature to limit the testing time required to determine the rheological characteristics of the bitumen.

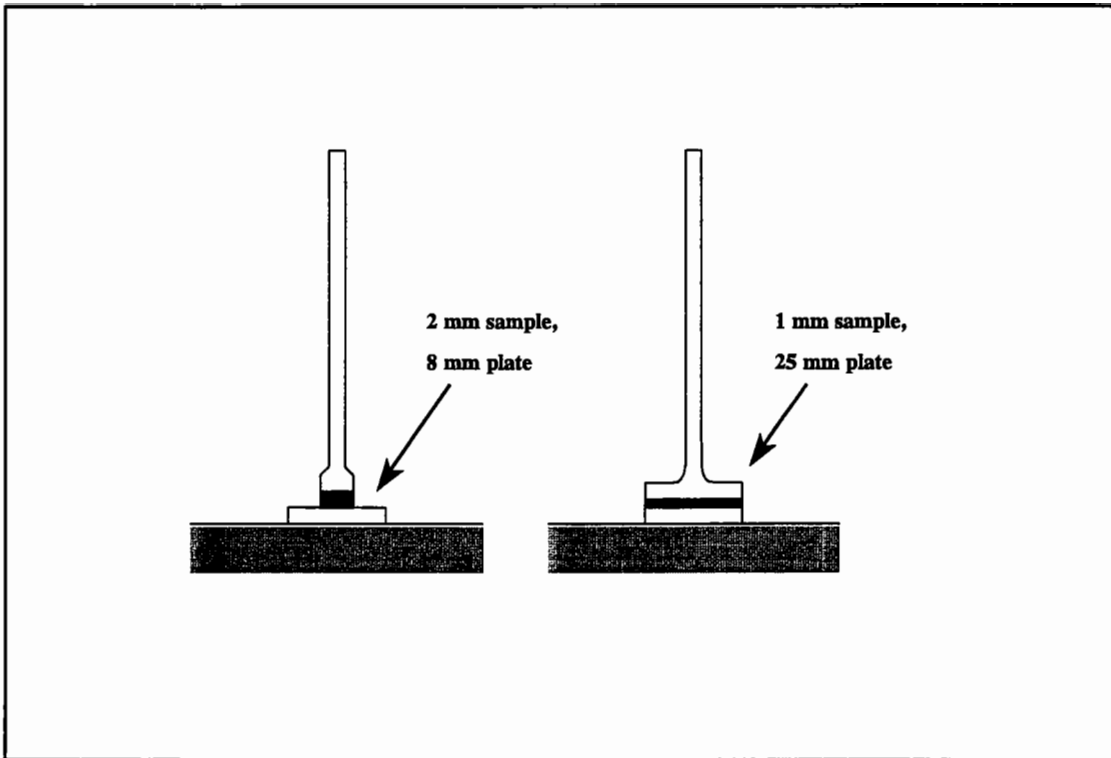


Figure A1: DSR bitumen test configurations

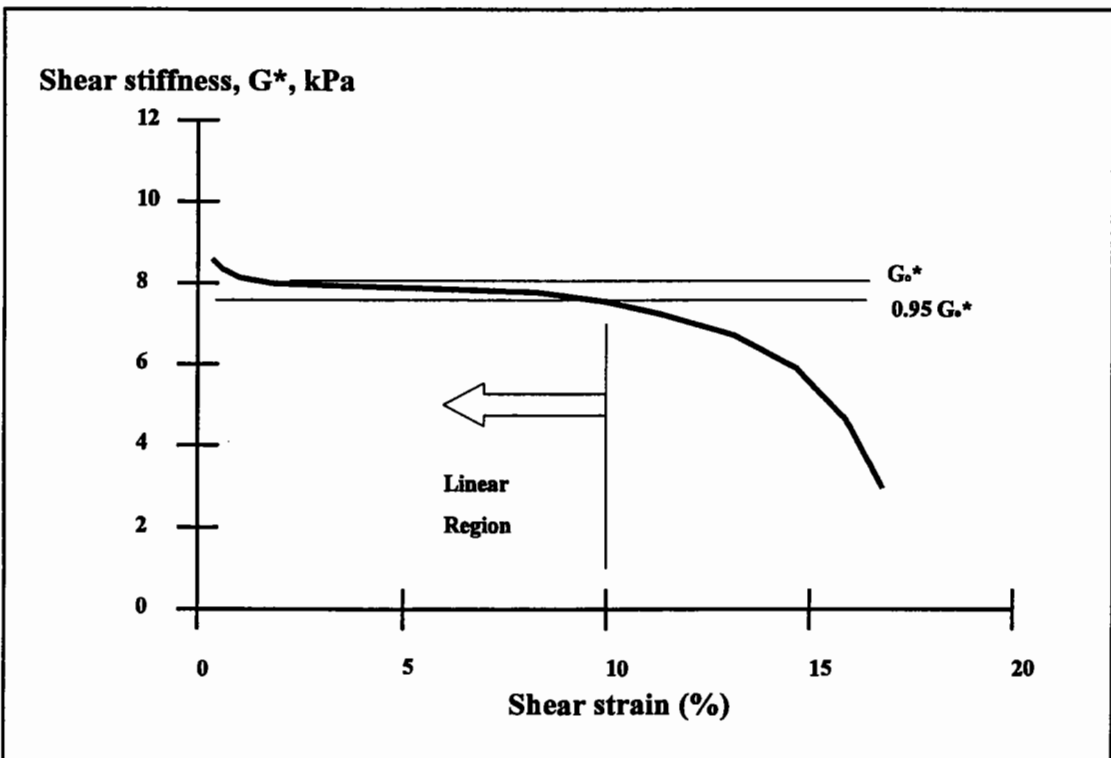


Figure A2: Strain sweeps used to determine linear region

**Appendix B**  
**DSR Data for Unaged Bitumens**  
**and PMB's**



## Middle East 80/100 penetration grade bitumen

### Complex modulus (Pa)

Freq\Temp	10°C	15°C	25°C	35°C	45°C	55°C	65°C	75°C
0.01 Hz	459500	142500	13200	1455	227	41	10	3
0.015 Hz	613500	200500	19000	2050	331	60	15	4
0.02 Hz	760000	252000	24800	2790	447	82	20	6
0.05 Hz	1490000	515000	54350	6455	1100	203	50	15
0.1 Hz	2360000	863500	97800	12300	2150	398	100	28
0.15 Hz	3110000	1150000	136000	18400	3135	599	150	44
0.2 Hz	3740000	1405000	173000	24000	4110	797	201	59
0.5 Hz	6565000	2650000	360000	54450	9720	1945	496	148
1 Hz	9725000	4155000	617500	99050	18500	3780	982	293
1.5 Hz	12100000	5385000	843500	139500	26800	5560	1455	439
2 Hz	14050000	6415000	1040000	177500	34750	7295	1935	583
5 Hz	22050000	10900000	1995000	368000	78300	17200	4665	1440
10 Hz	29700000	15600000	3170000	614000	140500	32000	8885	2760
15 Hz	34600000	18900000	4105000	804000	194500	46350	12600	3940

### Phase angle (degrees)

Freq\Temp	10°C	15°C	25°C	35°C	45°C	55°C	65°C	75°C
0.01 Hz	72	73	82	86	89	89	90	89
0.015 Hz	67	71	81	85	88	89	90	89
0.02 Hz	66	70	79	85	88	89	89	89
0.05 Hz	63	67	77	83	87	89	89	89
0.1 Hz	59	66	75	82	86	88	89	89
0.15 Hz	58	64	73	81	85	88	89	90
0.2 Hz	57	63	73	80	85	87	89	90
0.5 Hz	53	59	70	77	83	86	88	89
1 Hz	49	57	68	75	81	85	88	89
1.5 Hz	48	55	67	74	80	85	87	89
2 Hz	46	53	66	73	80	84	87	89
5 Hz	42	49	63	68	77	82	86	88
10 Hz	39	46	60	63	75	81	85	87
15 Hz	38	44	58	59	74	80	84	84

## Russian 80 penetration grade bitumen

### Complex modulus (Pa)

Freq\Temp	10°C	15°C	25°C	35°C	45°C	55°C	65°C
0.01 Hz	294000	100850	8530	1004	136	27	6
0.015 Hz	420500	147500	12400	1435	209	38	9
0.02 Hz	545500	186500	16050	1890	278	50	12
0.05 Hz	1120000	405000	37400	4450	686	127	31
0.1 Hz	1890000	700500	69350	8570	1355	250	63
0.15 Hz	2545000	957000	99300	12700	1990	372	93
0.2 Hz	3095000	1185000	127500	16650	2625	496	123
0.5 Hz	5645000	2330000	277500	38850	6365	1215	305
1 Hz	8575000	3745000	492500	73150	12350	2400	601
1.5 Hz	10850000	4880000	685000	105000	18150	3555	899
2 Hz	12700000	5855000	857000	136000	23750	4705	1190
5 Hz	20300000	10150000	1725000	301000	55500	11400	2915
10 Hz	27750000	14800000	2810000	527500	102500	21900	5655
15 Hz	32550000	17950000	3640000	713000	141500	31500	8190

### Phase angle (degrees)

Freq\Temp	10°C	15°C	25°C	35°C	45°C	55°C	65°C
0.01 Hz	75	79	84	84	87	89	89
0.015 Hz	73	76	84	86	88	89	90
0.02 Hz	71	76	83	86	88	89	89
0.05 Hz	67	73	81	85	87	88	89
0.1 Hz	64	70	79	85	87	88	89
0.15 Hz	62	68	78	84	87	88	89
0.2 Hz	61	67	77	83	86	88	89
0.5 Hz	56	63	75	82	86	87	88
1 Hz	53	60	73	80	85	87	88
1.5 Hz	51	58	71	79	84	87	88
2 Hz	49	56	70	78	84	87	88
5 Hz	44	52	66	74	82	86	88
10 Hz	41	48	63	69	80	85	87
15 Hz	39	46	61	65	79	84	86

## Venezuelan 70/100 penetration grade bitumen

### Complex modulus (Pa)

Freq\Temp	10°C	15°C	25°C	35°C	45°C	55°C	65°C	75°C
0.01 Hz	150500	48500	6720	901	143	29	7	2
0.015 Hz	207500	67800	9680	1290	213	42	11	3
0.02 Hz	265000	87000	12600	1730	286	58	14	5
0.05 Hz	536000	179000	28300	3970	708	146	36	11
0.1 Hz	918500	310000	53250	7655	1385	291	73	22
0.15 Hz	1180000	419000	75350	11000	2040	439	110	33
0.2 Hz	1415000	525000	95300	14350	2680	588	146	45
0.5 Hz	2650000	1050000	199500	32750	6300	1440	363	108
1 Hz	4165000	1740000	343000	59950	11850	2810	720	215
1.5 Hz	5370000	2290000	463500	85100	17200	4115	1070	323
2 Hz	6445000	2790000	572500	109000	22200	5395	1410	430
5 Hz	11100000	5060000	1060000	232500	49900	12600	3375	1070
10 Hz	16050000	7710000	1565000	401500	89200	23400	6465	2060
15 Hz	20000000	9520000	1845000	532500	124000	32550	9055	2980

### Phase angle (degrees)

Freq\Temp	10°C	15°C	25°C	35°C	45°C	55°C	65°C	75°C
0.01 Hz	73	76	81	85	89	89	90	90
0.015 Hz	70	73	80	86	89	89	90	90
0.02 Hz	70	73	80	85	88	89	90	89
0.05 Hz	67	71	77	83	87	89	89	89
0.1 Hz	65	69	76	82	86	89	90	89
0.15 Hz	64	68	75	81	85	88	89	89
0.2 Hz	63	68	74	80	85	88	89	89
0.5 Hz	60	65	73	78	83	86	89	89
1 Hz	57	63	72	77	81	85	88	89
1.5 Hz	55	61	70	75	81	85	87	88
2 Hz	54	60	70	74	80	84	87	88
5 Hz	50	57	68	71	78	82	85	87
10 Hz	47	54	66	67	76	81	84	86
15 Hz	45	52	65	65	76	81	83	85

### 3% EVA with 97% Middle East 80/100 pen bitumen

#### Complex modulus (Pa)

Freq\Temp	10°C	15°C	25°C	35°C	45°C	55°C	65°C	75°C
0.01 Hz	676000	256500	33300	4395	563	94	23	5
0.015 Hz	859000	341500	44750	6155	826	139	34	8
0.02 Hz	1070000	408500	56150	7865	1090	184	45	11
0.05 Hz	1940000	745500	104000	16450	2495	444	110	27
0.1 Hz	2950000	1200000	169500	28050	4630	875	217	54
0.15 Hz	3690000	1570000	230500	37800	6715	1290	325	82
0.2 Hz	4310000	1870000	286000	47250	8675	1685	431	109
0.5 Hz	7150000	3285000	545500	94150	18950	3890	1020	268
1 Hz	10200000	4920000	879000	157500	33400	7180	1920	524
1.5 Hz	12600000	6170000	1160000	211500	46300	10200	2760	775
2 Hz	14600000	7205000	1405000	261000	57800	13050	3540	1020
5 Hz	22500000	11700000	2535000	503500	117000	28100	7830	2400
10 Hz	30200000	16300000	3850000	819000	194000	48950	13900	4490
15 Hz	35100000	18900000	4740000	1075000	257000	66850	18800	6270

#### Phase angle (degrees)

Freq\Temp	10°C	15°C	25°C	35°C	45°C	55°C	65°C	75°C
0.01 Hz	58	63	69	78	84	85	88	88
0.015 Hz	58	61	67	78	85	87	88	88
0.02 Hz	57	60	67	78	84	86	87	87
0.05 Hz	54	58	65	74	82	85	87	88
0.1 Hz	53	57	64	72	80	84	86	88
0.15 Hz	52	56	63	71	79	83	85	88
0.2 Hz	51	56	63	70	78	82	85	88
0.5 Hz	48	53	61	68	75	80	83	87
1 Hz	46	51	60	66	73	78	81	87
1.5 Hz	44	50	59	66	72	77	80	86
2 Hz	43	49	59	65	71	76	80	86
5 Hz	40	46	57	64	69	74	78	84
10 Hz	37	43	55	62	67	73	77	82
15 Hz	36	42	54	61	65	72	76	80

## 5% EVA with 95% Middle East 80/100 pen bitumen

### Complex modulus (Pa)

Freq\Temp	10°C	15°C	25°C	35°C	45°C	55°C	65°C	75°C
0.01 Hz	899000	368500	55150	8810	1045	182	44	9
0.015 Hz	1170000	486000	70500	11750	1505	253	62	14
0.02 Hz	1355000	595000	87450	14350	1970	330	81	18
0.05 Hz	2385000	1013500	156500	27500	4300	769	190	44
0.1 Hz	3350000	1540000	251000	43150	7530	1420	360	86
0.15 Hz	4050000	1900000	330500	58350	10600	2070	523	128
0.2 Hz	4630000	2220000	392500	71600	13350	2670	681	171
0.5 Hz	7305000	3655000	691500	132000	26750	5880	1540	416
1 Hz	10150000	5210000	1055000	208000	44450	10400	2800	807
1.5 Hz	12250000	6390000	1345000	271000	59700	14400	3940	1185
2 Hz	14000000	7370000	1590000	325000	73150	18050	5005	1560
5 Hz	20600000	11450000	2695000	587000	138000	36250	10450	3620
10 Hz	27000000	15450000	3905000	902000	218500	60050	18050	6675
15 Hz	31200000	18050000	4760000	1175000	282500	78000	24250	9230

### Phase angle (degrees)

Freq\Temp	10°C	15°C	25°C	35°C	45°C	55°C	65°C	75°C
0.01 Hz	56	57	62	71	79	82	85	85
0.015 Hz	52	54	59	70	79	82	83	87
0.02 Hz	51	54	58	69	78	82	83	86
0.05 Hz	49	52	58	66	76	81	82	87
0.1 Hz	47	51	57	64	73	80	82	87
0.15 Hz	46	50	57	62	72	79	81	87
0.2 Hz	46	50	56	62	71	78	80	87
0.5 Hz	43	47	55	60	68	75	78	86
1 Hz	41	46	54	59	66	73	77	85
1.5 Hz	40	45	54	59	64	72	75	84
2 Hz	39	44	53	59	64	71	75	83
5 Hz	37	41	51	58	62	68	73	81
10 Hz	35	39	50	58	60	67	71	79
15 Hz	34	38	49	57	59	66	71	78

## 7% EVA with 93% Middle East 80/100 pen bitumen

### Complex modulus (Pa)

Freq\Temp	10°C	15°C	25°C	35°C	45°C	55°C	65°C	75°C
0.01 Hz	1420000	643500	105500	18700	2085	351	71	16
0.015 Hz	1675000	778000	140000	24300	2900	498	116	23
0.02 Hz	2010000	911000	163000	29600	3700	635	153	31
0.05 Hz	3095000	1495000	273000	54200	7780	1400	346	76
0.1 Hz	4380000	2155000	416500	83700	13050	2490	633	150
0.15 Hz	5430000	2730000	535500	106000	17400	3480	912	222
0.2 Hz	6140000	3110000	630500	125000	21600	4440	1180	292
0.5 Hz	9165000	4775000	1055000	218500	42500	9320	2540	700
1 Hz	12200000	6500000	1540000	332000	68800	16000	4470	1350
1.5 Hz	14400000	7735000	1915000	423000	90550	21850	6200	1950
2 Hz	16100000	8715000	2235000	502500	109500	27100	7765	2540
5 Hz	23000000	12850000	3605000	866500	193500	52900	15700	5650
10 Hz	29450000	16900000	5055000	1300000	292000	85750	25900	9890
15 Hz	33950000	19800000	6045000	1610000	366000	112000	34050	12900

### Phase angle (degrees)

Freq\Temp	10°C	15°C	25°C	35°C	45°C	55°C	65°C	75°C
0.01 Hz	51	50	55	68	72	69	75	84
0.015 Hz	46	49	54	65	73	75	79	85
0.02 Hz	46	48	53	65	73	75	79	85
0.05 Hz	44	46	52	61	71	75	79	86
0.1 Hz	42	46	52	58	69	75	78	86
0.15 Hz	41	45	51	56	68	74	77	86
0.2 Hz	41	44	51	55	67	74	77	85
0.5 Hz	39	43	50	54	63	71	74	84
1 Hz	38	41	49	54	61	69	73	83
1.5 Hz	37	40	48	54	59	68	71	82
2 Hz	36	40	48	54	58	67	71	81
5 Hz	34	38	46	53	56	65	68	78
10 Hz	33	37	45	53	54	63	66	75
15 Hz	32	36	44	52	53	62	65	73

### 3% EVA with 97% Russian 80 pen bitumen

#### Complex modulus (Pa)

Freq\Temp	10°C	15°C	25°C	35°C	45°C	55°C	65°C	75°C
0.01 Hz	486000	159000	16450	2280	400	111	11	3
0.015 Hz	705500	225500	23100	3350	639	152	18	4
0.02 Hz	860000	280500	29700	4380	796	181	24	5
0.05 Hz	1700000	546500	62250	8950	1615	340	58	13
0.1 Hz	2760000	956000	107500	15800	2780	594	106	26
0.15 Hz	3565000	1275000	148500	22400	3930	837	154	39
0.2 Hz	4230000	1565000	189000	28400	4980	1045	202	52
0.5 Hz	7365000	2950000	385500	60600	10750	2245	473	127
1 Hz	10850000	4610000	655000	107000	19200	4050	905	250
1.5 Hz	13600000	5930000	894000	148000	26900	5725	1310	372
2 Hz	15850000	7125000	1110000	186000	34200	7360	1710	490
5 Hz	24550000	12000000	2120000	378000	73100	16250	3970	1190
10 Hz	32850000	17150000	3375000	620000	128000	29350	7365	2310
15 Hz	37900000	20650000	4280000	803000	176500	41100	10400	3370

#### Phase angle (degrees)

Freq\Temp	10°C	15°C	25°C	35°C	45°C	55°C	65°C	75°C
0.01 Hz	69	72	71	73	61	11	74	90
0.015 Hz	65	69	71	72	64	53	82	90
0.02 Hz	65	69	72	73	65	55	83	89
0.05 Hz	61	66	71	73	69	64	83	89
0.1 Hz	59	64	71	74	72	69	83	89
0.15 Hz	57	63	71	74	73	71	83	90
0.2 Hz	56	62	70	73	73	72	83	89
0.5 Hz	52	59	69	73	75	75	83	89
1 Hz	49	56	67	73	75	76	83	88
1.5 Hz	47	54	66	72	75	77	82	88
2 Hz	46	53	65	72	75	77	82	87
5 Hz	42	49	62	71	74	77	81	85
10 Hz	39	46	60	69	73	77	81	84
15 Hz	37	44	58	67	72	77	80	82

## 5% EVA with 95% Russian 80 pen bitumen

### Complex modulus (Pa)

Freq\Temp	10°C	15°C	25°C	35°C	45°C	55°C	65°C	75°C
0.01 Hz	613500	224500	29800	6315	2100	842	47	4
0.015 Hz	791500	295500	40450	7875	2330	906	65	6
0.02 Hz	960500	359500	48850	9195	2570	948	77	8
0.05 Hz	1765000	665000	91200	16900	3760	1185	138	20
0.1 Hz	2715000	1055000	146500	26950	5815	1535	230	40
0.15 Hz	3495000	1380000	198500	35100	7520	1915	315	61
0.2 Hz	4140000	1660000	246000	42800	9090	2265	393	80
0.5 Hz	7020000	2965000	469500	81200	17350	4160	823	197
1 Hz	10250000	4510000	755500	133000	28600	6850	1455	390
1.5 Hz	12650000	5760000	991000	178500	38550	9340	2040	576
2 Hz	14750000	6815000	1205000	219500	47850	11600	2590	761
5 Hz	22900000	11250000	2210000	423500	94000	23200	5555	1800
10 Hz	30800000	16000000	3420000	690000	155500	39150	9755	3350
15 Hz	35700000	19050000	4350000	918000	204000	51750	13400	4690

### Phase angle (degrees)

Freq\Temp	10°C	15°C	25°C	35°C	45°C	55°C	65°C	75°C
0.01 Hz	61	60	59	44	24	13	36	88
0.015 Hz	59	60	59	52	28	17	48	87
0.02 Hz	58	60	59	54	33	19	51	88
0.05 Hz	56	58	61	59	45	29	60	88
0.1 Hz	55	59	62	61	52	41	65	88
0.15 Hz	54	58	62	62	55	47	68	88
0.2 Hz	53	57	62	63	58	51	69	88
0.5 Hz	50	55	62	64	62	60	72	88
1 Hz	48	53	61	64	65	64	73	86
1.5 Hz	46	52	60	64	65	65	73	86
2 Hz	45	51	60	64	66	66	74	85
5 Hz	41	48	58	64	66	68	74	83
10 Hz	38	45	56	64	66	69	74	81
15 Hz	37	43	55	63	65	69	74	79



## 7% EVA with 93% Russian 80 pen bitumen

### Complex modulus (Pa)

Freq\Temp	10°C	15°C	25°C	35°C	45°C	55°C	65°C	75°C
0.01 Hz	808500	330000	62500	16300	4565	1535	166	7
0.015 Hz	1035000	442000	80450	19550	5070	1650	167	10
0.02 Hz	1270000	505000	93700	22150	5635	1760	187	14
0.05 Hz	2090000	853000	147500	34700	8055	2210	303	36
0.1 Hz	3245000	1330000	227000	52050	11550	2885	486	69
0.15 Hz	4135000	1680000	289500	66150	14600	3535	639	102
0.2 Hz	4920000	1970000	342500	77800	17000	4100	776	135
0.5 Hz	8245000	3410000	596000	133500	29050	6995	1495	329
1 Hz	11900000	5090000	909000	202500	44100	10850	2480	634
1.5 Hz	14800000	6400000	1165000	259000	56750	14200	3355	925
2 Hz	17050000	7540000	1400000	310000	67850	17200	4150	1200
5 Hz	26550000	12500000	2455000	551000	121500	32000	8315	2700
10 Hz	35750000	17700000	3715000	852000	188000	51050	13750	4780
15 Hz	40750000	21300000	4640000	1085000	239000	66600	18400	6460

### Phase angle (degrees)

Freq\Temp	10°C	15°C	25°C	35°C	45°C	55°C	65°C	75°C
0.01 Hz	51	55	46	42	29	18	12	86
0.015 Hz	52	50	46	42	31	19	36	88
0.02 Hz	52	50	46	43	33	21	41	87
0.05 Hz	51	52	48	46	39	29	51	88
0.1 Hz	52	52	51	49	45	38	57	87
0.15 Hz	51	53	52	50	47	43	59	87
0.2 Hz	51	53	53	51	49	46	61	87
0.5 Hz	49	52	54	53	53	53	64	85
1 Hz	47	51	55	55	55	57	65	84
1.5 Hz	46	50	55	56	56	58	66	82
2 Hz	45	50	55	56	56	59	66	82
5 Hz	42	48	55	58	57	61	67	78
10 Hz	39	46	55	59	58	62	67	75
15 Hz	38	44	54	59	58	63	67	73

### 3% EVA with 97% Venezuelan 70/100 pen bitumen

#### Complex modulus (Pa)

Freq\Temp	10°C	15°C	25°C	35°C	45°C	55°C	65°C	75°C
0.01 Hz	313000	103500	15100	2685	447	80	15	5
0.015 Hz	393500	143000	20500	3605	610	117	26	7
0.02 Hz	481000	178500	26200	4400	797	155	35	9
0.05 Hz	897000	332500	52000	9395	1780	369	85	22
0.1 Hz	1380000	532000	87000	16550	3225	696	160	44
0.15 Hz	1790000	705500	125000	22400	4425	1008	233	66
0.2 Hz	2160000	856500	156000	27800	5615	1315	305	87
0.5 Hz	3795000	1570000	301000	56400	11950	2930	711	216
1 Hz	5690000	2425000	486000	95500	20900	5270	1340	426
1.5 Hz	7175000	3120000	640000	130000	29050	7385	1950	633
2 Hz	8410000	3730000	767000	162000	36450	9380	2520	837
5 Hz	13650000	6360000	1310000	319000	74600	19700	5690	1990
10 Hz	19100000	9265000	1830000	521000	125500	34150	10300	3770
15 Hz	22650000	11300000	2110000	680000	168000	46150	13800	5560

#### Phase angle (degrees)

Freq\Temp	10°C	15°C	25°C	35°C	45°C	55°C	65°C	75°C
0.01 Hz	64	64	70	74	79	82	77	88
0.015 Hz	61	63	69	74	81	85	84	88
0.02 Hz	61	63	69	74	81	85	83	88
0.05 Hz	58	61	67	72	78	83	83	88
0.1 Hz	57	61	66	71	76	81	83	89
0.15 Hz	57	60	65	70	75	80	83	89
0.2 Hz	56	60	65	70	75	79	83	89
0.5 Hz	53	58	64	68	73	77	83	88
1 Hz	51	56	64	68	72	76	82	87
1.5 Hz	50	55	63	67	71	75	81	86
2 Hz	49	54	63	67	71	75	81	85
5 Hz	46	51	61	67	70	73	79	83
10 Hz	43	49	59	65	69	73	78	81
15 Hz	42	48	58	63	68	72	76	81

## 5% EVA with 95% Venezuelan 70/100 pen bitumen

### Complex modulus (Pa)

Freq\Temp	10°C	15°C	25°C	35°C	45°C	55°C	65°C	75°C
0.01 Hz	491000	217000	40250	8730	1305	237	62	9
0.015 Hz	620000	266000	49500	10400	1790	359	83	14
0.02 Hz	723500	319000	60400	13000	2240	459	106	19
0.05 Hz	1235000	548000	103500	22100	4640	976	226	49
0.1 Hz	1860000	815000	154000	34200	7350	1700	400	98
0.15 Hz	2410000	1040000	211500	44000	9805	2350	560	146
0.2 Hz	2825000	1215000	257000	53000	11900	2935	707	193
0.5 Hz	4670000	2065000	454000	96900	22650	5995	1480	467
1 Hz	6720000	3065000	696500	152000	36400	10150	2570	897
1.5 Hz	8290000	3860000	900000	197000	48050	13650	3550	1310
2 Hz	9545000	4545000	1075000	237000	58800	16900	4470	1700
5 Hz	14950000	7485000	1870000	428000	109500	32650	9100	3790
10 Hz	20550000	10700000	2810000	669000	172000	52650	15100	6670
15 Hz	23800000	12950000	3405000	867000	221500	68600	19800	8330

### Phase angle (degrees)

Freq\Temp	10°C	15°C	25°C	35°C	45°C	55°C	65°C	75°C
0.01 Hz	55	57	53	60	68	66	36	88
0.015 Hz	52	53	54	59	69	74	74	88
0.02 Hz	52	53	54	58	69	74	75	87
0.05 Hz	51	53	54	56	66	73	74	88
0.1 Hz	51	52	56	56	65	71	73	87
0.15 Hz	50	52	55	57	64	71	73	87
0.2 Hz	50	52	55	57	64	70	73	86
0.5 Hz	48	51	55	58	62	69	72	85
1 Hz	47	50	55	58	62	67	72	84
1.5 Hz	46	50	55	58	61	67	71	82
2 Hz	46	49	55	58	61	66	71	81
5 Hz	44	48	54	59	60	65	69	78
10 Hz	42	46	53	59	59	64	68	75
15 Hz	41	45	52	57	59	64	67	73

## 7% EVA with 93% Venezuelan 70/100 pen bitumen

### Complex modulus (Pa)

Freq\Temp	10°C	15°C	25°C	35°C	45°C	55°C	65°C	75°C
0.01 Hz	455500	236000	59050	15750	4110	677	145	11
0.015 Hz	586000	274000	73250	19500	5150	873	185	17
0.02 Hz	672500	327500	84850	23000	5930	1055	223	22
0.05 Hz	1065000	526500	133500	35550	9520	1900	416	52
0.1 Hz	1595000	750000	196500	51850	14400	2950	682	106
0.15 Hz	1990000	928000	243500	67100	18400	3855	903	163
0.2 Hz	2310000	1080000	282000	79050	21700	4630	1095	217
0.5 Hz	3800000	1780000	457500	132500	36700	8380	2075	522
1 Hz	5515000	2620000	662500	194500	55000	13050	3380	1000
1.5 Hz	6895000	3295000	827500	243000	70000	16950	4510	1460
2 Hz	8070000	3860000	968000	286000	82800	20350	5510	1890
5 Hz	13000000	6420000	1620000	482000	143000	36350	10400	4110
10 Hz	18250000	9260000	2395000	719000	194000	55400	16550	6930
15 Hz	22200000	11450000	3045000	903000	397000	69750	20700	8310

### Phase angle (degrees)

Freq\Temp	10°C	15°C	25°C	35°C	45°C	55°C	65°C	75°C
0.01 Hz	46	51	47	47	51	50	61	89
0.015 Hz	47	46	46	46	51	54	61	88
0.02 Hz	47	47	46	46	51	55	61	88
0.05 Hz	46	48	46	47	50	57	61	87
0.1 Hz	49	47	48	49	51	57	62	87
0.15 Hz	48	48	48	49	51	57	62	86
0.2 Hz	49	49	48	49	51	58	63	86
0.5 Hz	49	49	49	50	52	58	64	84
1 Hz	48	49	50	51	52	58	64	82
1.5 Hz	48	49	50	51	52	58	64	81
2 Hz	48	49	50	51	52	58	64	80
5 Hz	46	49	51	52	53	57	63	75
10 Hz	44	48	51	52	53	58	63	72
15 Hz	43	47	51	51	53	58	62	69

### 3% SBS with 97% Russian 80 pen bitumen

#### Complex modulus (Pa)

Freq\Temp	10°C	15°C	25°C	35°C	45°C	55°C	65°C	75°C
0.01 Hz	387500	140500	15100	2360	402	60	29	11
0.015 Hz	555000	192500	21300	3330	564	118	32	13
0.02 Hz	705500	242500	28300	4320	724	153	42	17
0.05 Hz	1325000	491000	57500	9210	1660	355	97	36
0.1 Hz	2200000	816000	99200	16050	3080	668	181	65
0.15 Hz	2880000	1100000	134000	21900	4400	968	260	89
0.2 Hz	3465000	1345000	168000	27600	5645	1260	336	114
0.5 Hz	6045000	2525000	343000	58500	12050	2825	777	255
1 Hz	8905000	3965000	576000	103000	21100	5150	1455	474
1.5 Hz	11050000	5105000	765000	143000	29500	7275	2080	682
2 Hz	12900000	6060000	927000	180500	37300	9225	2685	884
5 Hz	20100000	10100000	1560000	370000	79300	19650	5925	2000
10 Hz	26950000	14400000	2090000	614500	139000	34300	10500	3660
15 Hz	31150000	17150000	2360000	795500	190000	46500	14200	5150

#### Phase angle (degrees)

Freq\Temp	10°C	15°C	25°C	35°C	45°C	55°C	65°C	75°C
0.01 Hz	69	72	72	79	72	72	40	78
0.015 Hz	67	70	72	78	80	81	77	74
0.02 Hz	65	69	71	77	80	81	78	73
0.05 Hz	62	67	71	74	79	81	80	75
0.1 Hz	60	65	71	73	77	81	80	76
0.15 Hz	58	64	71	72	76	80	81	77
0.2 Hz	57	63	71	72	76	80	81	78
0.5 Hz	52	59	69	72	74	78	81	79
1 Hz	49	56	67	72	73	77	80	80
1.5 Hz	47	54	66	72	73	76	80	80
2 Hz	46	53	65	72	73	76	79	80
5 Hz	42	49	63	71	73	75	77	79
10 Hz	39	46	60	82	72	74	76	77
15 Hz	37	44	58	25	71	74	75	76

## 5% SBS with 95% Russian 80 pen bitumen

### Complex modulus (Pa)

Freq\Temp	10°C	15°C	25°C	35°C	45°C	55°C	65°C	75°C
0.01 Hz	428500	150000	19500	3050	653	132	40	18
0.015 Hz	587000	203500	26400	4575	907	229	84	46
0.02 Hz	724500	259500	33700	5770	1145	285	98	54
0.05 Hz	1385000	498000	65900	12000	2365	569	182	90
0.1 Hz	2205000	815000	105000	20500	4165	1010	301	135
0.15 Hz	2875000	1115000	152000	28000	5745	1390	416	180
0.2 Hz	3415000	1365000	192000	34800	7225	1740	519	219
0.5 Hz	5865000	2500000	385000	70150	15000	3670	1100	435
1 Hz	8535000	3835000	629000	118500	25700	6460	1950	751
1.5 Hz	10550000	4870000	825000	161000	35150	8985	2745	1050
2 Hz	12150000	5700000	984000	200000	43800	11300	3490	1320
5 Hz	18600000	9315000	1640000	393500	88400	23400	7440	2805
10 Hz	24850000	13050000	2180000	639500	148500	39650	12950	4905
15 Hz	28750000	15300000	2450000	823000	199500	53450	17800	6695

### Phase angle (degrees)

Freq\Temp	10°C	15°C	25°C	35°C	45°C	55°C	65°C	75°C
0.01 Hz	67	67	70	68	59	40	50	45
0.015 Hz	64	66	69	71	67	62	55	49
0.02 Hz	63	66	69	71	69	63	57	49
0.05 Hz	60	64	67	70	70	68	63	53
0.1 Hz	57	63	67	69	71	71	68	58
0.15 Hz	56	61	67	69	71	72	69	61
0.2 Hz	55	61	67	69	71	72	71	63
0.5 Hz	51	57	66	68	71	73	73	68
1 Hz	48	54	65	68	70	73	74	71
1.5 Hz	46	53	64	68	69	72	74	72
2 Hz	45	51	63	68	69	72	74	72
5 Hz	41	48	60	68	68	71	73	73
10 Hz	38	45	58	67	68	70	72	73
15 Hz	36	43	57	65	67	70	72	72

## 7% SBS with 93% Russian 80 pen bitumen

### Complex modulus (Pa)

Freq\Temp	10°C	15°C	25°C	35°C	45°C	55°C	65°C	75°C
0.01 Hz	406500	164000	24050	4560	926	352	133	53
0.015 Hz	529500	210000	32000	5970	1355	438	199	105
0.02 Hz	642500	260000	39550	7360	1700	514	225	118
0.05 Hz	1145000	475000	75450	14400	3150	882	363	178
0.1 Hz	1750000	737000	124000	24100	5250	1495	538	254
0.15 Hz	2245000	967000	166000	32200	7265	2050	720	325
0.2 Hz	2650000	1170000	202500	39800	9080	2540	871	386
0.5 Hz	4370000	2030000	378000	77500	18050	5090	1695	705
1 Hz	6205000	3020000	600000	127000	30300	8565	2860	1155
1.5 Hz	7590000	3790000	784000	170000	41050	11600	3900	1555
2 Hz	8660000	4440000	940000	210000	50800	14350	4850	1935
5 Hz	13000000	7130000	1660000	396000	99050	28050	9780	3875
10 Hz	17100000	9810000	2485000	621000	161500	46350	16300	6540
15 Hz	19850000	11500000	3070000	791000	211500	61250	21550	8765

### Phase angle (degrees)

Freq\Temp	10°C	15°C	25°C	35°C	45°C	55°C	65°C	75°C
0.01 Hz	61	62	67	59	49	33	44	28
0.015 Hz	58	61	64	64	60	49	42	44
0.02 Hz	58	61	68	64	62	51	44	44
0.05 Hz	55	58	64	65	64	58	49	47
0.1 Hz	53	58	63	65	65	63	57	51
0.15 Hz	52	56	62	65	66	64	59	54
0.2 Hz	51	56	62	65	66	65	61	56
0.5 Hz	48	53	61	64	66	67	65	61
1 Hz	45	51	59	64	66	67	67	64
1.5 Hz	44	49	58	63	66	67	67	66
2 Hz	43	48	57	63	65	67	68	66
5 Hz	39	45	55	62	65	67	68	68
10 Hz	37	42	53	59	64	66	67	68
15 Hz	36	41	51	56	63	66	67	67

### 3% SBS with 97% Venezuelan 70/100 pen bitumen

#### Complex modulus (Pa)

Freq\Temp	10°C	15°C	25°C	35°C	45°C	55°C	65°C	75°C
0.01 Hz	255500	88750	14700	2570	390	85	23	7
0.015 Hz	334500	118500	19900	3530	608	132	33	11
0.02 Hz	422500	147000	24500	4470	798	174	44	14
0.05 Hz	805000	292500	49300	9345	1850	424	111	34
0.1 Hz	1275000	482000	84450	16200	3420	830	218	67
0.15 Hz	1695000	641500	112000	22200	4830	1220	325	97
0.2 Hz	2060000	788000	139000	27600	6105	1590	430	128
0.5 Hz	3685000	1495000	275500	55450	12700	3620	1011	308
1 Hz	5565000	2370000	452500	94050	21750	6545	1915	594
1.5 Hz	7030000	3080000	599000	128000	29750	9145	2755	872
2 Hz	8225000	3695000	726500	159000	37050	11550	3555	1140
5 Hz	13350000	6415000	1255000	313500	75050	23700	7755	2630
10 Hz	18600000	9400000	1740000	511000	126500	40050	13600	4770
15 Hz	22050000	11450000	2005000	657000	168500	53550	18100	6730

#### Phase angle (degrees)

Freq\Temp	10°C	15°C	25°C	35°C	45°C	55°C	65°C	75°C
0.01 Hz	67	69	70	79	83	81	89	85
0.015 Hz	65	66	69	77	83	87	88	87
0.02 Hz	64	66	69	76	83	86	87	87
0.05 Hz	62	65	68	72	80	85	87	87
0.1 Hz	60	64	68	71	77	83	86	86
0.15 Hz	59	63	67	70	76	82	85	86
0.2 Hz	58	63	67	69	75	81	85	86
0.5 Hz	55	60	67	69	72	78	83	85
1 Hz	52	58	66	69	70	75	81	84
1.5 Hz	51	57	65	68	70	74	79	83
2 Hz	50	56	64	69	70	73	79	82
5 Hz	46	52	62	68	69	71	76	80
10 Hz	43	50	60	79	68	70	74	77
15 Hz	42	48	59		68	70	73	76



## 5% SBS with 95% Venezuelan 70/100 pen bitumen

### Complex modulus (Pa)

Freq\Temp	10°C	15°C	25°C	35°C	45°C	55°C	65°C	75°C
0.01 Hz	335250	119000	23100	4340	704	174	46	11
0.015 Hz	436750	155000	31100	5640	1050	220	55	20
0.02 Hz	532500	197500	37800	7240	1370	285	73	27
0.05 Hz	969000	375500	70700	14700	3170	664	171	60
0.1 Hz	1530000	593500	116000	24700	5650	1240	327	113
0.15 Hz	2010000	753500	155000	33000	7620	1790	473	163
0.2 Hz	2387500	910500	190000	40300	9700	2290	613	212
0.5 Hz	4112500	1655000	357000	76800	19800	5040	1420	486
1 Hz	6052500	2555000	566000	125000	32900	8910	2640	911
1.5 Hz	7550000	3270000	734000	166000	44500	12200	3750	1310
2 Hz	8767500	3885000	881000	204000	54600	15200	4820	1700
5 Hz	13725000	6490000	1460000	387000	106000	29800	10300	3770
10 Hz	18750000	9285000	1990000	615000	172000	48800	17700	6650
15 Hz	21750000	11260000	2280000	793000	223000	62800	24000	9100

### Phase angle (degrees)

Freq\Temp	10°C	15°C	25°C	35°C	45°C	55°C	65°C	75°C
0.01 Hz	63	67	65	73	83	73	63	67
0.015 Hz	61	62	64	73	80	80	81	78
0.02 Hz	60	62	63	72	79	81	82	79
0.05 Hz	58	62	63	68	76	80	82	79
0.1 Hz	56	60	63	66	74	79	82	80
0.15 Hz	55	59	63	65	72	79	82	80
0.2 Hz	54	59	63	64	71	78	81	81
0.5 Hz	51	56	63	63	68	75	80	80
1 Hz	49	55	62	63	66	72	78	80
1.5 Hz	47	53	61	63	65	71	77	79
2 Hz	46	52	61	62	65	69	76	78
5 Hz	43	49	59	60	64	67	72	76
10 Hz	40	47	57	57	64	65	70	74
15 Hz	39	45	56	54	63	65	69	73

## 7% SBS with 93% Venezuelan 70/100 pen bitumen

### Complex modulus (Pa)

Freq\Temp	10°C	15°C	25°C	35°C	45°C	55°C	65°C	75°C
0.01 Hz	446000	174000	28700	5610	1180	179	74	25
0.015 Hz	585500	227000	38300	8080	1600	347	92	30
0.02 Hz	713500	270000	45900	10400	2060	455	122	39
0.05 Hz	1300000	499000	82300	19300	4480	1030	280	88
0.1 Hz	1990000	789000	133000	30200	7780	1900	533	167
0.15 Hz	2520000	1030000	174000	39800	10600	2690	764	239
0.2 Hz	2945000	1220000	213000	48500	13000	3450	985	309
0.5 Hz	4895000	2150000	396000	88700	24600	7260	2230	716
1 Hz	7025000	3230000	626000	140000	38900	12400	4040	1340
1.5 Hz	8640000	4040000	815000	183000	50900	16600	5650	1920
2 Hz	9945000	4750000	986000	221000	61200	20400	7150	2470
5 Hz	15300000	7690000	1750000	404000	113000	37900	14400	5380
10 Hz	20500000	10800000	2640000	622000	178000	59800	23300	9270
15 Hz	23750000	12900000	3270000	784000	232000	77400	29900	12500

### Phase angle (degrees)

Freq\Temp	10°C	15°C	25°C	35°C	45°C	55°C	65°C	75°C
0.01 Hz	58	64	61	68	80	70	79	68
0.015 Hz	58	59	57	69	77	79	79	79
0.02 Hz	57	59	57	67	76	79	80	79
0.05 Hz	54	59	59	62	72	78	80	81
0.1 Hz	54	57	60	60	69	76	80	81
0.15 Hz	52	56	60	60	67	75	80	81
0.2 Hz	51	56	60	59	66	74	79	81
0.5 Hz	49	53	60	60	62	70	77	80
1 Hz	46	52	59	61	60	67	74	79
1.5 Hz	45	50	58	61	60	65	73	78
2 Hz	44	49	58	61	60	64	71	77
5 Hz	41	46	56	61	60	61	67	73
10 Hz	38	44	54	61	60	61	64	70
15 Hz	37	43	54	61	60	61	63	68

**Appendix C**  
**DSR Data for RTFOT and PAV**  
**Aged Bitumens and PMB's**

## Middle East 80/100 penetration grade bitumen

RTFOT aged

### Complex modulus (Pa)

Freq\Temp	10°C	15°C	25°C	35°C	45°C	55°C	65°C
0.01 Hz	833000	283000	30200	3270	471	82	18
0.015 Hz	1035000	395500	43550	4690	708	121	26
0.02 Hz	1335000	509500	56150	6105	932	162	35
0.05 Hz	2405000	958500	116000	14200	2250	404	87
0.1 Hz	3650000	1555000	202500	26300	4305	801	174
0.15 Hz	4675000	2010000	275500	37450	6365	1185	261
0.2 Hz	5425000	2410000	340500	47850	8300	1570	347
0.5 Hz	8885000	4225000	672000	101650	18850	3735	852
1 Hz	12600000	6310000	1100000	177500	34600	7155	1660
1.5 Hz	15300000	7890000	1450000	244500	49050	10350	2450
2 Hz	17350000	9215000	1770000	303500	62500	13500	3215
5 Hz	26050000	14700000	3175000	608000	133000	30500	7540
10 Hz	34150000	20250000	4820000	997500	225000	55100	14150
15 Hz	39450000	23900000	5985000	1315000	293500	74750	20250

### Phase angle (degrees)

Freq\Temp	10°C	15°C	25°C	35°C	45°C	55°C	65°C
0.01 Hz	65	69	78	83	87	88	90
0.015 Hz	62	66	75	82	87	89	89
0.02 Hz	60	65	75	82	86	89	89
0.05 Hz	56	62	71	79	85	88	89
0.1 Hz	54	60	69	77	83	87	89
0.15 Hz	52	58	68	76	82	86	88
0.2 Hz	51	57	67	75	82	86	88
0.5 Hz	48	54	65	73	79	84	87
1 Hz	45	51	63	71	77	83	86
1.5 Hz	43	49	61	70	76	82	85
2 Hz	42	48	60	70	75	81	85
5 Hz	39	44	57	67	72	79	83
10 Hz	36	42	55	65	70	77	82
15 Hz	35	40	53	64	68	76	81

## Middle East 80/100 penetration grade bitumen

PAV aged

Complex modulus (Pa)

Freq\Temp	10°C	15°C	25°C	35°C	45°C	55°C	65°C	75°C
0.01 Hz	2575000	1065000	135000	17000	2040	320	59	14
0.015 Hz	3030000	1335000	189500	25050	2970	468	89	21
0.02 Hz	3635000	1620000	230500	30350	3895	627	118	28
0.05 Hz	5995000	2760000	447500	64500	8845	1525	294	70
0.1 Hz	8370000	4095000	710000	111500	16350	2930	583	136
0.15 Hz	10400000	5155000	941500	156500	23050	4275	866	206
0.2 Hz	11800000	6010000	1135000	190000	29350	5545	1135	274
0.5 Hz	17700000	9570000	2020000	364000	61650	12650	2720	677
1 Hz	23600000	13250000	3050000	588000	106000	23150	5195	1330
1.5 Hz	27950000	15950000	3860000	778000	144000	32500	7520	1960
2 Hz	31150000	18100000	4530000	942000	178000	41250	9745	2575
5 Hz	43500000	26400000	7365000	1720000	342500	85900	21650	6060
10 Hz	54100000	34200000	10300000	2650000	543000	144500	38650	11350
15 Hz	60400000	38950000	11950000	3320000	687000	190500	51400	15850

Phase angle (degrees)

Freq\Temp	10°C	15°C	25°C	35°C	45°C	55°C	65°C	75°C
0.01 Hz	55	58	68	77	84	88	88	90
0.015 Hz	51	56	66	76	83	87	89	90
0.02 Hz	50	55	65	74	82	87	89	90
0.05 Hz	46	51	61	71	79	85	88	89
0.1 Hz	44	50	60	69	77	83	87	89
0.15 Hz	43	48	59	68	75	82	87	89
0.2 Hz	42	47	58	67	75	82	86	88
0.5 Hz	39	44	55	64	72	79	84	87
1 Hz	37	42	53	62	69	77	82	86
1.5 Hz	35	40	51	61	67	75	81	85
2 Hz	34	39	51	61	66	74	80	85
5 Hz	31	36	47	58	62	72	78	83
10 Hz	29	34	45	56	58	69	76	81
15 Hz	28	33	44	55	55	68	75	80

## Russian 80 penetration grade bitumen

RTFOT aged

### Complex modulus (Pa)

Freq\Temp	10°C	15°C	25°C	35°C	45°C	55°C	65°C
0.01 Hz	580000	203000	21800	2335	296	49	11
0.015 Hz	791500	285000	30400	3535	430	73	17
0.02 Hz	1010000	361500	39600	4605	575	97	22
0.05 Hz	1820000	697000	89000	11250	1385	241	56
0.1 Hz	2885000	1170000	160000	21900	2750	484	112
0.15 Hz	3840000	1545000	227000	31400	4155	720	167
0.2 Hz	4540000	1870000	287000	40050	5485	949	224
0.5 Hz	7630000	3385000	579000	89250	13050	2315	554
1 Hz	10950000	5130000	938000	161000	24800	4535	1090
1.5 Hz	13450000	6465000	1200000	224500	35950	6680	1615
2 Hz	15350000	7595000	1420000	282500	46700	8820	2130
5 Hz	23000000	12300000	2170000	576000	104500	20850	5170
10 Hz	30250000	17050000	2690000	932500	186000	38950	9930
15 Hz	34800000	20450000	2890000	1170000	246000	56050	14650

### Phase angle (degrees)

Freq\Temp	10°C	15°C	25°C	35°C	45°C	55°C	65°C
0.01 Hz	67	73	81	83	86	88	89
0.015 Hz	65	70	80	85	87	89	90
0.02 Hz	63	69	79	84	87	89	90
0.05 Hz	59	66	76	83	87	88	89
0.1 Hz	57	63	74	81	86	88	89
0.15 Hz	55	61	73	80	85	88	89
0.2 Hz	53	60	72	80	85	87	89
0.5 Hz	49	56	69	78	83	87	88
1 Hz	46	53	66	76	82	86	88
1.5 Hz	44	51	65	75	81	85	87
2 Hz	43	50	64	74	80	85	87
5 Hz	39	46	60	72	78	83	86
10 Hz	36	43	57	69	75	82	85
15 Hz	34	41	55	66	74	81	85

## Russian 80 penetration grade bitumen

PAV aged

### Complex modulus (Pa)

Freq\Temp	10°C	15°C	25°C	35°C	45°C	55°C	65°C	75°C
0.01 Hz	2280000	911500	100400	12300	1435	192	37	9
0.015 Hz	2900000	1225000	140500	18400	2100	286	55	13
0.02 Hz	3510000	1475000	174500	21400	2815	395	73	18
0.05 Hz	5870000	2615000	345500	52200	6665	973	183	44
0.1 Hz	8385000	3985000	575500	95400	12650	1915	363	87
0.15 Hz	10180000	5115000	775000	128000	17650	2825	541	132
0.2 Hz	11700000	6010000	933500	161000	22650	3690	720	176
0.5 Hz	17850000	9670000	1720000	325000	50050	8665	1760	439
1 Hz	23800000	13450000	2650000	532000	89800	16250	3415	870
1.5 Hz	28100000	16100000	3370000	694000	125500	23400	5030	1295
2 Hz	31450000	18350000	4010000	835000	159000	30200	6570	1720
5 Hz	43600000	26550000	6685000	1410000	323000	65900	15350	4160
10 Hz	54000000	34250000	9535000	1940000	533000	116000	28400	7940
15 Hz	60250000	38750000	11400000	2230000	699000	154500	40750	11450

### Phase angle (degrees)

Freq\Temp	10°C	15°C	25°C	35°C	45°C	55°C	65°C	75°C
0.01 Hz	57	63	73	81	86	88	89	89
0.015 Hz	53	58	70	79	85	88	89	89
0.02 Hz	52	57	69	78	84	88	89	89
0.05 Hz	48	54	66	76	82	87	89	89
0.1 Hz	45	51	63	73	81	86	88	89
0.15 Hz	44	49	62	72	80	85	88	89
0.2 Hz	43	48	61	71	79	85	88	89
0.5 Hz	39	45	58	69	76	82	86	88
1 Hz	37	42	55	67	74	81	85	88
1.5 Hz	35	41	54	65	73	80	84	87
2 Hz	34	39	53	64	72	79	84	87
5 Hz	31	36	49	62	67	77	82	85
10 Hz	29	34	47	59	63	74	80	84
15 Hz	27	33	46	58	60	73	80	83

## Venezuelan 70/100 penetration grade bitumen

RTFOT aged

Complex modulus (Pa)

Freq\Temp	10°C	15°C	25°C	35°C	45°C	55°C	65°C
0.01 Hz	346500	116500	15500	2065	332	63	14
0.015 Hz	479000	163000	23100	3125	493	92	21
0.02 Hz	568500	199500	29500	4040	667	124	28
0.05 Hz	1085000	395500	64400	9325	1515	310	70
0.1 Hz	1710000	640000	110000	17350	2905	608	140
0.15 Hz	2255000	858500	147000	24550	4200	903	209
0.2 Hz	2685000	1045000	183000	30900	5470	1185	276
0.5 Hz	4705000	1930000	359000	65150	12350	2815	678
1 Hz	7040000	3005000	582000	113000	22500	5335	1325
1.5 Hz	8895000	3880000	760000	155000	31850	7685	1950
2 Hz	10450000	4605000	907000	192500	40600	9915	2555
5 Hz	16850000	7850000	1510000	379500	86500	22050	5980
10 Hz	23350000	11400000	2020000	612000	149500	39250	11100
15 Hz	27650000	14000000	2270000	767500	206000	53200	16050

Phase angle (degrees)

Freq\Temp	10°C	15°C	25°C	35°C	45°C	55°C	65°C
0.01 Hz	68	68	76	83	87	88	89
0.015 Hz	64	67	74	82	87	89	89
0.02 Hz	63	67	74	81	86	89	89
0.05 Hz	61	64	71	78	84	88	89
0.1 Hz	58	63	70	77	83	86	89
0.15 Hz	58	62	69	75	82	86	88
0.2 Hz	57	61	69	75	81	85	88
0.5 Hz	53	59	67	73	79	83	87
1 Hz	51	57	66	72	77	82	85
1.5 Hz	49	55	64	71	76	81	85
2 Hz	48	54	64	70	75	80	84
5 Hz	45	51	61	69	73	78	82
10 Hz	42	49	59	68	71	77	81
15 Hz	40	47	58	67	69	76	80



## Venezuelan 70/100 penetration grade bitumen

PAV aged

### Complex modulus (Pa)

Freq\Temp	10°C	15°C	25°C	35°C	45°C	55°C	65°C	75°C
0.01 Hz	1255000	489500	67000	11600	1775	289	54	13
0.015 Hz	1600000	597500	93150	15800	2565	431	80	19
0.02 Hz	1910000	725000	113500	20900	3385	553	107	26
0.05 Hz	3205000	1290000	215000	42400	7415	1295	266	63
0.1 Hz	4645000	1935000	348500	71900	13250	2505	523	124
0.15 Hz	5895000	2465000	457500	95100	18950	3655	774	187
0.2 Hz	6815000	2885000	552000	117000	23900	4705	1019	249
0.5 Hz	10650000	4780000	997000	223000	49650	10450	2400	604
1 Hz	14750000	6870000	1535000	356000	84250	18550	4510	1170
1.5 Hz	17700000	8420000	1965000	464000	114500	25850	6495	1710
2 Hz	20150000	9735000	2330000	555000	141000	32700	8360	2245
5 Hz	29250000	15000000	3945000	952000	271500	66800	18350	5160
10 Hz	37650000	20350000	5715000	1340000	434000	113000	32500	9500
15 Hz	42650000	23750000	6930000	1580000	555500	151500	44150	13600

### Phase angle (degrees)

Freq\Temp	10°C	15°C	25°C	35°C	45°C	55°C	65°C	75°C
0.01 Hz	60	61	67	76	82	86	89	90
0.015 Hz	53	58	64	73	81	86	89	89
0.02 Hz	52	57	64	72	80	85	89	90
0.05 Hz	50	54	61	69	77	83	87	89
0.1 Hz	47	53	60	67	75	82	86	88
0.15 Hz	46	52	59	66	73	80	85	88
0.2 Hz	46	51	59	66	72	79	84	87
0.5 Hz	43	48	57	64	70	77	82	86
1 Hz	41	46	55	62	68	75	80	85
1.5 Hz	40	45	54	62	66	73	79	84
2 Hz	39	44	54	61	65	73	78	83
5 Hz	36	42	51	59	62	70	76	81
10 Hz	34	40	50	57	59	68	74	79
15 Hz	33	39	48	56	58	68	73	78

### 3% EVA with 97% Middle East 80/100 pen bitumen

RTFOT aged

#### Complex modulus (Pa)

Freq\Temp	10°C	15°C	25°C	35°C	45°C	55°C	65°C	75°C
0.01 Hz	1260000	551000	70100	9760	1160	205	43	11
0.015 Hz	1585000	667000	95750	13400	1695	297	64	17
0.02 Hz	1890000	799000	119000	16800	2225	395	83	23
0.05 Hz	3185000	1390000	219000	33900	5125	957	205	55
0.1 Hz	4640000	2090000	347500	58900	9425	1840	403	111
0.15 Hz	5780000	2670000	453000	76500	13300	2680	597	166
0.2 Hz	6650000	3120000	548000	94200	16900	3505	790	221
0.5 Hz	10450000	5130000	986000	182000	35600	7890	1860	536
1 Hz	14400000	7330000	1510000	294000	60850	14350	3505	1040
1.5 Hz	17200000	9010000	1925000	386000	82200	20150	5040	1520
2 Hz	19400000	10300000	2285000	471000	101500	25500	6465	1990
5 Hz	28250000	15900000	3855000	864000	194500	52600	14050	4615
10 Hz	36350000	21400000	5585000	1340000	309500	88650	24500	8555
15 Hz	41450000	25000000	6750000	1720000	397000	118000	33200	11700

#### Phase angle (degrees)

Freq\Temp	10°C	15°C	25°C	35°C	45°C	55°C	65°C	75°C
0.01 Hz	58	61	65	78	84	88	89	84
0.015 Hz	52	56	64	76	83	87	89	86
0.02 Hz	52	56	63	75	83	87	89	86
0.05 Hz	49	53	60	70	79	85	88	86
0.1 Hz	47	51	59	68	77	83	86	86
0.15 Hz	46	51	58	66	76	82	86	86
0.2 Hz	45	50	58	65	74	81	85	86
0.5 Hz	43	47	56	63	71	78	82	85
1 Hz	41	45	55	62	68	76	80	85
1.5 Hz	39	44	54	61	67	74	79	84
2 Hz	38	43	53	61	66	74	78	83
5 Hz	36	41	51	59	63	70	75	81
10 Hz	34	39	49	58	60	68	73	80
15 Hz	33	38	49	58	59	68	73	79

### 3% EVA with 97% Middle East 80/100 pen bitumen

PAV aged

#### Complex modulus (Pa)

Freq\Temp	10°C	15°C	25°C	35°C	45°C	55°C	65°C	75°C	85°C
0.01 Hz	3045000	1430000	237500	39200	5960	938	178	44	13
0.015 Hz	3695000	1730000	316500	51200	8400	1345	261	72	21
0.02 Hz	4355000	2070000	364500	62300	10800	1780	347	94	27
0.05 Hz	6450000	3220000	636500	117000	22500	4060	826	225	64
0.1 Hz	8700000	4490000	955500	183500	39000	7450	1590	434	123
0.15 Hz	10350000	5440000	1195000	239500	53100	10600	2335	631	182
0.2 Hz	11600000	6180000	1400000	284000	66000	13550	3050	821	244
0.5 Hz	16550000	9240000	2285000	497000	126000	28750	6855	1925	597
1 Hz	21250000	12300000	3255000	749000	200000	49200	12300	3595	1160
1.5 Hz	24650000	14400000	3985000	951000	260000	66750	17050	5160	1720
2 Hz	27250000	16200000	4580000	1115000	312000	82400	21550	6640	2260
5 Hz	36700000	22800000	7020000	1875000	540000	155500	43400	14500	5270
10 Hz	44950000	28700000	9480000	2715000	789000	242000	71550	25500	9610
15 Hz	50000000	32600000	11100000	3320000	958000	304000	92400	35000	13400

#### Phase angle (degrees)

Freq\Temp	10°C	15°C	25°C	35°C	45°C	55°C	65°C	75°C	85°C
0.01 Hz	45	55	60	66	78	85	87	74	84
0.015 Hz	43	47	56	64	76	84	87	84	83
0.02 Hz	42	47	55	63	75	83	87	84	82
0.05 Hz	39	45	52	60	71	80	85	84	85
0.1 Hz	38	42	51	59	69	78	83	84	86
0.15 Hz	37	41	50	57	67	76	82	84	86
0.2 Hz	37	41	49	57	66	75	80	83	87
0.5 Hz	34	38	47	55	62	71	77	82	86
1 Hz	33	37	46	53	60	68	74	80	85
1.5 Hz	31	36	45	52	59	67	73	79	84
2 Hz	31	35	44	52	58	65	72	78	83
5 Hz	29	33	42	50	57	62	68	76	81
10 Hz	27	31	41	49	56	60	66	74	79
15 Hz	27	30	40	48	55	58	66	73	78

## 5% EVA with 95% Middle East 80/100 pen bitumen

RTFOT aged

### Complex modulus (Pa)

Freq\Temp	10°C	15°C	25°C	35°C	45°C	55°C	65°C	75°C
0.01 Hz	1970000	847500	142000	23050	2555	387	77	20
0.015 Hz	2280000	1100000	185500	30450	3615	566	118	30
0.02 Hz	2750000	1275000	221000	36950	4675	722	157	42
0.05 Hz	4425000	2060000	386000	68100	10200	1715	378	103
0.1 Hz	5985000	3045000	591500	107000	17800	3225	723	200
0.15 Hz	7385000	3780000	756500	138500	24400	4695	1050	297
0.2 Hz	8330000	4355000	888500	166000	30150	6070	1370	389
0.5 Hz	12450000	6795000	1500000	296000	58500	13150	3095	932
1 Hz	16650000	9300000	2200000	453500	94050	22750	5570	1775
1.5 Hz	19600000	11150000	2745000	582000	123500	30900	7765	2570
2 Hz	21900000	12650000	3205000	697000	149000	38300	9780	3335
5 Hz	30750000	18450000	5140000	1215000	266500	73050	19950	7505
10 Hz	38800000	24050000	7175000	1815000	407000	117000	33550	13350
15 Hz	43900000	27550000	8560000	2265000	510500	147500	44650	17850

### Phase angle (degrees)

Freq\Temp	10°C	15°C	25°C	35°C	45°C	55°C	65°C	75°C
0.01 Hz	51	51	59	71	80	83	84	77
0.015 Hz	47	50	56	68	78	84	86	84
0.02 Hz	47	49	55	67	77	83	86	85
0.05 Hz	44	46	54	63	73	81	84	86
0.1 Hz	42	46	53	60	71	79	83	86
0.15 Hz	41	45	52	59	69	78	82	85
0.2 Hz	41	45	52	58	67	76	81	85
0.5 Hz	38	42	51	56	64	73	77	84
1 Hz	37	41	50	56	62	70	75	83
1.5 Hz	36	40	49	55	60	68	73	82
2 Hz	35	39	48	55	59	67	72	81
5 Hz	33	37	46	54	57	64	70	79
10 Hz	31	35	45	53	55	63	68	77
15 Hz	30	34	44	52	53	62	67	75

## 5% EVA with 95% Middle East 80/100 pen bitumen

PAV aged

### Complex modulus (Pa)

Freq\Temp	10°C	15°C	25°C	35°C	45°C	55°C	65°C	75°C	85°C
0.01 Hz	5095000	2540000	498000	89000	13600	1590	327	85	21
0.015 Hz	6310000	3160000	610500	111000	18600	2340	480	124	37
0.02 Hz	7165000	3570000	707000	135500	22800	3060	629	162	50
0.05 Hz	9970000	5450000	1165000	235000	44800	6615	1470	387	121
0.1 Hz	13650000	7545000	1655000	355000	72500	11900	2760	749	242
0.15 Hz	16250000	8775000	2110000	453500	94500	16350	3875	1080	361
0.2 Hz	18050000	9840000	2445000	537500	114000	20600	4935	1405	478
0.5 Hz	24900000	14150000	3830000	906500	205000	41450	10500	3220	1150
1 Hz	31100000	18250000	5295000	1325000	313000	68100	18100	5925	2190
1.5 Hz	35350000	21100000	6395000	1655000	394000	89850	24500	8395	3170
2 Hz	38650000	23450000	7250000	1930000	467000	109000	30300	10700	4110
5 Hz	50650000	31900000	10700000	3085000	792000	195500	57650	22550	9130
10 Hz	60750000	39550000	14100000	4320000	1160000	295500	91250	38150	16300
15 Hz	66600000	44300000	16250000	5145000	1450000	365500	116500	47350	21300

### Phase angle (degrees)

Freq\Temp	10°C	15°C	25°C	35°C	45°C	55°C	65°C	75°C	85°C
0.01 Hz	44	48	54	61	74	81	84	75	83
0.015 Hz	38	43	52	59	72	80	84	82	83
0.02 Hz	38	42	51	58	71	79	84	83	84
0.05 Hz	36	40	48	55	67	76	81	83	86
0.1 Hz	34	38	47	54	64	73	79	82	86
0.15 Hz	33	37	46	53	63	72	77	82	86
0.2 Hz	33	37	45	52	61	71	76	81	86
0.5 Hz	31	35	43	50	57	67	72	79	84
1 Hz	30	34	42	49	55	64	70	78	83
1.5 Hz	29	32	41	48	54	62	68	76	82
2 Hz	28	32	40	48	54	61	67	76	81
5 Hz	26	30	38	46	53	57	64	73	78
10 Hz	25	29	37	45	52	55	62	71	76
15 Hz	25	28	36	45	52	54	61	69	75

## 7% EVA with 93% Middle East 80/100 pen bitumen

RTFOT aged

### Complex modulus (Pa)

Freq\Temp	10°C	15°C	25°C	35°C	45°C	55°C	65°C	75°C	85°C
0.01 Hz	2025000	895000	182000	31000	5920	842	167	28	9
0.015 Hz	2295000	1140000	216000	38700	7880	1170	252	45	14
0.02 Hz	2720000	1320000	248000	46400	9560	1390	329	62	19
0.05 Hz	4025000	1990000	396000	81900	17600	3030	745	154	48
0.1 Hz	5360000	2770000	599000	122000	28500	5340	1350	301	97
0.15 Hz	6485000	3330000	773000	157000	36700	7400	1890	441	145
0.2 Hz	7340000	3760000	892000	184000	43900	9220	2400	578	193
0.5 Hz	10600000	5590000	1420000	313000	76900	18400	5050	1370	472
1 Hz	13750000	7420000	1990000	460000	116000	30100	8610	2600	920
1.5 Hz	16000000	8790000	2420000	577000	148000	39800	11600	3730	1350
2 Hz	17750000	9880000	2770000	675000	177000	48400	14400	4830	1760
5 Hz	24400000	14000000	4240000	1110000	303000	87700	27100	10500	4060
10 Hz	30450000	17900000	5730000	1590000	452000	133000	43300	18200	7320
15 Hz	34150000	20300000	6690000	1950000	564000	166000	54800	22200	9420

### Phase angle (degrees)

Freq\Temp	10°C	15°C	25°C	35°C	45°C	55°C	65°C	75°C	85°C
0.01 Hz	49	45	53	64	70	75	81	75	85
0.015 Hz	41	45	52	61	71	76	80	85	86
0.02 Hz	41	43	51	60	70	75	80	85	86
0.05 Hz	39	40	51	57	66	74	78	86	87
0.1 Hz	37	41	48	54	63	72	76	85	88
0.15 Hz	37	40	47	53	61	70	75	85	87
0.2 Hz	36	40	47	52	60	69	73	84	87
0.5 Hz	34	38	45	51	57	66	70	83	86
1 Hz	34	37	44	50	55	63	68	81	85
1.5 Hz	33	36	43	50	54	61	66	80	84
2 Hz	32	36	43	49	54	60	65	79	83
5 Hz	31	35	41	48	53	57	63	76	80
10 Hz	30	33	40	47	53	56	61	73	78
15 Hz	29	33	40	46	52	55	61	71	75

## 7% EVA with 93% Middle East 80/100 pen bitumen

PAV aged

### Complex modulus (Pa)

Freq\Temp	10°C	15°C	25°C	35°C	45°C	55°C	65°C	75°C	85°C
0.01 Hz	6040000	3010000	605000	125000	25100	5110	692	163	43
0.015 Hz	6660000	3320000	781000	162000	32200	7050	1040	247	75
0.02 Hz	7430000	3860000	922000	189000	39300	8880	1330	337	99
0.05 Hz	10500000	5680000	1410000	316000	71400	15800	2870	763	257
0.1 Hz	13100000	7250000	2030000	476000	107000	26500	5100	1420	495
0.15 Hz	15300000	8520000	2440000	600000	141000	34900	7150	2090	726
0.2 Hz	16500000	9500000	2780000	705000	166000	42800	8910	2710	972
0.5 Hz	22100000	13300000	4160000	1130000	286000	75300	17600	5970	2340
1 Hz	27600000	16900000	5550000	1590000	422000	115000	28700	10600	4280
1.5 Hz	31600000	19500000	6550000	1940000	523000	148000	38200	14400	6020
2 Hz	34400000	21400000	7390000	2230000	605000	174000	45800	18100	7800
5 Hz	44800000	28700000	10500000	3400000	954000	294000	81800	36000	16400
10 Hz	53700000	35200000	13500000	4600000	1350000	438000	124000	57200	27100
15 Hz	58000000	39200000	15400000	5360000	1620000	557000	155000	60300	29400

### Phase angle (degrees)

Freq\Temp	10°C	15°C	25°C	35°C	45°C	55°C	65°C	75°C	85°C
0.01 Hz	37	43	49	54	67	74	78	81	77
0.015 Hz	36	40	47	54	65	72	77	81	83
0.02 Hz	35	39	46	53	64	72	77	81	85
0.05 Hz	31	36	43	49	61	68	74	80	85
0.1 Hz	31	35	43	50	58	66	72	79	85
0.15 Hz	31	34	41	48	56	65	71	79	84
0.2 Hz	31	34	41	48	55	64	69	78	83
0.5 Hz	29	32	39	46	51	60	65	75	81
1 Hz	28	31	38	44	50	57	62	73	79
1.5 Hz	27	30	37	43	49	56	61	72	78
2 Hz	27	29	36	43	49	55	60	71	77
5 Hz	25	28	35	41	48	52	57	68	73
10 Hz	24	28	34	41	47	51	55	66	71
15 Hz	24	27	33	40	47	49	54	64	70

### 3% EVA with 97% Russian 80 pen bitumen

RTFOT aged

#### Complex modulus (Pa)

Freq\Temp	10°C	15°C	25°C	35°C	45°C	55°C	65°C	75°C
0.01 Hz	1100000	408500	45150	5830	870	161	26	5
0.015 Hz	1500000	529000	61050	8090	1220	222	41	8
0.02 Hz	1890000	655000	74350	10200	1610	288	55	10
0.05 Hz	3195000	1190000	140000	21300	3470	662	128	25
0.1 Hz	4920000	1855000	231500	35800	6120	1220	245	51
0.15 Hz	6255000	2430000	324500	48800	8555	1740	358	76
0.2 Hz	7345000	2870000	400000	61400	10900	2235	465	101
0.5 Hz	11900000	4950000	767500	124000	22750	4925	1055	251
1 Hz	16700000	7325000	1235000	206000	39450	8870	1950	496
1.5 Hz	20200000	9190000	1620000	274000	54300	12450	2780	737
2 Hz	23150000	10700000	1950000	339000	68000	15800	3565	975
5 Hz	34050000	17000000	3500000	638000	139000	33700	7925	2350
10 Hz	44250000	23300000	5305000	984000	233000	58700	14250	4455
15 Hz	50600000	27750000	6750000	1220000	309000	79900	19450	6445

#### Phase angle (degrees)

Freq\Temp	10°C	15°C	25°C	35°C	45°C	55°C	65°C	75°C
0.01 Hz	63	62	68	71	74	72	81	88
0.015 Hz	57	61	67	72	77	81	83	88
0.02 Hz	56	61	66	71	77	81	83	88
0.05 Hz	54	58	66	71	75	80	82	89
0.1 Hz	51	57	65	69	74	79	82	89
0.15 Hz	50	56	64	69	74	78	82	89
0.2 Hz	49	55	64	69	73	78	81	88
0.5 Hz	46	52	62	68	72	76	80	88
1 Hz	43	50	61	67	71	76	80	87
1.5 Hz	42	48	60	67	71	75	79	87
2 Hz	41	47	59	66	70	75	79	86
5 Hz	37	44	56	65	69	74	79	84
10 Hz	34	41	54	63	67	73	78	83
15 Hz	33	39	53	61	65	73	77	83



## 5% EVA with 95% Russian 80 pen bitumen

RTFOT aged

Complex modulus (Pa)

Freq\Temp	10°C	15°C	25°C	35°C	45°C	55°C	65°C	75°C
0.01 Hz	1180000	510500	82850	13850	2295	422	77	10
0.015 Hz	1435000	650000	102500	17650	3050	576	102	15
0.02 Hz	1725000	762500	124500	21300	3690	686	129	19
0.05 Hz	2825000	1295000	222000	39250	7125	1385	274	48
0.1 Hz	4065000	1930000	333000	61400	11700	2410	494	98
0.15 Hz	5050000	2425000	433000	79100	16000	3310	693	144
0.2 Hz	5855000	2850000	513000	94750	19600	4105	884	190
0.5 Hz	9235000	4700000	888500	172000	37150	8315	1880	463
1 Hz	12850000	6725000	1340000	271000	59650	14050	3335	897
1.5 Hz	15450000	8280000	1705000	353500	78750	19050	4660	1315
2 Hz	17600000	9565000	2005000	422500	95750	23600	5870	1710
5 Hz	25900000	14700000	3380000	758500	177000	46100	12300	3930
10 Hz	33750000	19850000	4910000	1170000	278000	75450	21050	7055
15 Hz	38800000	23000000	5980000	1480000	354500	98600	28550	9310

Phase angle (degrees)

Freq\Temp	10°C	15°C	25°C	35°C	45°C	55°C	65°C	75°C
0.01 Hz	54	54	57	57	65	56	51	87
0.015 Hz	50	52	55	57	65	64	70	87
0.02 Hz	50	51	55	58	65	65	71	87
0.05 Hz	48	50	55	57	65	68	73	87
0.1 Hz	47	50	54	58	64	68	74	87
0.15 Hz	46	49	55	58	64	69	74	87
0.2 Hz	45	49	55	58	63	69	74	87
0.5 Hz	43	47	54	58	62	68	74	86
1 Hz	42	46	53	59	62	68	73	84
1.5 Hz	40	44	53	58	61	67	73	83
2 Hz	40	44	52	58	61	67	73	82
5 Hz	37	41	51	58	60	66	71	80
10 Hz	35	40	50	58	59	66	71	78
15 Hz	33	39	49	57	58	66	71	75

## 5% EVA with 95% Russian 80 pen bitumen

PAV aged

### Complex modulus (Pa)

Freq\Temp	10°C	15°C	25°C	35°C	45°C	55°C	65°C	75°C	85°C
0.01 Hz	3650000	1670000	323000	44900	6200	990	202	50	14
0.015 Hz	4215000	2090000	376000	57200	8530	1410	279	68	21
0.02 Hz	4960000	2470000	445000	70700	11000	1810	367	89	27
0.05 Hz	7495000	3810000	758000	128000	22400	3840	858	213	68
0.1 Hz	9935000	5440000	1090000	198000	37200	7020	1580	418	133
0.15 Hz	12000000	6630000	1380000	254000	50400	10000	2270	617	198
0.2 Hz	13550000	7500000	1610000	303000	61100	12800	2920	821	261
0.5 Hz	19450000	11100000	2600000	528000	115000	26600	6450	1940	638
1 Hz	25200000	14700000	3700000	793000	182000	44900	11500	3670	1250
1.5 Hz	29150000	17200000	4520000	1010000	235000	60100	15900	5320	1840
2 Hz	32200000	19200000	5220000	1190000	281000	73900	20000	6880	2430
5 Hz	43400000	27100000	8010000	2000000	485000	139000	40000	15100	5570
10 Hz	53150000	34100000	10800000	2880000	709000	218000	65900	26400	10200
15 Hz	58800000	38100000	12700000	3540000	863000	277000	87600	32900	13400

### Phase angle (degrees)

Freq\Temp	10°C	15°C	25°C	35°C	45°C	55°C	65°C	75°C	85°C
0.01 Hz	49	52	59	65	74	77	82	80	84
0.015 Hz	42	45	54	61	73	78	81	84	84
0.02 Hz	42	44	53	60	72	78	81	84	84
0.05 Hz	40	43	51	58	69	76	80	85	87
0.1 Hz	37	41	49	56	66	74	79	85	88
0.15 Hz	37	40	49	55	65	73	78	85	88
0.2 Hz	36	40	48	55	64	72	77	84	87
0.5 Hz	34	38	46	53	60	69	75	83	86
1 Hz	33	36	45	53	58	67	73	81	85
1.5 Hz	32	36	44	52	58	65	71	80	84
2 Hz	31	35	44	51	58	64	70	79	84
5 Hz	29	33	42	50	57	61	68	76	81
10 Hz	27	31	41	49	57	59	66	74	79
15 Hz	27	31	40	48	56	58	65	73	77

## 7% EVA with 93% Russian 80 pen bitumen

RTFOT aged

### Complex modulus (Pa)

Freq\Temp	10°C	15°C	25°C	35°C	45°C	55°C	65°C	75°C	85°C
0.01 Hz	1495000	707000	138000	30600	7210	1560	266	15	4
0.015 Hz	1830000	850000	176000	39000	9120	1930	335	24	7
0.02 Hz	2045000	986000	202000	44800	10600	2260	402	33	9
0.05 Hz	3285000	1500000	303000	70100	17000	3940	753	78	24
0.1 Hz	4735000	2090000	446000	103000	25300	6030	1230	152	48
0.15 Hz	5705000	2610000	544000	127000	31900	7670	1640	224	69
0.2 Hz	6440000	3010000	635000	146000	37500	9100	2000	298	93
0.5 Hz	9960000	4760000	1020000	234000	61300	16100	3780	715	232
1 Hz	13750000	6670000	1450000	338000	88200	24500	6080	1360	459
1.5 Hz	16550000	8180000	1790000	424000	110000	31300	8040	1960	685
2 Hz	18900000	9400000	2070000	500000	129000	37600	9760	2530	905
5 Hz	28100000	14400000	3360000	841000	216000	66000	18300	5410	2110
10 Hz	36750000	19500000	4790000	1240000	318000	101000	28900	9230	3860
15 Hz	42100000	23000000	5860000	1540000	394000	127000	36900	11500	5160

### Phase angle (degrees)

Freq\Temp	10°C	15°C	25°C	35°C	45°C	55°C	65°C	75°C	85°C
0.01 Hz	50	41	45	48	52	52	61	88	87
0.015 Hz	42	43	42	45	51	53	60	87	88
0.02 Hz	43	43	42	45	50	53	61	87	88
0.05 Hz	44	41	43	46	48	55	61	87	89
0.1 Hz	43	45	45	47	50	55	63	86	89
0.15 Hz	43	44	45	47	50	55	62	86	88
0.2 Hz	43	44	45	47	50	55	62	85	88
0.5 Hz	42	44	46	48	51	55	62	83	87
1 Hz	41	44	47	49	51	55	62	81	86
1.5 Hz	40	43	47	49	52	55	62	80	85
2 Hz	39	43	48	50	52	55	62	79	84
5 Hz	37	42	48	51	54	55	62	75	81
10 Hz	35	40	48	52	54	56	62	72	78
15 Hz	33	39	47	52	53	56	62	70	75

## 7% EVA with 93% Russian 80 pen bitumen

PAV aged

### Complex modulus (Pa)

Freq\Temp	10°C	15°C	25°C	35°C	45°C	55°C	65°C	75°C	85°C
0.01 Hz	5120000	2460000	474000	89500	16000	3270	443	74	16
0.015 Hz	5426667	3010000	613000	118000	21100	4290	634	115	25
0.02 Hz	6096667	3350000	712000	137000	25400	5170	822	146	37
0.05 Hz	8740000	4670000	1090000	229000	45700	10000	1790	345	94
0.1 Hz	11200000	6280000	1560000	336000	68000	16100	3150	671	187
0.15 Hz	13533333	7380000	1900000	429000	86400	21400	4250	923	279
0.2 Hz	14933333	8250000	2180000	504000	103000	25700	5280	1200	371
0.5 Hz	20733333	11800000	3330000	820000	178000	45600	10400	2760	914
1 Hz	26233333	15100000	4490000	1170000	266000	70300	17200	4960	1755
1.5 Hz	30000000	17600000	5350000	1430000	339000	90200	22800	6880	2540
2 Hz	33000000	19500000	6070000	1650000	400000	107000	27700	8750	3290
5 Hz	43866667	26800000	8900000	2580000	674000	188000	51500	18100	7400
10 Hz	53333333	33500000	11700000	3560000	992000	286000	80400	29900	13000
15 Hz	58833333	37600000	13400000	4220000	1230000	361000	100000	33500	15950

### Phase angle (degrees)

Freq\Temp	10°C	15°C	25°C	35°C	45°C	55°C	65°C	75°C	85°C
0.01 Hz	39	40	48	54	65	70	74	85	88
0.015 Hz	37	39	47	53	64	69	73	81	88
0.02 Hz	36	38	46	52	63	69	73	81	88
0.05 Hz	34	35	43	50	60	67	72	82	87
0.1 Hz	34	37	44	50	57	66	71	81	87
0.15 Hz	33	36	42	49	56	64	70	81	87
0.2 Hz	33	35	42	48	55	63	69	80	87
0.5 Hz	31	34	41	47	52	60	66	79	85
1 Hz	30	33	40	46	52	58	64	77	83
1.5 Hz	29	32	39	46	51	57	63	76	82
2 Hz	29	32	39	46	51	56	62	75	81
5 Hz	27	31	38	44	51	54	60	72	78
10 Hz	26	30	36	44	50	52	59	70	75
15 Hz	25	29	36	43	49	51	58	67	73

### 3% EVA with 97% Venezuelan 70/100 pen bitumen

RTFOT aged

#### Complex modulus (Pa)

Freq\Temp	10°C	15°C	25°C	35°C	45°C	55°C	65°C	75°C
0.01 Hz	624000	277000	45450	7270	1115	213	57	13
0.015 Hz	776000	368000	58200	9770	1590	299	78	19
0.02 Hz	952500	429000	70250	12100	2025	389	102	25
0.05 Hz	1610000	750500	130500	23500	4335	905	230	64
0.1 Hz	2420000	1155000	206500	39000	7600	1690	425	125
0.15 Hz	3110000	1475000	268000	51000	10500	2390	610	187
0.2 Hz	3640000	1745000	323500	62300	13100	3030	783	247
0.5 Hz	5885000	2930000	587500	117000	26050	6435	1755	596
1 Hz	8310000	4265000	910500	187000	43350	11150	3205	1145
1.5 Hz	10150000	5265000	1170000	245000	58250	15300	4515	1660
2 Hz	11600000	6135000	1400000	297000	71550	19050	5775	2150
5 Hz	17600000	9670000	2410000	532000	136500	38250	12350	4860
10 Hz	23500000	13350000	3560000	800000	218500	63350	21400	8780
15 Hz	27400000	15750000	4360000	998000	282000	84300	28400	11750

#### Phase angle (degrees)

Freq\Temp	10°C	15°C	25°C	35°C	45°C	55°C	65°C	75°C
0.01 Hz	56	61	63	69	79	84	79	86
0.015 Hz	54	55	61	68	78	84	82	87
0.02 Hz	53	55	60	67	77	83	81	87
0.05 Hz	51	54	59	65	74	81	79	87
0.1 Hz	50	52	59	64	71	79	79	87
0.15 Hz	49	52	58	63	70	77	79	87
0.2 Hz	48	51	58	63	69	76	78	86
0.5 Hz	46	49	57	62	67	73	78	85
1 Hz	44	48	56	61	66	71	77	83
1.5 Hz	43	47	55	61	65	70	76	82
2 Hz	42	46	55	61	65	70	76	82
5 Hz	40	44	53	60	63	68	74	79
10 Hz	38	42	51	59	62	67	72	77
15 Hz	37	41	51	59	61	67	72	76

## 5% EVA with 95% Venezuelan 70/100 pen bitumen

RTFOT aged

Complex modulus (Pa)

Freq\Temp	10°C	15°C	25°C	35°C	45°C	55°C	65°C	75°C
0.01 Hz	1015000	451000	91500	17600	3210	479	106	17
0.015 Hz	1225000	547000	116000	22400	4070	698	173	28
0.02 Hz	1385000	663000	140000	27600	5210	891	217	40
0.05 Hz	2220000	1030000	222000	46900	9770	1850	451	99
0.1 Hz	3140000	1540000	333000	72900	15100	3140	769	198
0.15 Hz	3900000	1930000	417000	97600	19800	4260	1040	299
0.2 Hz	4485000	2190000	494000	116000	23800	5280	1300	397
0.5 Hz	6945000	3480000	828000	198000	43100	10200	2660	934
1 Hz	9570000	4880000	1200000	297000	67000	16500	4520	1750
1.5 Hz	11550000	5900000	1490000	377000	87100	21700	6160	2500
2 Hz	13100000	6790000	1740000	445000	105000	26200	7620	3200
5 Hz	19600000	10400000	2810000	755000	187000	47600	14900	6790
10 Hz	26050000	14200000	4010000	1120000	287000	73300	23900	11300
15 Hz	30200000	16700000	4890000	1330000	369000	93100	30300	12400

Phase angle (degrees)

Freq\Temp	10°C	15°C	25°C	35°C	45°C	55°C	65°C	75°C
0.01 Hz	50	54	56	60	68	73	61	88
0.015 Hz	45	47	51	57	66	74	72	87
0.02 Hz	46	48	51	56	65	73	72	87
0.05 Hz	45	47	51	55	61	71	70	86
0.1 Hz	44	46	50	54	60	68	70	85
0.15 Hz	44	46	50	54	59	67	70	84
0.2 Hz	43	45	49	54	59	66	69	84
0.5 Hz	42	45	49	53	58	64	69	82
1 Hz	42	44	49	53	57	62	68	80
1.5 Hz	41	44	49	53	57	61	68	78
2 Hz	40	43	48	53	57	61	67	77
5 Hz	39	42	48	53	57	59	66	74
10 Hz	38	41	47	53	57	59	65	72
15 Hz	37	41	47	53	56	59	64	70

## 5% EVA with 95% Venezuelan 70/100 pen bitumen

PAV aged

### Complex modulus (Pa)

Freq\Temp	10°C	15°C	25°C	35°C	45°C	55°C	65°C	75°C	85°C
0.01 Hz	3170000	1480000	351500	74100	13500	2535	603	166	48
0.015 Hz	3385000	1730000	405000	86600	18200	3450	836	249	66
0.02 Hz	3950000	2010000	474000	103000	21800	4380	1055	330	88
0.05 Hz	5780000	2970000	764000	175000	37100	8120	2070	772	201
0.1 Hz	7380000	3990000	1050000	255000	57400	13350	3395	1420	396
0.15 Hz	8875000	4750000	1325000	309000	77100	18100	4555	2035	580
0.2 Hz	9890000	5310000	1530000	352000	92300	22300	5625	2595	755
0.5 Hz	13900000	7720000	2355000	571000	158000	40450	10800	5520	1710
1 Hz	17900000	10200000	3210000	816000	233000	62000	17450	9475	3090
1.5 Hz	20800000	11900000	3860000	1010000	292000	79550	22800	12750	4290
2 Hz	22900000	13300000	4370000	1180000	343000	94450	27650	15700	5450
5 Hz	31300000	18700000	6445000	1870000	566000	160000	49850	29300	11100
10 Hz	39000000	23800000	8545000	2630000	825000	234000	76150	45150	18200
15 Hz	43600000	27100000	9880000	3290000	1010000	280000	93900	44650	20700

### Phase angle (degrees)

Freq\Temp	10°C	15°C	25°C	35°C	45°C	55°C	65°C	75°C	85°C
0.01 Hz	41	49	50	56	63	70	70	80	84
0.015 Hz	39	41	48	53	60	68	71	82	85
0.02 Hz	38	41	47	53	59	67	70	82	84
0.05 Hz	35	40	45	50	57	64	68	80	84
0.1 Hz	35	38	44	49	56	62	67	78	83
0.15 Hz	35	38	44	49	54	61	66	76	82
0.2 Hz	35	37	43	49	54	60	65	76	81
0.5 Hz	33	36	42	47	52	57	63	73	78
1 Hz	32	35	41	46	52	56	62	70	76
1.5 Hz	32	35	40	46	51	54	61	69	75
2 Hz	32	34	40	46	51	54	61	68	74
5 Hz	31	34	39	45	50	52	59	66	71
10 Hz	30	33	39	44	50	51	58	64	69
15 Hz	29	32	39	44	50	51	58	64	68

## 7% EVA with 93% Venezuelan 70/100 pen bitumen

RTFOT aged

### Complex modulus (Pa)

Freq\Temp	10°C	15°C	25°C	35°C	45°C	55°C	65°C	75°C	85°C
0.01 Hz	789500	425000	114000	31100	8120	2100	267	24	7
0.015 Hz	910000	470000	125000	36000	9670	2430	376	39	10
0.02 Hz	1030000	548000	148000	42300	11300	2890	454	52	13
0.05 Hz	1600000	848000	231000	68000	18900	4970	811	126	32
0.1 Hz	2220000	1130000	317000	94600	26600	7510	1240	241	64
0.15 Hz	2705000	1410000	392000	119000	33200	9340	1650	345	97
0.2 Hz	3065000	1600000	448000	136000	38600	10800	1990	447	129
0.5 Hz	4740000	2470000	697000	217000	63700	18300	3660	1030	314
1 Hz	6610000	3440000	975000	309000	92800	27200	5790	1890	609
1.5 Hz	8025000	4200000	1180000	381000	116000	34200	7590	2650	895
2 Hz	9235000	4810000	1360000	441000	136000	40400	9120	3370	1170
5 Hz	14250000	7520000	2140000	703000	222000	68500	16500	6840	2610
10 Hz	19550000	10400000	3010000	993000	322000	101000	25200	11300	4620
15 Hz	23150000	12500000	3650000	1200000	392000	450000	30300	12900	5830

### Phase angle (degrees)

Freq\Temp	10°C	15°C	25°C	35°C	45°C	55°C	65°C	75°C	85°C
0.01 Hz	47	44	49	49	51	57	61	79	86
0.015 Hz	40	43	44	46	49	53	59	86	88
0.02 Hz	41	42	44	46	49	53	59	86	88
0.05 Hz	42	41	44	46	48	53	58	85	88
0.1 Hz	42	42	43	45	48	52	59	83	87
0.15 Hz	42	42	44	45	48	53	59	83	87
0.2 Hz	42	43	44	45	48	53	60	82	87
0.5 Hz	43	43	44	45	48	53	60	80	86
1 Hz	43	44	44	46	49	52	61	78	84
1.5 Hz	43	44	44	46	49	53	61	77	83
2 Hz	43	44	45	46	49	52	61	76	82
5 Hz	42	44	45	47	49	53	60	72	78
10 Hz	41	44	46	48	50	53	60	69	75
15 Hz	41	43	47	48	48		59	68	73



## 7% EVA with 93% Venezuelan 70/100 pen bitumen

PAV aged

### Complex modulus (Pa)

Freq\Temp	10°C	15°C	25°C	35°C	45°C	55°C	65°C	75°C	85°C
0.01 Hz	3285000	1825000	521000	115000	28400	6360	1210	343	89
0.015 Hz	3955000	2115000	569000	145000	34300	8330	1630	510	130
0.02 Hz	4310000	2435000	663000	168000	41300	10000	1960	683	173
0.05 Hz	5795000	3450000	1020000	264000	66700	18100	3640	1530	404
0.1 Hz	7770000	4560000	1370000	384000	98800	27900	5790	2730	731
0.15 Hz	8945000	5370000	1660000	461000	124000	35800	7600	3690	1050
0.2 Hz	9910000	5945000	1870000	526000	144000	41200	9150	4620	1320
0.5 Hz	13650000	8320000	2730000	808000	227000	70400	16500	9210	2840
1 Hz	17200000	10650000	3610000	1100000	322000	103000	25500	15100	4880
1.5 Hz	19750000	12350000	4240000	1330000	399000	127000	33000	19800	6690
2 Hz	21800000	13650000	4740000	1510000	457000	148000	39100	23500	8260
5 Hz	29550000	18850000	6770000	2260000	717000	242000	67000	40100	15500
10 Hz	36650000	23750000	8800000	3040000	1010000	345000	99100	57900	24200
15 Hz	41050000	26800000	10200000	3580000	1240000	413000	117000	48900	25400

### Phase angle (degrees)

Freq\Temp	10°C	15°C	25°C	35°C	45°C	55°C	65°C	75°C	85°C
0.01 Hz	38	41	49	53	53	62	63	80	84
0.015 Hz	33	37	43	47	53	59	63	79	84
0.02 Hz	33	36	43	47	52	59	63	78	83
0.05 Hz	32	35	41	46	49	57	61	75	80
0.1 Hz	32	34	39	44	49	54	61	73	79
0.15 Hz	32	34	39	43	48	53	60	72	78
0.2 Hz	32	34	39	43	48	53	60	71	77
0.5 Hz	31	33	37	42	46	51	59	67	74
1 Hz	31	33	37	41	46	50	58	65	72
1.5 Hz	30	32	36	41	45	50	58	64	70
2 Hz	30	32	36	41	45	49	57	64	69
5 Hz	30	32	36	40	45	49	56	62	67
10 Hz	29	31	35	40	45	49	55	60	65
15 Hz	29	31	35	40	44	48	55	61	65

### 3% SBS with 97% Russian 80 pen bitumen

RTFOT aged

#### Complex modulus (Pa)

Freq\Temp	10°C	15°C	25°C	35°C	45°C	55°C	65°C	75°C
0.01 Hz	848000	329000	37450	4890	703	136	31	10
0.015 Hz	1150000	451000	50950	7090	1050	183	45	15
0.02 Hz	1450000	546500	62500	9170	1345	242	59	19
0.05 Hz	2640000	1040000	130500	18800	3045	570	139	45
0.1 Hz	4010000	1685000	219000	31000	5595	1085	268	84
0.15 Hz	5165000	2225000	293500	44600	8090	1565	391	123
0.2 Hz	6065000	2650000	363000	56500	10400	2030	510	159
0.5 Hz	9930000	4625000	714000	117000	22150	4610	1185	370
1 Hz	14050000	6850000	1165000	198000	38750	8445	2220	700
1.5 Hz	17000000	8545000	1540000	269000	53650	11950	3190	1015
2 Hz	19450000	9960000	1870000	334000	67250	15250	4125	1320
5 Hz	28800000	15700000	3355000	644000	138000	32700	9080	3010
10 Hz	37300000	21350000	5065000	1010000	234000	56600	16150	5515
15 Hz	42400000	25100000	6265000	1280000	306000	77900	22100	7730

#### Phase angle (degrees)

Freq\Temp	10°C	15°C	25°C	35°C	45°C	55°C	65°C	75°C
0.01 Hz	66	69	72	77	78	83	76	74
0.015 Hz	61	65	70	76	81	84	85	82
0.02 Hz	60	64	69	75	80	84	84	81
0.05 Hz	56	62	68	73	79	82	84	82
0.1 Hz	53	59	67	72	77	82	83	82
0.15 Hz	52	58	67	71	76	81	83	82
0.2 Hz	51	57	66	71	75	80	83	82
0.5 Hz	47	53	64	70	73	78	82	82
1 Hz	44	50	62	69	72	77	80	82
1.5 Hz	42	48	61	69	71	76	80	81
2 Hz	41	47	60	69	71	75	79	81
5 Hz	37	43	57	67	70	73	77	79
10 Hz	34	41	54	64	68	73	76	78
15 Hz	33	39	53	62	67	72	75	77

### 3% SBS with 97% Russian 80 pen bitumen

PAV aged

#### Complex modulus (Pa)

Freq\Temp	10°C	15°C	25°C	35°C	45°C	55°C	65°C	75°C	85°C
0.01 Hz	2405000	930000	136000	18800	2860	444	91	20	6
0.015 Hz	3035000	1250000	188000	25800	3980	689	127	30	9
0.02 Hz	3525000	1490000	227000	33100	5000	876	167	39	11
0.05 Hz	5570000	2510000	410000	61100	10300	1920	406	97	29
0.1 Hz	7900000	3720000	659000	104000	18100	3510	777	193	59
0.15 Hz	9525000	4520000	842000	141000	24700	5060	1140	287	85
0.2 Hz	10800000	5240000	1010000	171000	30900	6440	1470	376	113
0.5 Hz	15750000	8200000	1780000	326000	60800	13400	3300	891	273
1 Hz	20600000	11100000	2640000	523000	103000	23000	5920	1680	531
1.5 Hz	24000000	13200000	3310000	683000	139000	31400	8310	2380	777
2 Hz	26600000	14900000	3880000	824000	169000	39100	10500	3070	1020
5 Hz	36000000	21300000	6220000	1460000	328000	78300	22000	6720	2340
10 Hz	44300000	27200000	8600000	2200000	529000	130000	37300	11600	4230
15 Hz	48950000	30900000	10200000	2750000	681000	170000	49300	15300	5690

#### Phase angle (degrees)

Freq\Temp	10°C	15°C	25°C	35°C	45°C	55°C	65°C	75°C	85°C
0.01 Hz	52	57	64	70	75	83	85	87	89
0.015 Hz	48	53	62	67	74	82	86	88	89
0.02 Hz	47	52	61	68	73	81	86	88	89
0.05 Hz	43	49	59	66	71	78	84	87	88
0.1 Hz	42	47	58	65	70	76	82	86	88
0.15 Hz	40	46	56	64	69	75	81	86	88
0.2 Hz	39	45	56	63	69	73	80	85	87
0.5 Hz	36	42	53	62	67	71	77	83	86
1 Hz	34	40	51	60	66	70	75	81	85
1.5 Hz	33	38	49	59	66	69	74	79	84
2 Hz	32	38	49	58	65	69	73	78	83
5 Hz	30	35	46	56	64	68	71	76	81
10 Hz	28	33	43	54	62	66	70	74	79
15 Hz	27	32	42	52	60	65	70	72	76

## 5% SBS with 95% Russian 80 pen bitumen

RTFOT aged

Complex modulus (Pa)

Freq\Temp	10°C	15°C	25°C	35°C	45°C	55°C	65°C	75°C
0.01 Hz	906500	353000	43750	7170	1195	217	46	14
0.015 Hz	1155000	447000	56350	9420	1720	314	71	22
0.02 Hz	1440000	552000	72750	11900	2210	409	94	29
0.05 Hz	2500000	1050000	139500	23400	4700	936	222	69
0.1 Hz	3665000	1610000	229500	39200	8070	1735	425	133
0.15 Hz	4780000	2095000	309000	53000	11000	2485	619	192
0.2 Hz	5630000	2500000	378000	65200	13800	3175	807	253
0.5 Hz	9125000	4290000	720500	129000	27550	6720	1830	587
1 Hz	12750000	6290000	1155000	214000	46250	11550	3325	1100
1.5 Hz	15450000	7810000	1505000	288000	62350	15650	4660	1580
2 Hz	17450000	9020000	1815000	354000	77250	19450	5910	2030
5 Hz	25550000	14050000	3205000	657000	152500	38550	12200	4450
10 Hz	32950000	19000000	4755000	999000	250500	64250	20600	7745
15 Hz	37200000	22200000	5875000	1240000	326500	86500	27450	10350

Phase angle (degrees)

Freq\Temp	10°C	15°C	25°C	35°C	45°C	55°C	65°C	75°C
0.01 Hz	60	65	68	71	75	80	85	81
0.015 Hz	59	62	66	69	77	82	85	84
0.02 Hz	58	62	66	69	76	82	84	84
0.05 Hz	53	59	65	68	73	79	83	84
0.1 Hz	52	57	64	67	70	78	82	83
0.15 Hz	50	56	64	67	69	76	82	83
0.2 Hz	49	55	63	67	69	75	81	83
0.5 Hz	45	51	61	66	67	72	78	81
1 Hz	42	48	60	66	67	70	76	80
1.5 Hz	41	47	59	65	67	69	75	79
2 Hz	40	46	58	65	67	69	74	78
5 Hz	36	42	55	64	66	68	71	75
10 Hz	34	40	52	63	65	68	70	73
15 Hz	33	38	51	62	64	68	70	72

## 5% SBS with 95% Russian 80 pen bitumen

PAV aged

Complex modulus (Pa)

Freq\Temp	10°C	15°C	25°C	35°C	45°C	55°C	65°C	75°C	85°C
0.01 Hz	2075000	911000	137000	25000	4360	703	145	38	10
0.015 Hz	2760000	1230000	170000	33600	5890	1050	215	52	15
0.02 Hz	3205000	1440000	208000	41300	7370	1400	284	69	20
0.05 Hz	5015000	2390000	388000	78900	14900	3080	672	169	51
0.1 Hz	7235000	3510000	595000	129000	24700	5400	1260	329	99
0.15 Hz	8655000	4320000	774000	172000	33300	7430	1800	484	142
0.2 Hz	9730000	4970000	917000	206000	40400	9230	2310	637	187
0.5 Hz	14350000	7760000	1600000	377000	78400	18500	4980	1460	451
1 Hz	18800000	10600000	2380000	581000	129000	30800	8670	2700	864
1.5 Hz	21850000	12600000	2960000	745000	172000	41500	11900	3830	1260
2 Hz	24350000	14100000	3460000	876000	211000	51300	14900	4860	1620
5 Hz	33200000	20200000	5560000	1390000	393000	99300	29600	10200	3620
10 Hz	40950000	25700000	7710000	1840000	607000	161000	48500	17300	6410
15 Hz	45550000	29000000	9280000	2100000	759000	208000	65500	23500	8860

Phase angle (degrees)

Freq\Temp	10°C	15°C	25°C	35°C	45°C	55°C	65°C	75°C	85°C
0.01 Hz	52	54	66	67	72	78	81	88	88
0.015 Hz	47	53	61	65	70	80	85	88	89
0.02 Hz	47	52	61	65	70	79	84	87	89
0.05 Hz	44	48	59	64	68	75	82	86	88
0.1 Hz	42	47	57	63	66	72	79	85	87
0.15 Hz	40	45	56	63	66	71	78	84	87
0.2 Hz	39	45	55	62	66	70	77	83	87
0.5 Hz	36	42	53	61	65	68	73	80	85
1 Hz	34	40	51	59	64	67	71	77	83
1.5 Hz	33	38	49	59	64	66	70	76	81
2 Hz	32	37	48	58	64	66	69	75	80
5 Hz	29	35	46	56	62	65	68	72	77
10 Hz	28	33	44	54	61	63	67	70	75
15 Hz	26	32	42	52	58	63	67	69	73

## 7% SBS with 93% Russian 80 pen bitumen

RTFOT aged

### Complex modulus (Pa)

Freq\Temp	10°C	15°C	25°C	35°C	45°C	55°C	65°C	75°C	85°C
0.01 Hz	788000	296000	41100	7680	1200	321	48	16	9
0.015 Hz	970000	404000	59000	10500	2000	422	111	37	17
0.02 Hz	1200000	490000	66700	12900	2510	555	149	47	22
0.05 Hz	1985000	864000	133000	25100	5100	1180	333	104	45
0.1 Hz	2870000	1350000	217000	40600	8760	2080	604	192	79
0.15 Hz	3610000	1700000	283000	51600	11900	2930	860	275	110
0.2 Hz	4190000	2000000	339000	63300	14900	3700	1100	355	142
0.5 Hz	6575000	3310000	611000	122000	28700	7600	2400	786	307
1 Hz	9040000	4740000	938000	198000	46900	12800	4260	1440	555
1.5 Hz	10900000	5820000	1200000	263000	62400	17200	5910	2040	791
2 Hz	12400000	6730000	1430000	318000	76200	21000	7420	2610	1010
5 Hz	17850000	10200000	2410000	581000	145000	40100	15000	5540	2200
10 Hz	23050000	13600000	3500000	875000	233000	64900	24600	9470	3930
15 Hz	26300000	15900000	4260000	1060000	300000	85400	32200	12400	5400

### Phase angle (degrees)

Freq\Temp	10°C	15°C	25°C	35°C	45°C	55°C	65°C	75°C	85°C
0.01 Hz	56	61	64	68	69	80	67	56	52
0.015 Hz	55	58	62	66	72	75	75	75	71
0.02 Hz	53	57	61	65	71	74	75	74	71
0.05 Hz	50	55	61	64	69	74	76	76	72
0.1 Hz	49	53	60	63	67	73	77	77	73
0.15 Hz	47	52	59	63	66	72	77	78	74
0.2 Hz	46	51	59	63	65	72	76	78	75
0.5 Hz	43	48	57	62	64	69	75	77	76
1 Hz	41	46	56	62	63	67	73	77	76
1.5 Hz	39	45	55	61	63	66	71	76	76
2 Hz	39	44	54	61	63	65	71	75	76
5 Hz	36	41	52	59	63	64	68	72	75
10 Hz	34	39	50	58	62	64	66	71	74
15 Hz	33	38	49	57	61	64	66	69	73

## 7% SBS with 93% Russian 80 pen bitumen

PAV aged

### Complex modulus (Pa)

Freq\Temp	10°C	15°C	25°C	35°C	45°C	55°C	65°C	75°C	85°C
0.01 Hz	3090000	1470000	213000	34300	6190	1190	236	58	16
0.015 Hz	3800000	1730000	288000	43800	8330	1650	356	81	24
0.02 Hz	4460000	2070000	368000	54000	10300	2110	463	108	33
0.05 Hz	7000000	3560000	664000	102000	19700	4450	1100	262	81
0.1 Hz	9665000	5090000	997000	162000	31500	7630	1990	513	162
0.15 Hz	11700000	6180000	1160000	215000	43100	10200	2810	752	237
0.2 Hz	13200000	6980000	1380000	260000	51800	12600	3550	973	315
0.5 Hz	19150000	10600000	2350000	476000	97500	24200	7330	2190	752
1 Hz	24800000	14400000	3420000	741000	157000	39100	12300	3950	1410
1.5 Hz	28800000	17000000	4260000	959000	204000	51400	16500	5470	2010
2 Hz	31850000	19200000	4960000	1140000	247000	63000	20200	6850	2590
5 Hz	42900000	27200000	7830000	1980000	455000	118000	38300	13600	5510
10 Hz	52400000	34500000	10800000	2910000	709000	188000	60600	22300	9220
15 Hz	58000000	38900000	12900000	3580000	891000	245000	76200	29800	11900

### Phase angle (degrees)

Freq\Temp	10°C	15°C	25°C	35°C	45°C	55°C	65°C	75°C	85°C
0.01 Hz	49	58	61	65	68	77	84	84	87
0.015 Hz	47	51	58	61	66	77	84	87	88
0.02 Hz	45	50	57	61	65	76	83	87	88
0.05 Hz	42	48	56	61	63	71	80	85	88
0.1 Hz	40	44	54	60	62	68	77	83	87
0.15 Hz	39	44	54	60	62	66	75	82	86
0.2 Hz	38	43	53	60	62	65	74	81	85
0.5 Hz	35	40	51	58	62	63	69	77	83
1 Hz	33	38	49	57	62	63	67	74	80
1.5 Hz	32	37	47	56	61	62	66	72	78
2 Hz	31	36	47	55	61	62	65	71	77
5 Hz	29	33	44	53	60	62	64	67	73
10 Hz	27	31	42	52	59	61	63	65	70
15 Hz	26	30	41	51	58	60	63	65	68

### 3% SBS with 97% Venezuelan 70/100 pen bitumen

RTFOT aged

Complex modulus (Pa)

Freq\Temp	10°C	15°C	25°C	35°C	45°C	55°C	65°C	75°C
0.01 Hz	451000	170500	33800	5480	982	179	40	11
0.015 Hz	618000	234000	42500	7860	1425	271	60	16
0.02 Hz	748500	285500	55300	9830	1825	365	80	22
0.05 Hz	1335000	525500	108000	20200	4010	850	196	53
0.1 Hz	2075000	860500	173000	32200	6990	1535	382	105
0.15 Hz	2645000	1125000	232000	42600	9580	2180	560	158
0.2 Hz	3115000	1355000	283000	52600	11950	2800	732	209
0.5 Hz	5245000	2395000	521000	105000	23950	5955	1670	502
1 Hz	7580000	3605000	802000	174000	40200	10350	3055	959
1.5 Hz	9345000	4530000	1020000	234000	54700	14200	4285	1385
2 Hz	10800000	5310000	1190000	288000	67800	17700	5430	1805
5 Hz	16750000	8610000	1840000	539000	134000	35750	11400	3995
10 Hz	22650000	12050000	2350000	832000	220500	59650	19350	7065
15 Hz	26300000	14200000	2590000	1030000	291000	79700	25900	9620

Phase angle (degrees)

Freq\Temp	10°C	15°C	25°C	35°C	45°C	55°C	65°C	75°C
0.01 Hz	62	67	69	72	79	84	88	88
0.015 Hz	59	62	66	70	79	85	88	88
0.02 Hz	58	62	66	70	78	84	87	88
0.05 Hz	56	60	65	69	74	81	86	88
0.1 Hz	54	58	64	67	72	79	84	87
0.15 Hz	53	57	64	67	71	78	83	86
0.2 Hz	52	57	63	67	70	76	82	86
0.5 Hz	50	54	62	66	68	73	79	84
1 Hz	47	52	61	66	68	71	77	82
1.5 Hz	46	51	60	65	67	70	76	81
2 Hz	45	50	59	65	67	70	75	80
5 Hz	42	47	57	64	66	69	72	77
10 Hz	39	45	55	63	64	68	71	75
15 Hz	38	44	54	61	63	68	70	73



### 3% SBS with 97% Venezuelan 70/100 pen bitumen

PAV aged

#### Complex modulus (Pa)

Freq\Temp	10°C	15°C	25°C	35°C	45°C	55°C	65°C	75°C	85°C
0.01 Hz	1470000	694000	110000	18100	3980	784	187	40	12
0.015 Hz	1970000	831000	137000	25200	5170	1120	259	62	17
0.02 Hz	2305000	983000	173000	30600	6630	1430	338	83	23
0.05 Hz	3545000	1690000	311000	58900	12900	3120	760	195	52
0.1 Hz	5190000	2460000	473000	99000	21800	5390	1350	377	109
0.15 Hz	6435000	3030000	614000	127000	29000	7200	1920	565	166
0.2 Hz	7430000	3510000	734000	157000	35500	8920	2440	736	221
0.5 Hz	11400000	5610000	1280000	286000	68000	17600	5160	1650	533
1 Hz	15300000	7830000	1920000	444000	110000	29200	8890	2960	1010
1.5 Hz	18150000	9470000	2420000	575000	145000	39400	12200	4120	1440
2 Hz	20400000	10700000	2840000	692000	177000	48300	15200	5190	1840
5 Hz	28950000	16000000	4660000	1210000	322000	93600	30500	10800	3950
10 Hz	36750000	21200000	6570000	1820000	492000	151000	50600	18300	6870
15 Hz	41100000	24500000	7880000	2240000	611000	196000	66700	23900	9440

#### Phase angle (degrees)

Freq\Temp	10°C	15°C	25°C	35°C	45°C	55°C	65°C	75°C	85°C
0.01 Hz	52	59	63	66	72	78	84	82	89
0.015 Hz	49	53	59	63	69	77	83	87	89
0.02 Hz	48	53	59	63	69	76	82	86	88
0.05 Hz	45	51	57	62	67	72	79	84	87
0.1 Hz	45	48	56	61	65	70	77	82	86
0.15 Hz	43	48	55	60	65	69	75	81	85
0.2 Hz	42	47	55	60	64	69	74	80	85
0.5 Hz	40	45	53	59	63	67	72	77	82
1 Hz	38	43	51	58	62	66	70	75	80
1.5 Hz	37	42	51	57	62	65	69	74	78
2 Hz	36	41	50	57	62	65	69	73	78
5 Hz	34	39	48	55	61	63	67	71	75
10 Hz	32	37	46	53	60	62	67	70	74
15 Hz	31	36	45	52	58	61	66	70	73

## 5% SBS with 95% Venezuelan 70/100 pen bitumen

RTFOT aged

Complex modulus (Pa)

Freq\Temp	10°C	15°C	25°C	35°C	45°C	55°C	65°C	75°C	85°C
0.01 Hz	459000	201000	43700	8240	1810	393	80	28	9
0.015 Hz	600000	246000	57800	11700	2390	540	128	34	13
0.02 Hz	733000	299000	71500	13600	3020	691	168	46	16
0.05 Hz	1285000	544000	130000	27100	6080	1530	396	109	40
0.1 Hz	1965000	843000	204000	43800	10200	2780	738	211	78
0.15 Hz	2455000	1080000	268000	57600	14000	3870	1040	309	115
0.2 Hz	2870000	1280000	325000	69700	17300	4810	1340	403	150
0.5 Hz	4700000	2220000	576000	131000	33400	9590	2900	924	351
1 Hz	6670000	3280000	859000	210000	54200	15900	5080	1700	660
1.5 Hz	8125000	4080000	1070000	274000	72000	21300	7030	2390	947
2 Hz	9335000	4770000	1230000	332000	87600	26200	8750	3060	1220
5 Hz	14100000	7570000	1820000	593000	165000	50600	17300	6400	2670
10 Hz	18800000	10400000	2250000	884000	262000	81400	28800	10900	4640
15 Hz	21800000	12400000	2450000	1080000	337000	105000	38800	14600	6110

Phase angle (degrees)

Freq\Temp	10°C	15°C	25°C	35°C	45°C	55°C	65°C	75°C	85°C
0.01 Hz	60	64	66	66	72	78	76	82	85
0.015 Hz	56	58	61	66	73	79	83	85	85
0.02 Hz	55	58	62	65	72	79	83	85	84
0.05 Hz	53	57	61	64	68	76	81	84	84
0.1 Hz	51	55	60	62	66	73	79	83	84
0.15 Hz	50	54	60	63	65	72	78	83	83
0.2 Hz	50	54	60	62	65	71	77	82	83
0.5 Hz	47	51	58	62	64	68	74	79	82
1 Hz	45	50	57	62	64	66	71	77	80
1.5 Hz	44	49	57	61	64	65	70	76	79
2 Hz	43	48	56	61	63	65	69	75	78
5 Hz	40	45	54	60	63	64	67	71	76
10 Hz	38	43	52	59	62	64	66	69	74
15 Hz	37	42	51	58	60	64	66	68	72

## 5% SBS with 95% Venezuelan 70/100 pen bitumen

PAV aged

Complex modulus (Pa)

Freq\Temp	10°C	15°C	25°C	35°C	45°C	55°C	65°C	75°C	85°C
0.01 Hz	1385000	648000	125000	29200	6540	1470	357	92	29
0.015 Hz	1755000	846000	155000	38700	9040	2100	498	142	33
0.02 Hz	2055000	995000	187000	46500	10500	2690	645	195	44
0.05 Hz	3230000	1630000	329000	81400	20100	5260	1360	448	109
0.1 Hz	4585000	2400000	493000	134000	32600	8580	2410	791	208
0.15 Hz	5620000	2950000	650000	177000	42400	11400	3310	1130	301
0.2 Hz	6465000	3410000	766000	209000	51200	14000	4050	1440	394
0.5 Hz	9770000	5360000	1300000	364000	93700	26400	7980	3050	893
1 Hz	13100000	7380000	1900000	538000	147000	42200	13100	5240	1595
1.5 Hz	15450000	8810000	2380000	666000	191000	55400	17300	7070	2220
2 Hz	17300000	10000000	2750000	773000	228000	67600	21400	9140	2790
5 Hz	24400000	14700000	4410000	1200000	402000	124000	39900	17400	5710
10 Hz	30950000	19200000	6120000	1590000	596000	193000	63500	28000	9580
15 Hz	34800000	21900000	7280000	1790000	734000	243000	83100	34300	12650

Phase angle (degrees)

Freq\Temp	10°C	15°C	25°C	35°C	45°C	55°C	65°C	75°C	85°C
0.01 Hz	51	57	59	60	65	70	74	84	86
0.015 Hz	47	50	57	60	63	71	78	83	86
0.02 Hz	46	50	56	60	63	69	77	81	86
0.05 Hz	44	48	54	58	61	66	73	79	84
0.1 Hz	43	46	53	58	61	64	70	77	82
0.15 Hz	42	45	53	58	61	63	69	75	81
0.2 Hz	41	45	52	57	61	63	68	74	80
0.5 Hz	39	42	50	56	60	62	66	70	77
1 Hz	37	41	49	55	59	61	65	68	75
1.5 Hz	36	40	48	55	59	61	64	67	73
2 Hz	35	39	48	54	59	60	63	67	72
5 Hz	33	37	46	53	57	59	63	65	70
10 Hz	31	35	44	51	56	58	62	64	68
15 Hz	30	34	43	50	53	57	62	64	68

## 7% SBS with 93% Venezuelan 70/100 pen bitumen

RTFOT aged

Complex modulus (Pa)

Freq\Temp	10°C	15°C	25°C	35°C	45°C	55°C	65°C	75°C	85°C
0.01 Hz	718500	293000	50200	11000	2400	563	114	29	11
0.015 Hz	935000	393000	65800	14000	3590	804	180	48	17
0.02 Hz	1120000	469000	84100	17000	4380	1020	237	64	22
0.05 Hz	1835000	800000	146000	30700	8540	2200	549	153	52
0.1 Hz	2690000	1230000	230000	48900	13600	3830	1010	292	100
0.15 Hz	3350000	1550000	295000	63200	17800	5240	1420	424	148
0.2 Hz	3865000	1810000	354000	75400	21300	6490	1820	549	194
0.5 Hz	6110000	2980000	629000	138000	38900	12400	3770	1240	450
1 Hz	8450000	4250000	961000	217000	61400	19700	6340	2240	839
1.5 Hz	10200000	5220000	1240000	280000	80400	25800	8540	3130	1200
2 Hz	11600000	6020000	1480000	337000	97000	31400	10500	3930	1540
5 Hz	17100000	9260000	2500000	601000	176000	57300	19600	7970	3310
10 Hz	22300000	12600000	3620000	916000	271000	89800	30900	13000	5670
15 Hz	25700000	14800000	4450000	1180000	342000	114000	39400	17100	7630

Phase angle (degrees)

Freq\Temp	10°C	15°C	25°C	35°C	45°C	55°C	65°C	75°C	85°C
0.01 Hz	53	57	60	60	63	72	78	73	77
0.015 Hz	52	54	57	60	70	78	82	85	84
0.02 Hz	51	54	58	59	67	77	82	84	84
0.05 Hz	48	52	57	59	64	73	80	83	84
0.1 Hz	48	52	57	58	61	69	77	82	83
0.15 Hz	46	50	56	59	60	67	76	81	83
0.2 Hz	46	50	56	59	60	66	74	80	82
0.5 Hz	43	48	55	59	59	63	70	77	80
1 Hz	42	46	54	59	59	61	67	74	79
1.5 Hz	40	45	53	58	59	61	65	72	77
2 Hz	40	44	52	58	58	60	65	71	76
5 Hz	37	42	50	57	58	60	62	68	73
10 Hz	35	40	49	56	56	60	61	65	70
15 Hz	35	39	48	55	56	59	61	64	69

## 7% SBS with 93% Venezuelan 70/100 pen bitumen

PAV aged

### Complex modulus (Pa)

Freq\Temp	10°C	15°C	25°C	35°C	45°C	55°C	65°C	75°C	85°C
0.01 Hz	1900000	847000	145000	29500	7320	1840	438	102	28
0.015 Hz	2335000	1010000	191000	38200	9520	2480	625	157	42
0.02 Hz	2645000	1200000	226000	45800	11500	3020	777	211	54
0.05 Hz	4095000	1950000	381000	83900	20200	5630	1670	477	130
0.1 Hz	5700000	2740000	599000	128000	32300	9140	2840	865	252
0.15 Hz	6985000	3430000	777000	167000	42600	11900	3910	1230	372
0.2 Hz	7930000	3930000	904000	199000	51100	14400	4790	1550	487
0.5 Hz	11700000	6060000	1500000	353000	91600	26400	8930	3190	1080
1 Hz	15400000	8220000	2170000	538000	141000	41500	14200	5350	1900
1.5 Hz	18100000	9830000	2650000	688000	182000	53800	18600	7160	2610
2 Hz	20100000	11100000	3080000	811000	217000	65100	22300	8770	3230
5 Hz	27900000	16100000	4820000	1380000	375000	116000	40700	16500	6410
10 Hz	34850000	20700000	6640000	1990000	552000	178000	63200	26000	10400
15 Hz	39050000	23700000	8030000	2450000	673000	224000	81800	33000	13700

### Phase angle (degrees)

Freq\Temp	10°C	15°C	25°C	35°C	45°C	55°C	65°C	75°C	85°C
0.01 Hz	46	50	60	59	60	68	79	80	87
0.015 Hz	46	50	54	58	60	67	77	83	86
0.02 Hz	45	49	54	58	59	66	76	82	86
0.05 Hz	41	45	53	56	58	62	71	79	84
0.1 Hz	41	45	52	56	59	60	68	76	82
0.15 Hz	40	44	51	56	58	60	66	74	80
0.2 Hz	39	44	51	56	58	60	65	73	79
0.5 Hz	37	42	49	55	58	59	63	69	75
1 Hz	35	40	48	54	58	59	62	66	73
1.5 Hz	34	39	47	53	57	58	61	65	71
2 Hz	34	38	46	53	57	58	61	64	70
5 Hz	32	36	44	52	56	57	60	63	67
10 Hz	30	34	43	50	55	56	60	62	65
15 Hz	29	34	42	50	54	56	60	62	64

**Appendix D**  
**DSR Data for Unaged, RTFOT and**  
**PAV Aged Sealoflex PMB**

## Sealoflex

### Unaged

#### Complex modulus (Pa)

Freq\Temp	10°C	15°C	25°C	35°C	45°C	55°C	65°C	75°C	85°C
0.01 Hz	149000	55300	9050	2200	390	93	50	28	10
0.015 Hz	190500	72200	12500	2870	712	246	107	60	43
0.02 Hz	239000	94900	15500	3470	880	279	118	67	50
0.05 Hz	433500	173000	28900	6740	1730	525	204	96	69
0.1 Hz	684000	272000	46700	11600	2880	867	314	144	93
0.15 Hz	902500	369000	63600	15600	3910	1180	425	183	113
0.2 Hz	1070000	433000	77900	18900	4780	1460	524	220	131
0.5 Hz	1840000	766000	149000	35700	9170	2900	1040	417	224
1 Hz	2705000	1160000	245000	57800	14900	4850	1770	692	352
1.5 Hz	3345000	1470000	327000	76800	19900	6540	2420	932	465
2 Hz	3865000	1730000	398000	93800	24400	8060	3010	1160	575
5 Hz	6040000	2890000	723000	179000	47000	15500	5970	2320	1130
10 Hz	8240000	4140000	1070000	288000	76900	24900	9780	3920	1910
15 Hz	9675000	5070000	1300000	369000	99600	32500	12900	5230	2540

#### Phase angle (degrees)

Freq\Temp	10°C	15°C	25°C	35°C	45°C	55°C	65°C	75°C	85°C
0.01 Hz	64	62	62	47	65	26	43		
0.015 Hz	61	62	62	64	62	56	46	40	40
0.02 Hz	60	62	62	64	63	56	48	40	39
0.05 Hz	58	60	62	64	64	62	55	47	42
0.1 Hz	56	60	63	63	65	64	60	52	44
0.15 Hz	55	59	63	63	65	65	63	55	47
0.2 Hz	54	58	63	63	65	66	64	57	49
0.5 Hz	51	56	63	63	64	66	67	63	56
1 Hz	49	55	62	64	63	66	67	65	60
1.5 Hz	47	53	61	64	63	65	67	66	62
2 Hz	46	52	61	64	64	65	67	67	63
5 Hz	43	49	59	63	64	64	67	67	66
10 Hz	41	47	57	62	65	64	66	67	67
15 Hz	40	45	56	61	65	65	66	65	65

## Sealoflex

### RTFOT aged

#### Complex modulus (Pa)

Freq\Temp	10°C	15°C	25°C	35°C	45°C	55°C	65°C	75°C	85°C
0.01 Hz	208000	86700	23000	5420	1370	405	101	62	34
0.015 Hz	275000	111000	29800	6920	1660	435	141	58	29
0.02 Hz	331000	136000	36500	8300	2020	539	172	69	36
0.05 Hz	570000	236000	69000	15000	3840	1090	331	127	64
0.1 Hz	856500	371000	111000	24300	6510	1830	577	215	97
0.15 Hz	1080000	484000	147000	31700	8220	2450	784	295	127
0.2 Hz	1265000	567000	177000	39000	9910	3040	965	371	157
0.5 Hz	2050000	965000	325000	74100	18300	5760	1920	756	311
1 Hz	2875000	1420000	502000	119000	29200	9190	3190	1290	528
1.5 Hz	3490000	1770000	640000	156000	38700	12100	4290	1750	723
2 Hz	3990000	2040000	755000	189000	47500	14700	5270	2180	907
5 Hz	6010000	3210000	1220000	345000	90400	27600	9950	4260	1850
10 Hz	7975000	4420000	1630000	530000	146000	44100	15800	6930	3110
15 Hz	9220000	5230000	1870000	656000	192000	56700	20500	9040	4190

#### Phase angle (degrees)

Freq\Temp	10°C	15°C	25°C	35°C	45°C	55°C	65°C	75°C	85°C
0.01 Hz	57	58	61	54	36	65			
0.015 Hz	55	58	60	60	63	64	60	55	54
0.02 Hz	54	57	60	60	64	65	61	57	54
0.05 Hz	51	55	60	60	62	65	66	62	58
0.1 Hz	51	55	59	60	61	65	67	66	61
0.15 Hz	49	54	59	61	61	65	67	67	63
0.2 Hz	48	53	59	61	61	64	67	68	64
0.5 Hz	46	51	58	61	61	63	67	69	67
1 Hz	44	49	57	61	61	62	66	69	69
1.5 Hz	43	47	56	60	62	62	64	68	69
2 Hz	42	47	55	60	62	62	64	68	69
5 Hz	39	44	54	59	62	62	63	66	69
10 Hz	38	43	52	56	62	63	63	65	68
15 Hz	37	41	51	51	61	63	63	65	67



## Sealoflex

PAV aged

### Complex modulus (Pa)

Freq\Temp	10°C	15°C	25°C	35°C	45°C	55°C	65°C	75°C	85°C
0.01 Hz	2440000	500000	87600	20600	4880	913	295	55	18
0.015 Hz	2666667	662000	109000	25300	5910	1380	353	97	31
0.02 Hz	3170000	772000	134000	30100	7050	1710	447	125	42
0.05 Hz	4630000	1200000	236000	53800	12500	3350	948	270	94
0.1 Hz	5976667	1740000	348000	81300	19900	5440	1650	490	170
0.15 Hz	7173333	2120000	437000	111000	26200	7160	2250	688	232
0.2 Hz	7953333	2410000	509000	130000	31900	8620	2750	879	297
0.5 Hz	11270000	3610000	837000	227000	57500	15700	5250	1830	655
1 Hz	14450000	4830000	1200000	339000	89300	24600	8350	3110	1170
1.5 Hz	16600000	5700000	1480000	428000	115000	32000	10900	4160	1630
2 Hz	18333333	6430000	1700000	499000	137000	38700	13200	5130	2070
5 Hz	24666667	9160000	2640000	801000	240000	70700	24100	9600	4140
10 Hz	30266667	11700000	3620000	1090000	360000	111000	37800	15200	6750
15 Hz	33533333	13400000	4290000	1260000	448000	141000	48500	19400	8760

### Phase angle (degrees)

Freq\Temp	10°C	15°C	25°C	35°C	45°C	55°C	65°C	75°C	85°C
0.01 Hz	47	52	55	58	59	41	64	71	81
0.015 Hz	41	47	55	57	59	68	73	76	77
0.02 Hz	41	46	54	57	59	67	73	76	76
0.05 Hz	39	45	52	56	57	64	71	75	77
0.1 Hz	37	43	52	57	58	61	68	74	77
0.15 Hz	36	42	51	56	58	60	67	73	77
0.2 Hz	36	41	50	56	58	60	66	72	76
0.5 Hz	34	39	48	55	58	59	63	69	75
1 Hz	33	38	47	54	58	59	61	67	73
1.5 Hz	32	37	46	53	58	59	60	65	71
2 Hz	31	36	45	53	58	59	60	64	70
5 Hz	29	35	43	51	57	59	60	62	67
10 Hz	28	33	42	49	55	58	60	61	65
15 Hz	28	33	41	47	52	58	60	61	64